Coastal Protection and Restoration Authority
450 Laurel Street, Baton Rouge, LA 70804 | coastal@la.gov | www.coastal.la.gov

Louisiana Flood Protection Design Guidelines (LFPDG)

Geotechnical Section

Report: Version I.0

Date: July 16, 2015

Coastal Protection and Restoration Authority

This document was prepared by the Louisiana Coastal Protection and Restoration Authority (CPRA) to support the 2012 Coastal Master Plan. CPRA Board was established by the Louisiana Legislature in response to Hurricanes Katrina and Rita through Act 8 of the First Extraordinary Session of 2005. Act 8 of the First Extraordinary Session of 2005 expanded the membership, duties, and responsibilities of CPRA, and charged the Board to develop and implement a comprehensive coastal protection plan, consisting of a Master Plan (revised every 5 years) and annual plans. CPRA was established in accord with La. R.S. 49:214.1 and 49:214.6.1 to be the implementation and enforcement arm of the Board. CPRA's mandate is to develop, implement, and enforce a comprehensive coastal protection and restoration Master Plan. As part of CPRA's mandate, the Authority has oversight over all matters relating to the study, planning, engineering, design, construction, extension, improvement, repair, and regulation of integrated coastal protection projects and programs, including hurricane protection, flood control, and storm damage reduction and is authorized to develop guidelines for cost-sharing agreements with public and private entities participating in approved integrated coastal protection projects.

Hurricanes Katrina and Rita caused tremendous loss of life and destruction of property when they struck Coastal Louisiana in 2005. As a result, The Hurricane and Storm Damage Risk Reduction System Design Guidelines (HSDRRSDG) were published in 2007 by the U.S. Army Corps of Engineers (USACE). The latest revision of the HSDRRSDG is dated June 14, 2012, which to date has been the main design and construction resource for Coastal Louisiana flood protection projects. Major projects in the West Bank & Vicinity (WBV) and Lake Pontchartrain & Vicinity (LPV) have been designed and constructed using HSDRRSDG to reduce flood risk from a 100-year event, or the 1 percent Annual Exceedance Probability (AEP) flood event in a given year. The Louisiana Flood Protection Design Guidelines (LFPDG) have been drafted to accommodate CPRA and State of Louisiana Projects based on lessons learned and experience gained from Louisiana projects by various non-federal sponsors and engineering consultants. The LFPDG will serve as the minimum standard consistent with sound engineering practices for those engaged in designing or constructing flood protection projects and systems where state funding is utilized.

The LFPDG is a living document and CPRA will continue to improve and update these guidelines as new information is discovered and as design techniques evolve.

Engineering Design Documents, Plans, and Specifications shall be prepared by or under the direct supervision of a licensed professional engineer and registered in the state of Louisiana following professional engineering standards as per La. R.S. Title 37, and Louisiana Administrative Code Title 46, Part LXI, Professional and Occupational Standards, as governed by the Louisiana Professional Engineering and Land Surveying Board.

Questions, corrections, or suggestions should be submitted in writing to the following email address coastal@la.gov. Please include LFPDG in the subject line.

Acknowledgements

The authors would like to acknowledge the following people and agencies that were instrumental in the development of these guidelines.

- Permission by the Louisiana Coastal Protection and Restoration Authority (CPRA) to adapt the June 2015 version of the Louisiana Flood Protection Design Guidelines (LFPDG).

- Continual support by Mr. Kyle Graham, Executive Director, CPRA

- The support by Mr. Jerome Zeringue, former Executive Director CPRA.

- Mr. Brad Barth, P.E., Mr. Brian Powell, P.E., Mr. Scott Breen, P.E., Mr. David St. Marie, P.E. and Mr. Jared Sommers, E.I., for authoring and facilitating the preparation of this document and coordinating reviews.

- Finally, for the technical reviews and recommendations provided by Mr. Ignacio Harrouch, P.E., Mr. Russ Joffrion, P.E., Mr. Rickey Brouillette, P.E., and Mr. Jaskaran Singh, P.E. of the CPRA, are gratefully acknowledged.

Executive Summary

The Coastal Protection and Restoration Authority (CPRA) is developing the Louisiana Flood Protection Design Guidelines (LFPDG) to be used as the minimum standard consistent with sound engineering practices for the implementation of CPRA and State of Louisiana funded flood protection projects and systems within the Louisiana Coastal Zone. This document consists of the Geotechnical Section of the LFPDG, with subsequent sections to be developed.

The Hurricane and Storm Damage Risk Reduction System Design Guidelines (HSDRRSDG), developed by the U.S. Army Corps of Engineers (USACE), were considered in the development of these guidelines. The latest version of the USACE HSDRRSDG should be utilized as guidance for flood protection projects pertaining to the 1 percent Annual Exceedance Probability (AEP) flood event. The LFPDG were developed to provide guidance for flood protection projects of the Interim Level of Protection, i.e. for more frequent events or events greater than the 1 percent AEP flood event, i.e. 2, 4, 10, 20 percent AEP flood events.

The LFPDG Geotechnical Section provides guidance pertaining to subsurface investigations, soil boring/CPT layout, laboratory testing requirements, levee embankment design, slope stability design, I-Wall Design (Z-Sheet/Combi-Wall), Pile Foundations, Anchored or Braced Sheet Pile Walls, Borrow Material, and Construction.

This document is intended as a guide for designing and constructing flood protection systems and is not intended to replace the professional engineering judgment of the design engineer.

Table of Contents

Illustration

List of Tables

List of Figures

List of Abbreviations

CPRA	Coastal Protection and Restoration Authority
USACE	United States Army Corps of Engineers
LFPG	Louisiana Flood Protection Guidelines
HSDRRSDG	Hurricane and Storm Damage Risk Reduction System Design Guidelines
USGS	United States Geological Survey
USCS	Unified Soil Classification System
NAVFAC	Naval Facilities Engineering Command
ASTM	American Society of Testing and Materials
FOS	Factor of Safety
EM	USACE - Engineering Manual
EC	USACE - Engineering Circular
ER	USACE - Engineering Regulations
ETL	USACE - Engineering Technical Letter
CPT	Cone Penetrometer Test
AEP	Annual Exceedance Probability

List of Project Definitions

AEP	The level of protection can be defined through a frequency or return period of a given storm such as a 1 in 25, 50, 100, etc., percent Annual Exceedance Probability (AEP). These flood events are commonly referred to 25, 50, 100-year, etc., events. See Figure 1.
CG	Water at construction grade (CG) is the water level to the construction grade prior to consolidation. Construction Grade or levee overbuild accounts for levee settlement as a result of primary consolidation. Levee overbuild is the difference between CG and Project Grade (PG). See Figure 1.
PG	Water at project grade (PG) is the water level to a levee elevation above the Still Water Level (SWL) to account for wave action and run-up minus overtopping height. Overbuild for primary consolidation settlement is not included in the PG. See Figure 1.
SWL	Water at design grade or also commonly known as Still Water Level (SWL) is the water level to a levee elevation for a level of authorized protection for a given design hurricane loading condition. This level of protection is determined through a design AEP. See Figure 1.
LWL (hurricane condition)	Low Water Level (LWL) hurricane condition is the water level to a levee elevation on the floodside that occurs when hurricane winds are directed away from the levee and the water is drawn down on the floodside. LWL can also occur in a non-hurricane event on the protected side when water levels in a nearby drainage feature are lowered by pumping in advance of a storm with anticipated high amounts of rainfall. See Figure 1.
NWL	Normal water level or operating pool. See Figure 1.
NWL (non-hurricane condition) S-case	Normal Water Level (NWL) non-hurricane condition is the water level to a typical levee elevation on both the floodside and protected side of the levee with normal drainage or pumping operations occurring. These conditions may be considered the long-term water and/or ground water conditions and stability is analyzed in terms of effective stress (S-case analysis). See Figure 1.
TOW	Top of Wall (I-Walls, T-Walls, etc.) water elevation is the top of wall which accounts for the SWL plus wave action and may include structural superiority.
Design Life	Design life is the length of time a project loading will remain valid.
Service Life	Service life is the length of time a project will remain in use to provide its intended function.

Interim Level of Protection	Specified as more frequent events greater than the 1 percent AEP flood event, i.e. 2, 4, 10, 20 percent AEP events.
Flood Protection System	Structures, walls, dikes, levees, gates, used to minimize the risk of flooding.
Soil Boring	An investigatory method to advance, collect/conduct samples or in-situ tests by rotary or direct push methods. Undisturbed types include 3-inch, 5-inch, while general type, include 3-inch with open tube samplers, SPTs, and CPTs. Alternate tests include Vane Shear Tests.

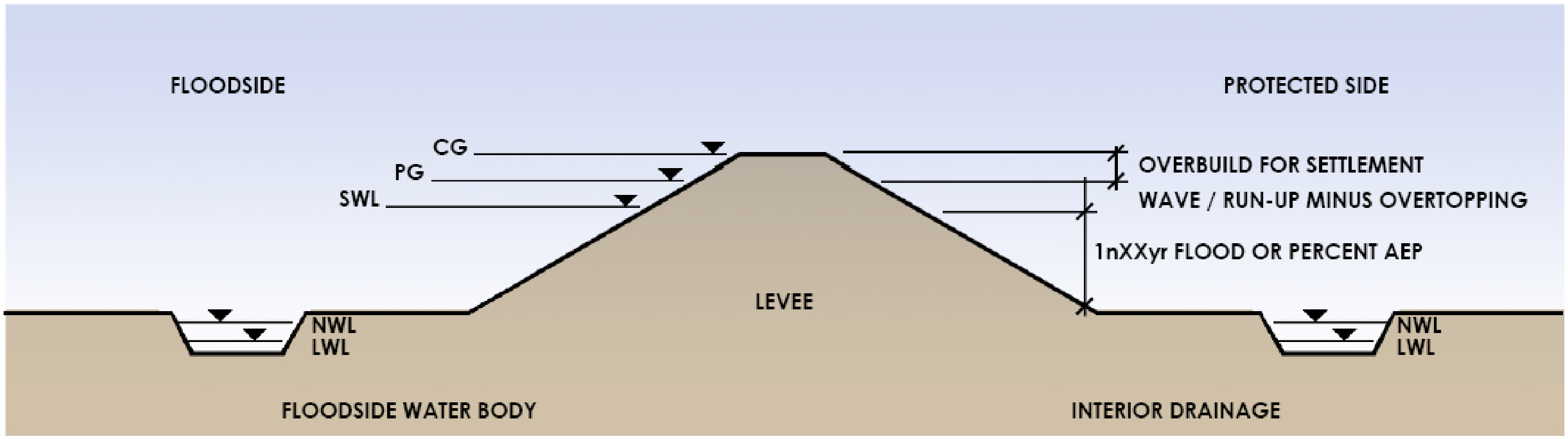

Figure 1: Project Elevation Schematic.

1.0 Introduction

This document has been prepared by CPRA to provide flood protection design guidance for the State of Louisiana and local flood protection projects.

This is a living document and is subject to change based on new conditions, data, analyses, or regulatory guidelines, as coordinated between CPRA, state and local entities.

The primary purpose of this document is to provide a consistent framework for the geotechnical evaluation, design, and construction of flood protection projects within the Louisiana Costal Zone. These design guidelines are intended to provide uniformity, expedite analysis, and reduce the timeframe and number of reviews by CPRA, State, local agencies, and Architectural/Engineer (A/E) firms. This design methodology should be used by all parties working on projects directly or indirectly affecting State and local flood protection projects and systems where State funding is utilized. In lieu of these guidelines, HSDRRSDG may be used, if warranted, by the design percent Annual Exceedance Probability (AEP), project design life, risk analyses, incorporation into the Federal Levee Safety Program, and/or funding available.

The intent of these guidelines is to summarize current applicable project information, design information, and guidelines and methodology for the analysis and design of flood protection projects. The summary includes but is not limited to listing of geotechnical design guidelines, hydraulic definitions, design references, design methodologies, design computer programs, pertinent data, loadings, load cases, materials, and unit weights. These guidelines are not intended to be all inclusive of any proposed project. Engineering judgment is necessary for projects or conditions which may go beyond the scope of this guidance. Because each project is unique, exceptions to the following guidance may exist which will require additional and/or alternative analyses. As such, it is recommended project and site specific design criteria, design approaches, methodologies and acceptance criteria be developed for each project. While considered applicable to the majority of flood protection projects, this document is intended to provide geotechnical engineering guidance for your specific project. Additional coordination is recommended with CPRA if projects or conditions cannot be partially or fully addressed by these guidelines.

2.0 Subsurface Investigation

2.1 General

The purpose of this section is to provide guidance and establish standards to be followed for geotechnical subsurface investigation, documentation of field testing, sample descriptions, field logging, instrumentation, and the handling and storage of samples.

The guidelines and procedures presented herein are intended to be of general use. A specific Subsurface Investigation Plan, including any modifications to these guidelines, should be prepared and documented prior to beginning the subsurface investigation. Additionally, as work progresses, appropriate revisions may be made based on field conditions.

The specific requirements of each drilling contract are presented in the Subsurface Investigation Plan to be prepared by the project Geotechnical Engineer. Field personnel should be familiar with the requirements of the Subsurface Investigation Plan.

2.2 Investigation Requirements

Adequate site characterization is dependent upon the degree of understanding of the site prior to the field investigation. At a minimum, the review of available geologic maps, geomorphic maps, aerial topography, bathymetry, soils maps, existing soil boring logs and cone penetrometer tests (CPTs), well logs, published papers, reports, and available information from local, state and federal agencies, such as the United States Geological Survey (USGS) and the United States Army Corps of Engineers (USACE), should be conducted prior to the development of the Subsurface Investigation Plan.

The quantity and quality of existing subsurface information will influence the scope of work and schedule of a proposed subsurface investigation. Other factors to consider when developing a Subsurface Investigation Plan include location, levee size, levee type, geology, geomorphology, groundwater, borrow material, knowledge of the area, and risk tolerance.

In some cases it may be prudent to approach the subsurface investigation in phases to develop a more comprehensive plan. For example, Cone Penetration Testing (CPTs) could be advanced quickly and in greater numbers to characterize a site, then a targeted soil boring program could be developed to supplement the preliminary CPT results. Likewise, CPTs may be incorporated in phased or staged investigations to confirm foundation shear strength gain from the placement of previous lifts.

2.2.1 Soil Boring Spacing

The following spacing below should be considered as typical spacing guidance for Flood Protection Systems and may be altered based on past knowledge/experience of a particular site. Flood protection systems are commonly referred to as levees, regardless if they are an earthen embankment, wall, structure, or gate. Additionally, for sites or projects where Interim Protection (>1 percent AEP) is being considered subsurface investigations may consider a combination of CPTs and 3-inch undisturbed soil borings as outlined below. Soil shear strength data generated from 3-inch undisturbed soil borings may be up to 10 to 30 percent weaker as compared to 5-inch soil borings. As such, the construction costs may be substantially higher in comparison to any cost savings in subsurface investigation. CPRA is currently exploring research efforts to further evaluate the shear strength differences based on different sample and specimen sizes.

<u>Soil Boring Spacing for Existing Levees</u>

Soil Borings shall be spaced in accordance with Table 1 for existing levees.

Table 1: Suggested Soil Boring Spacing (EM 1110-1-1804)*.

Levee Height	Suggested Soil Boring Spacing, L
Feet	**Feet**
< 20	1000
20 to 40	750
> 40	500

*Note: Suggested Spacing Taken from EM 1110-1-1804, Appendix F, Table 2-4

To maximize subsurface investigation coverage along a levee alignment, soil borings, CPTs, and/or vane shear testing should be staggered from centerline to toe as shown in Figure 2. A geotechnical engineer or geologist experienced in levee subsurface investigations may utilize a different spacing and soil boring type layout based on engineering experience and judgment, and by also considering many factors, such as available data, data quality, geology, levee history, levee performance, and risk and consequences to life and property. Soil borings should alternate between "Undisturbed" soil borings and "General Type" soil borings. Vane shear tests may be incorporated into the geotechnical Subsurface Investigation Plans at the discretion of the geotechnical engineer or geologist.

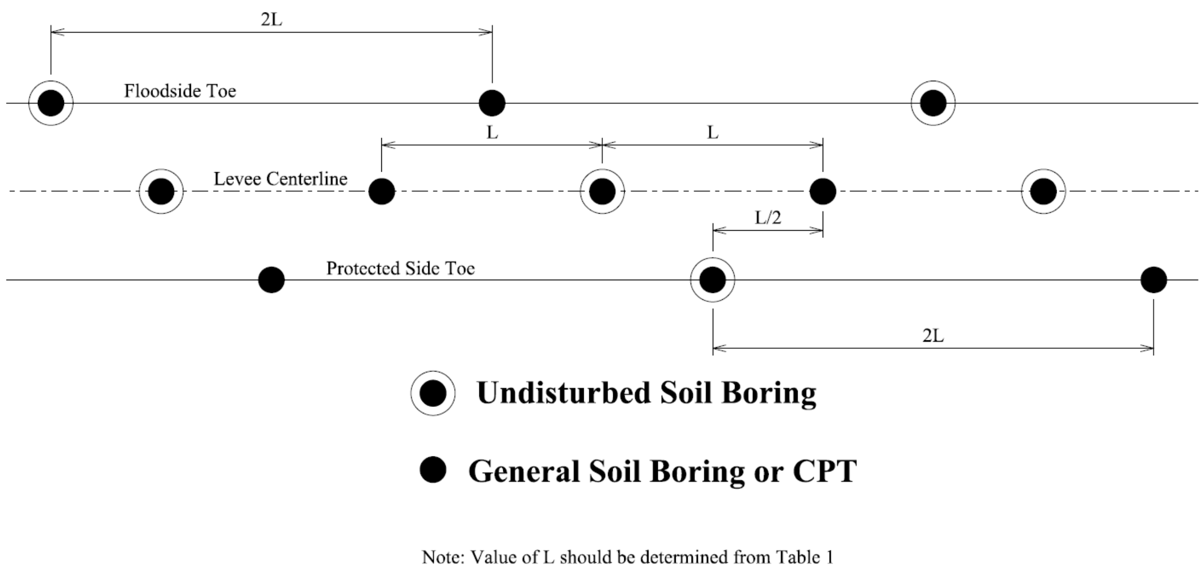

Figure 2: Soil Boring/CPT Spacing and layout Recommendations for Existing Levees.

<u>Soil Boring Spacing for New Levees</u>

For new levees, the foundation likely has not had the previous additional overburden along the centerline as compared to an existing levee. Therefore, significant variations in unit weight, shear strength, or differences in the stress-strain history of the foundation soil may not be expected. Only centerline borings are expected to be needed for new levees. However, engineering judgment and consideration of geology and geomorphology conditions should be also used to determine if toe borings are also necessary. Exceptions may exist because of geology or geomorphology, such as a proposed levee centerline located along natural levee deposits. This example would result in backswamp deposits along the floodside toe, while the centerline and protected side toe would be underlain by natural levee deposits, thus only centerline and floodside toe borings may be warranted.

The soil boring and CPT spacing illustrated in Figure 3 is recommended for new levees. This spacing is recommended because less is known about the subsurface conditions of a virgin levee. As a result, a more extensive subsurface investigation plan may be necessary to set the basis for the geologic data. Soil boring spacing, as shown in Figure 3, for centerline and toe borings should be considered for new levees which are anticipated to have large footprints or future lifts, or for areas where the known geology of the area dictates toe borings. In these scenarios, engineering judgment may warrant using a centerline and toe soil boring layout.

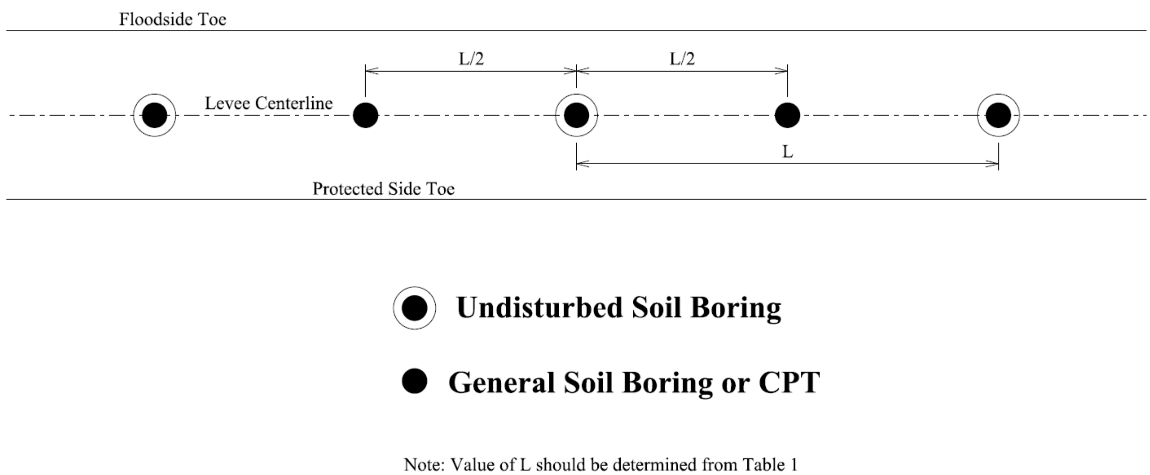

Figure 3: Soil Boring/CPT Spacing Recommendations for New Levees.

Dependent on the proposed levee size and the potential for future lifts, the new levee soil boring layout may need to have a pattern similar to that shown for existing levees to potentially capture the future levee toe position, see Figure 2.

<u>I-Walls</u>

Where I-Walls are planned in long reaches, and not used as transitions, additional soil borings and CPTs should be performed prior to final design to reduce the soil boring spacing, "L", to 100 to 250 feet based on experience and engineering judgment.

<u>Phased Investigations using CPT</u>

The use of phased investigations to quickly capture site wide geotechnical data through the use of CPTs may be considered where multiple subsurface investigations are planned to refine data and information for a levee site, with each phase refining the investigation spatially or by capturing more geotechnical testing information and data. In a phased investigation the initial or preliminary investigation may use CPTs in lieu of soil borings, if the subsequent investigations further refine the overall site investigation with CPTs, soil borings, and vane shear tests to adequately characterize the site, and thoroughly identify foundation shear strengths and compressibility.

Staged Construction

In many cases, levees are built via a staged construction utilizing several lifts of placed fill material, where the entire or a limited amount of fill is placed along the alignment and allowed to settle. After the foundation soil has consolidated and/or gained sufficient strength, as required to safely support additional lift material, another lift of material is added to the levee footprint and the process repeated until the design elevation can be maintained or until a future project elevation is reached. If the levee is designed to be constructed in staged lifts, a staged Subsurface Investigation Plan may be used to capture shear strength gain for the future levee lifts, thus reducing the future levee lift footprint. The soil boring spacing for subsequent lifts may vary based on engineering judgment because the base geotechnical explorations would have been performed for the new construction or existing condition. These investigations may include CPTs, soil borings, or vane shear tests based on engineering judgment.

Typically very soft to soft Coastal Louisiana soils trend or are normally consolidated. As such they will typically follow a trend of 0.17 to 0.30 C/P', where C/P' is the ratio of undrained shear strength (C) to effective stress (P'). The change in shear strength since the previous lift may be estimated using typical effective stress estimates of past and current levee configurations by assuming a C/P' of 0.22 to 0.24, which is a relationship independent of plasticity index established by Mesri (1975) for normally consolidated. This relationship may be utilized to evaluate the validity of the newly collected staged construction geotechnical data.

Borrow Pits

Borrow pit soil boring spacing is recommended to be performed on a 200- to 500-foot grid spacing

Additional Investigations

Depending on factors, such as geologic variability, weak or compressible soil profiles, levee history, past performance, or critical structures and/or levee penetrations, closer soil boring spacing may be necessary, and should be based on engineering judgment. Executed Subsurface Investigation Plans should be reviewed for their desired outcome. For example, if unanticipated zones of weak soils were encountered, unusable samples obtained from a soil boring, or more information is needed within an area because of unexpected variability, then further exploration should be planned.

2.2.2 Soil Boring Depth

In Coastal Louisiana, soil borings and CPTs should extend through soft compressible soils or soft fine-grained soils into competent material of suitable bearing capacity, such as dense sands or the Pleistocene formation.

It is recommended soil borings extend to a minimum depth of 50 feet below the natural ground surface. Selected soil boring depths should be based on the type of structure/foundation, the use of geosynthetics, the presence of adjacent excavations/water bodies, evaluation of the critical slope stability failure surfaces, evaluation of deep foundations, the zone of stress increase, and the presence of incompressible strata.

The depth of investigation should also extend deep enough below the foundation load or deep transferred load to adequately evaluate stress increase to the foundation soils, foundation index and physical properties, and to adequately determine the extent of foundation compressibility or consolidation due to the structure or load applied. Ultimately, the depths of soil borings should be determined by the geotechnical engineer based on experience and engineering judgment.

Typical levee soil borings may be on the order of 50 to 100 feet in depth, while structure soil borings may be on the order to 100 to 150 feet in depth, exclusive of levee embankment thickness.

2.2.3 Soil Boring Type and Sampling

Soil Boring Types

- Undisturbed – Continuous 3-inch or 5-inch diameter Shelby Tubes with a fixed-piston sampler
- General Type – Cone Penetration Tests, 3-inch diameter Shelby Tubes
- Vane Shear

Fixed-piston type sampling shall be utilized for fine-grained soil classified by USCS as OH, OL, CH, CL, CL-ML, MH, and ML for "Undisturbed" soil borings. Likewise, Standard Penetration Tests (SPT) shall be performed on all cohesionless soils such as sands or gravels. Where 3-inch Undisturbed Soil Borings are used, CPTs shall be used for the General Type Soil Boring.

In Coastal Louisiana, rotary wash drilling with hydraulically pushed thin-walled tube samplers is the commonly accepted method of obtaining undisturbed samples. The disadvantages of using open-drive samplers include the potential for obtaining samples with disturbed material or soil cuttings from a poorly cleaned borehole, which can be non-representative of overall sample characteristics. Open-drive thin-walled tube samplers may cause excess pressure over the sample during the drive causing the sample to be pushed aside within the sampler, and may not be effective in reducing the pressure over the sample during withdrawal, both of which result in poor quality and sample recovery. Hvorslev (1949) does not recommend open-drive samplers be used for undisturbed sampling of soft or loose soils for those aforementioned reasons.

Open-drive Shelby Tube sampling may also be used to retrieve samples considering the level of investigation necessary, soil conditions, and engineering judgment.

Sampling Intervals

Sampling intervals are recommended to be consistent with the current standard of practice, which consists of continuous sampling regardless of boring type. Vane shear tests should be performed based on engineering judgment, but 5- to 10-foot interval for the zone of interest may be appropriate.

Drill Advancement Methods

Soil borings shall be advanced by rotary wash with a side or upward discharging bit. Borehole stability shall be maintained and soil cuttingsshall be displaced to the surface through the use of a bentonite slurry during borehole advancement.

The following mud rotary guidelines shall be implemented to reduce soil sample disturbance:

- Limit excess down pressure or excess drill penetration rates to reduce damage to levee embankments or clay formations.
- Drilling penetration shall be limited to 1-foot depth of advancement per minute, which limits clay “balling” during the removal of soil cuttings.
- The drill interval shall be re-washed or cleaned if the drill pump experiences an excessive pump surge or pressure increase during the drilling of an advancement interval. The pump shall be operated at the lowest pressure possible to keep the bit clean and to flush cuttings to the surface.
- Do not drill by quickly raising and lowering the drill stem. Cleaning of an advancement interval shall be done in a controlled slow manner to prevent excessive pressures.
- Once the borehole is completed to the sample interval the pump shall be run for a sufficiently long time period to flush and clean the base of the borehole. This time may vary and should be based on experience and physical measurements of the borehole cleanliness prior to sampling.
- Borehole cleanliness shall be measured with a weighted tape, and shall be free of soil cuttings prior to taking a sample; otherwise the borehole shall be re-cleaned prior to taking the sample.

Borehole drilling mud shall consist of the following:

- Maximum Mud Weight 72 lbs/ft^3 per ASTM D 4380, 1984: R 2012 Standard Test Method for Density of Bentonitic Slurries. Virgin mud shall be used once mud weights exceed 72 lbs/ft^3.
- Mud Viscosity as measured by a Marsh Funnel shall be maintained within 60 to 70 seconds per API RP 13B-1 (2003).

Mud properties shall be continuously monitored and measured frequently during the drilling and sampling process.

2.2.3.1 Undisturbed Sampling

The 3- and 5-inch diameter relatively undisturbed clay and silt strata samples are obtained using thin-walled Shelby Tubes with a fixed-piston type sampler. This sampler and sample tube system consists of a piston that is connected to the piston rod (sometimes referred to as the inner rod). Within the sampler head, a locking mechanism (double-thread locking block type) allows the piston to be locked to the head in the down position (just inside the cutting edge of the sample tube), preventing the piston from falling out of the sample tube when in a vertical position. The piston rods or inner rods are then threaded inside the drill pipe during the lowering of the sampler to the sample interval. Once in position to sample, the piston is unlocked from the sampler head and the inner rod is fixed to the drilling rig. The steps used in obtaining the undisturbed sample using a fixed-piston sampler are as follows:

- A 30- to 36-inch and 54-inch long Shelby tube(s) is slipped over the piston and connected to the header with four bolts, for 3-inch and 5-inch samplers, respectively.

- The piston is positioned at the bottom of the tube (just inside the cutting edge) and locked (double-thread locking block type).
- The piston rod is connected to the smaller inner rods within outer drill rods.
- Once the piston is released (double-thread locking block type), the top of the inner rod is held in position (mechanically fixed to the drill rig) while the outer rod is pushed downward using the drill rig (i.e., the piston remains at the top of the sampling interval during the push).
- After pushing the Shelby tube in one continuous push to obtain the sample, the inner rod is removed from the outer drill rod and the sampler and Shelby tube are removed from the borehole.
- The push shall be measured and marked, and be approximately 6 inches less than the sample tube length.
- Prior to retrieval, the drill rod and attached sampler shall be rotated to shear the sample from the underlying formation.
- Once at the ground surface, the piston sampler, while still attached to the sample tube, is placed horizontally on a table, saw horses, or appropriate work surface.
- The vacuum breaker screw is removed to release the vacuum on the sample.
- The sample will then be field classified by a qualified geologist, geotechnical engineer, or a soil technician and prepared for transport to the laboratory.

Shelby tubes shall meet the requirements of ASTM D 1587-08(2012) e1 – Standard Practice for Thin-walled Tube Sampling of Soils for Geotechnical Purposes. In cases of less cohesive or leaner materials, such as silts, straight-sided Shelby tubes with inside clearance ratios of approximately zero may be considered based on actual field recovery and sampling experience of the geotechnical engineer.

The Shelby tube is pushed using the drill rig to obtain the sample and then removed from the borehole. All sampling shall be from a "clean" borehole. Potential very stiff to hard clays may be present in the upper overburden soils; therefore, if needed to ensure adequate recovery, Split-Spoon Sampling (SPT) may be considered during the field exploration. The soil recovered is field classified by a geologist or geotechnical engineer.

For sample intervals where little to no recovery is encountered, the sample interval shall be drilled out or cleaned to the bottom of the sampled or pushed interval. Then, a standard penetration test (SPT) will be taken, regardless of soil type. In the event back-to-back samples with less than 25 percent recovery occurs, the sample interval in question will be re-drilled and sampled. At a minimum, the zone should be over sampled by one sample above to one sample below.

To identify any re-drilled locations, an "R" shall be incorporated in the last string of the boring identification.

Drill cuttings or softened material from the top of the sample and a portion of the material at the bottom of the sample shall be removed by a soil lathe. Field classifications shall be determined from the bottom material removed for placement of the expandable packer. The top softened materials shall be discarded. Prior to capping the recovery shall be recorded by the soil logger. Shelby tubes shall then be sealed with expandable packers and capped, taped and labeled prior to shipment to the laboratory for extrusion. Labels shall clearly identify the soil boring name, the sample name and interval, direction of sample push, and date sampled. Labels shall be conspicuous and shall be located on the tube. The top cap should also be labeled with the boring name and sample name.

The prepared samples will then be transported from the drill site, typically on a daily basis, to the laboratory using special care to reduce disturbance of the soil sample.

The samples will be kept "shaded" during hot weather periods with a tarp or canopy until they are picked up for daily transport. The samples shall be secured vertically and cushioned to reduce sample disturbance. The samples are then transported to a laboratory for moisture content determination, classification, and testing.

2.2.3.2 Shelby Tube Storage, Extrusion and Shipment

Transportation

ASTM D 4220/D 4220M-14 – Standard Practices for Preserving and Transporting Soil Samples allows various modes of transportation and shipping containers that vary depending on the type of soil testing being performed and the sensitivity of the soil being tested. Based on the ASTM D 4220 groupings, a majority of the soils in Coastal Louisiana would be classified as "Group D" soils because of their sensitivity to disturbance for consolidation, strength, and other more sophisticated soil testing. Following the "Group D" classification, the most common transportation technique is to place the sealed samples in the back of a vehicle in a wood shipping container that provides cushioning and insulation to reduce vibration, shock, and protect against extreme heat for each sample within the shipping container. However, the amount of cushioning material recommended in ASTM D 4220 varies from the recommendations provided in EM 1110-1-1804.

Because reducing sample disturbance is paramount to yield quality samples for shear strength testing, EM 1110-1-1804 should be followed for sample transport.

Soil samples should be transported to the laboratory as quickly as feasible. EM 1110-1-1804 states samples must be stored snuggly to prevent rolling and bumping, and protected from changes in moisture content, shock, vibration, temperature extremes and chemical changes during transport. If samples are transported in tubes, a 1/2-inch to 3/4-inch thick marine plywood box with 3 to 6 inches of cushioning material between the samples, and bottom and sides of the container, or similar container, is recommended.

Extrusion

Though field extrusion is beneficial to reduce disturbance caused by soil-tube adhesion and friction during extrusion, the risk of disturbance from handling soft cohesive soils in the field and transport is increased. This is especially true with the very soft to soft soils typically found in Coastal Louisiana. For this reason, it is recommended that tube samples be sealed in the field and extruded in the laboratory. Field extrusion is recommended when cohesive samples are medium stiff or stiffer in consistency and can be handled and transported with less potential disturbance.

A hydraulic sample jack should be used to extrude a tube sample in one continuous uniform push. Mechanical and pneumatic jacks should not be used for extrusion.

Where it is anticipated extrusion is causing significant additional disturbance to the soil samples for testing, two methods may be used to help reduce disturbance. Cut the tube adjacent to the sampling location or use a hypodermic tube to feed a thin wire along the soil-tube interface and rotate the wire around the perimeter of the tube to break the bond.

Extruded samples shall be carefully caught within a core catcher to reduce disturbance, sample breakage, or bending the sample.

Preservation

After extrusion of the sample, samples should be wrapped in plastic wrap and stored in air-tight containers. It is recommended the designated tests be performed as soon as possible. When tests cannot be performed immediately following extrusion, samples should be waxed. Medium stiff or stiffer soils may, alternatively, be preserved by wrapping in plastic wrap, aluminum foil, and placed in a plastic bag. Because of the quality of pore water in some samples, they may have chemical reactions to the aluminum foil, which may affect the sample quality.

Samples to be waxed should follow:

- Wrap the sample in plastic wrap and wrap in aluminum foil;
- Place sample in two plastic bags (for easier removal of the inner bag with the sample); and,
- Place bagged sample in concrete cylinder mold or similar container and cover with molten wax (wax temperature shall not exceed 180° F).
- Minimum wax thickness above the sample is 0.4 inch or 10 mm.

Storage

Samples shall be temporarily stored within a temperature controlled laboratory environment until testing is complete. Samples slated for long-term storage shall be preserved and stored in a humid room. If mold or fungus growth, or slow chemical changes are anticipated, the samples should be properly refrigerated in accordance with EM 1110-1-1804.

Sample Schedule upon Sample Retrieval

- Extrusion should be performed as soon as feasible, at a minimum within 5 days of field sampling.
- Moisture Contents and Extrusion Logs should be performed within 7 days of field sampling.
- Samples not designated for Index or Physical tests shall be waxed within 7 days of extrusion.
- Index and physical tests such as Atterberg limits, Grain Size analysis, Hydrometer, Percent Passing U.S. No. 200 Sieve, Organics, Unconfined Compression, Unconsolidated-Undrained Triaxial Tests, Consolidated-Undrained Triaxial Tests, Direct Shear, Consolidation, and Permeability tests shall begin within 15 days of field sampling.

The remaining usable portions of specimens shall be waxed as recommended above at the time of test specimen preparation.

2.2.4 Standard Penetration Tests (SPT) with Split-Spoon Sampling

Where cohesionless strata are encountered, the Standard Penetration Test (SPT) shall be performed, ASTM D 1586-11 - Standard Test Method for Standard Penetration Test (SPT) and Split-Barrel Sampling of Soils. The SPT consists of a standard split-barrel sampler with a 2-inch outer diameter, 1.50- or 1.38 –inch inner diameter, and 18 to 24 inches in length, excluding the driving shoe. The SPT sample is collected by driving a total of 18 inches, using a 140-pound hammer falling 30 inches.

The SPT test is performed by recording the blows for three consecutive 6-inch intervals, with the first interval being a seating interval. The test is considered complete if any of the following occurs during the test:

- Sampler moves less than 1-inch in 10 blows;
- Total blows exceed 50 for any 6-inch interval; or
- Total blows exceed 100.

The SPT value is determined by adding the number of blows for the last two 6-inch test intervals, or recording a value of 50 and the inches driven for the termination interval, if the test is completed prior to driving 18 inches. The test intervals shall be clearly measured and marked to a stationary reference for the soil logger.

CPRA prefers the use of an automatic trip hammer, to maintain consistency of hammer fall. However, if a safety hammer and cathead are used, a maximum of 1-3/4 wraps (CCW cathead rotation) and 2 ¼ wraps (CW cathead rotation) are allowed. Prior to using a safety hammer, the 30-inch fall shall be measured and clearly marked. Regardless of the hammer type, hammers used and/or hammer used by individual drillers shall be calibrated for energy at least on a yearly basis. Rig /operator calibration shall follow ASTM D 4633-10 – Standard Test Method for Energy Measurement for Dynamic Penetrometers. Hammer efficiency information as well as the date of hammer calibration should be reported on the soil boring log.

SPT samplers shall be equipped with a "core catcher" with an appropriate stiffness for every test. Plastic bags or glass jars with screw-on lids shall be used to retain representative split-spoon sample(s). Samples with multiple representative portions shall be split and sampled separately, with sampling interval depths described on each sample jar or bag, and described on the boring log.

Disturbed soil samples placed into sample containers should be labeled to indicate: project name, project number, blows per 6 inches of penetration (or blow for penetrations less than 6 inches), date of sampling, boring number, sample number, top and bottom elevations for the sample. In addition, if jars are used, the lid should also be marked with project number, boring number, sample number, blow counts, and top and bottom elevation of the sample. Examples for labeling disturbed samples are illustrated below in Figure 4.

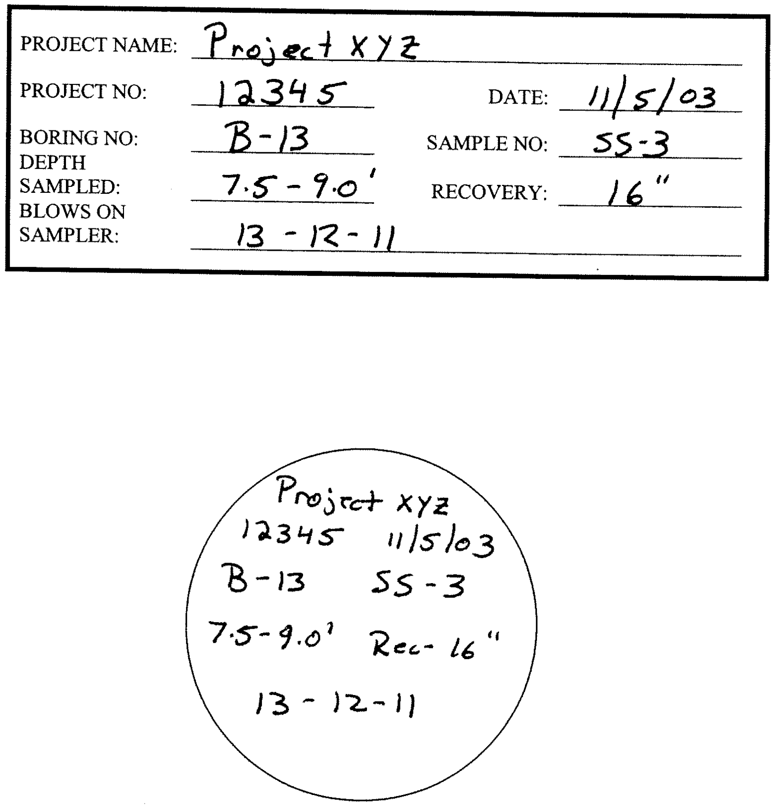

Figure 4: Example SPT sample container label.

Representative sample portions shall be saved in sample containers for each sample interval. Within a sample interval where lenses or layers are evident, multiple samples shall be taken from a single spilt-spoon sample. Multiple samples should be noted with an alphabetic suffix on the sample number SS-2a, SS-2b, etc. The samples should be labeled in alphanumeric sequence with increasing depth. For a given sample interval, sample A should be from the top 6 inches of the sample, B from the middle, and C from the bottom 6 inches.

If the jar samples are to be temporarily stored on-site, they shall be protected from the weather, including direct sunlight, heat and freezing.

2.2.5 Cone Penetrometer Test (CPT) Procedure

CPTs are to be used as a General Type soil boring. CPTs should be done according to ASTM D 5778-12 – Standard Test Method for Electronic Friction Cone and Piezocone Penetration Testing of Soils, and the following.

<u>CPT Equipment</u>

Items to consider for CPTs, tooling, push rods, and the thrust vehicle include:

- Cones, either 10 cm^2 or 15 cm^2 Type 2 Piezocones, should have a net area ratio closest to 0.80, ratios of 0.60 to 0.90 may be acceptable for the level of the work being considered. The 10 cm^2 cone is the preferred standard per ASTM D 5778-12.
- Cones should include tip, friction, inclinometer, and pore water pressure sensors or channels. It is also recommended the cone include a temperature sensor.
- Cones shall be properly calibrated in accordance with ASTM D 5778 -12 and shall include a net area ratio curve.
- Thrust equipment shall have a minimum dead weight reaction of 10 tons, minimum. The use of screw augers to anchor the rig and obtain additional thrust will not be allowed within levee embankments.
- Thrust equipment shall include a hydraulic rig leveling system which is connected to a rigid frame to prevent flexure of the reaction system.
- The CPT provider must be able to meet the criteria of ASTM D 3740.

<u>CPT General Procedure</u>

The CPT rig is positioned over the location of the sounding and the leveling jacks are lowered to raise the machine mass off the rig's suspension system. The hydraulic rams of the penetrometer thrust system are set to as near vertical as possible by adjusting the leveling jacks. Once the rig is set level, the following procedures are performed:

- Power up the penetrometer tip and data acquisition system according to the manufacturer's recommendations, typically 15 to 30 minutes prior to use.
- Measure the average diameter of the tip and sleeve to be sure that the sleeve is slightly larger than the tip (approximately 0.01-inch), and both are within ASTM D 5778-12.
- CPT cones will be de-aired on the bench of the truck vertically, and the porous element will be assembled under the de-airing fluid without applying a vacuum (standard method).
- Obtain initial zero readings for the cone in an unloaded condition at a temperature as close as possible to existing ground conditions.
- Record on the project data sheet other pertinent information such as Project Number, Date and Time, Cone Identification, and starting point of each test.
- CPT operator will record the initial and final zero readings on his daily logs/data sheet for each sounding. The percent change should be recorded for the tip, sleeve, and the pressure transducers.
- Set steel casing, as needed, for cone rod support.
- Advance the cone into the soil at a rate of approximately 2 centimeters per second. The depth, tip resistance, sleeve friction, and probe inclination are recorded at 2-centimeter long intervals.
- During the progress of sounding, monitor tip and sleeve forces continuously for signs of proper operation. It is helpful to monitor other indicators such as ram pressure or probe inclination to ensure that damage will not occur if highly resistant layers or obstructions are encountered. Probe inclination is a particularly useful indicator of imminent danger to the system.
- Soundings should be advanced to the planned tip depth or refusal.

- Pore pressure dissipation tests should be obtained at the direction of the Geotechnical Engineer.
- At the end of a sounding, extract the penetrometer tip, obtain a final set of zero readings from the unloaded cone prior to cleaning, and check them against the initial zero readings. Record initial and final baselines on all documents related to the sounding.
- Inspect the cone assembly after each push for damage to the components or seals and replace parts as needed. Clean the cone per manufacturer's recommendations.
- Raw CPT data, the Operator's daily log, preliminary processed data and CPT plots will be available, and submitted weekly to CPRA.
- If CPTs are being conducted in conjunction with a "calibration soil boring," the CPT shall be conducted prior to the Undisturbed type soil boring.
- When CPTs are included in a subsurface investigation, calibration soil borings should be performed for every approximately 10 CPTs, or based on engineering judgment.

<u>CPT Quality</u>

The CPT data collection operator shall be directly supervised a qualified engineer, geologist, or geoprofessional. Readings from the cone penetrometer are recorded in digital format with a digital data acquisition system. The calibration information is stored in the cone. This information is read from the cone before each test and recorded in the data files. Zero readings are recorded before and after each test automatically and stored in the data file. The cone should be checked for cross-talk between tip and the friction sleeve prior to starting the test and at the test completion. Zero and final readings should be recorded by the operator in his log as well. The raw data files should include the calculated initial / final baseline percent difference, which should be less than 2 percent for the tip, sleeve, and the pressure transducers. The cone and sleeve device units will be cleaned after each sounding. No "rotating wheel on the CPT rod" shall be used for the CPT depth encoder.

On a regular basis, the field data are transmitted electronically or by overnight mail to the appropriate office, where it is processed, reviewed, and finalized. The original unprocessed data is stored on large capacity, limited access storage medium where it is kept indefinitely for future reference as confidential records.

The integrity of the measurements shall be checked and verified to ensure that the logs generated are as accurate as possible. Rod spikes, which are generated naturally when the pushing is stopped such as when adding rods while advancing the sounding, are identified and edited out. These are displayed as negative spikes on the field generated CPT plot and when left uncorrected, may affect data integrity when further processing is done on the data.

The edited CPT plot is examined to ensure there are no problems with the data, such as negative values for tip or friction, cross talk between the tip and friction, or friction ratios which are excessive.

Prior to the release of the final report, the entire set of data will be reviewed by the CPT Manager. In this process, the reviewer conducts a thorough assessment of the data set checking its consistency and accuracy.

<u>CPT Data Presentation and Interpretation</u>

Data developed from a CPT shall follow ASTM D 5778 and include the following information:

- Ground surface elevation
- Raw tabular data including depth, cone tip resistance (q_c), friction (f_s), pore pressure (u_2), inclinometer (x, y), and temperature in electronic format.
- Calibration information
- Cone type and size
- Net area ratio
- Initial and final baselines, including percent difference calculation for the tip, sleeve, and pore pressure transducers
- Interpreted data files utilizing programs such as CONEPLOT, RAPID CPT, or others.
- Undrained shear strengths may be determined by N_U, N_C, N_K, or the N_{KT} methods, see Table 2, based on engineering judgment
- Drained shear strengths shall be interpreted by engineering judgment
- Data plots including corrected total cone tip resistance($q_t = q_c + u_2(1\text{-}a)$), frictional sleeve resistance (f_s), pore pressure (u_2), friction ratio (FR%), and with interpreted soil classifications based on methods such as those illustrated by Robertson et. al (1986) for non-normalized behavior or Robertson et. al (1990) for normalized soil behavior
- CPT soil classifications shall be interpreted with USCS classifications based on ASTM D 2487-11 Standard Practice for Classification of Soils for Engineering Purposes (Unified Soil Classification System) and ASTM D 2488-09a Standard Practice for Description and Identification of Soils (Visual-Manual Procedure) at paired CPT/Boring calibration locations

Table 2: Undrained Shear Strength from CPT Data*.

Method	Undrained Shear Strength
N_U	$S_u = (u_2 - u_o) / N_U$
N_{KT}	$S_u = (q_t - \sigma_{vo}) / N_{KT}$
N_K	$S_u = (q_C - \sigma_{vo}) / N_K$
N_C	$S_u = q_t / N_C$

*Note: Equations as shown in the RapidCPT Manual.
Where σ_{vo} is the total overburden.

2.2.6 Field Vane Shear Test Procedures

Field vane shear tests are normally performed for the purpose of measuring the undrained shear strength of subsurface silts and clays in cased boreholes that have been conventionally drilled. Field vane shear tests shall be performed in accordance with ASTM D 2573-08 Standard Test

Method for Field Vane Shear Test in Cohesive Soils. The following considerations shall be made for vane shear testing:

- Field vane shear tests may be considered for very soft to medium stiff clayey soils (S_U < 750 psf).
- Field vane shear test results shall be overseen by an experienced geotechnical engineer or geologist.
- Both the peak and remolded undrained shear strengths should be determined.
- Shelby tube over-sampling shall be taken from the test zone after the completion of the shear test for confirmation of material and Atterberg Limits. Material examination shall identify test zones which may have been conducted in undesirable drainage or dilatant soils such as stiff clays, sands, sandy silts, or soils with shells which may influence results.
- Spacing of tests within a specified zone shall be determined by the Geotechnical Engineer. Typical spacing may be on 2.5-, 5-, to 10-foot centers.
- The torque measuring device shall be calibrated in accordance with ASTM D 2573-08.
- Vane shear results shall be corrected (Bjerrum, 1972). Several correction methods are available considering plasticity index, effective overburden, over-consolidation ratio, and time to failure.
- Vane shear tests results, including laboratory test results for the over-sampling of the test zone, shall follow the reporting requirements of ASTM D 2573-08.

2.2.7 Borehole Abandonment

Boreholes, CPTs, auger holes, and/or vane shear tests shall be grouted full-depth in accordance with the State of Louisiana regulations or these recommendations, whichever is more stringent. Boreholes should be grouted with 24 hours of completion, with the top three feet backfilled with native soil cuttings. Grout backfill shall be tremie grouted and should consist of a 3 to 8 percent (by weight) cement-bentonite grout. Listed in Table 3 are typical cement-bentonite mixes.

Table 3: Suggested One Sack Cement-Bentonite Grout Mixes

Mix (% bentonite by weight)	Bentonite (lbs)	Water (Gallons)	Grout Weight (lbs/ft^3)	Yield per Sack (ft^3)
3	2.0	7.0	14.4	1.45
4	3.8	7.8	14.1	1.54
5	4.7	8.5	13.8	1.64
6	5.6	9.1	13.5	1.74
7	6.6	9.8	13.3	1.83
8	7.5	10.5	13.1	1.93

2.3 Laboratory Requirements

At a minimum, laboratories will be required to meet ASTM E329 Standard Specification for Agencies Engaged in Construction Inspection, Testing, or Special Inspection, which among other items states in Section 9.4.1 that a lab shall demonstrate evidence of meeting requirements set forth in Specification ASTM E329 through accreditation in the field of its operation by a recognized accreditation authority. For example AASHTO Materials Reference Laboratory (AMRL) accreditation for the specified laboratory tests would meet this requirement. CPRA prefers USACE validated laboratories be used for testing in accordance with ER 1110-1-261 and ER 1110-1-8100.

2.4 Laboratory Moisture/Classification Log

All samples are to be classified in accordance with the Unified Soil Classification System (USCS) classification system following ASTM D 2487-11 and D 2488-09a as applicable. At a minimum, the moisture content of each sample shall be determined. Samples are considered to be in 1-foot intervals for cohesive materials from Shelby Tube samplers and a maximum of 18-inch intervals for SPT samples. Moisture content tests shall be in accordance with ASTM D 2216-10 Standard Test Methods for Laboratory Determination of Water (Moisture) Content of Soil and Rock by Mass. This data is recorded on a laboratory moisture/classification log sheet.

2.5 Logging and Reporting of Soil Borings and Lab Tests

The results of field soil borings and laboratory tests will be shown and furnished by the geotechnical contractor. The borings will be reported and furnished as a stratified plotted boring log. In addition, the logs will be furnished and labeled with alphanumeric characters as specified on the proposed boring plan. The original "field log" for each boring will be recorded by the field logger, maintained by the geotechnical contractor as needed for analysis purposes.

2.6 Lab Testing Frequency and Methods

Lab Testing is anticipated to be assigned at the following frequency, pending actual materials encountered and engineering judgment:

Table 4: Lab Testing frequency and Methods.

Test	Frequency	Method	Comments
Moisture Content and USCS Classification	On all samples.	ASTM D 2216-10, D 2487-11, D 2488-09a	None
Atterberg Limits	On representative samples of embankment and foundations soils and for every consolidation, UCT, UU, CIU and unit weight test specimen.	ASTM D 4318-10	Method B
Unconfined Compression Tests (UCT)	On representative samples of embankment and foundation soils from Undisturbed or General type soil borings. Minimum of 1 every 5 feet of drilling, limited to the embankment and the upper 10 feet of foundations soils.	ASTM D 2166 / D 2166M-10	1.4-inch, 2.8-inch diameter specimens; trimmed from the center of 3-inch samples or from the center of a quadrant of 5-inch samples. Specimens shall be sheared to reach a constant axial load at 15 percent strain, otherwise shall be sheared to 20 percent strain, per EM 1110-2-1906.
Unconsolidated Undrained (UU or Q) Triaxial Test	On representative samples of embankment and foundation soils from Undisturbed or General type soil borings. Minimum of 1 every 5 feet of drilling.	ASTM D 2850-03a (2007)	1.4-inch, 2.8-inch diameter specimens; trimmed from the center of 3-inch samples or from the center of a quadrant of 5-inch samples. For 3-inch samples, a

Test	Frequency	Method	Comments
			minimum of 2 specimens from the same/adjacent sample interval(s), trimmed vertically. A third specimen shall be reserved for testing, if needed. Specimens shall be sheared to reach a constant axial load at 15 percent strain, otherwise shall be sheared to 20 percent strain, per EM 1110-2-1906.
Isotropic Consolidated Undrained (CIU or S) Triaxial Test with pore pressure measured	Assigned considering project, loads, anticipated drainage conditions (effective stress conditions), and engineering judgment.	ASTM D 4767-11	1.4-inch, 2.8-inch diameter specimens; trimmed from the center of 3-inch samples or from the center of a quadrant of 5-inch samples. For 3-inch samples, specimens from the same/adjacent sample interval(s), trimmed vertically.
Consolidated Drained (S) Direct Shear Test	Assigned considering project, loads, anticipated drainage conditions (effective stress conditions), and engineering judgment.	ASTM D 3080 / D 3080M-11	None
Consolidation Test	On representative samples of embankment and foundation soils from	ASTM D 2435-11	Test Method B Minimum 2.0-inch diameter specimens,

Test	Frequency	Method	Comments
	Undisturbed soil borings. Assigned considering project, loads, primary consolidation zone, and engineering judgment. Pending the size of the levee project and the material within the zone of consolidation, the number of tests shall be enough to adequately characterize the consolidation properties for settlement evaluation.		and Minimum D/H ≥ 2.5
Gradation/Hydrometer	On representative samples of embankment and foundation soils. If any gradation does not obtain D_{10} size, a hydrometer test will need to be performed.	ASTM D 421-85 (Reapproved 2007) and D 422-63 (Reapproved 2007)	None
P_{200} Test	On representative samples of embankment and foundation soils. P_{200} tests will also be needed on all borrow material.	ASTM D 1140-00 (Reapproved 2006)	None
Organic Content	On representative cohesive samples with organics. All materials classified as OH, OL or Pt should be tested for organics.	ASTM D 2974-13	None
Unit Weight Tests	Test is included as part of consolidation, UCT, UU, and CIU tests. Additional unit weight tests shall be assigned based on engineering judgment.	ASTM D 7263-09	Included with consolidation, UCTs, UUs, and CIUs.
Specific Gravity	On each consolidation and CIU Triaxial Test.	ASTM D 854-14	None

Test	Frequency	Method	Comments
Salinity and Sulfate Tests	As appropriate for Levee Embankment Soil Borings, Borrow Pit Soil Borings, and Test Pits	ASTM D 4542 (Salinity)	None

2.7 Shear Strengths and Consolidation Data

2.7.1 Unconfined Compression Tests

Unconfined compression tests (UCTs) samples obtained from either 3-inch or 5-inch diameter tubes are allowed. Specimens with 1.4-inch or 2.8-inch diameter shall have a height to diameter ratio between 2 to 2.5. Specimens should be trimmed from the center of the sample or sample quadrant for testing, in accordance with ASTM and USACE guidelines. This practice will help minimize specimen disturbance. It is recommended EM 1110-2-1906 be followed for specimen shearing (i.e. samples are sheared to reach a constant axial load or 20 percent strain).

2.7.2 Triaxial Compression Tests

For triaxial shear tests, samples obtained from either 3-inch or 5-inch diameter tubes are allowed. Specimens with 1.4-inch or 2.8-inch diameter shall have a height to diameter ratio between 2 to 2.5. Specimens should be trimmed from the center of the sample or sample quadrant for testing, in accordance with ASTM and USACE guidelines. The three specimens shall be tested under different confining pressures with the maximum confining pressure at least equal to the maximum normal pressure expected in the field with the project in place. The selected confining pressures shall consider the overburden stress, the existing pore pressures, the consolidation state such as under-, normally, and over-consolidated, and the anticipated future load or stress increase. These confining pressures should be selected by the geotechnical engineer based on experience and engineering judgment. Triaxial shear tests may be run for three different stress states: unconsolidated-undrained (UU) or Q-test, isotropic consolidated-undrained (CIU) with pore pressure measurements or the R-test, and consolidated-drained (CD) tests or S-test. A minimum of 3-points, or 3 specimens are recommended to estimate the shear strength envelope. For over-consolidated soils, consideration shall be given to testing 4 specimens or selecting two confining pressures on the over-consolidated portion of the shear strength envelope.

It is recommended EM 1110-2-1906 be followed for specimen shearing where samples are sheared at a rate of 1.0 percent per minute until a constant axial load is reached or 20 percent strain.

2.7.3 Consolidation Tests

Specimens trimmed from 3-inch or 5-inch thin-walled tube samples may be used. Minimum specimen size of 2.0-inches may be used provided the diameter to height ratio is greater or equal to 2.5. Consolidation tests shall follow ASTM D 2435-11 Test Method B. The specimen should be loaded in the following increments; 0.25, 0.5, 1.0, 2.0, 4.0, 8.0, and 16.0 tons per square foot (tsf) unless otherwise specified. A higher loading increment of 32 tons may be necessary depending on soil conditions and/or proposed project loading. Deformation readings should be recorded at increments of 0.1, 0.2, 0.5, 1.0, 2.0, 4.0, 8.0, 15.0 and 30.0 minutes, and at 1, 2, 4, 8 and 24 hours. If primary consolidation has not completed within the first 24 hours of testing, testing will be extended in 24 hour increments until primary consolidation has completed.

EM 1110-2-1906 provides guidance for the estimation of the preconsolidation pressure (P'c) and EM 1110-1-1904 provides guidance for the compression index (Cc), and the recompression index (Cr). EM 1110-1-1904 Chapter 3, including Figure 3-12 and Table 3-6, and NAVFAC (1986) Figure 4 page 7.1-144, shown in LFPDG Figure 5, may be used for laboratory test data interpretations. It is recommended the interpretation of the preconsolidation pressure, the compression and recompression indices be based on the Casagrande graphical construction method. Additional methods are available to estimate the preconsolidation pressure and compression indices and may be used based on engineering judgment. Differences in P'c, Cc, Cr, may arise between software based interpreted values within commercially available consolidation test software and the Casagrande graphical procedure. Therefore, the consolidation test data shall be evaluated and interpreted by the geotechnical engineer. Regardless, design calculations shall clearly document the methodologies of data interpretation.

EM 1110-2-1906 does not provide guidance for estimation of the effective overburden pressure ($\sigma v'$) or the coefficient of consolidation (Cv). The effective overburden pressure is typically calculated from the basic soil mechanics principles of effective stress.

The coefficient of consolidation may be interpreted from the laboratory consolidation test data within the range of anticipated design pressures. However, the time rate of settlement in the field can often be orders of magnitude different than estimated from laboratory tests. Experience in Coastal Louisiana suggests the rate of settlement in the field is often quicker than calculated by using the laboratory estimated coefficient of consolidation. This is typically because of the non-homogeneity of the in-situ soils in comparison to the laboratory sample, which allows for quicker pore pressure dissipation or because shorter drainage paths exist in-situ. The Naval Facilities Engineering Command (NAVFAC) Design Manual 7.01 provides a figure (see Figure 5) to estimate the coefficient of consolidation based on the soil's liquid limit, which has been used in local practice.

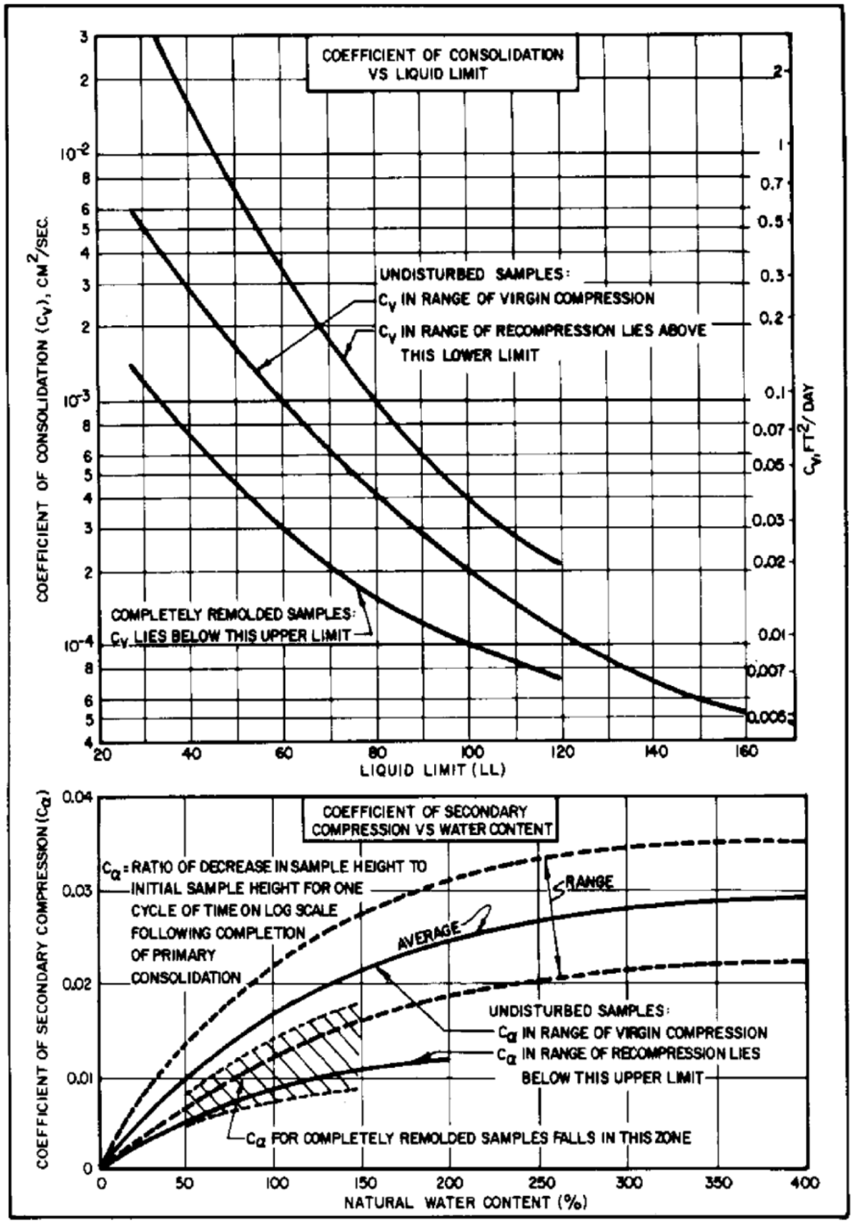

Figure 5: Correlations for Consolidation Characteristics of Silts and Clays (NAVFAC DM 7.01, Fig-4, pg. 7.1-144). Boring/CPT Spacing Recommendation for Existing Levees.

3.0 Levee Embankment Design and Design Parameters

3.1 Levee Embankment Geometry

Minmum10-foot crown width, minimum 1V:3H levee side slopes, minimum 1V:50H levee berm slopes to promote drainage away from levee, and minimum 1V:3H levee berm toe slopes are required. Levee lifts for existing levees with 8-foot crown widths may keep the 8-foot levee crown width to minimize the levee footprint.

3.2 Typical Levee Embankment Fill Properties

Table 5: Typical Levee Embankment Soil Parameters (HSDRRSDG 2012)*.

Soil Type (USCS - CH or CL)	Unit Weight (pcf)	Undrained Shear Strength (psf)	Friction Angle, ϕ (deg.)
Compacted Clay (90% Standard Proctor)	115	600	0
Uncompacted Clay (from dry borrow pit)	100	200	0

*Note: Typical values Taken from HSDRRSDG (2012) Table 3.2

Table 6: Typical Values for Silts, Sands, and Riprap Parameters (HSDRRSDG 2012)*.

Soil Type (per USCS)	Unit Wt (pcf)	Undrained Shear Strength (psf)	Friction Angle, ϕ (deg.)
Silt (undrained)[1]	117	200	15
Silty Sand	122	0	30
Poorly graded Sand (Sand Core)	122	0	33
Riprap	132	0	40

*Note: Typical values Taken from HSDRRSDG (2012) Table 3.3

[1]Silt properties for S-Case analysis, c' = 0 psf, Φ'=28°

For S-case analysis typically clay properties used for stability analysis are c' = 0 psf, Φ'=23° and for Silts c' = 0 psf, Φ'=28°. Engineering judgment or laboratory tests should be used to determine S-case soil properties for clayey silts, clayey sands and sandy silts. Design values may vary from the typical values when site specific information is available.

3.3 Levee Shear Strength Lines

Shear strength lines should be developed and plotted for all applicable cross sections and/or levee reaches. Shear strength lines should be based on the results of current or new subsurface data, but should consider any available historic soil information previously used for stability analysis. Generally new shear lines for existing levees will include a historic strength gain along the observed centerline soil borings.

For new levee construction, one shear strength line may only need to be developed along the center line of the proposed levee. Exceptions to this may be, for example, a levee which may be positioned along a natural levee/back swamp deposit where different shear strength lines for different positions across the levee section may be appropriate considering the site geology. However for existing levees, the floodside, protected side, and center levee shear strength lines should be developed for a given cross section for a representative soils reach to account for different stress histories at these locations. Shear strength lines on the protected side and floodside are typically weaker than through the center of the levee. The existence of wave or stability berms on the floodside and stability berms on the protected side may also influence the shear strength below those levee features. In the case of levees with berms, it may be necessary to develop a fourth and/or fifth shear line to account for the levee centerline, berms, and virgin toes shear strengths.

A line indicating the ratio of cohesion (undrained shear strength) to effective overburden pressure (C/P') of 0.22 to 0.24, historically observed in Coastal Louisiana, should also be superimposed on the shear strength plots. The effective overburden pressure can be determined by treating the levee embankment section as a distributed load, calculate the change in stress with depth using an appropriate method, such as Boussinesq load distribution values, and adding the overburden pressure calculated by starting at the base of the existing levee section. EM 1110-1-1904 Appendix C may be considered for estimating the stress increase from the levee embankment load.

Shear strength lines for the center line, berms, floodside and protected side toe plots (as applicable), plotted by elevation, should include at a minimum the following:

- Design shear strength lines;
- Historic shear strength lines (if applicable);
- Ground water elevation;
- C/P' line = 0.17 and 0.22;
- UU (solid symbols) and UC (hollow symbols) test results;
- Moisture contents;
- Unit weights;
- Correlated CPT shear strengths;
- Generalized stratigraphy (USCS); and
- Corresponding friction angles for sand and silt layers.

The design shear strength line generally should be selected considering laboratory shear strengths, CPT shear strength estimates, and engineering judgment.

Because of the quantity of data points, the design should color code the data points by soil boring, CPT, or Vane Shear Test, and present the data in 11 x 17 landscape format. An example Shear Line is illustrated in Figure 6.

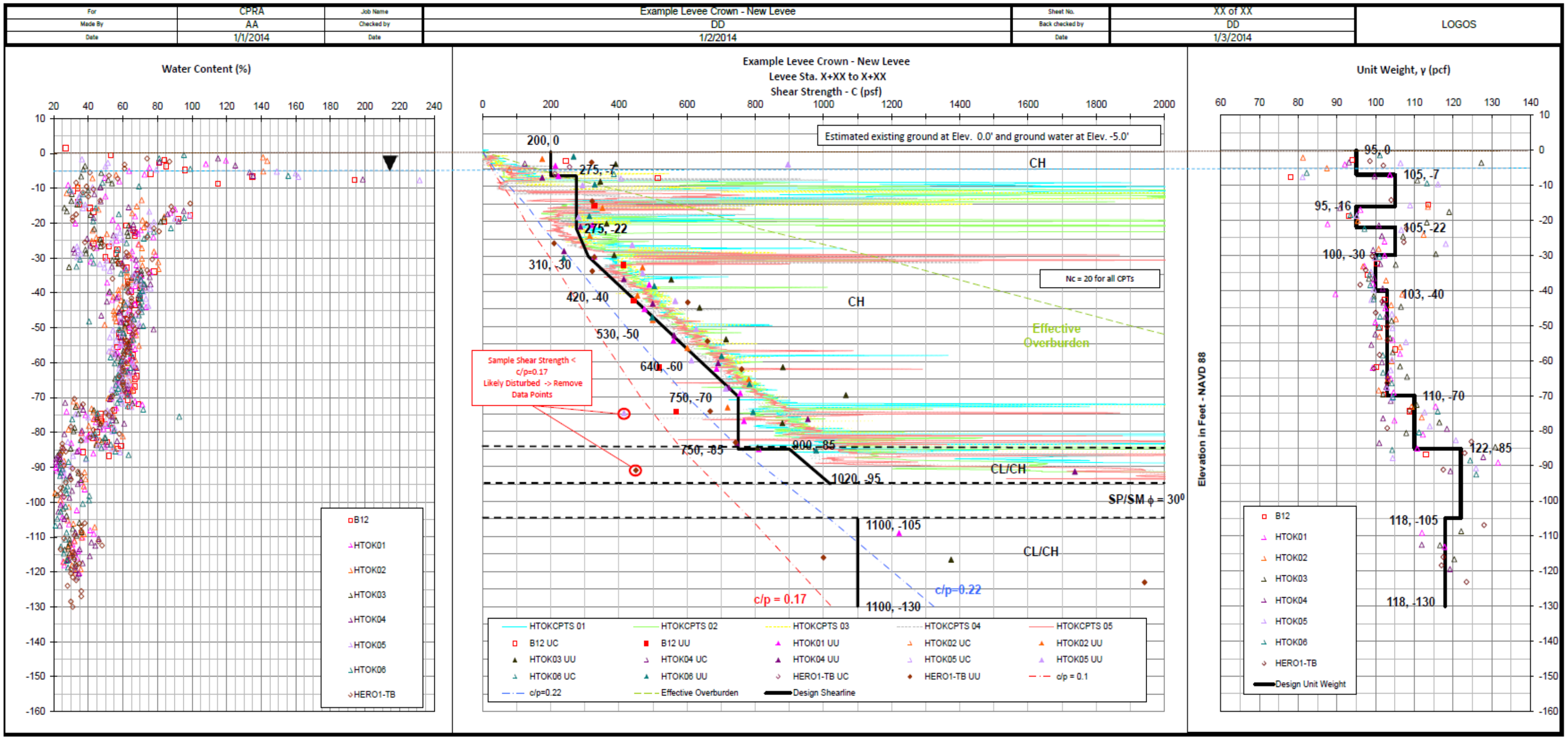

Figure 6: Example Design Shear Strength Line.

Undrained shear strengths may be estimated from CPT data by one of the methods presented in Table 2 of these guidelines.

Typically, without any calibration, N_c values of 18 to 21 are used for southern Louisiana soils (Brandon et. al., 2010). However, when a CPT is done near the location of an undisturbed boring, calibration of the undrained shear strength is possible. The undrained shear strengths from the undisturbed borings can be compared with the measured CPT tip resistance, so a "calibrated" N_c value can be back calculated. A fair amount of scatter is possible with this approach, but overall selected N_c values below 10 and above 30 are not typically considered.

3.4 Levee Stability Factors of Safety (FOS)

Based on the background research and the evaluations, the following slope stability FOSs, stress/pore water conditions, and analyses methods listed in Table 7 are recommended for Coastal Louisiana or hurricane levees:

Table 7: Recommended Design Slope Stability Factors of Safety.

Case	Shear Strength Condition	Pore Water Pressure Condition / Water Level	Required Minimum Factor of Safety[1]
End-of-Construction (EOC)[2]	Undrained – Floodside and Protected Side	NWL	1.3
Hurricane at Design Grade (SWL)	Undrained – Protected Side	SWL	1.4
Hurricane at Construction Grade (CG)	Undrained – Protected Side	CG	1.3
Hurricane at Water Low Grade (LWL)	Undrained – Floodside	LWL	1.4 (1.3)[3]
Hurricane at Design Grade (SWL)	Drained – Protected Side[4]	SWL	1.4 (1.5)[5]
NWL Non-Hurricane (S-Case)	Drained – Floodside and Protected Side	NWL	1.4

Notes: [1] Spencer's Method used for analysis.

[2] EOC case is not required for Coastal Levees if SWL or CG cases are checked.

[3] The FOS of 1.3 may be used where the water levels are not anticipated to be withdrawn from the hurricane.

[4] Long-term slope stability is not typically a critical failure mode for Louisiana coastal levees, so this case should be a design check on a limited number of sections. Use FOS of 1.5 where steady state seepage may occur.

[5] Where Rapid Drawdown slope stability conditions may occur, a FOS of 1.1 to 1.3 shall be used for levees, drainage canals, or sumps regardless of levee location.

3.5 Levee Consolidation Settlement

3.5.1 Stress Estimation Theory and Methodology

Consolidation settlement analysis of levee embankments requires an estimate of the existing effective stress and proposed effective stress increase. In the case of an existing levee that requires a future lift, the use of superposition to estimate stresses is often used to account for the load shape and magnitude. Otherwise, overestimation of the stress increase could occur for future levee lifts.

Common methods used to estimate the stress in a soil mass in the form of 2-D or 3-D solutions include: the 2:1 Method, Boussinesq, and Westergaard theories. Further discussion on these stress estimation theory's and methods are available in soil mechanics publications, and in EM 1110-1-1904 Appendix C. More advanced methods or software such as finite element may better account for untypical load shapes.

The effective stress and stress increase estimation should be based on engineering judgment and experience, and will not be addressed in detail within these guidelines. Stress changes can also be estimated with commercially available software, such as USACE's CSETT settlement software, and Settle3D.

3.5.2 Consolidation Settlement Calculations

Consolidation Settlement calculations shall address immediate settlement of foundation soils, consolidation settlement of foundation soils, shrinkage and consolidation settlement of the levee embankment, and regional subsidence. The time rate of settlement estimate is also required for evaluation of the levee design grade over the design life of the project.

Similar to the levee shear lines, consolidation parameters for each levee soil reach shall be developed from consolidation data and should include the following at a minimum:

- Void ratio versus elevation and/or depth;
- Compression (C_C) and re-compression (C_R) indices (or Ratios strain based); and,
- Overconsolidated ratios.

Within normally consolidated zones moisture contents may be utilized to estimate the void ratio and the compression index.

In Coastal Louisiana, soils are typically normally consolidated, however based on engineering judgment and site geology, some soil profiles may need to be considered as overconsolidated, particularly in the upper zones and within the upper portions of deeper geologic formations. EM 1110-1-1904 Settlement Analysis provides settlement theory and methodologies for the calculation of settlement. Settlement calculations are typically presented as hand written calculations or in spreadsheet format, but commercially available settlement software, such as CSETT or Settle3D may also be used for providing output reports.

3.5.3 Levee Lift Schedule

Levee designs should consider the existing and the future design grade. This estimation will give the designer an idea of how many levee lifts may be necessary over the life of the project. Once an idea as to how many lifts may be necessary to maintain the design elevation, the time rate of settlement may be determined for each lift. These estimates may be used to produce a graph such as the one presented below. The levee lift schedule below includes a design grade increase over time; however, for some levee systems the design grade may be the same over the life of the design. This type of levee lift schedule may be used to optimize the number and magnitude of levee lifts.

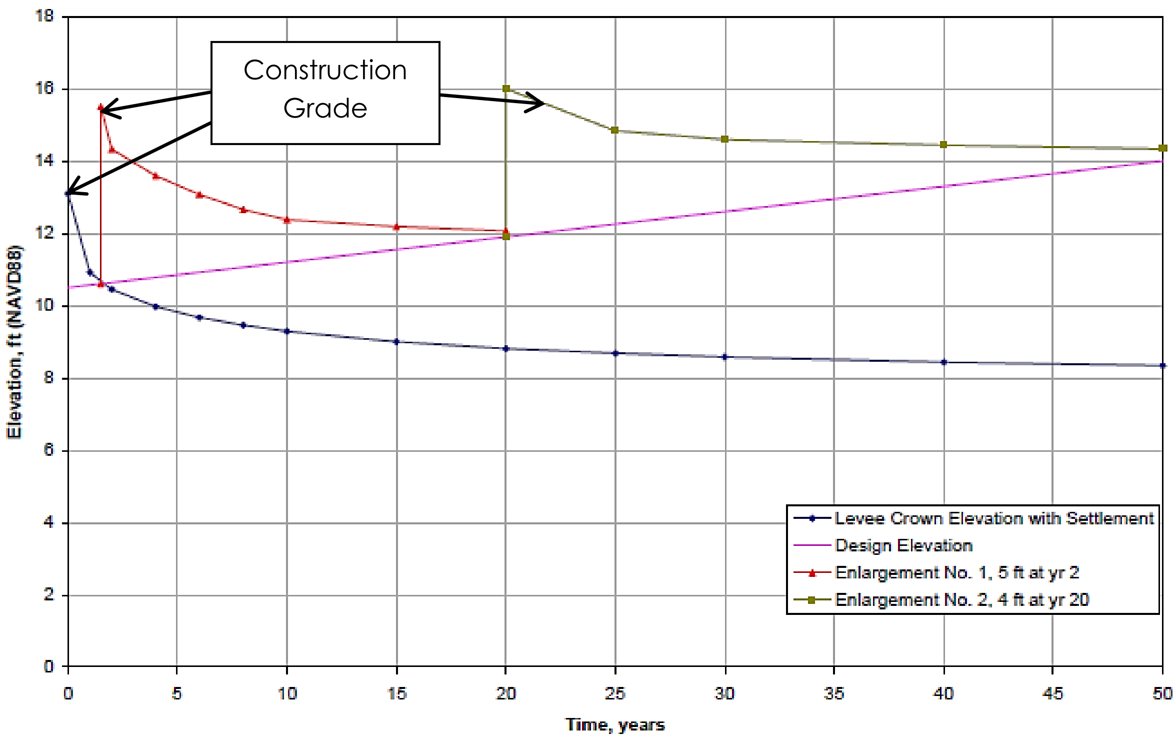

Figure 7: Example of Levee Lift Schedule.

As shown in Figure 7 the levee is a new levee to be constructed and remain above the design grade for 50 years. The current design elevation is 11 feet and the future elevation is 14 feet at year 50. Based on the settlement analyses and the time rate of settlement analyses, this levee is estimated to be constructed at year zero with two future levee lifts or two enlargements. Considering the time rate of settlement, design elevation, and the initial overbuild, the above graph may be developed to demonstrate the construction elevations of the initial levee and the two future enlargements, as well as the time to implement the two future enlargements. Settlement monitoring real-time in the field may be utilized to adjust this schedule based on the observed actual time rate and magnitude of settlement.

The levee lift schedule may also be used in conjunction with shear strength gain evaluations. Each time settlement curve for each lift provides an estimated time to reach completion of primary consolidation of the load applied. Such a developed schedule may be used with shear strength gain estimates or be used to determine when new soil borings may be taken to capture the shear strength gain for use in the next lift design. Incorporation of such a method will reduce the future lift levee footprints.

4.0 Slope Stability Design Criteria

4.1 Slope Stability Modes of Failure

The following slope stability modes should be evaluated for levees, as appropriate.

End-of-Construction Stability Analysis:

Short-term (Undrained or End-of-Construction) stability analysis applies to the stability evaluation during construction or at the end-of-construction (EOC). This analysis is appropriate for new levee construction, levee shifts, levee raises, and/or levee berms or benches. Effective stress analysis with drained shear strength parameters are typically used for free-draining soils, and total stress analysis with undrained shear strength parameters are typically used for low-permeability soils. Soil with a hydraulic conductivity greater than 10^{-3} cm/s (3.3 x 10^{-5} ft/s) is commonly considered free-draining (Duncan and Wright 2005). Triaxial unconsolidated-undrained shear strength testing data (UU or Q test) and/or CPTs are used to estimate the total Mohr-Coulomb failure envelope, which for saturated clays is typically represented by a straight line with $\varphi = 0°$ (internal angle of friction, phi) . However, the Mohr-Coulomb envelope may have a curved portion when the soils are not saturated, as illustrated in EM 1110-2-1906 Figure 14b.

Long-term Stability Analysis:

This case applies to the stability evaluation for steady-state seepage condition. The steady-state seepage condition represents a period when the excess pore pressure generated during construction has dissipated in the levee and foundation. This condition occurs when the flood water remains at full flood stage long enough to fully saturate and form a condition of steady-state seepage. This loading condition represents the “working condition” of the levee.

Rapid Drawdown Stability Analysis:

This case occurs when the flood stage water is high enough and is present long enough to saturate a major part of the floodside embankment and then flood waters recede faster than the soil can drain. This causes the development of excess pore water pressure within the soil that cannot drain fast enough, which in turn causes the floodside embankment slope to become less stable. This procedure requires the input of effective and total strengths for poorly drained soils. Generally, soils with hydraulic conductivities less than 10^{-4} cm/sec may be considered poorly drained. Well drained soils with hydraulic conductivities greater than 10^{-4} cm/sec may use drained strengths. The rapid drawdown case is generally critical for the floodside slope when the water level drops rapidly but also can be observed on the protected side when an interior drainage canal is rapidly pumped down prior to a rainfall event to provide additional storage capacity in the system. Hurricane storm surges or hydrographs are generally not of sufficient duration to reach a long-term steady-state seepage condition within the levee embankments.

Seismic (Earthquake) Stability Analysis:

Historical seismic events in Coastal Louisiana have not produced ground motions sufficient to require this analysis.

4.2 Required FOS

Experience is cited by multiple sources, EM 1110-2-1902 and (Duncan 2000) for example, as being one of the key drivers in selection of slope stability FOS. A FOS of 1.3 for force equilibrium method, USACE-MVN's Method of Planes (MOP) analyses for the hurricane loading condition utilizing undrained strength and total stresses, has provided sections which have historically not failed during hurricane loads. However, Spencer's method with the use of currently available computer software is a more sophisticated tool and a more rigorous method for slope stability analyses. Considering recent construction in Coastal Louisiana it is known that the use of a 1.5 FOS with Spencer's method has generally provided more robust sections than sections which previously performed satisfactorily based on MOP analyses with a FOS of 1.3.

Long-term slope stability typically does not control for Coastal Louisiana levees because of higher drained shear strength compared to undrained shear strength, and possibly because of short-term hydraulic loads (little to no excessive pore pressures). The hurricane load may not be in-place long enough to induce steady-state seepage within the foundation and/or the embankment itself. As such USACE-MVN does not require long-term stability analyses with the hurricane load in place (HSDRRSDG 2012).

Global stability is to be checked by Spencer's Method, a force-moment equilibrium method. Both block and circular searches with optimization should be performed to identify the critical failure surface. Optimization subdivides the traditional slip surface, circular or wedge, into a series of straight line segments. The process then starts at the entry point and randomly varies this point until the lowest FOS is found, then proceeds to adjust the next point along the straight line segments. This process is repeated until all points have been varied along the slip surface, generally resulting in a lower FOS than traditional circular or wedge surfaces. Once the critical failure surface has been identified, two stratums above and two stratums below the critical surface should be checked using the optimized block search method to demonstrate the critical failure surface has been bracketed. Both manual and automatic tension crack searches should be utilized to estimate the tension crack (if required) depth to eliminate tension from the upper slices. Regions used to model the soil strengths and unit weights, which can vary horizontally and vertically within each layer as needed.

Required FOSs for levee embankments, I-Walls, and T-Walls, may be found in Sections 3.0, 6.0, and 8.0, respectively.

4.3 Optimization Methodology

As discussed above, critical slip surfaces should be optimized with commercially available software. The selected number of optimized surface iterations, convergence criterion, and number of points along the critical slip surface should be selected such that the FOS is consistent toward the end of the iterations. If the FOS is still dropping, then the number of iterations or other optimization inputs may need to be adjusted to reach a consistent FOS towards the end of optimized slip surface.

During the optimization procedure, there may be a tendency to form convex surfaces along the critical failure surface. Considerable debate exits relating to the admissibility of convex slip surfaces. When performing optimization, inter-slice forces should be reviewed for unrealistic tension forces. Adjustments to the default optimization settings may be required to prevent tension from occurring in the critical slip surface.

4.4 Tension Crack Methodology

Tension cracks should be used when tension appears in the critical slip surface as determined by evaluation of the free body diagram or force polygons of individual slices. The following are ways tension may appear in the analysis:

- Negative inter-slice forces (i.e. normal side forces on the slice are not compressive, or shear side forces on the slice are negative);
- Negative total or effective normal forces on the bases of the slices;
- Line of thrust (or inter-slice forces resultant) acts outside the slice boundaries; and/or,
- The shear resistance resultant force switches direction (from a resisting to a driving force).

Some commercially available software packages may specifically indicate an error code when a tension crack may be needed. Regardless, the engineer should examine the slice forces in the output file to determine the need for a tension crack. If geotextile reinforcement is present in the levee section, care should also be taken when using a program's automatic search for tension crack feature as this may result in a tension crack which extends through the geotextile in a reinforced levee. As a result of a tension crack passing through the reinforcement, the fabric capacity would be ignored which is not appropriate.

EM 1110-2-1902 gives guidance on tension cracks for stability analysis. Generally, finding the appropriate tension crack depth is an iterative process of performing several analyses with various tension crack depths from relatively shallow to relatively deep. Ultimately the goal is to find the shallowest tension crack at which tensile stresses in the slices are removed from the analysis.

5.0 Seepage Design Criteria

Levee's should be evaluated for uplift and through seepage considering the design flood event or hurricane loading using analysis criteria as outlined in these guidelines and as part of the EMs, ETLs and DIVRs for levees. Levee profiles and foundation materials consisting of clayey materials may not require significant engineering analyses for through seepage or uplift based on experience and engineering judgment.

Levees should be evaluated for seepage considering the following requirements:

- Through seepage should be evaluated for levees where the combination of levee material type (silts and sands) and the duration of the flood event causes the levee to be susceptible to a phreatic surface break out on the protected side levee face.

- Uplift should be evaluated where an underlying clean transmissible sand aquifer material exists which is connected to a floodside source, e.g. borrow pit, canal, bayou, river, lake, or water body.
- Levees which do not meet the above requirements for through seepage or uplift, should at a minimum be evaluated based on Lane's Weighted Creep Flow Theory (1935).

Through seepage, uplift, and Lane's Weighted Creep may be evaluated using the guidelines presented in Sections 5.1 to 5.3.

5.1 Through Seepage / Severity

For through seepage evaluations in silty or sandy levee embankments consideration should be given to the factor of safety against piping through sands using the average and point method based on Schmertmann's paper "The No-Filter Factor of Safety Against Piping Through Sands" (Schmertmann 2000).

In addition, for through seepage, the average gradient across the sand layer and the critical gradient for evaluation of internal erosion should be considered. Similar to section 5.2 below, the through seepage exit gradient should be determined by using Equation (1) in Section 5.2 below. Where Δh is the change in head across the levee embankment and $\Delta \ell$ is the representative distance across the levee.

Further consideration should also be given to the estimated volume of water flow (Qs) through/under the levee template. EM 1110-2-1913 suggests if Qs exceeds 200 gallons per minute (gpm) per 100 lineal feet of levee, additional measures should be considered to limit the infiltration on the floodside of the levee. TM 3-424 also characterizes the severity of seepage beneath the levee by relating the flow (Qs) per 100 lineal feet of levee to the excess head (H) from the floodside to protected side of the levee by the following:

Table 8: Severity of Seepage.

Qs/H (gpm per 100 feet per foot head)	**Severity of Seepage**
Greater than 10	Heavy
5 to 10	Medium
Less than 5	Light

5.2 Effective Uplift (Piping)

Seepage should be evaluated using analysis criteria as outlined in this section. USACE's semi-empirical procedure known as Blanket Theory, as published in EM-1110-2-1913 and updated guidance provided in ETL 1110-2-569, should be utilized to evaluate underseepage of the selected levee section. The exit gradient should be determined by calculation of the effective uplift at the levee toe or beyond, such as at the sumps or ditches.

$$i_{exit} = \frac{\Delta h}{\Delta \ell} \qquad (1)$$

Where Δh is the excess total head within the aquifer or basal sand, and $\Delta \ell$ is the blanket thickness.

The effective uplift or piping factor of safety, FOS_{piping}, is the ratio of the critical gradient divided by the exit gradient, as shown in Equation (2). The critical gradient is defined as the gradient required to induce piping or a quick condition (boils or heaving) of the protected side top stratum and is taken as the ratio of the buoyant saturated unit weight of soil and the unit weight of water, or the critical gradient, i_{crit}, is the numerical difference between the saturated unit weight, γ_{sat}, and the unit weight of water, γ_w, divided by the unit weight of water, as shown by Equation (3). The exit gradient i_{ex} is the change in total head at the critical exit block divided by the length of the flow path across the critical exit block. The seepage FOS_{piping} should be calculated at the critical exit block, which is typically the shortest equal potential head drop for the shortest flow path, as viewed from a typical flow net diagram.

$$FOS_{piping} = \frac{i_{crit}}{i_{ex}} \qquad (2) \qquad\qquad i_{crit} = \frac{\gamma_{sat} - \gamma_w}{\gamma_w} \qquad (3)$$

Seepage at the protected side levee toe should be evaluated for the SWL and PG event and will be required to meet a FOS of 1.6 (SWL) and 1.3 (PG), respectively, against piping Equation (2). In Coastal Louisiana the total saturated unit weight of soil could often be less than 112 pcf so by observation a traditional exit gradient of 0.5 would not meet the minimum required FOS for soils with unit weights less than 112 pcf.

The minimum allowable FOS at the bottom of drainage ditches located at the protected side levee toe to a distance of 150 feet landward will decrease linearly from a FOS of 1.6 to 1.0 (approximately a maximum exit gradient of 0.5 to 0.8). Beyond 150 feet landward the minimum allowable FOS should be a FOS of 1.0 (approximately a maximum exit gradient of 0.8), at the bottom of the ditch. All protected side ditches regardless of distance from the levee shall be analyzed with the water level at the bottom of the ditch, unless the ditch is near a pump station's influence, which shall incorporate the LWL pool elevations, as appropriate.

A factor of safety against uplift of the protected side blanket can also be determined using total stress parameters as follows;

$$FOS_{TSuplift} = \frac{h_{stratum} * \gamma_{sat}}{H_{water} * \gamma_w} \qquad (4)$$

Where $h_{stratum}$ is the blanket thickness, γ_{sat} is the saturated unit weight of the blanket soil, H_{water} is the total head relative to the aquifer material, and γ_w is the unit weight of water. For Total Stress uplift, typically a FOS of 1.2 is utilized.

5.3 Alternate Analysis Method's

Blanket theory is adequate for most general levee underseepage analysis. However, as a model becomes more complicated, computer seepage analysis using commercially available finite element software may be a more appropriate tool. Finite element software can also aid in modeling short term loading by using transient analysis to reflect the rise and fall of water levels during a relatively short flood event such as those generated by a hurricane. As always, appropriate engineering judgment is required when evaluating seepage using computer software especially in defining hydraulic soil properties and the seepage model boundary conditions, as computer seepage models may be used to project or predict seepage pressures which have not been observed.

Levee sections not meeting the analysis criteria as shown in Section 5.0 for through seepage or effective uplift, should be evaluated using finite element software and/or by considering Lane's Weighted Creep (Lane, 1935) as shown in TM-3-424.

$$Cw = \frac{\sum {}^{L_H}\!/_{3} + \sum L_V}{H} \qquad (5)$$

Where L_H and L_V are the horizontal and vertical flow paths and H is the floodside to protected side exit total Head differential. See Table 9 for Creep Ratios (C_W).

Table 9: Lane's Recommended Weighted Creep Ratios (C_W).

Material	**Cw**
Very Fine Sand and Silt	8.5
Fine Sand	7.0
Medium Sand	6.0
Coarse Sand	5.0
Fine Gravel	4.0
Medium Gravel	3.5
Coarse Gravel Including Cobbles	3.0
Boulders with Some Cobbles and Gravel	2.5
Soft Clay	3.0
Medium Clay	2.0
Hard Clay	1.8
Very Hard Clay or Hardpan	1.6

The weighted creep shall be evaluated for seepage along the embankment – foundation interface for the Project Grade water level case.

5.4 Seepage Reduction Measures

Levee sections which do not meet the seepage requirements of Sections 5.1 and 5.2 shall include seepage reduction measures. Reduction measures may include seepage berms, relief wells, cut-offs, or drains. The most common reduction measure in Coastal Louisiana has been protected side seepage berms when the right of way is available.

When seepage berms are required, it is recommended the following FOSs be required for berm design:

Table 10: Recommended FOS Against Uplift at the Seepage Berm Toe (HSDRRSDG 2012)*.

Seepage Berm Width to Levee Height	FOS	
	SWL	PG
4	1.5	1.2
8	1.3	1.1
12	1.1	1.0
>16	1.0	1.0

*Note: Typical values Taken from HSDRRSDG (2012) Table 3.5.

Additional guidance for seepage analyses and seepage reduction measures may be found in USACE TM 3-425, EM-1110-2-1913, ETL 1110-2-569 and USACE Mississippi Valley Division (MVD) DIVR 1110-1-400.

6.0 I-Wall (Z-Sheet or Combi-Wall) Design Criteria

Design of the I-Wall /levee section less than 4 feet in height should follow the criteria as outlined in the HSDRRS design guidelines, which is summarized below. This section is applicable to classic cantilevered Z-type sheet pile or Combi-type sheet pile. I-Walls should not use cold formed steel. For I-Walls greater than 4 feet in height the design should follow the guidelines established in EC 1110-2-6066 Design of I-Walls (2011). I-Walls should not be used along navigable water ways.

If I-Walls are to be used for significant lengths and not primarily for transition zones (T-Wall to Levee) where other types of flood barriers are not practical, a lateral load test should be performed.

6.1 I-Wall Sheet Piling Gap Estimates

As a result of lessons learned from Hurricane Katrina, the formation of a floodside gap along the soil sheet pile interface has been documented, modeled, and researched. As the wall is loaded permanent deflection causes a gap to form between the floodside soils and the sheet pile. This gap should be accounted for in design when analyzing global stability and seepage of I-Walls. I-

Walls should be designed to be stable with a floodside gap present between the sheeting and the soil.

The depth of the gap should be determined by analyzing the Top of the Wall (TOW) case with a FOS of 1.0 for Q-case shear strengths utilizing the fixed and sweep search methods in CWALSHT. The lower of the two embedments calculated should be considered for the gap depth. In addition, the following conditions should be checked and the lowest or deepest gap depth should be considered from:

- CWASLHT gap depth (Fixed/Sweep - FOS=1.0);
- if the gap depth is within 5 feet of sand, silt, or peat layer, use depth to layer; and,
- the equivalent point of the hydrostatic water pressure to the at rest earth pressure or $\gamma_w * h_W = \gamma_S * h_s * K_o$.

6.2 I-Wall Sheet Piling Tip Penetration

Sheet pile tip elevation should be evaluated using the USACE Sheet pile Wall Design/Analysis computer program CWALSHT. CWALSHT provides the sheet pile tip elevation for the cantilevered wall analysis which satisfies static equilibrium.

The cantilever case should be analyzed with a FOS of 1.5 on both active and passive soil parameters, using "Q" shear strength parameters. The analysis should be performed for a water level to SWL plus the wave load. The design tip elevation should be evaluated using both the fixed surface wedge method and the sweep search method. In addition, a design check with water to the Top of the Wall (TOW) using "Q" strengths and minimum required FOS of 1.3. The lower or deepest tip should be selected based on the SWL plus wave load case.

An additional load case consisting of "S" shear strengths with water at LWL with a minimum required FOS of 1.5 should also be checked. This case may not be necessary where the LWL does not provide a differential head from the floodside to the protected side.

At a minimum the I-Wall sheeting should be embedded a minimum of:

- Three times the wall height;
- 10 feet below the lowest adjacent grade; and/or,
- Through any shallow peat, silt, sand layers tipped into clayey substratum.

Considering lessons learned from Hurricane Katrina, even when calculations do not dictate sheeting tips below or through any shallow peats, silts, and sands, it is generally considered good engineering practice to extend the sheeting tips below these shallow layers into a less permeable clay substratum.

6.3 I-Wall Global Stability Analysis

Slope stability analysis of the I-Wall/embankment section should be analyzed with Spencer's method to the SWL with a minimum required FOS of 1.5. Slope stability should also be checked to the TOW with a minimum required FOS of 1.4. A minimum required FOS of 1.5 should be utilized if steady-state seepage conditions may develop during a hurricane loading. Global stability should be checked for tension crack and no tension crack cases. For the Tension crack case, the full hydrostatic load should be assumed on the floodside, this may be accomplished by removing the floodside soils from the model to the determined gap depth.

6.4 Piping and Seepage Analysis

The steel sheet piling in the I-Wall is designed for structural support and to control seepage. Seepage analyses may be performed by the Method of Fragments, Lane's Weighted Creep, Blanket Theory, or finite element modeling.

Effective stress (piping, Eqn. 2) heave analyses should be evaluated to the TOW condition, see Sections 5.0 to 5.3 for methodology. The depth of the tension crack should be accounted for within the analyses.

In addition to piping analyses, the section should also be checked for heave or total stress uplift, see Eqn. 4. The design section should meet a minimum FOS of 1.2 to the TOW case.

7.0 Piles

The use of spiral welded pipe piles will generally be permitted in Coastal Louisiana soil conditions provided they meet requirements set forth in ETL 1110-2-577. The proposed spiral welded pipe pile section intended for production driving shall also be used for installation of test piles.

7.1 Axial Pile Capacity

Analysis criteria is outlined in HSDRRSDG 2012 Section 3.3 and EM 1110-2-2906, Design of Pile Foundations. Alternately, analysis methods may follow Louisiana Highway Department of Transportation and Development (LADOTD) or the Federal Highway Administration (FHWA) for determining axial pile capacity.

Tables 11 to 16 below present typical recommended values for use in pile design.

Table 11: Recommended Adhesion (α) vs. Undrained Shear Strength (HSDRRSDG 2012)*.

Adhesion (α), psf	Undrained Shear Strength (S_U), psf
500	>1,500
500	1,500
1,000	500
1,000	<500

*Note: Typical values Taken from HSDRRSDG (2012) Figure 3.6, use linear interpretation between S_U=500 to 1,500 psf.

Table 12: Recommended Minimum FOS Axial Pile Capacity (HSDRRSDG 2012)*.

Method of Determining Capacity	Loading Condition	Minimum FOS	
		Compression	Tension
Theoretical prediction verified by static pile load test	Q-Case	2.0	2.0
	S-Case	1.5	1.5
Theoretical prediction verified by pile driving analyzer	Q-Case	2.5	3.0
	S-Case	1.5	1.5
Theoretical prediction NOT verified by load test	Q-Case	3.0	3.0
	S-Case	1.5	1.5

*Note: Typical values Taken from HSDRRSDG (2012) Table 3.7.

Table 13: Typical Q-case Soil Dependent Pile Design Coefficient Values (HSDRRSDG 2012)*.

Q-Case			
Soil Type	Friction Angle, ϕ' (deg.)	Nc	Nq
Clay	0	9.0	1.0
Silt	15	12.9	4.5
Silty Sand	30	0	22.5
Poorly graded Sand	33	0	30.0

*Note: Typical values Taken from HSDRRSDG (2012) Table 3.8

Table 14: Typical S-case Soil Dependent Pile Design Coefficient Values (HSDRRSDG 2012)*.

S-Case			
Soil Type	**Friction Angle, ϕ' (deg.)**	**Nc**	**Nq**
Clay	23	0	10.0
Silt	28	0	19.5
Silty Sand	30	0	22.5
Poorly graded Sand	33	0	30.0

*Note: Typical values Taken from HSDRRSDG (2012) Table 3.9

Table 15: Typical Lateral Earth Pressure Coefficient Values for Pile Design (HSDRRSDG 2012)*.

Soil Type	Displacement Piles		Non Displacement Piles	
	Compression (Kc)	**Tension (Kt)**	**Compression (Kc)**	**Tension (Kt)**
Sand	1.25	0.70	1.25	0.50
Silt	1.0	0.50	1.0	0.35
Clay	1.0	0.70	1.0	0.70

*Note: Typical values Taken from HSDRRSDG (2012) Table 3.10

Table 16: Typical Angle of Friction Values Between Soil and Pile (HSDRRSDG 2012)*.

Pile Material	δ
Steel	0.67Φ to 0.83Φ
Concrete	0.90Φ to1.0Φ
Timber	0.80Φ to 1.0Φ

*Note: Typical values Taken from HSDRRSDG (2012) Table 3.11

The overburden pressure is limited to 3,500 pounds per square foot (psf) and no end bearing is calculated for piles tipping in soils with short-term shear strengths below 1,000 psf. The additional embedment length due to pile batter should be neglected for skin friction calculations.

7.2 Pile Settlement

Individual and pile group settlement should be evaluated for load transfer settlement relationship. Individual pile foundations are typically limited to less than ½ to 1-inch of deflection to initial movement to develop the required resistance. Individual pile and group or pile cap deflections should be limited the criteria established in EM 1110-2-2906 and HSDRSSDG T-Wall procedures; see Section 8.0 of this manual.

Pile load transfer movement for single and group piles may follow the methods identified in Section 4-4 as shown in EM 1110-2-2906.

7.3 Lateral Pile Capacity

Analysis criteria are outlined in HSDRRSDG 2012 Section 3.3.1 and EM 1110-2-2906, Design of Pile Foundations. Typically, for lateral analyses, p-y curves are developed for each stratum or derived from recognized empirical methodologies, utilizing such parameters such as the modulus of soil reaction. Typical p-y curve methods such as Matlock (1970) for soft clays would be considered appropriate for preliminary design.

Lateral deflection of the substructure and drift of the superstructure are primarily due to hydrostatic loads, waves, wind, seismic, and operation of equipment or the structure. Deflection criteria for I-Walls and T-Walls should follow HSDRRS design guidelines. However, for special pile foundations, such as anchored or braced sheet pile walls or braced pile frames without a pile cap, detailed soil structure interaction (SSI) modeling is recommended for final design to evaluate the estimated deflection, p-y curves, and the elastic/plastic state of stress within the soil.

For anchored/braced sheet pile walls or braced pile frames, based on the guidelines researched and current practice, deflection should be limited to keeping the mobilized soil stresses within the soil's elastic range while also considering the loads, load combinations, allowable drift and deflections without negative impact to the structure function and operational requirements. Where upper profile soils are susceptible to disturbance or are very soft to soft it may be impractical or unreasonable to keep the mobilized soil stresses within the elastic zone when loaded, or repeatedly loaded, by the structure foundation. Therefore, it may be necessary to ignore those upper soils for SSI analyses. Pile types, sections, and depths should be explored such that deflections are within the project's acceptable tolerance. Operational requirements during load cases may dictate more ridged restrictions and deformations and requires communication between all designers (e.g., a maintenance crane may not need to operate; however, gates need to remain sealed). Allowable horizontal movement should be established for the entire structure/foundation based on the tolerable lateral movement with consideration for the structure height and stiffness. Further site specific deflection limits or maximum deflection, should be based on engineering judgment and the design purpose of the structure. Where flexible braced cantilevered walls and relatively non-flexible braced pile abutments intersect or are connected, detailed analyses should be performed to account for strain compatibility or viability of connections.

User defined p-y curves may be developed from site specific lateral load tests and are recommended for anchored or braced sheet pile walls or braced pile frame structures.

7.4 Downdrag and Bending Moments in Battered Piles

Interim guidance for determination of drag loads and downdrag was provided by the St. Louis, MO USACE district in April 2009, and should be followed as outlined in Section 3.3.2.1 of the HSDRRSDG. The approach to drag load and downdrag follows the Fellenius method for determining the neutral plane. Details and the step-by-step approach for determining downdrag and drag load are presented in HSDRRSDG Section 3.3.2.1.

In accordance with the guidance, the drag load on the piles is calculated as the total load associated with negative skin friction acting on the pile above the neutral plane. The elevation of the neutral plane is determined by plotting pile load and resistance vs. elevation over the full design length of the pile. The load curve is calculated as the dead load at the pile. The resistance curve is calculated as the end bearing resistance at the pile toe plus the resistance due to positive skin friction. The neutral plane is located at the elevation where the pile load and resistance are equal. Negative skin friction is assumed to act above the neutral plane as drag load, while positive skin friction contributes to pile capacity below the neutral plane.

The maximum load in the pile (dead load plus drag load) must be less than the computed allowable structural strength of the pile in compression.

In accordance with the guidance, long-term settlement of the pile cap consists of the following components:

- Elastic compression of the pile above the neutral plane due to the average permanent load;
- the free-field settlement at the neutral plane due to the external increase in effective stress causing ground settlement; and
- the settlement below the neutral plane from the transfer of the structure dead load.

The free field settlement at the neutral plane is based on the estimated levee consolidation settlement. The settlement below the neutral plane is analyzed using an "equivalent footing". An imaginary footing equal in width to the distance between the batter piles, with the structural dead load uniformly distributed, is modeled at the neutral plane. Stress increase below the equivalent footing is calculated assuming a 2V:1H distribution.

Final guidance for determination of bending moments in battered piles subjected to drag loads provided by Virginia Tech in September 2012, the "LPILE Method for Evaluating Bending Moments in Battered Piles Due to Ground Settlement for Pile-Supported Floodwalls in New Orleans and Vicinity" should be followed to determine if settlement induced bending moments in battered piles exceed acceptable limits. Details and the step-by-step approach are also presented in Appendix 1.

7.5 Pile Drivability

Pile drivability should be examined by an experienced engineer to ensure the pile may reach the desired tip elevation, develop the required resistance, and be successfully installed without damage. Drivability issues may exist related to very soft cohesive layers which may present tension issues in driven piles or dense sands which could lead to compression issues or pile not being able to reach a required tip elevation and/or not being able to develop the required resistance.

Drivability analyses are critical for precast prestressed concrete (PPC) piles which are subject to tension stresses during pile driving. Wave Equation analyses should be performed to assess hammer selection, estimated pile driving stresses, penetration rates to the desired tip elevation, and estimated dynamic and static pile capacities. Drivability analyses may also be used to assess jetting, spudding, or preboring for pile installation.

7.6 Pile Group Capacity

Analysis criteria are outlined in HSDRRSDG 2012 Section 3.3.6 and EM 1110-2-2906, Design of Pile Foundations.

Consideration should be given to evaluating group effect of piles driven in clusters of 4 or more piles. Typical pile spacing should be driven with a minimum center to center spacing of no less than 3 pile diameters. Experience has shown a group effect of large pile clusters is best accounted for through the use Perimeter Shear equations. These equations assume the material enclosed within the pile cluster tends to act as a large block. Thus the ultimate capacity of the group is compared to the ultimate capacity of the summation of the individual piles. Individual pile capacity is limited to the lower of the two group values divided by the number of the piles in the group.

7.7 Pile Load Tests

Analysis criteria are outlined in HSDRRSDG 2012 Section 3.3.1.1, 3.3.1.2, 3.3.4, and 3.3.5 and EM 1110-2-2906, Design of Pile Foundations.

Consideration should be given to implementing a pile load test program to minimize pile foundation costs or to increase the engineer's confidence for the pile tip elevation selection. Implementation of a pile load test program is typically used to reduce the design FOS for the type of load test performed, dynamic with a pile driving analyzer (PDA), static compression, or static tension. Design FOSs with pile load tests are presented in Table 12.

Dynamic pile load tests consist of using a PDA during the driving of a test or production pile. The PDA uses accelerometers and strain gauges to estimate the driving resistance or capacity of the pile. The PDA may also be used to assess the pile drivability, selected hammer equipment, and for evaluation of compression and tensile stresses within the pile. Considering the end of drive pile capacities pile restrikes are typically necessary at 24-hours, and 14- to 21-days to assess pile setup. The dynamic pile capacity should be estimated by an experienced pile driving engineer with a CAPWAP® analyses. PDA testing should follow ASTM D 4945-12 Standard Test Method for High-Strain Dynamic Testing for Deep Foundations.

Axial compression pile load tests should follow ASTM D 1143 / D 1143M-07 (Reapproved 2013) Standard Test Method for Deep Foundations Under Static Axial Compressive Load. Axial tension pile load tests should follow ASTM D 3689/D 3689M-07 (Reapproved 2013) Standard Test Method for Deep Foundations Under Static Axial Tensile Load. While lateral pile load tests should follow ASTM D 3966/ D 3966M-07 (Reapproved 2013) Standard Test Methods for Deep Foundations Under Lateral Load.

Interpretation of axial pile load tests should follow the criteria established in HSDRRSDG Section 3.3.5.

If pile corrosion protection/painting of piles is required for production piles, then all test piles shall be painted or treated with the same corrosion protection prior to driving.

8.0 T-Wall Design Criteria

Design of T-Wall sections should follow the criteria as outlined in the HSDRRS design guidelines, which is summarized below.

- Lateral slope stability to determine any unbalanced forces;
- Calculation of the elastic moduli at the base of the structures for use in the CE Pile Group Analysis (CPGA) program;
- Calculation of the repositioned unbalanced force, if required, to be input at the base of the structure, Fcap, for use in the CPGA program;
- Drag load and downdrag calculations;
- Determination of the pile capacities for the structures; and
- Seepage analysis to determine the sheet pile embedment elevation.

8.1 T-Wall Slope Stability

The stability of the proposed structures should be determined using software which is capable of performing Spencer's Method with a robust search procedure. The slope stability analysis should be performed with only water loads acting on the ground surface floodside of the heel of the T-wall. Any water, soil, or surcharge loads acting directly on the structures are not included because these loads are presumed to be carried by the piles to deeper soil layers. A second piezometric surface should be utilized for sand layers to model the anticipated more gradual drop of the piezometric surface within the sand layers. Global slope stability for the protected side should be analyzed for 2 cases, water at Still Water Level (SWL), and water at the top of the wall as noted in the following table. Floodside stability is also checked using the LWL cases.

Table 17: Recommended Design T-Wall Slope Stability Factors of Safety.

Case	Shear Strength Condition	Pore Water Pressure Condition / Water Level	Required Minimum Factor of Safety[1]
Hurricane at Design Grade (SWL)	Undrained – Protected Side[3]	SWL	1.5
Hurricane at Top of Wall	Undrained – Protected Side	PG	1.4 (1.5)[6]
Hurricane at Water Low Grade (LWL)[7]	Undrained – Floodside	LWL	1.4
NWL Non Hurricane Water (S-Case)[8]	Drained – Floodside and Protected Side	NWL	1.4

Notes: [1] Spencer's Method non-circular search used for analysis.

[6, 7, 8] For Footnotes 6, to 8 see HSDRRS Design Guidelines, 14 JUN 12, Table 3.1.

Non-circular or block searches are used to analyze only the short-term shear strength soils beneath the footing. Block searches generate wedge-shaped failure surfaces that satisfy force and moment equilibrium by an iterative process where the factor of safety is determined.

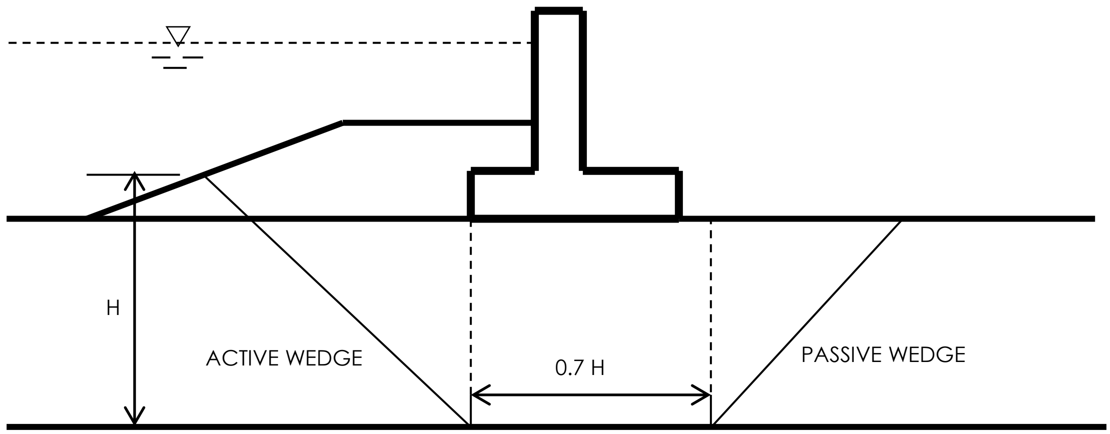

Figure 8: Typical Failure Plane beneath a T-Wall (HSDRRSDG 2012 Figure 3.7).

As noted above, only non-circular failure planes are investigated horizontally along the critical failure surface. This horizontal distance (H) is referred to as the neutral block. The neutral block should have a minimum dimension of the greater of 0.7 H, or the base length of the T-Wall or structure. H is defined as the vertical distance from the failure surface to the intersection of the failure plane with the ground surface (see Figure 8 above). For closure gates, the minimum width of the neutral block will be 0.7 H, or the width of the footing, as it is assumed the failure surfaces will not penetrate through the structure.

All of the soil layers should be checked using a large global search. The soil layers should be a maximum of 15 feet in depth. After the most critical layer(s) are determined, the failure surfaces should be optimized by defining a block around the entry and exit points of that layer. All the reported failure surfaces should be optimized. The critical layer and the failure surfaces to two soil layers above and below the critical surface should also be reported.

Spencer's Method considers shear and normal interslice forces, satisfies moment and force equilibrium, and assumes a constant interslice force function. Each layer is investigated to determine the position resulting in the lowest factor of safety.

Local stability analysis of the berm should also be conducted. In the case where the factor of safety is determined to be lower than the design criteria, unbalanced forces are calculated for the T-Wall and gate structures. The maximum unbalanced force should be determined by increasing a horizontal line load at a fixed elevation until the minimum safety factor is attained. The location of the line load has an X-coordinate at the heel of the wall or gate. The Y-coordinate is located at an elevation that is halfway between the ground surface at the heel of the wall or gate and the lowest elevation of the critical failure surface.

The largest unbalanced load does not necessarily coincide with the failure surface with the lowest factor of safety; therefore, multiple failure surfaces at various elevations may need to be analyzed to determine the corresponding unbalanced forces. The unbalanced load should be determined for the slip surface with lowest factor of safety and the slip surface with the highest unbalanced load.

8.2 Subgrade Moduli

The modulus of horizontal subgrade reaction (Es) value is used within the CPGA program to model the soil-pile interface and is used for calculating the resultant force (Fcap) based on the unbalanced forces determined from Spencer's Method. The USACE provided direction for determining Es in the New Orleans District is based on the following equations:

*Es (pci) = 0.444 * Cohesion (psf) (*Clays) (6)

*Es (pci) = 1.5 *γ' (pcf) * z (ft)* (Sands) (7)

Where:

γ' is the effective unit weight above the sand layer
z is the depth of the sand layer

The Es equations shown above do not account for reduced group capacity from pile spacing, and may need to be further reduced by the structural engineer after the initial pile layout is determined. Typically, only the upper ten pile diameters/widths provide significant reaction when piles are horizontally loaded. Therefore, a weighted Es average of the soils to this depth should be calculated.

If unbalanced forces are determined in the Spencer's Method slope stability analyses, the Es value directly beneath the structure's footing is reduced. The Es is reduced with reduced global stability factors of safety to account for lack of support from the less stable soil mass located above the critical failure plane. For cases where the global factor of safety without piles is less than 1.0, Es is input in the CPGA program at an extremely low value, such as 0.00001 kips per square inch. For conditions where the factor of safety is between 1.0 and the target factor of safety, Es is computed by multiplying the percentage of the computed factor of safety between 1.0 and the target factor of safety by the actual estimated value of Es. For example, if the FS = 1.2, the target factor of safety is 1.5, and the estimated value of Es below the foundation is 100 pounds per square inch (psi), Es is input at 40 percent of the actual estimated value, 40 psi. This accounts for the fact that, with higher factors of safety, the unbalanced force is a small percentage of the total force, and the soil is able to resist some amount of the lateral forces from the wall.

8.3 Fcap

When unbalanced forces are determined in the Spencer's Method slope stability analyses, the unbalanced force is converted to an "equivalent" force applied to the bottom of the T-Wall or gate structure. It is calculated by a ratio derived by computing equivalent moments at the location of the maximum moment in the pile below the critical failure surface. The equivalent force (excluding the unbalanced force above the base of the T-Wall), Fcap, is calculated as follows:

$$F_{cap} = F_{ub}\left[\frac{\left(\frac{L_p}{2}+R\right)}{\left(L_p+R\right)}\right]\frac{L_p}{L_u} \qquad (8)$$

Where:

F_{ub} *=unbalanced force calculated in Spencer's Method*
L_u *=distance from ground to lowest critical failure surface*
L_p *=distance from bottom of footing to lowest critical failure surface*

$$R = (EI/E_s)^{1/4} \qquad (9)$$

Where:
E = Elastic Modulus of the pile
I = Moment of Inertia of the pile
E_s *= Modulus of subgrade reaction below critical failure surface*

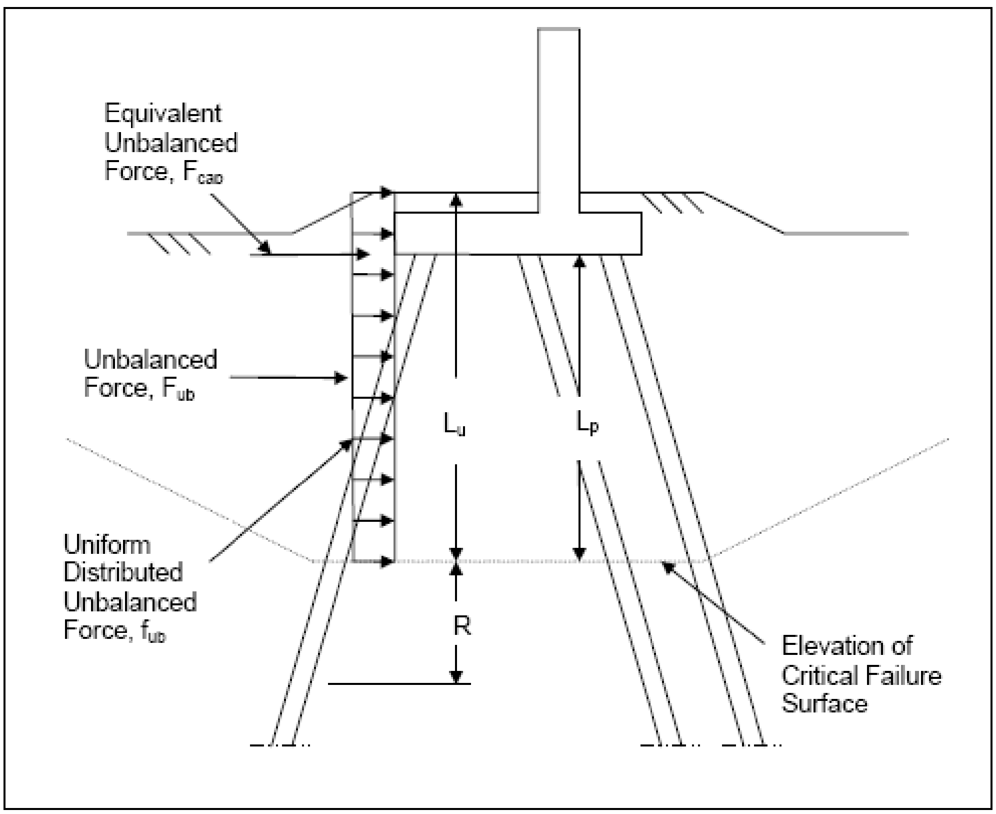

Figure 9: Unbalanced forces (HSDRRSDG 2012 Figure 3.10).

8.4 Pile Capacities

Ultimate compression and uplift pile capacity values should be generated to determine lengths required to support the structures per section 7.1 of these guidelines. The foundations for T-Walls will derive lateral capacity from battered piles. If unbalanced loads exist, pile capacity above the critical failure surface should be neglected.

8.5 Seepage

All seepage analyses should consider steady-state conditions and factors of safety against erosion and piping defined in Section 5.0 in the LFPDG.

Seepage should be analyzed using blanket theory and assuming no cutoff. If the minimum factors of safety are met for all conditions, the sheet pile cutoff beneath the T-Wall should be determined using Lane's Weighted Creep Ratio values and a head differential based on the SWL.

- For T-Walls to be built on levees, several seepage paths should be checked. The seepage paths begin at the top of the cutoff (bottom of wall footing) assuming a gap can develop around/below the T-Wall footing. Several paths should be analyzed considering different exit locations on the protected side.
- For T-Walls and gates to be built directly on existing ground without a levee, the seepage path should be twice the cutoff length in the vertical direction.
- The minimum cutoff extended through any levee material, and at least 5 feet into the surrounding grade. The minimum cutoff also needs to meet all other applicable HSDRRSDG.

8.6 Settlement

Settlement calculations should address immediate settlement of foundation soils, primary consolidation settlement of foundation soils, shrinkage and primary consolidation settlement of the levee embankment, and regional subsidence. The foundation support piles should be designed to limit the vertical and differential settlement of the structure to acceptable limits as determined by the structural engineer. Settlement calculations should also account for adverse effects drag forces have on sheet pile cutoff and support piles.

9.0 Anchored or Braced Sheet Pile Walls

Anchored/braced sheet pile walls may be considered for floodwalls in lieu of traditional T-Walls. This type of wall should be expected to deflect more than a traditional T-Wall. Design should include the following steps based on EM 1110-2-2504:

1. Determine design loads (usual, unusual, and extreme).
2. Determine hydrostatic and lateral earth pressures (Coulomb earth theory)

3. Check external stability or "rigid" rotation about the anchor position, fixed-earth method, finding the factored depth of minimum penetration, factored maximum moment, and unfactored anchor force.
4. Anchor/Brace Design (axial pile design and flow through (arching)).
5. Check Deep Seated Global Stability (around sheet pile).
6. Check Seepage.
7. Structural Design Sheet Pile, Anchor Components (whalers/braces, tie rods, bolt/welds).
8. Corrosion Analyses.
9. Soil-Structure Interaction (SSI) analyses to refine classic design shown in steps 2 through 3.

In addition to EM 1110-2-2504, USACE 2011 Interim Measures Design Manual, Sections 1.2.3 through 1.2.6 should be determined. This includes performing the external stability with unbalanced loads to determine the minimum sheet pile tip elevation, maximum bending moment, anchor force, and determining the appropriate zone to neglect pile capacity for the anchor design. Only the Fixed-earth method is required for determining the factored minimum sheet pile tip elevation, corresponding maximum bending moment, and unfactored anchor load. Considering the required section modulus, larger steel sheet piles or even combi-wall steel sheet piles may be utilized to stiffen the system, potentially reducing deflection of the sheeting.

See Section 7.0 of these guidelines for Piles.

10.0 Braced Pile Foundations

Braced pile frame abutments and receiving structures may be considered for closure structures. These types of structures should generally follow a combination of the HDSDRRS T-Wall design procedure and recommendations in EM 1110-2-2705, Structural Design of Closure Structures for Local Flood Protection Projects. Section 4-3 of EM 1110-2-2705 refers to Chapters 4 and 5 in EM 1110-2-2502, Retaining and Flood Walls, for overturning and sliding requirements. EM 1110-2-2705 refers to EM 1110-2-2906, Design of Pile Foundations, for the design of pile foundations.

1. Perform global stability using Spencer's Method.
2. Determine unbalanced loads.
3. Determine allowable axial capacity and allowable shear loads. Neglect axial capacity above the critical plane determined from the global stability analysis.
4. Check lateral pile capacity and Soil-Structure Interaction (SSI) analyses.
5. Check seepage. Neglect axial component of sheet pile for foundation analysis.
6. Corrosion analyses.
7. Where braced foundations are used in conjunction with braced cantilever floodwalls, the strain compatibility between the components should be evaluated. Engineering judgment should be used to determine the allowable deflections at each component.

See Section 7.0 of these guidelines for Piles.

11.0 Levee Transitions

Transitioning from floodwalls to an earthen levee section should follow HSDRRS design guidelines section 5.6.9, which includes the requirement of a minimum of 30 lineal feet of un-capped sheet piling extending into a full levee section for erosion and seepage control. It is recommended the sheet pile tip elevation remain at the same elevation as the adjacent walls unless it is indicated by seepage analysis that a lesser tip elevation is adequate.

In addition to evaluation of seepage exit gradient at the sheet pile transition section, velocity, flow, and internal gradients within a connected aquifer should be evaluated around the sheet pile end. If increases in velocity and internal exit gradients are observed locally around the end of the transition wall, the sheet pile should be extended further horizontally in the levee section until acceptable velocities and gradients are observed, see Section 12.0 Erosion.

12.0 Erosion

Design of scour protection for levee tie-ins, transitions, and floodwalls should follow the criteria as outlined in the HSDRRS design guidelines Section 5.6.9. At a minimum, scour protection for I-walls on the protected side should extend 8 feet out from the wall and a minimum of 5 feet down embankment slopes.

Well-established and maintained turf increases the levees resistance to erosion, and is important to the resiliency of the levee during a flood event. Well established turf consisting of unreinforced Bermuda grass, founded on clay embankment material specified in Section 14.0 in these guidelines, has been shown in tests to resist average wave overtopping discharges up to 1.0 ft^3/s per foot (cfs/foot) in studies performed by Colorado State University, provided the grass has been well established and maintained for more than 2 years.

If average wave overtopping discharges greater than 1.0 cfs/foot are anticipated, Bermuda grass reinforced with a high performance turf reinforcement mat (HPTRM) may be necessary.

13.0 Utilities/Penetrations

Design of utilities/penetrations should follow the criteria as outlined in the HSDRRS design guidelines Section 3.6.

14.0 Embankment Recommendations

14.1 Borrow Material

Borrow material used for levee embankment construction should consist of homogenously processed naturally occurring or blended earthen materials classified as CL or CH in accordance with ASTM D 2487. Material should also meet the following requirements:

- Plasticity Index greater than 10,
- contain less than 35 percent sand by weight,
- an Organic Content of less than 9 percent by dry weight, ASTM D 2974, Method C
- salinity properties amenable to growing turf, and
- be free of deleterious materials which may include organic matter (leaves or plant matter), sticks, branches, trees, logs, stumps, roots, trash, and/or construction debris.

Embankment borrow may contain deleterious materials, which should be removed at the borrow pit prior to transporting to the levee site. Material may be removed by hand, mechanical means, or wasting the borrow that contains the deleterious materials.

14.2 Working Platforms in the Wet

Working platforms should be considered where levee alignments require placement through wet areas, bayous, ponds, or water bodies which are not practicably dewatered. Such working platforms or bridge lifts are typically uncompacted, and may be used to help develop a platform to a sufficient elevation above the water surface to work from. Consideration should be given to the uncompacted fill type, and generally a granular material would be expected to reduce water-related fill placement issues at the time of construction. Regardless of material type, consideration may need to be given to positive cutoff, material encapsulation, and the use of high strength geotextiles. Designs should address slope stability, settlement, and seepage related to the working platform or the bridge lift.

14.3 Field Placement and Compaction

During levee lift placement any remaining deleterious materials should be removed by similar methods as discussed in Section 14.1. Up to 1 percent by volume of deleterious materials per in-place cubic yard may be permitted in the embankment material as directed by the Engineer, if the deleterious materials are relatively uniform in size, evenly distributed, less than 12 inches in length, less 4 square inches in cross-sectional area, or less than 48 cubic inches in volume. All deleterious materials longer than 12 inches in length, greater than 4 square inches in cross-sectional area, or greater than 48 cubic inches in volume shall be removed.

The following items should be considered for contract documents:

- Levee embankment shall not be placed in water.
- Uncompacted lift thickness shall not exceed 6 inches for the first lift, unless placed on top of a geotextile.

- Uncompacted lift thickness shall be a minimum of 15 inches plus or minus 3 inches for the first lift placed on top of a geotextile.
- Uncompacted lift thickness for intermediate lifts should not exceed 12 inches.
- Uncompacted lift thickness shall not exceed 6 inches for the last two levee lifts.

Uncompacted lift thickness may need to be reduced depending on the approved levee embankment material and the approved compaction equipment. Embankment material shall be compacted to at least 90 percent of maximum dry density at a moisture content within the limits of plus 5 to minus 3 percentage points of optimum moisture content as determined by ASTM D 698. Different compaction percentages may be required to meet the levee embankment design wet unit weight. Likewise, erodibility of the levee embankment material relative to the degree of compaction must also be considered.

14.4 Quality Control

14.4.1 Preconstruction Material Testing

Prior to levee embankment placement and compaction embankment borrow shall be tested for conformance to these requirements. A minimum of 2 test suites shall be performed and submitted to the Owner for approval for each material type and source. The following tests shall be performed:

- Water Content ASTM D 2216;
- Atterberg Limits ASTM D 4318;
- Sand Content ASTM D 1140;
- Organics ASTM D 2974, Method C;
- Soil Classification (USCS Classification) ASTM D 2487; and,
- Standard Proctor ASTM D 698 if material meets the requirements of Section 14.1.

If the material is determined to be acceptable, these initial 2 proctor curves will serve as the upper and low bound of the family of curves.

14.4.2 Construction Material Testing

During levee construction the suite of tests as defined in Section 14.3.1 shall be performed at a minimum every 10,000 truck cubic yards, and at every source change and material change as determined by the Engineer following soil classification based on ASTM D 2488, or 1-point proctor testing.

14.4.3 Density Control Testing and Inspection

In-place density testing (ASTM D 2922), moisture content (ASTM D 4643), Atterberg Limit (ASTM D 4318), and field classification (ASTM D 2488) shall be performed every 500 lineal feet of levee per lift, not to exceed one test per 1,500 compacted cubic yards of levee per lift, or a minimum of one per shift of levee compaction work. The test location shall be representative of the area being tested. The percentage of the maximum dry density, the water content as related to the optimum water content using the representative proctor curve shall be determined by experience and judgment from visual soil classifications (ASTM D 2488) and/or 1-point proctors.

The in-place dry density shall be determined by calculation from the nuclear density gauge measurement of wet density and the in-place field moisture content.

In-place density tests (nuclear method) shall be checked with the Sand Cone Method ASTM D 1556, at a rate of 1 Sand Cone for every 10 Nuclear Tests. If the Nuclear Wet Density varies by more than 3 percent, then a wet density correction factor should be applied. The correction factor should be based off of a minimum of 5 comparison tests.

At a minimum a 1-point proctor shall be performed at every 5th in-place density test at the same location of the sand cone confirmation test. Material shall be moisture adjusted, if required, to be within 3 percentage points or 80 percent of optimum on the dry side of the proctor curve as determined from the family of curves. The 1-point dry density shall be plotted on the family of curves, and a similarly shaped projected proctor curve should then be sketched to match the slope and shape of the family of curves determined by ASTM D 698. If the 1-point proctor moisture content is not within 3 percentage points or 80 percent of the optimum moisture to the dry side of the curves or is outside the family of curves, a new suite of tests in per Section 14.3.1 shall be performed. The new proctor curve may then be added to the family of curves.

Bulk test pits or trenches for determination of compliance with the volume of deleterious materials per Section 14.1 shall be performed as needed based on visual inspection and judgment.

14.4.4 Quality Assurance Inspection

The Engineer of Record, or the Engineer's representative, and/or the Owner shall provide Quality Assurance (QA). The Contractor or Quality Control representative shall make samples available for splitting with the QA representative upon request. The QA Representative may request additional tests by the Contractor or Quality Control representative in accordance with Sections 14.1 and 14.3.1, 14.3.2, and 14.3.3.

15.0 References

Abramson, L.W., Lee, T.S., Sharma, S. and Boyce, G.M. (2002). Slope Stability and Stabilization Methods. 2nd Ed., John Wiley and Sons, New York.

American Society of Civil Engineers (2010), "So You Live Behind a Levee!" Link: http://content.asce.org/files/pdf/SoYouLiveBehindLevee.pdf

API RP 13B-1 – American Petroleum Institute Recommended Practice for Field Testing Water-based Drilling Fluids.

ASTM E 329 - Standard Specification for Agencies Engaged in Construction Inspection, Testing, or Special Inspection.

ASTM D 421 - Standard Practice for Dry Preparation of Soil Samples for Particle-Size Analysis and Determination of Soil Constants.

ASTM D 422 - Standard Test Method for Particle-Size Analysis of Soils.

ASTM D 698 - Standard Test Methods for Laboratory Compaction Characteristics of Soil Using Standard Effort.

ASTM D 854 - Standard Test Methods for Specific Gravity of Soil Solids by Water Pycnometer.

ASTM D 1140 - Standard Test Methods for Amount of Material in Soils Finer than No. 200 (75-μm) Sieve.

ASTM D 1556 - Standard Test Method for Density and Unit Weight of Soil in Place by the Sand-Cone Method.

ASTM D 1586 - Standard Test Method for Standard Penetration Test (SPT) and Split-Barrel Sampling of Soils.

ASTM D 1587 - Standard Practice for Thin-Walled Tube Sampling of Soils for Geotechnical Purposes.

ASTM D 2166 - Standard Test Method for Unconfined Compressive Strength of Cohesive Soil.

ASTM D 2216 - Standard Test Methods for Laboratory Determination of Water (Moisture) Content of Soil and Rock Mass.

ASTM D 2435 - Standard Test Methods for One-Dimensional Consolidation Properties of Soils Using Incremental Loading.

ASTM D 2487 - Standard Practice for Classification of Soils for Engineering Purposes (Unified Soil Classification System).

ASTM D 2488 - Standard Practice for Description and Identification of Soils (Visual-Manual Procedure).

ASTM D 2573 - Standard Test Method for Field Vane Shear Test in Cohesive Soil.

ASTM D 2850 - Standard Test Method for Unconsolidated-Undrained Triaxial Compression Test on Cohesive Soils.

ASTM D 2922 - Standard Test Methods for Density of Soil and Soil-Aggregate in Place by Nuclear Methods (Shallow Depth).

ASTM D 2974 - Standard Test Methods for Moisture, Ash, and Organic Matter of Peat and Other Organic Soils.

ASTM D 3080 - Standard Test Method for Direct Shear Test of Soils Under Consolidated Drained Conditions.

ASTM D 3740 - Standard Practice for Minimum Requirements for Agencies Engaged in Testing and/or Inspection of Soil and Rock as Used in Engineering Design and Construction.

ASTM D 4220 / D 4220M - Standard Practices for Preserving and Transporting Soil Samples.

ASTM D 4318 - Standard Test Methods for Liquid Limit, Plastic Limit, and Plasticity Index of Soils.

ASTM D 4380 - Standard Test Method for Density of Bentonitic Slurries.

ASTM D 4542 - Standard Test Method for Pore Water Extraction and Determination of the Soluble Salt Content of Soils by Refractometer.

ASTM D 4633 - Standard Test Method for Energy Measurement for Dynamic Penetrometers.

ASTM D 4767 - Standard Test Method for Consolidated-Undrained Triaxial Compression Test for Cohesive Soils.

ASTM D 5778 - Standard Test Method for Electronic Friction Cone and Piezocone Penetration Testing of Soils.

ASTM D 7181 - Standard Test Method for Consolidated Drained Triaxial Compression Test for Soils.

ASTM D 7263 - Standard Test Methods for Laboratory Determination of Density (Unit Weight) of Soil Specimens.

Bouwer, H. (1989), The Bouwer and Rice Slug Test – An Update, in Ground Water, Vol. 27, No. 3, May-June.

Bowles, J. E. (1988), Foundation Analysis and Design. 4th Ed., McGraw-Hill, Inc.

Bjerrum, L. (1972), Embankments on soft ground. Performance of Earth and Earth-Supported Structures, Vol. II, (Purdue Conference), ASCE, Reston, VA, 1-54.

Brandon, T., L. Martin, and T. Grifka (2010), Cone Penetration Test Correlations in New Orleans Area Practice, Report Submitted to USACE-New Orleans District, Virginia Polytechnic Institute and State University, Blacksburg, 2010, 33 pages.

Cedergren, H.R. (1989), Seepage, Drainage, and Flow Nets. 3rd Ed., John Wiley and Sons, New York.

Duncan, J. M., Horz, R. C., and Yang, T. L. (1989). Shear Strength Correlations for Geotechnical Engineering. Virginia Polytechnic Institute and State University, Blacksburg, August, 1989, 100 pages.

Duncan, J.M. and Wright, S.G. (2005). Soil Strength and Slope Stability. John Wiley and Sons, New York.

FHWA (2002). Geotechnical Engineering Circular 5 (GEC5) - Evaluation of Soil and Rock Properties. Report No FHWA-IF-02-034. Authors: Sabatini, P.J, Bachus, R.C, Mayne.

Harr, M.E. (1962). Groundwater and Seepage. McGraw-Hill Book Company, New York.

Kulhawy, F.H. and Mayne, P.W. (1990), "Manual on Estimating Soil Properties for Foundation Design," Research Project 1493-6, Electric Power Research Institute.

Lade, P. V. (2010). "The Mechanics of Surficial Failure in Soil Slopes." Engineering Geology, Vol 114, pp. 57-64.

Lane, E. W., (1935) "Security from Under-Seepage - Masonry Dams on Earth Foundations." Transactions, ASCE Transactions, Paper 1919, p 1235.

Matlock, H. (1970), "Correlation for design of laterally loaded piles in soft clay", Presented at the Second Annual Offshore Technology Conference, Houston, Texas, 1970, Vol. 1, pp 577-588.

Schmertmann, J. H. (2000). "The No-Filter Factor of Safety Against Piping Through Sands".

Skempton, A.W. (1964). Long Term Stability of Clay Slopes. Geotechnique, Vol. 14(2), pp. 77-102.

Terzaghi, K, Peck, R. B., and Mesri, G. (1996), "Soil Mechanics in Engineering Practice", 3rd Edition, John Wiley and Sons, New York.

US Army Corps of Engineers (2012), "Hurricane and Storm Damage Risk Reduction System Design Guidelines - Interim", New Orleans District Engineering Division with Revisions through June 2012.

US Army Corps of Engineers (1956), "Investigation of Underseepage and its Control Lower Mississippi River Levees", Technical Memorandum No. 3-424.

US Army Corps of Engineers (1999), "Engineering and Design: Quality Assurance of Laboratory Testing Procedures" Engineering Regulation 1110-1-261.

US Army Corps of Engineers (1998), "Soil Mechanic Data." Division Regulation (DIVR) 1110-1-400.

US Army Corps of Engineers (2001), "Engineering and Design: Geotechnical Investigations." Engineer Manual 1110-1-1804.

US Army Corps of Engineers (1990), "Engineering and Design: Settlement Analysis." Engineer Manual 1110-1-1904.

US Army Corps of Engineers (1997), "Engineering and Design: Laboratory Investigations and Testing" Engineering Regulation 1110-1-8100.

US Army Corps of Engineers (2003), "Engineering and Design: Slope Stability." Engineer Manual 1110-2-1902.

US Army Corps of Engineers (1986), "Engineering and Design: Laboratory Soils Testing." Engineer Manual 1110-2-1906.

US Army Corps of Engineers (2000), "Design and Construction of Levees." Engineer Manual 1110-2-1913.

US Army Corps of Engineers (1989), "Engineering and Design: Retaining and Flood Walls." Engineer Manual 1110-2-2502.

US Army Corps of Engineers (1994), "Engineering and Design: Design of Sheet Pile Walls." Engineer Manual 1110-2-2504.

US Army Corps of Engineers (1994), "Engineering and Design: Structural Design of Closure Structures for Local Flood Protection Projects." Engineer Manual 1110-2-2705.

US Army Corps of Engineers (1991), "Engineering and Design: Design of Pile Foundations." Engineer Manual 1110-2-2906.

US Army Corps of Engineers (1999), "Engineering and Design: Quality Assurance of Laboratory Testing Procedures." Engineering Regulation 1110-1-261.

US Army Corps of Engineers (1997), "Engineering and Design: Laboratory Investigations and Testing." Engineering Regulation 1110-1-8100.

US Army Corps of Engineers (2005), "Design Guidance for Levee Underseepage." Engineer Technical Letter 1110-2-569.

US Army Corps of Engineers (2011), "Engineering and Design: Evaluation of I-Walls" Engineer Technical Letter 1110-2-575.

US Army Corps of Engineers (2012), "Engineering and Design: Use of Spiral Welded Pipe Piles" Engineer Technical Letter 1110-2-577.

US Army Corps of Engineers (2011), "Engineering and Design: Design of I-Walls" Engineer Circular 1110-2-6066.

U.S. Army Corps of Engineers (2011), 2011 Interim Measures Design Manual, US Army Corps of Engineers, New Orleans District, June, 8.

THIS PAGE INTENTIONALLY LEFT BLANK

Appendices

Appendix 1: "LPILE Method for Evaluating Bending Moments in Battered Piles Due to Ground Settlement for Pile-Supported Floodwalls in New Orleans and Vicinity"

FINAL CONTRACT REPORT
Contract No. W912P8-07-D-0062

LPILE METHOD FOR EVALUATING BENDING MOMENTS IN BATTER PILES DUE TO GROUND SETTLEMENT FOR PILE-SUPPORTED FLOODWALLS IN NEW ORLEANS AND VICINTY

for
US Army Corps of Engineers

by

Michael P. McGuire, Virginia Tech
George M. Filz, Virginia Tech
Michael P. Navin, US Army Corps of Engineers
Kent D. Hokens, US Army Corps of Engineers

September 2012

Table of Contents

Appendices

1 Introduction

This report describes development, validation, and use of a method to estimate bending moments in batter piles induced by downdrag settlements. This project was performed under US Army Corps of Engineers (USACE) Contract No. W912P8-07-D-0062. The method is referred to as the "LPILE Method", and it was developed for the design of pile-supported T-Walls in the New Orleans area and vicinity. The LPILE Method utilizes the program LPILE, developed by Ensoft, Inc. (2008), combined with conventional geotechnical procedures to calculate consolidation settlements and correlations generated for this project. This approach is intended for practical use by designers, and it was developed to be as straightforward as possible while retaining the capability to address complexities of the soil-structure interactions that occur for pile-supported T-Walls.

This is the final report prepared under the contract. It supersedes the draft report dated May, 2010 and previous memoranda. Since issuing the draft report, there have been several significant revisions made to the LPILE Method and its application to design problems.

1.1 Objective

Batter piles used to support T-Walls in the New Orleans area and vicinity may be subject to downdrag loads produced by consolidation of soft clay foundation soils under the weight of a levee embankment. When a pile is battered, a component of the total downdrag load on the pile acts normal to the pile axis and produces bending moments. The bending moments due to downdrag can be significant, and they can influence the design of the piling system used to support the T-Wall. The objective of this report is to provide guidance for estimating the bending moments produced by downdrag for the relatively complex soil-structure interaction characteristics of pile-supported T-Walls.

1.2 Scope of Work

The original scope of work, as outlined in the January 20, 2010 Statement of Work in the project contract, was limited to:

1. Reviewing existing methods used by A/E firms and identified in published sources to estimate downdrag-induced bending moments in batter piles.
2. Evaluate the existing methods
3. Recommend minor changes to an existing method for use on projects in the New Orleans area and vicinity.

None of the existing methods used by A/E firms or identified during the literature review were sufficiently validated or detailed enough to address the characteristics of typical pile-supported T-walls used by the USACE in New Orleans and vicinity. Consequently, an extensive effort was undertaken to develop and validate a method that would satisfy USACE requirements. This included comparing the results from analyses using LPILE with published data from an instrumented field case history and laboratory experiments. LPILE analyses were also compared with a series of numerical analyses that were performed by Dr. Michael Navin of the USACE as part of this project. These comparisons resulted in two new components for the LPILE Method: (1) a chart that accounts for the stiffening effect of battered piles on ground settlements in the vicinity of the battered piles and (2) a chart that accounts for lateral movement of the soil when asymmetric fill loads are applied around the T-wall.

Some of the numerical analyses performed for the project addressed the effects of the lack of a distinct bearing layer, the presence of a second row of batter piles on the protected-side of the T-Wall, the presence of a sheet pile cutoff wall, and whether the T-Wall is positioned within the compressible clay foundation or within an existing levee.

An effort was also made to provide recommendations for interpreting and combining the maximum downdrag-induced bending moment estimated using the LPILE Method with estimates of bending moment produced from other sources, such as flood loading.

1.3 Limitations

The LPILE Method presented in this report was developed using the assumptions listed in Table 2.1 and the specific T-Wall geometry, pile properties, pile spacing, and soil conditions shown in Figures 2.5 and 2.6 and Tables 2.3 and 2.4 located in Section 2.1. The LPILE Method is applicable to the cases outlined in Table 2.2. The LPILE Method may not be accurate for conditions that are substantially different from those used to develop the method.

The bending moment estimated using the LPILE Method is the component of the total bending moment in the batter pile due to downdrag. Other sources of bending moment, such as flood loading, can contribute to the total bending moment in the pile.

1.4 Organization of the Report

This report is written and organized so that information related to usage of the LPILE Method is quickly accessible by designers. The supporting content related to the background and development of the LPILE Method is contained in a series of appendices that follow the main body of the report.

The main body of the report is organized into three chapters following the introduction provided in Chapter 1. Chapter 2 presents a concise step-by-step outline of the LPILE Method. Chapter 3 presents a detailed example problem showing complete application of the method. The list of references is in Chapter 4. Three appendices follow the main body of the report.

Appendix A covers the findings from the literature review performed for the project. Appendix B presents a detailed discussion of the background and development of the LPILE Method for calculating downdrag-induced bending moments in battered piles. Appendix C provides an example of the calculation of settlement used for input in the LPILE Method and the process used to account for the stiffening effect of the piles on settlements. Appendix D summarizes the analysis performed to determine how the LPILE Method should be applied when a T-Wall with three batter piles is positioned within an existing embankment.

2 Description of the LPILE Method

This chapter describes usage of the LPILE Method for calculating bending moments induced in batter piles for T-Walls subject to downdrag. Section 2.1 provides key definitions and essential details regarding the assumptions and calibration of the LPILE Method. Section 2.2 provides a step-by-step procedure for applying the LPILE Method.

2.1 Key Definitions, Assumptions, and Calibration of the LPILE Method

Figure 2.1 provides a definition sketch for application of the LPILE Method to batter piles supporting T-Walls subject to downdrag. In this figure, L_e equals the length of pile within the existing embankment, L_c equals the length of pile in the foundation clay, and z equals the distance along the pile starting from an origin at the base of the T-wall. The method was developed for practical use by designers of USACE T-Walls in the New Orleans area, and it is based on the assumptions listed in Table 2.1. Table 2.2 describes the applicability of the LPILE Method to the flood-side, middle, and outer protected-side piles for different loading conditions and T-Wall locations. The bending moments determined using the LPILE Method are only the moments due to downdrag. Additional bending moments may be produced by other factors, such as flood loading.

The LPILE Method uses the soil movement option in LPILE 5.0 Plus to apply the component of downdrag that acts normal to the pile axis when the pile is battered. As shown in Figure 2.2, the soil movement is treated as displacement of the back side of the nonlinear p-y springs that act on the pile at a particular location. For embankment loading that produces symmetrical compression on the flood side and protected side of the T-Wall, the primary direction of soil displacement due to consolidation under the embankment surcharge is assumed to be vertical. For embankment loading that is asymmetric, there may be a significant component of lateral soil displacement. The most straightforward approach to estimating the component of soil displacement that acts normal to the pile axis, $d_{N,z}$, is to multiply the vertical soil displacement, $d_{V,z}$, by the sine of the batter angle taken from vertical and add the result to the product of the horizontal soil displacement, $d_{H,z}$, and the cosine of the batter angle. Downward vertical soil movements have positive sign for piles on both the flood and protected sides. For the flood-side batter pile, horizontal soil movement from the flood side to the protected side has a positive sign. For piles on the protected side, horizontal soil movement from the protected side to the flood side has a positive sign.

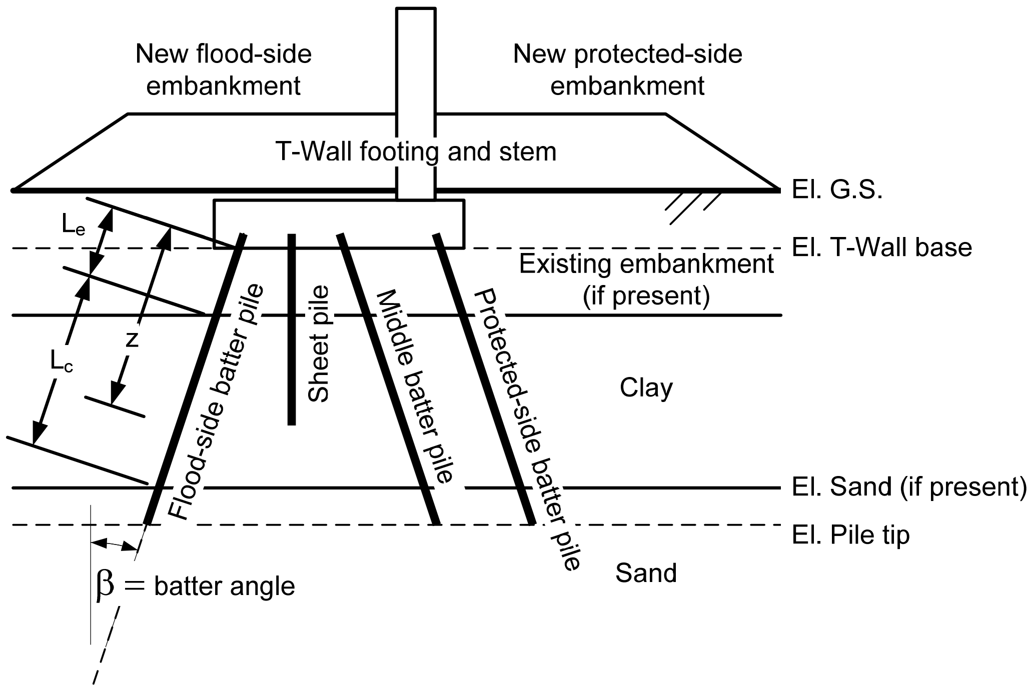

Figure 2.1: Schematic diagram of pile-supported T-Wall, embankment, and sub-surface profile.

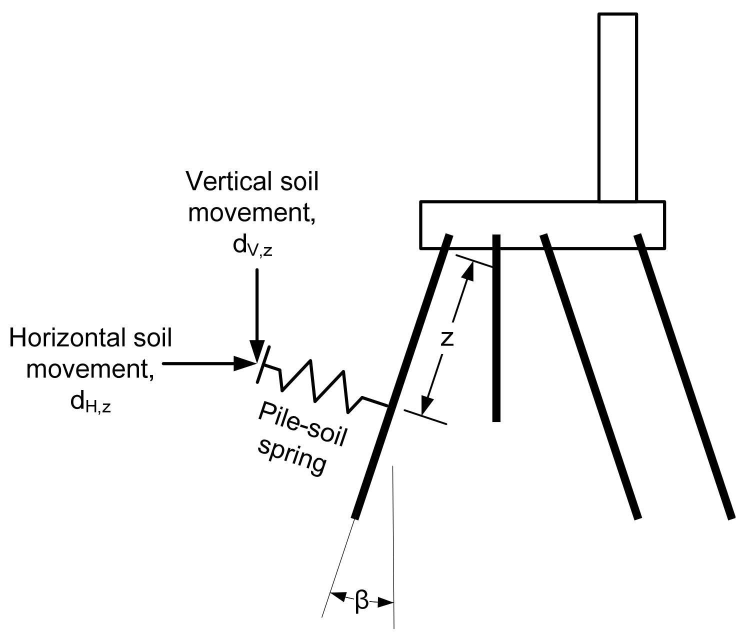

Figure 2.2: Soil movement applied to pile-soil spring

Table 2.1 Assumptions used to develop LPILE Method for calculating downdrag-induced bending moments

1	The piles are battered at 3V:1H, corresponding to a batter angle, β, of 18.4^{o} from vertical.
2	The connection of the piles to the T-Wall has little moment resistance and can be reasonably approximated by a pin support.
3	The foundation soils consist primarily of compressible clay and may include a sand bearing layer, as shown in Figure 2.1.
4	The clay is slightly overconsolidated near the ground surface but is otherwise normally consolidated.
5	For T-Walls located within an existing embankment, compression of the existing embankment material is insignificant compared to the compression of the foundation soils due to the surcharge applied by the new embankment.
6	For T-Walls located within an existing embankment, the foundation soils have reached equilibrium with the stress imposed by the existing embankment and no additional compression occurs due to the existing embankment. However, compression of the clay foundation does occur in response to the new embankment load.
7	For T-Walls located within an existing embankment, the undrained strength of the existing embankment is between 400 and 1600 psf.
8	For T-Walls located within an existing embankment, the effects of lateral spreading on downdrag-induced bending moments can be conservatively ignored when calculating downdrag-induced bending moments.
9	Soil movement normal to the pile axis is responsible for the downdrag-induced bending moment. When the new embankment produces the same compressions on both sides of the T-Wall, the component of vertical soil movement normal to the pile axis of interest is solely responsible for producing downdrag-induced bending moment. When the new embankment produces asymmetrical compressions on either side of the T-Wall and the resulting normal component of horizontal soil movement acts in the same direction as the normal component of the vertical soil movement for the pile of interest, the magnitude of the downdrag-induced bending moment increases.
10	Axial loading in the pile does not significantly impact the downdrag-induced bending moments, i.e., the P-Δ effect is not included in this method.

Table 2.1 (cont): Assumptions used to develop LPILE Method for calculating downdrag-induced bending moments

11	Soil movements normal to the pile axis used in the LPILE Method can be reasonably estimated based on conventional one-dimensional calculations of settlement performed along vertical profiles on either side of the T-Wall as shown in Figures 2.3 and 2.4. Vertical soil movements can be determined by adjusting the compression calculated on the same side of the T-wall as the pile of interest to account for the stiffening effect of the piles and the presence of the T-Wall using a specially-developed chart presented in this report. When fill is asymmetrical, the downdrag-induced bending moment due to horizontal soil movement along the pile of interest can be accounted for in the LPILE Method using a specially-developed chart and the difference between the compressions calculated on either side of the T-Wall.
12	The total bending moment developed in the batter piles is produced from three sources: (1) the self-weight of the T-wall, weight of fill directly overlying the T-Wall base, weight of the flood water on the T-Wall base, and lateral load on the T-Wall produced by the flood, (2) downdrag, (3) the "unbalanced forces" produced by the weight of the flood on the flood-side soils and asymmetric fill loads (USACE, 2012). Moments from different sources where both the sign and magnitude of the moments are known can be combined by adding moments having the same sign and using the moment with the largest absolute value for moments having opposite signs. This approach conservatively considers that maximum bending moments from different sources occur at the same location along the pile and ignores counteracting moments with different sign. Moments from different sources where only the magnitude of the moments is known can be conservatively combined by adding the magnitude of the moments.
13	The presence of a sheet pile cut-off has a negligible effect on downdrag-induced bending moments produced in the batter piles.
14	When the T-Wall is positioned within the clay foundation soil, the maximum calculated compressions on either side of the T-Wall are between 4.5 and 43 inches. When the T-Wall is positioned within an existing embankment, the maximum calculated compressions on either side of the T-Wall are between 6.5 and 30 inches. The difference between calculated compressions on either side of the T-Wall is less than 21 inches for cases where the T-Wall is positioned within the foundation soil and 14 inches for cases where the T-Wall is positioned within an existing embankment.
15	When the new fill produces symmetrical compressions on either side of the T-Wall, the flood-side pile experiences higher downdrag-induced bending moment than the protected-side pile or the middle pile. When the pile of interest is the either the protected-side or middle piles, it is conservative to ignore the reduction in bending moment compared to the flood-side pile due to additional shielding from the T-Wall and adjacent piles.

Table 2.2: Application of the LPILE Method to flood-side, middle, and protected-side batter piles for different combinations of fill and T-Wall position.

Fill condition & T-Wall position[1]	Pile of interest[2]	Use of LPILE Method[3]
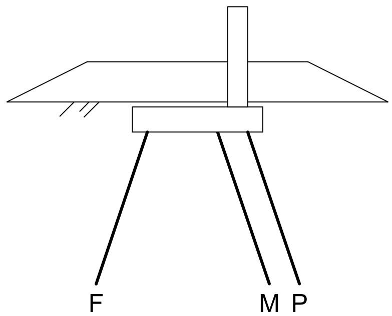 Symmetrical fill, T-Wall in clay foundation	Flood-side pile (F)	Okay
	Middle pile (M)	Very conservative
	Protected-side pile (P)	Somewhat conservative when middle pile is not present. Fairly conservative when middle pile is present.
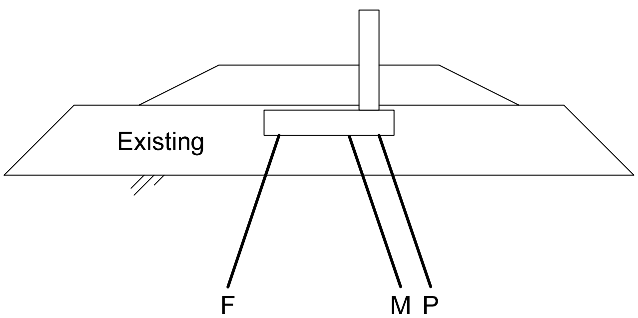 Symmetrical fill, T-Wall in existing embankment	Flood-side pile (F)	Okay
	Middle pile (M)	Expected to be fairly to very conservative
	Protected-side pile (P)	Okay when middle pile is not present. Expected to be somewhat conservative when middle pile is present.
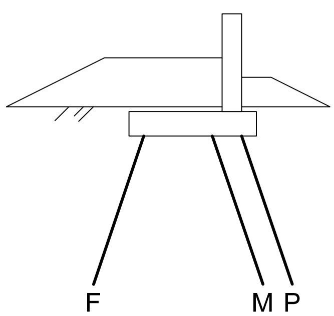 Asymmetrical fill producing more compression on flood side, T-Wall in clay foundation	Flood-side pile (F)	Okay
	Middle pile (M)	Does not apply, but a conservative design can be obtained by using the magnitude of the maximum moment from the LPILE Method for the flood-side pile.
	Protected-side pile (P)	

Table 2.2 (continued): Application of the LPILE Method to flood-side, middle, and protected-side batter piles for different combinations of fill and T-Wall position.

<table>
<tr><th>Fill condition & T-Wall position[1]</th><th>Pile of interest[2]</th><th>Use of LPILE Method[3,4]</th></tr>
<tr><td rowspan="3">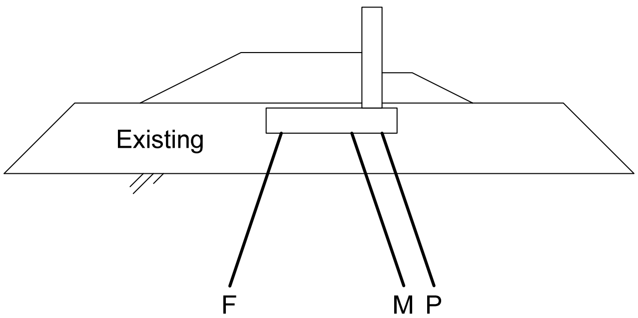

Asymmetrical fill producing more compression on flood side, T-Wall in existing embankment</td><td>Flood-side pile (F)</td><td>Okay when middle pile is not present

Expected to be okay if maximum moment is increased by 7% when middle pile is present</td></tr>
<tr><td>Middle pile (M)</td><td>Does not apply, but it is expected that a conservative design can be obtained by using the magnitude of the maximum moment from the LPILE Method for the flood-side pile.</td></tr>
<tr><td>Protected-side pile (P)</td><td>Does not apply, but a conservative design can be obtained by using the magnitude of the maximum moment from the LPILE Method for the flood-side pile.</td></tr>
<tr><td rowspan="3">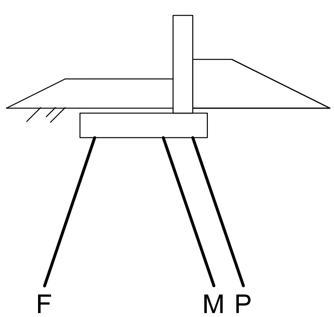

Asymmetrical fill producing more compression on protected side, T-Wall in clay</td><td>Flood-side pile (F)</td><td>Does not apply, but it is expected that a conservative design can be obtained by using the magnitude of the maximum moment from the LPILE Method for the protected-side pile</td></tr>
<tr><td>Middle pile (M)</td><td>Expected to be fairly to very conservative</td></tr>
<tr><td>Protected-side pile (P)</td><td>Expected to be okay when middle pile is not present

Expected to be somewhat conservative when middle pile is present</td></tr>
</table>

Table 2.2 (continued): Application of the LPILE Method to flood-side, middle, and protected-side batter piles for different combinations of fill and T-Wall position.

Fill condition & T-Wall position[1]	**Pile of interest**[2]	**Use of LPILE Method**[3,4]
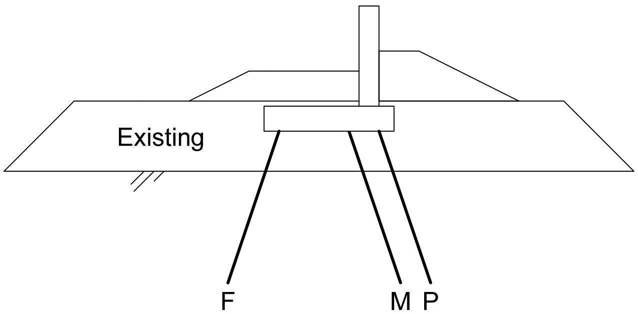 Asymmetrical fill producing more compression on protected side, T-Wall in existing embankment	Flood-side pile (F)	Does not apply, but it is expected that a conservative design can be obtained by using the magnitude of the maximum moment from the LPILE Method for the protected-side pile
	Middle pile (M)	Expected to be fairly conservative
	Protected-side pile (P)	Expected to be okay

Notes:
1. The FLAC analyses used to calibrate the LPILE Method evaluated symmetrical fill and fill producing more compression on the flood side for the T-Wall positioned in the clay foundation or within an existing embankment.
2. The LPILE Method is calibrated to calculate the maximum moment in the flood-side pile for the conditions evaluated in the FLAC analyses. Expected results for other piles are based on available information from the FLAC analyses and the authors' judgment.
3. Values of maximum moment calculated by the LPILE Method that are 'somewhat' conservative are less than 25% greater than the FLAC results, values that are 'fairly' conservative are between 25 and 50% greater than the FLAC results, and values that are 'very' conservative are more than 50% greater than the FLAC results.
4. For cases in which the designer judges that applying the LPILE Method using the guidelines in this table produce results that are too conservative, FLAC analyses can be performed to estimate the pile bending moments

Soil movements acting on the pile analyzed in LPILE are determined by settlements calculated along vertical profiles over the elevation interval from the base of the T-Wall to the top of the pile bearing layer, or pile tip, for profiles lacking a distinct bearing layer. The locations of the profiles for calculating settlement are shown in Figures 2.3 and 2.4. The settlement on the flood side of the T-Wall, s_F, is determined along a profile that intersects the flood-side pile at 25 percent of the vertical distance from the base of the T-Wall footing to the top of the bearing layer, or pile tip if no bearing layer is present. On the protected side, the settlements s_M and s_P are determined along profiles that intersect the middle and protected-side piles, respectively, at 25 percent of the vertical distance from the base of the T-Wall footing to the top of the bearing layer, or pile tip if no bearing layer is present. The profiles used to calculate s_F, s_M, and s_P are a horizontal distance equal to $0.25(L_e + L_c)\sin(\beta)$ from the location where the corresponding pile intersects the T-Wall base.

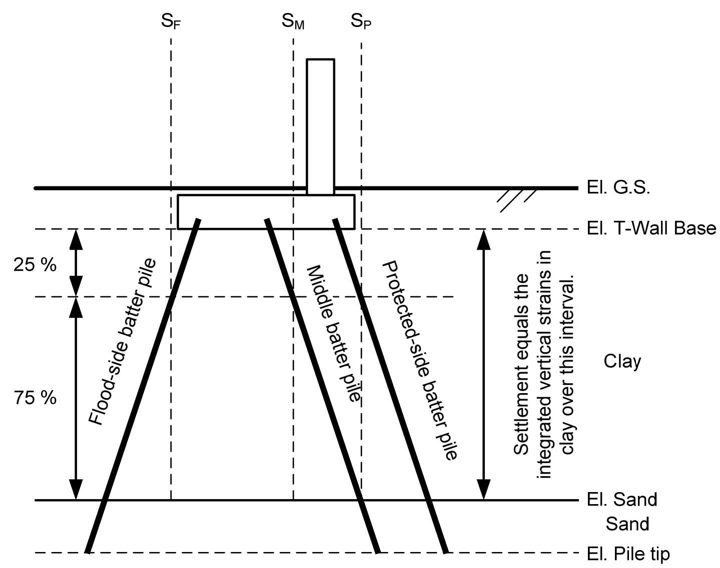

Figure 2.3: Location of settlement profiles, when the T-Wall is positioned within the clay foundation, for determining soil movements used in LPILE

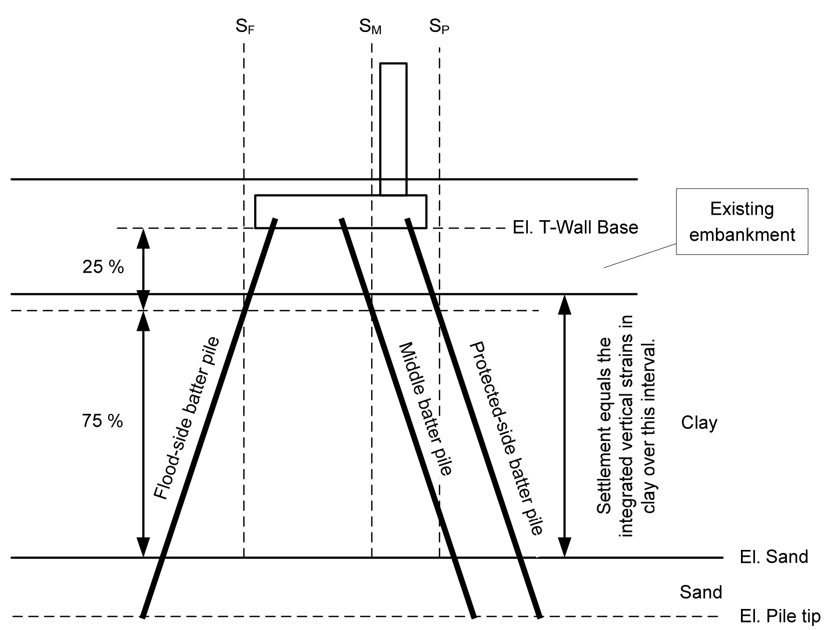

Figure 2.4: Location of settlement profiles, when the T-Wall is positioned within an existing embankment, for determining soil movements used in LPILE

Figures 2.5 and 2.6 and Tables 2.3 and 2.4 provide a summary of the geometry and properties modeled in FLAC which served as the basis for calibrating the LPILE Method to conditions applicable to pile-supported T-Walls in the New Orleans area. The embankment geometry for the surcharge pressure extended laterally such that the mid-point of the side slopes was 75 ft from the protected-side face of the T-Wall stem in both directions for cases where the fill is symmetric and only on the flood side for cases with asymmetric fill. The existing embankment layer included in some of the analyses was of broad lateral extent.

Further details regarding the development of the LPILE Method and the conditions and procedures used for calibration can be found in Appendix B. When project conditions deviate substantially from the conditions used to calibrate the LPILE Method, engineering judgment should be exercised to determine whether the LPILE Method would be expected to produce reliable estimates of bending moment. For other situations, alternative/supplemental methods, such as numerical modeling, should be considered.

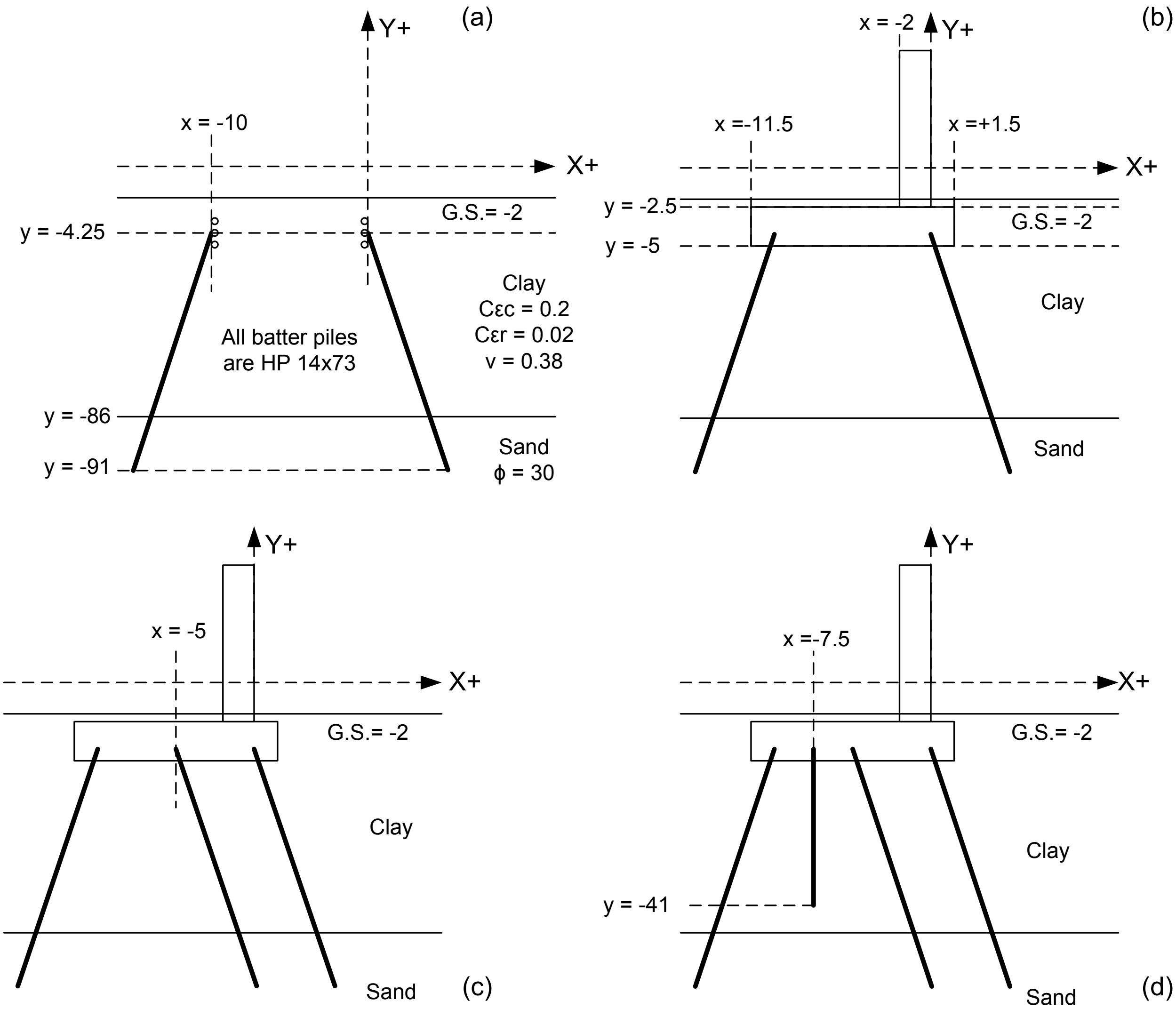

Figure 2.5: Geometries evaluated in FLAC for the purpose of developing the LPILE Method with T-Wall positioned in soft clay: (a) Pair of batter piles with roller supports, (b) Pair of batter piles pinned at base of T-Wall footing, (c) Three batter piles pinned at base of T-Wall footing, (d) Three batter piles plus sheet pile pinned at base of T-Wall footing. In all cases shown, the flood side is to the left of the T-Wall stem. The coordinate values shown for each portion of the figure also apply to all subsequent portions of the figure. All piles at 3V:1H batter. All distances and elevations in feet.

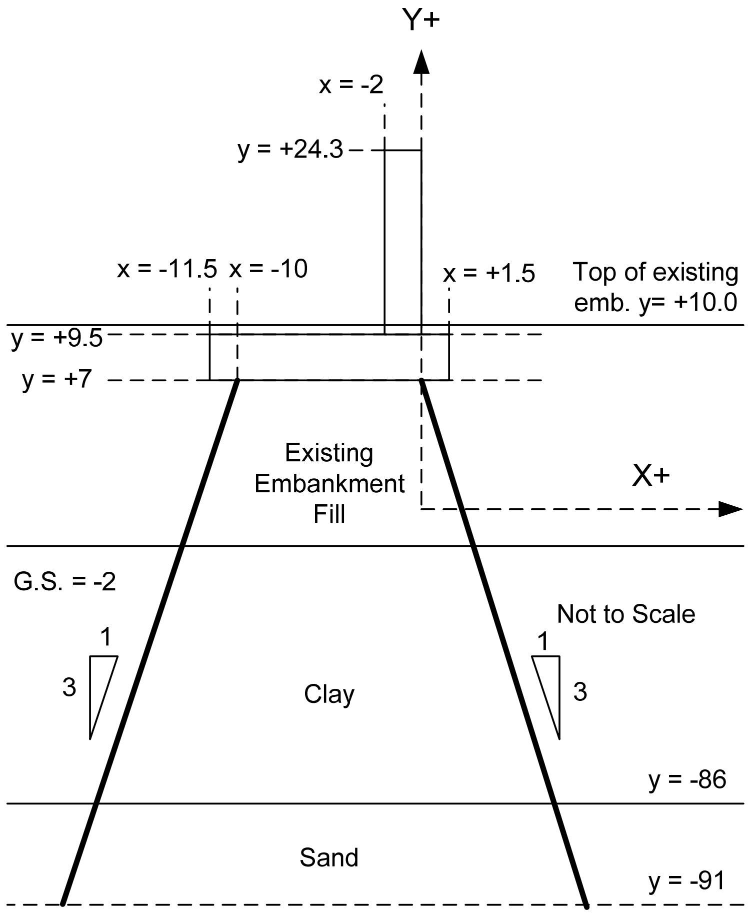

Figure 2.6: Geometry (e) evaluated in FLAC for the purpose of developing the LPILE Method with the T-Wall positioned within existing embankment. The flood side is to the left of the T-Wall stem. All distances and elevations in feet.

Table 2.3: Relevant H-Pile (HP 14x73) properties used in FLAC analyses to calibrate LPILE Method

Moment of Inertia (in.^{4})	726
Depth and Width of Section (in.)	13.6 x 14.6
Cross-Sectional Area (in.^{2})	21.4
Young's Modulus (psi)	29 x 10^6

Table 2.4: Relevant soil properties used in FLAC analyses to calibrate LPILE Method

Parameter	Existing Embankment	Soft Clay	Sand
Effective unit weight[1], γ (pcf)	110	50	60.5
Compression ratio, $C_{\varepsilon c}$ Recompression ratio, $C_{\varepsilon r}$		0.2 0.02	
Preconsolidation pressure, p_p (psf)		$\text{Max}\begin{cases}900\\ \sigma'_v\end{cases}$	
Undrained strength, s_u (psf)	800	$\text{Max}\begin{cases}200\\ 0.22(\sigma'_v)\end{cases}$	
Effective friction angle, φ' (deg)		23	30
Effective cohesion, c (psf)		0	0
Effective Poissons Ratio, ν		0.38	0.35
Youngs Modulus, E (psf)	500(s_u)	varies[2]	423,000

1. Ground water was located at the elevation of the original ground surface, El. -2
2. $E = (\Delta p/\varepsilon)(1+\nu)(1-2\nu)/(1-\nu)$ where

$$\varepsilon = C_{\varepsilon r}\log\frac{p_0+\Delta p}{p_o}\ \text{for}\ \left(p_o+\Delta p\right)\le p_p,\quad \varepsilon = C_{\varepsilon r}\log\frac{p_p}{p_o}+C_{\varepsilon c}\log\frac{p_0+\Delta p}{p_p}\ \text{for}\ p_p<\left(p_o+\Delta p\right)$$

p_o = vertical overburden stress prior to application of new embankment load
Δp = change in vertical stress due to application of new embankment load

2.2 Step-by-Step Procedure

The step-by-step procedure for the LPILE Method to estimate downdrag-induced bending moments in batter piles is given below.

1. Calculate the settlement, s, of the soil at the elevation of the T-Wall base due to the new embankment load using ordinary one-dimensional geotechnical analysis procedures, without considering the stiffening effect of the batter piles. Table 2.5 provides the settlement calculations required depending on the pile being analyzed by the LPILE Method. Only combinations of pile and fill condition where the LPILE Method is applicable, as listed in Table 2.2, are provided in Table 2.5. The difference in settlement on the flood and protected sides, Δs, is only required for cases where the fill is asymmetrical.

Table 2.5: Settlements required to determine soil movements in LPILE

Pile of interest	Fill condition	s (in.)	Δs (in.)
Flood-side pile	Symmetrical	s_F	not needed
Middle pile	Symmetrical	s_M	not needed
Protected-side pile	Symmetrical	s_P	not needed
Flood-side pile	Asymmetrical, more compression on flood side	s_F	s_F - s_P
Middle pile	Asymmetrical, more compression on protected side	s_M	s_M - s_F
Protected-side pile	Asymmetrical, more compression on protected side	s_P	s_P - s_F

Settlement should be evaluated by integrating the compression of the foundation soils from a depth equal to L_e*cos(β) below the base of the T-Wall to a depth equal to (L_e + L_c)*cos(β) below the base of the T-Wall. This approach neglects any compression of existing embankment materials. The locations of the profiles used to determine s_F, s_M, and s_P are defined in Figures 2.3 and 2.4.

2. Determine the vertical soil movement, $d_{V,0}$, to be applied in the LPILE Method using the value of s determined in Step 1 and Figure 2.7 to account for the stiffening effect of the piles on soil compression. Note that the relationship between s and $d_{V,0}$ provided in Figure 2.7 is different depending on whether the T-Wall is positioned within the clay foundation soil or an existing embankment. For the case where the T-Wall is positioned within an existing embankment, the LPILE Method was calibrated using a 12-foot thick embankment. In situations where the existing embankment is less than 12 feet thick, the relationships shown in Figure 2.7 should be interpolated to determine $d_{V,0}$. In situations where the existing embankment is greater than 12 feet thick, the relationship in Figure 2.7 for the T-Wall positioned in an existing 12-foot thick embankment should be used to determine $d_{V,0}$. The relationships in Figure 2.7 should not be applied for settlements, s, larger than 42 inches for a T-Wall with base in the clay foundation or larger than 30 inches for a T-Wall with base in a 12-ft thick embankment.

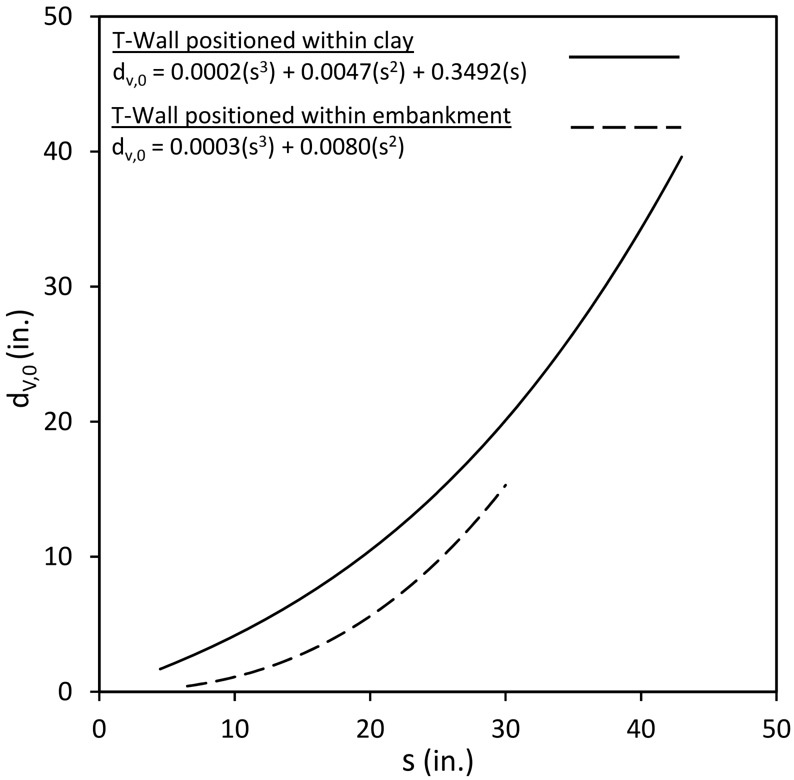

Figure 2.7: Vertical soil movement, $d_{V,0}$, considered in LPILE Method versus calculated settlement, s.

3. For conditions where the embankment surcharge produces asymmetric compression of the foundation soils (i.e. $\Delta s \neq 0$), the guidance provided in Table 2.6 should be used to determine whether horizontal soil movement, $d_{H,0}$, is applied to the top of the pile in LPILE in addition to $d_{V,0}$ to account for the influence of asymmetry on bending moments. As indicated in Table 2.6, the components of soil movement applied in LPILE may be different if the maximum bending moment, M_{max}, estimated by the LPILE Method is combined with the maximum bending moment from the USACE "unbalanced force" calculation.

Table 2.6: Guidance for accounting for fill asymmetry in the LPILE Method.

Pile of interest	Fill condition	Components of soil movement applied in LPILE	
		M_{max} based on LPILE only	M_{max} based on LPILE + USACE "unbalanced force" calculation
Flood-side pile	Asymmetrical, more compression on flood side	$d_{V,0}$ and $d_{H,0}$	$d_{V,0}$ only ($d_{H,0} = 0$)
Middle pile	Asymmetrical, more compression on protected side	$d_{V,0}$ and $d_{H,0}$	$d_{V,0}$ and $d_{H,0}$
Protected-side pile	Asymmetrical, more compression on protected side	$d_{V,0}$ and $d_{H,0}$	$d_{V,0}$ and $d_{H,0}$

4. If Step 3 indicates that horizontal soil movement, $d_{H,0}$, should be applied to the top of the pile in LPILE, the magnitude of $d_{H,0}$ can be determined using Figure 2.8 and the value of Δs determined in Step 1.

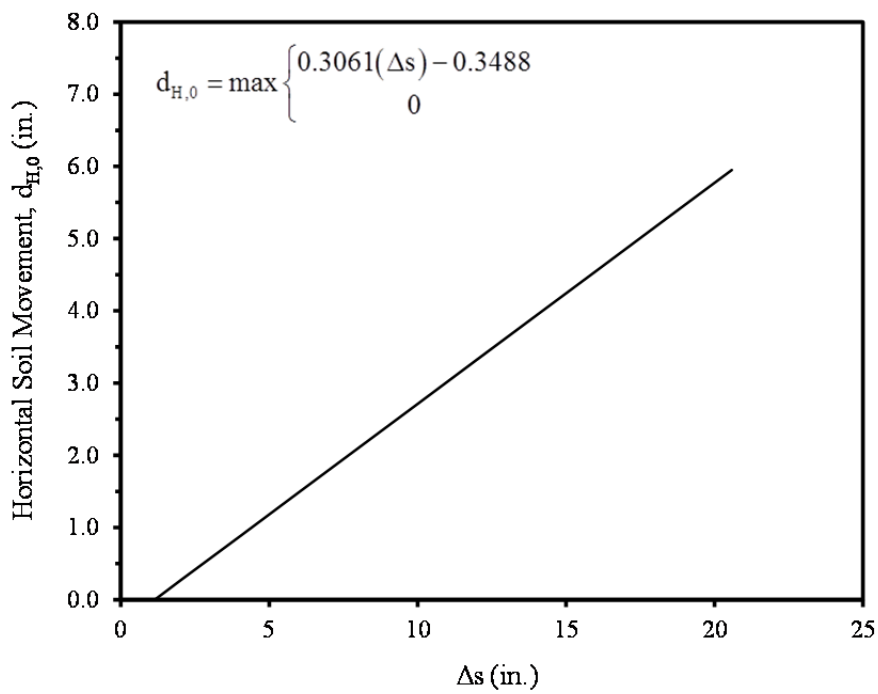

Figure 2.8: Horizontal soil movement, $d_{H,0}$, considered at the top of the pile in LPILE Method versus Δs

5. Determine the soil movement to be used in LPILE as displacement of the spring supports at the top of the pile, $d_{N,0}$, by summing the components of $d_{V,0}$ and $d_{H,0}$ that act normal to the pile.

$$d_{N,0} = d_{V,0} * \sin(\beta) + d_{H,0} * \cos(\beta) \tag{1}$$

6. Apply soil movement along the pile, $0 \leq z \leq (L_c + L_e)$, according to Equations 2 and 3 where $s_{z*\cos(\beta)}$ is the settlement at a depth below the T-Wall base equal to z*cos(β).

$$d_{N,z} = d_{N,0} \text{ for } 0 \leq z \leq L_e \tag{2}$$

$$d_{N,z} = d_{N,0}\left(\frac{s_{z*\cos(\beta)}}{s}\right) \text{ for } L_e < z \leq (L_e + L_c) \tag{3}$$

Soil movements applied along the pile in LPILE should be determined at enough locations to reasonably capture non-linearity in the distribution of soil compression along the settlement profile. Figure 2.9 provides an example of the settlement profile over the depth range occupied by the pile above the bearing stratum, $(L_c+L_e)*\cos(\beta)$, versus the corresponding position along the pile, z.

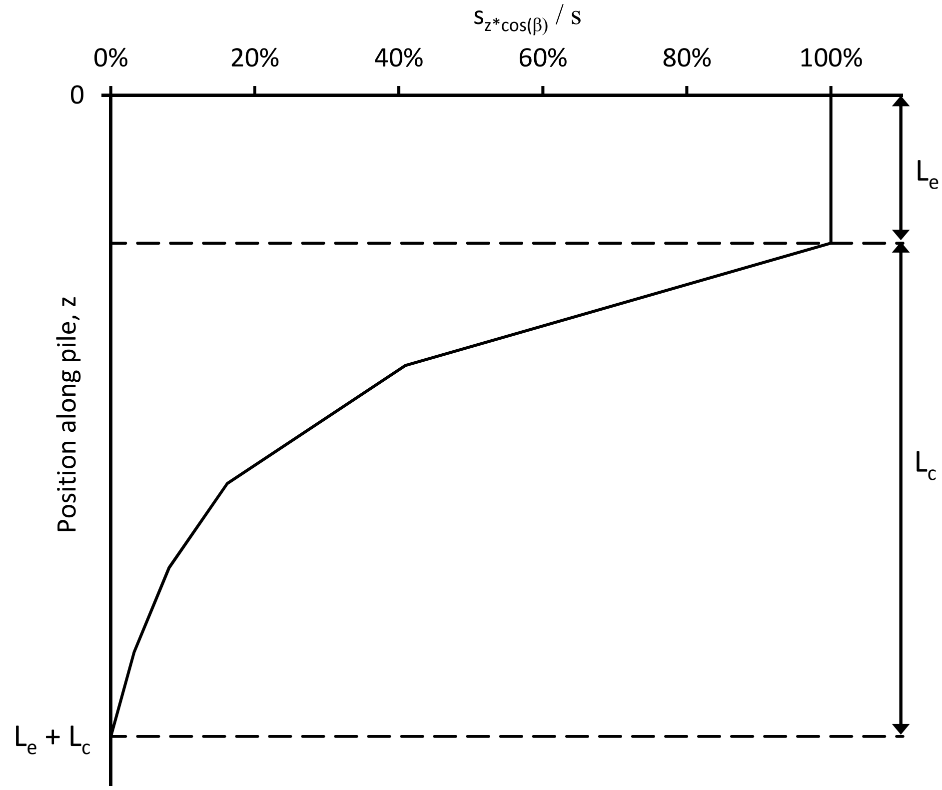

Figure 2.9: Sample distribution of settlement along the pile

7. Determine the pile batter angle according to the convention shown in Figure 2.10 for soil moving against the pile, which is opposite of the convention given in the LPILE 5.0 Plus User's Manual for soils resisting lateral movement of the pile.

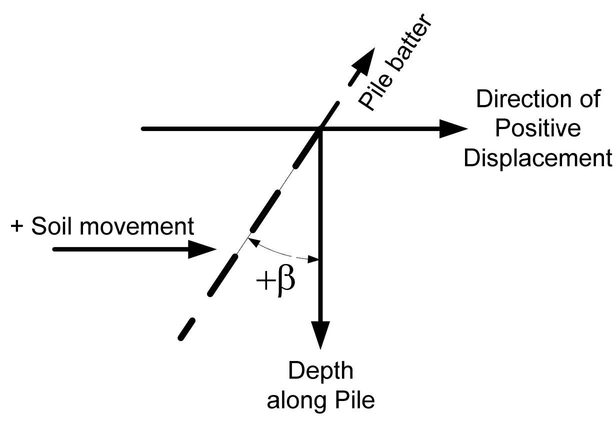

Figure 2.10: Sign convention to be used in LPILE for soil movement and pile batter

8. Transform the soil profile according to Figure 2.11 to match the coordinate system used in LPILE, which is parallel to the pile axis.

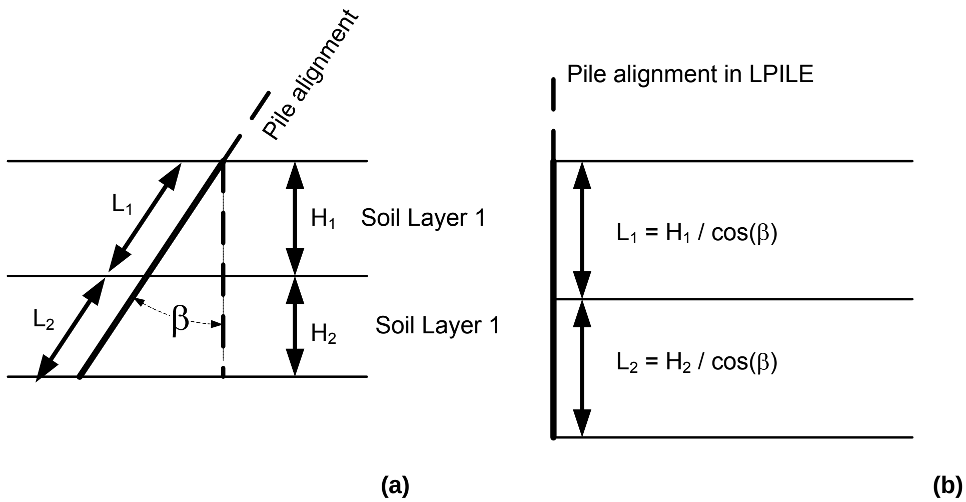

Figure 2.11: (a) Actual soil stratigraphy, (b) Soil stratigraphy modified for pile batter angle

9. Determine the factored unit weight, γ_z, for each soil layer considered in LPILE according to $\gamma_z = \gamma * \cos(\beta)$ where γ is the effective unit weight.

10. Determine the LPILE spring stiffness parameters using default values for strain at 50% maximum stress, ε_{50}, for clay layers and the stiffness modulus, k, for sand layers. Default values are assigned in LPILE by entering zero in the fields for ε_{50} and k. The undrained strength for clay layers and friction angle for sand layers used in LPILE to assign the available spring force should reflect the actual soil strengths and not be reduced by a factor of safety. As described in Appendix B, the maximum bending moment calculated using LPILE was sensitive to the assigned undrained strength of the existing embankment material, whereas the maximum bending moment calculated in FLAC did not exhibit significant sensitivity to undrained strength of the existing embankment material over the range from 400 to 1,600 psf. Since the LPILE Method is calibrated to the FLAC results, an undrained strength of 800 psf should be used in LPILE for existing embankment materials with undrained strength in the range of 400 to 1,600 psf.

11. Specify the pile properties and number of pile increments in LPILE using the standard guidance in the LPILE User's Manual. A pinned restraint (zero moment and zero displacement) with no axial load should be specified at the top of the pile.

12. Perform an LPILE analysis to determine the maximum moment, M_{max}, using the spring support displacements from Step 6, the soil properties from Steps 9 and 10, the pile properties from Step 11, and the pile-head boundary conditions from Step 11.

13. The maximum downdrag-induced bending moment estimated using the LPILE Method can be conservatively combined with maximum bending moments from other sources using the convention provided in Table 2.7.

Table 2.7: Recommendations for combining maximum moment from LPILE Method with moments from other sources

<table>
<tr><th>Fill condition</th><th>Pile of interest</th><th>Recommendation for combining maximum moment from LPILE Method with moments from other sources[1]</th></tr>
<tr><td>Symmetrical</td><td>Flood-side, Middle, or Protected-side piles</td><td rowspan="3">When the step-by-step procedure of the LPILE Method is followed, LPILE calculates a maximum bending moment with a negative sign for pile bending toward the centerline of the T-Wall. Using this sign convention, moments from other sources can be combined with the moment due to downdrag by adding moments having the same sign and using the moment with the largest absolute value for moments having opposite signs.</td></tr>
<tr><td>Asymmetrical fill producing more compression on flood side</td><td>Flood-side pile</td></tr>
<tr><td>Asymmetrical fill producing more compression on protected side</td><td>Middle or Protected-side pile</td></tr>
<tr><td>Asymmetrical fill producing more compression on flood side</td><td>Middle or Protected-side pile</td><td rowspan="2">The LPILE Method only provides an estimate of the magnitude of the downdrag-induced bending moment (i.e. the direction of pile bending is unknown). Moments from other sources can be conservatively combined with the magnitude of the moment due to downdrag by adding the absolute values of the moments.</td></tr>
<tr><td>Asymmetrical fill producing more compression on protected side</td><td>Flood-side</td></tr>
<tr><td colspan="3">1. For some of the cases listed in this table, the LPILE Method has to be applied in a special way, as described in Table 2.2. For example, in some cases the moment in the flood-side pile is used as an estimate of the magnitude of bending moment in the middle or protected-side piles. Thus, the LPILE Method needs to be applied with consideration of the recommendations in Table 2.2 prior to combining the results with moment from other sources.</td></tr>
</table>

3 Example Problem

3.1 Introduction to Example Problem

This example problem illustrates the LPILE Method for calculating downdrag-induced bending moments. The example problem is similar to the embankment and T-Wall geometry described in the report "Overview of FLAC Analysis for St. Bernard Parish" (Navin, 2009) and the foundation soil profile considered in the numerical model developed by Geomatrix Consultants, Inc. (2007) for T-Walls in the New Orleans area. Figure 3.1 shows the embankment, T-Wall, piling, and foundation soil profile for the example. The embankment includes a wave run-up berm on the flood side, which is not symmetric with the embankment fill on the protected side. Two batter piles are used on the protected-side and a sheet pile cut-off is also included. The tables included in Figure 3.1 provide the relevant information for the batter piles, as well as information about the soil properties. The goal of this analysis is to estimate the maximum bending moment in the critical flood-side batter pile due to downdrag and consolidation effects of asymmetric fill loading. Other sources of bending moment, such as flood loading, are not considered in this example.

3.2 Step-by-Step Procedure for Example Problem

1. Calculate the settlements, s_F and s_P, of the soil from the bottom of the T-wall to the top of the bearing layer at the plan view locations where the flood-side and protected-side battered piles intersect the elevation corresponding to 25% of the depth from the bottom of the T-wall to the top of the bearing layer.

   Figure 3.2 shows subdivision of the embankment load into uniform area loads. Alternatively, solutions for linear varying surcharge pressure could be applied. The fill directly overlying the base of the T-Wall is not included in calculations of stress change in the clay for the LPILE Method. Two-dimensional conditions are assumed for calculating stress change, and this can be approximated by assuming that the loaded areas extend a great length in the direction of the T-Wall alignment.

   Based on the area loads shown in Figure 3.2, the change in vertical stress with depth is determined using Boussinesq elastic theory for the two locations where compression is to be determined. Using the results of the stress analysis, and the soil properties provided in Figure 3.1, the settlement on the flood side at the location of the left cross-hair, s_F, and on the protected side at the location of the right cross-hair, s_P, were calculated to be 10.32 and 8.23 inches, respectively. In this case, the value of s used to determine $d_{V,0}$ is equal to 10.32 inches and the value of Δs used to determine $d_{H,0}$ is equal to 2.09 inches.

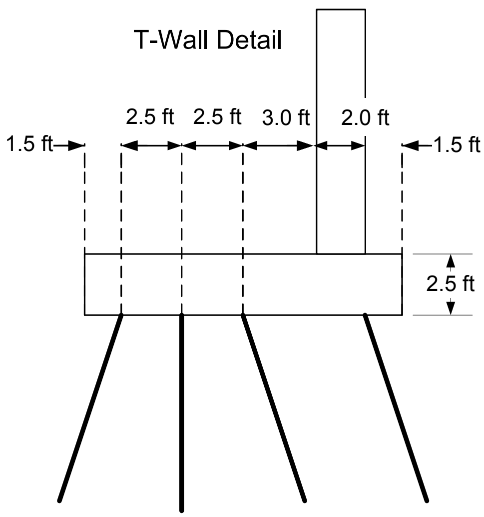

Relevant H-Pile (HP 14x73) Details	
Moment of Inertia (in.^{4})	726
Depth and Width of Section (in.)	13.6 x 14.6
X-Sectional Area (in.^{2})	21.4
Young's Modulus (psi)	29 x 10^6

Relevant Soil Properties	Soft Clay	Sand
Bouyant unit weight, γ (pcf)	50	60.5
Compression ratio, $C_{\varepsilon c}$ Recompression ratio, $C_{\varepsilon r}$	0.2 0.02	
Preconsolidation pressure, P_p (psf)	$\text{Max}\begin{cases} 900 \\ \sigma'_v \end{cases}$	
Undrained strength, S_u (psf)	$\text{Max}\begin{cases} 200 \\ \frac{2}{9}(\sigma'_v) \end{cases}$	
Effective friction angle, ϕ' (deg)		30

Unit weight of embankment (pcf)	110

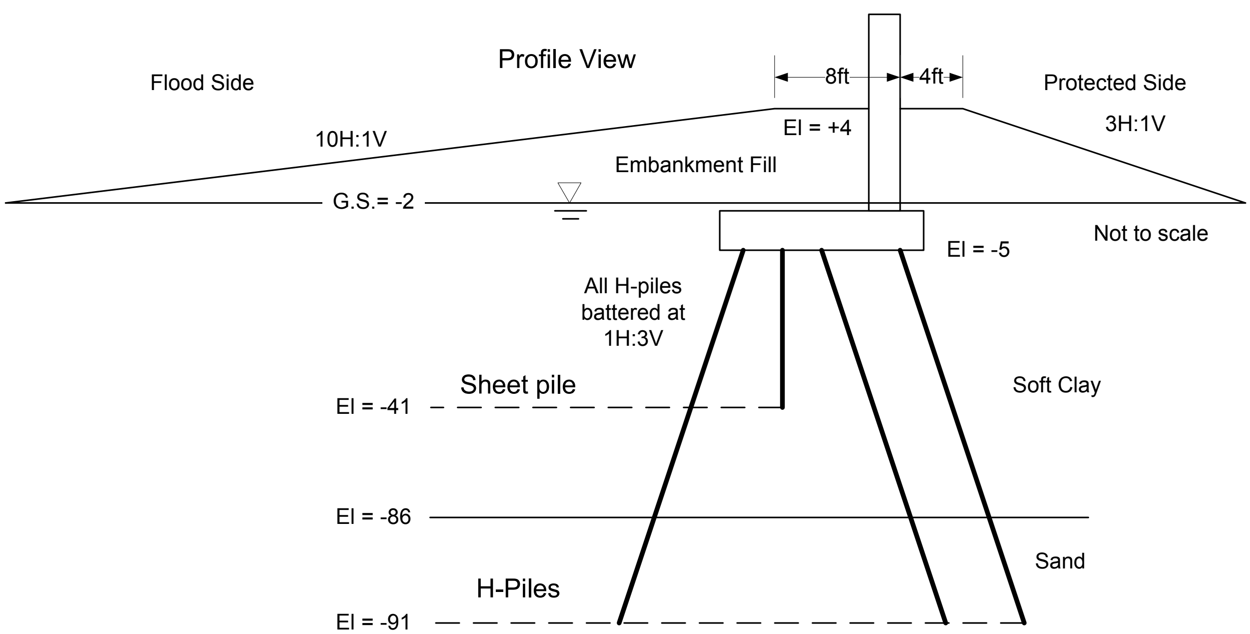

Figure 3.1: T-Wall, piling, embankment geometry, and relevant information for example problem

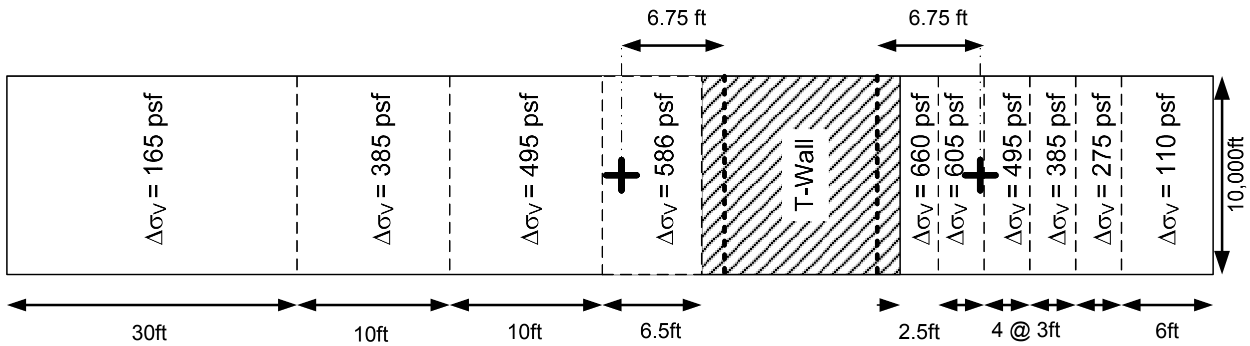

Figure 3.2: Plan view showing subdivision of fill into uniform area loads, excluding the fill overlying the T-Wall base. The locations where compression will be determined on the flood side and protected side are indicated with cross-hairs

2. Determine the vertical soil movement, $d_{V,0}$, to be applied in the LPILE Method using the value of s determined in Step 1 and Figure 2.7 to account for the stiffening effect of the piles on soil compression. Using the equation for the best fit line, $d_{V,0}$ can be determined as:

$$d_{V,0} = 0.0002(10.32)^3 + 0.0047(10.32)^2+0.3492(10.32)$$
$$d_{V,0} = 4.32 \text{ inches}$$

3. Horizontal soil movement in addition to vertical soil movement should be applied to the pile in LPILE, as indicated by Table 2.6, since the fill surcharge is asymmetric ($s_F \neq s_P$) and the bending moment from the LPILE Method will not be combined with moment from the USACE "unbalanced force" calculation.

4. Determine the horizontal soil movement applied at the top of the pile, $d_{H,0}$, to be considered in the LPILE analysis using the value of Δs equal to 2.09 inches determined in Step 1 and Figure 2.8. Using the equation for the best fit line, $d_{H,0}$ can be determined as:

$$d_{H,0} = \max\{0.3061(2.09) - 0.3488, 0\}$$
$$d_{H,0} = 0.29 \text{ inches}$$

5. The soil movement used in LPILE as displacement of the spring supports at the top of the pile, $d_{N,0}$, is equal to the components of $d_{V,0}$ and $d_{H,0}$ that act normal to the pile. In this case, the batter angle, β, is equal 18.43 degrees, which is obtained from the arctan of the slope of the pile given as 1H:3V. The value of $d_{N,0}$ is calculated using Equation 1, as follows:

$d_{N,0} = 4.32*\sin(18.43) + 0.29*\cos(18.43)$

$d_{N,0} = 1.64$ inches

6. Determine the distribution of the soil movements applied in LPILE. In the current problem, the T-Wall has its base in the clay foundation soil, therefore L_c = the length of the pile from the bottom of the T-wall to the top of the bearing layer and $L_e = 0$. The solid line in Figure 3.3 shows the distribution of settlement over the vertical profile that was used in Step 1 to calculate s. The horizontal axis provides the percentage of the settlement at a particular depth below the base of the T-Wall, $s_{z*\cos(\beta)}$, to the settlement at the elevation of the T-Wall base, s. The vertical axis provides the position along the pile, z, corresponding to the depth, $z*\cos(\beta)$. Interpreting the plot indicates that settlement equal to 50% of s (10.32 in. / 2 = 5.16 in.) occurs at a position along the pile equal to 320 inches below the T-Wall base, corresponding to a depth equal to 304 inches below the T-Wall base (320 in.*cos(18.43) = 304 in.).

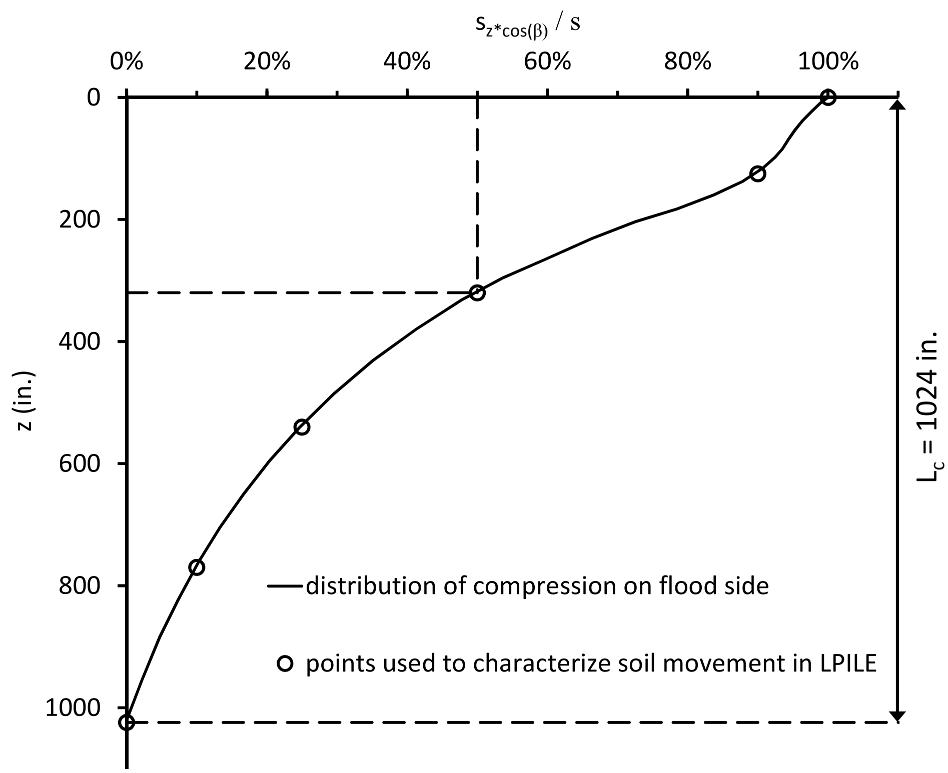

Figure 3.3 Vertical settlement profile used to determine distribution of soil movement along the pile in LPILE.

LPILE uses linear interpolation between specified values to assign soil movement to the supports of the pile-soil springs, therefore soil movement should be specified at enough locations to adequately represent the non-linear distribution of compression. The circle symbols in Figure 3.3 correspond to the entries in Table 3.1 for position, z, and the corresponding percentage of s used to determine the soil movements used as input in LPILE.

Table 3.1: Soil movement specified in LPILE for example

Column (1)	Column (2)	Column (3)
Position along pile, z (in.)	$s_{z*\cos(\beta)}$ / s	$d_{N,z} = d_{N,0}$ * Column (2) (in.)
0	100%	1.64
125	90%	1.48
320	50%	0.82
540	25%	0.41
770	10%	0.16
1024	0%	0.00

A screen shot of the detail for this aspect of LPILE input for the example problem is shown in Figure 3.4. Since LPILE assumes zero soil movement below the largest depth entered, it is not necessary to specify zero soil movement at the tip of the pile for piles terminating in a bearing layer.

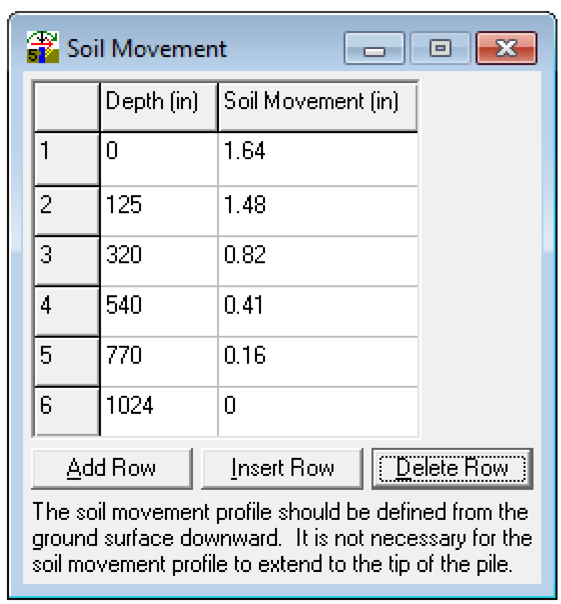

Figure 3.4: Input of soil movement in LPILE

7. The batter pile angle for this example problem equals 18.43 degrees based on the sign convention defined in this report.

8. Since the depth axis in LPILE is axial to the pile, a transformed soil profile needs to be developed from the information given in the example problem statement. The first step is to determine the transformed soil layer thicknesses according to Figure 2.11.

   For the example problem, the transformed thickness of the clay from Elevation -5 to -86 is (12)(86-5)/cos(18.43) = 1024 inches, while the sand from Elevation -86 to the bottom of the pile has a thickness of (12)(91-86)/cos(18.43) = 64 inches.

9. The transformed unit weight, γ_β, is determined for each soil according to $\gamma_z = \gamma * \cos\beta$, where γ is the total unit weight of soils above the water table and γ is the buoyant unit weight of soils below the water table. This step is needed for LPILE to determine the correct overburden pressure for the transformed soil stratigraphy. For this problem, the transformed buoyant unit weight for the soft clay, in units of pounds per cubic inch, pci, is equal to (50 pcf)cos(18.43)/(12 in/ft)^3 = 0.027 pci. For the sand, the transformed buoyant unit weight is equal to (60.5 pcf)cos(18.43)/(12 in/ft)^3 = 0.033pci.

10. Enter the remaining soil properties into LPILE. Due to overconsolidation of the upper soft clay, a minimum undrained shear strength of 200 psf (1.39 psi) was given in the problem statement. For LPILE to properly assign undrained strengths to each pile-soil increment, the clay layer will be divided into two sublayers. The upper layer will be assigned an undrained strength of 1.39 psi, while the lower layer will increase linearly with effective overburden pressure. The boundary between these two layers in the transformed profile can be determined according to

$$z = \frac{12}{\cos(18.43)}\left[\frac{200}{50 * 0.22} - 3\right] \tag{7a}$$

$$z = 190 \text{ inches} \tag{7b}$$

   The undrained strength of the clay at the top of the sand bearing layer is equal to

$$s_u = (0.22)[50 * (86 - 2)]/144 \tag{8a}$$
$$s_u = 6.48 \text{ psi} \tag{8b}$$

   LPILE spring stiffness parameters ε_{50} for the clay and k for the sand are assigned default values by entering zero in the input fields.

   Screen shots of the soil profile used in LPILE for the example problem are shown below in Figures 3.5 and 3.6.

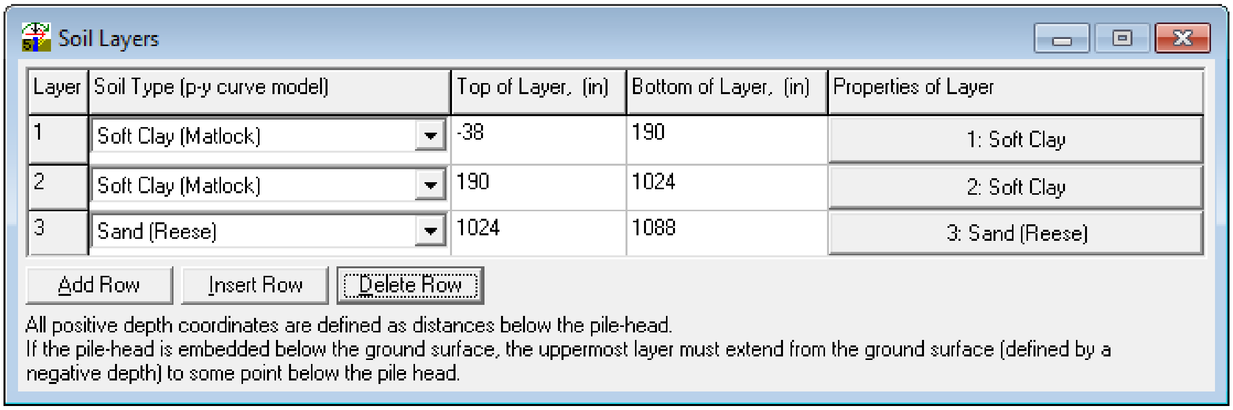

Soil Layers

Layer	Soil Type (p-y curve model)	Top of Layer, (in)	Bottom of Layer, (in)	Properties of Layer
1	Soft Clay (Matlock)	-38	190	1: Soft Clay
2	Soft Clay (Matlock)	190	1024	2: Soft Clay
3	Sand (Reese)	1024	1088	3: Sand (Reese)

Add Row Insert Row Delete Row

All positive depth coordinates are defined as distances below the pile-head.
If the pile-head is embedded below the ground surface, the uppermost layer must extend from the ground surface (defined by a negative depth) to some point below the pile head.

Figure 3.5: Soil profile used in LPILE for example problem

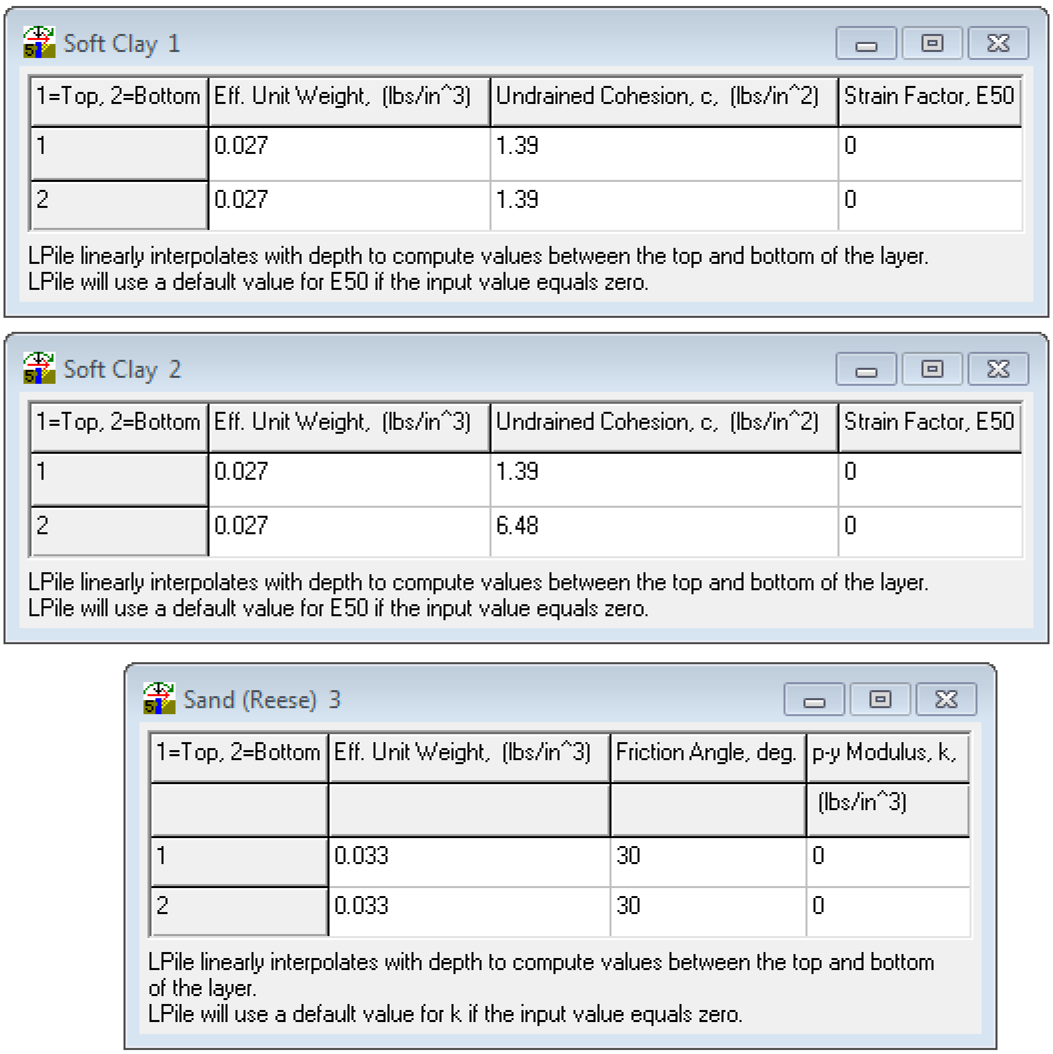

Soft Clay 1

1=Top, 2=Bottom	Eff. Unit Weight, (lbs/in^3)	Undrained Cohesion, c, (lbs/in^2)	Strain Factor, E50
1	0.027	1.39	0
2	0.027	1.39	0

LPile linearly interpolates with depth to compute values between the top and bottom of the layer.
LPile will use a default value for E50 if the input value equals zero.

Soft Clay 2

1=Top, 2=Bottom	Eff. Unit Weight, (lbs/in^3)	Undrained Cohesion, c, (lbs/in^2)	Strain Factor, E50
1	0.027	1.39	0
2	0.027	6.48	0

LPile linearly interpolates with depth to compute values between the top and bottom of the layer.
LPile will use a default value for E50 if the input value equals zero.

Sand (Reese) 3

1=Top, 2=Bottom	Eff. Unit Weight, (lbs/in^3)	Friction Angle, deg.	p-y Modulus, k,
			(lbs/in^3)
1	0.033	30	0
2	0.033	30	0

LPile linearly interpolates with depth to compute values between the top and bottom of the layer.
LPile will use a default value for k if the input value equals zero.

Figure 3.6: Soil properties assigned in LPILE

11. Enter the pile properties into LPILE. The length of the pile is the total pile length from Elevation -5 to -91 and is therefore equal to (12)(91-5)/cos(18.43) = 1088 inches. The distance from the ground surface (El. -2) to the top of the pile (El. -5) is equal to 12[(5 - 2)/cos(18.43)] = 38 inches. Using guidance given in the LPILE 5.0 Plus User's Manual, the pile was divided into 180 increments, the distance between the pile top the ground surface was entered as -38 inches, and the pile was assigned a batter angle of 18.43 degrees as described in Step 7. Next, the properties of the pile section are entered into LPILE. The cross sectional area, moment of inertia, and Young's modulus are provided in the problem statement. An equivalent pile diameter is input for the HP 14 x 73 piles using an equal area approach based on the section depth and width provided in the problem statement, such that the equivalent diameter equals the square root of $4*13.6*14.6/\pi$ = 15.9 inches. Screen shots of the LPILE input are provided in Figure 3.7.

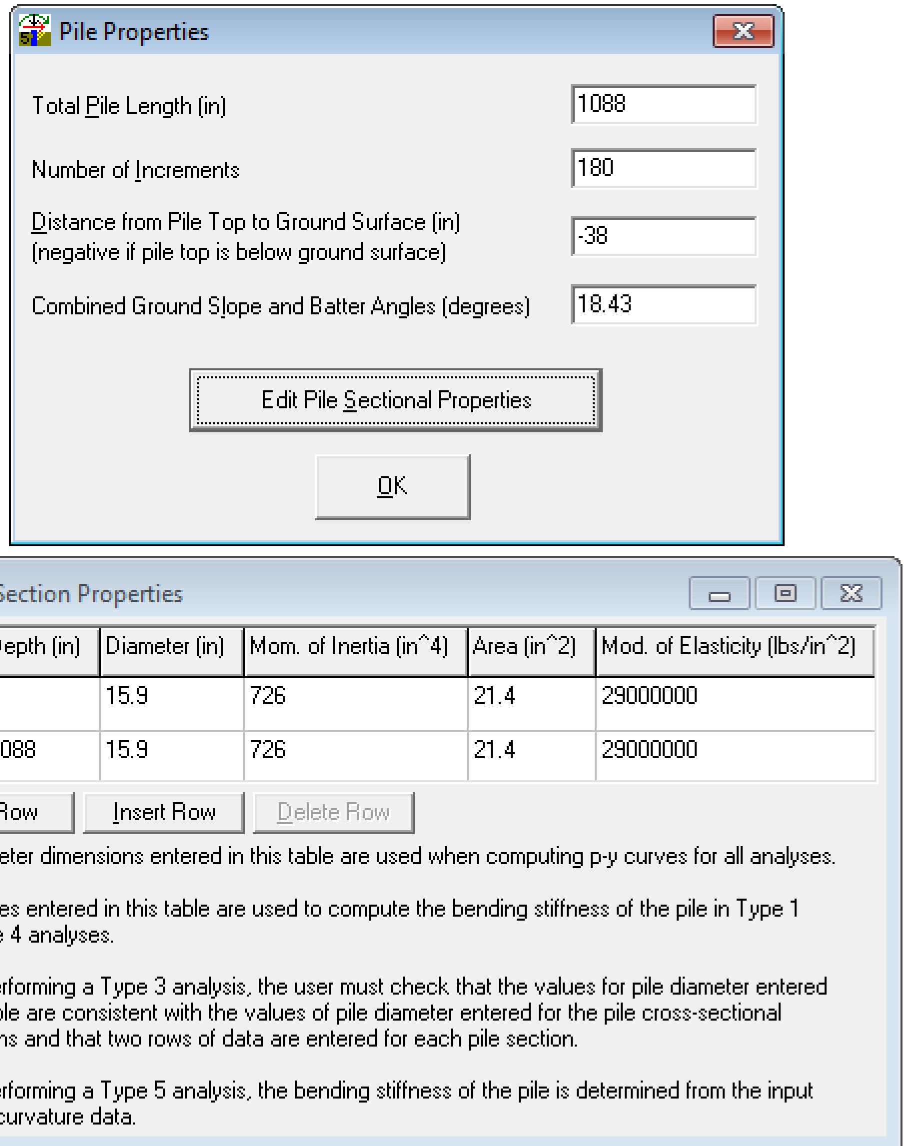

Figure 3.7: Pile properties used in LPILE

Use the static loading type under the "Loading Type" drop-down menu and a zero displacement, zero moment boundary condition at the top of the pile. No axial load should be specified since the LPILE Method does not include an axial-load contribution to downdrag-induced bending moment. A screen shot of the boundary condition specified for this problem is shown in Figure 3.8.

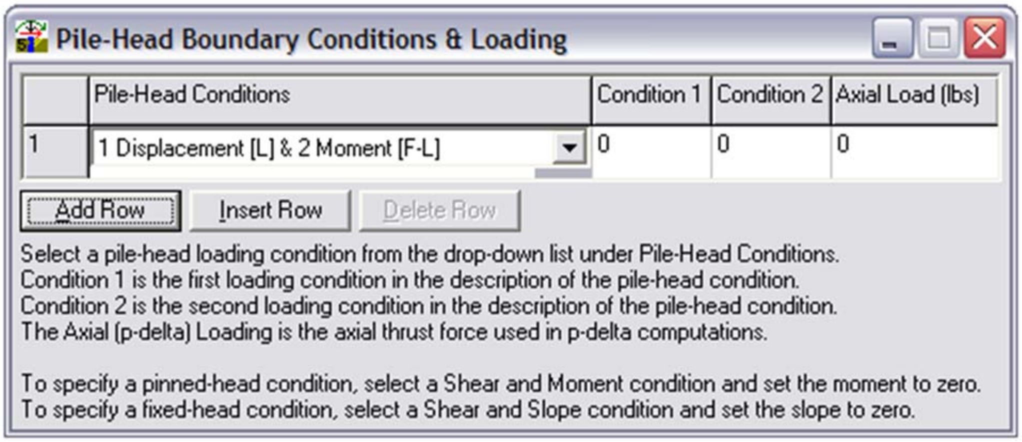

Figure 3.8: Boundary condition at the top of the pile used in LPILE

12. Perform an LPILE analysis to determine the maximum moment, M_{max}, due to downdrag. For the example problem, the absolute value of the maximum moment was determined to be 82 k-ft. Figure 3.9 shows the bending moment distribution predicted by the LPILE analysis.

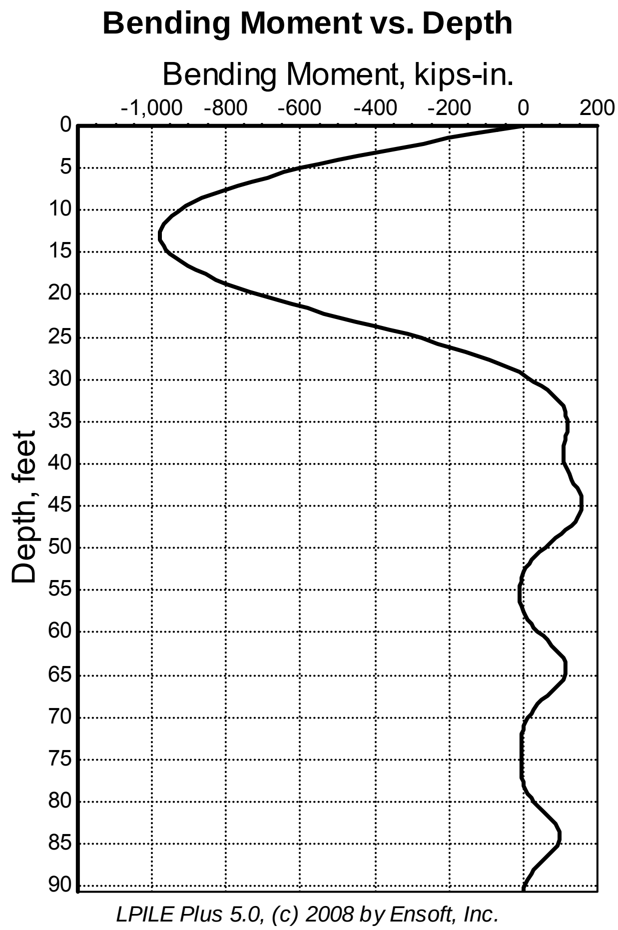

Figure 3.9: Moment distribution estimated by LPILE analysis

13. This example does not include the component of the total bending moment in the pile from the USACE "unbalanced force" procedure for T-Wall design. If the bending moment due to "unbalanced force" were included in this example, the outcome of Step 3 would have resulted in $d_{H,0} = 0$ and maximum moment from downdrag would have been combined with maximum moment from "unbalanced force". If the maximum moments had the same sign, they would be combined by adding the moments. If the maximum moments had opposite signs, they would be combined by using the moment with the largest absolute value.

4 References Cited in Report and Appendices

Broms, B., and Fredericksson, A. (1976). "Failure of pile-supported structures caused by settlements." Proceedings of the 6th European Conference on Soil Mechanics and Foundation Engineering, 383-386.

Ensoft. (2008). *LPILE 5.0 Plus User's Manual, Ensoft, Inc.*, Austin, TX.

Geomatrix Consultants, I. (2007). "Soil-structure interaction and load transfer mechanism of pile-supported T-Wall for New Orleans levees, Project 12048.001." Prepared for U.S. Army Engineer Research & Development Center, Waterways Experiment Station, Vicksburg, Mississippi, Okland, California.

ITASCA. (2002). *FLAC Fast Lagrangian Analysis of Continua.,* ITASCA Consulting Group, Minneapolis, Minnesota.

Matlock, H. (1970). "Correlations for design of laterally loaded piles in sift clay." 2nd Annual Offshore Technology Conference, OTC1204 Vol 1, Houston, Texas, pp. 577-594.

Rao, S. N., Murthy, T. V. B. S. S., and Veeresh, C. (1994). "Induced bending moments in batter piles in settling soils." *Soils and Foundations*, 34(1), 127-133.

Reese, L. C., Cox, W. R., and Koop, F. D. (1974). "Analysis of laterally loaded piles in sand." 5th Annual Offshore Technology Conference, OTC 2080, Houston, Texas.

Sato, S., Akai, K., Funahashi, T. (1970). "Study on methods to calculate negative skin friction and bending in a batter pile." Laboratory Report of Japan Road Corporation, pp. 31-49 (in Japanese).

Sato, S., Iwashita, F., and Ohmori, H. (1987). "The calculation method on the bending moment of a batter pile induced by ground settlement." *Soils and Foundations*, 27(2), 75-84 (in Japanese).

Sawaguchi, M. (1989). "Prediction of bending moment of a batter pile in subsiding ground." *Soils and Foundations*, 29(4), 120-126.

Shibata, T., Sekiguchi, H., and Yukitomo, H. (1982). "Model test and analysis of negative friction acting on piles." *Soils and Foundations*, 22(2), 29-39.

Takahashi, K. (1985). "Bending of a batter pile due to ground settlement." *Soils and Foundations*, 25(4), 75-91.

USACE (2012). "Hurricane and Storm Damage Risk Reduction System Design Guidelines." New Orleans District Engineering Division.

A. Literature Review

The literature review for this project consisted of evaluating information from two primary source categories. The first source was unpublished documents, hand calculations, and electronic files pertaining to methods used by A/E firms working on USACE projects to estimate downdrag-induced bending moments. In total, three such methods were identified. Two of the methods were used by Eustis Engineering, Inc., while the third was used by Burns Cooley Dennis, Inc.

Published journal and conference papers were the other main source of information about downdrag-induced bending moments in batter piles. Several databases were used for the literature review including: the ASCE Research Library, Virginia Tech's Newman Library, Compendex, and the Transportation Research Institute Search engine (TRIS).

This appendix is organized into the following sections:

- Section A.1: Overview and initial impressions of existing methods to calculate downdrag-induced bending moment in batter piles
- Section A.2: Overview of experimental and numerical studies related to downdrag-induced bending moments in batter piles
- Section A.3: Summaries of selected literature
- Section A.4: List of all published literature reviewed for the project

Appendix A.1, Overview and initial impressions of existing methods to calculate downdrag-induced bending moment in batter piles

<table>
<tr><th>Method</th><th>Pros/Cons</th><th>Assumptions</th><th>Remarks/ Other findings of study</th></tr>
<tr><td rowspan="2">Sato et al. (1970)
(in Japanese)</td><td>• Simple closed-form solution
• Selection of loading zone dimensions is subjective and has significant impact on results</td><td>• Pile considered to be elastic beam
• Clay divided into loading zone and supporting zone.
• Loading zone carries weight of clay over “effective length” and “effective width”
• Supporting zone treats clay as Winkler soil, therefore ground reaction is linear.
• Pile considered to be pinned at base of clay layer, no tip settlement
• Moments and deflections are zero at either end of pile</td><td>• Sato’s method is very sensitive to the choice of ‘effective width’ and ‘effective length’ for defining the loading zone. The recommendation is to use an effective width of three times the pile diameter, but there is no guidance on selecting an effective length.
• When calibrated, Takahashi (1985) showed that this model has good ability to predict bending moments.</td></tr>
<tr><td colspan="3">Assessment
• Since there is no English version of this paper, pursuing this method further would be difficult.
• This method appears to have no advantages to the method by Sawaguchi (1989).
• Usage of this method requires defining the dimensions of an upper loading zone. Although some guidance is provided in the paper regarding the selection of the width of the loading zone, the choice of the length of the zone is rather arbitrary and has significant effect of the predicted maximum bending moment. Therefore, it would be difficult to assess the reliability of the bending moments predicted using this method.</td></tr>
<tr><td>Broms and Fredriksson (1976)</td><td>• Use of trigonometric series for solution of the analytical model makes this method impractical for general use</td><td>• Bending moments in piles are due to downdrag forces
• Axial loads in pile have insignificant impact on predicted bending moment
• Clay is considered as Winkler soil, therefore ground reaction is linear
• Settlement assumed to be uniform over the length of the pile</td><td>• Broms and Fredriksson use the concept of virtual work to equate the internal work in the pile due to the induced moment and the external work due to displacement of the soil
• They use an empirical relationship between the coefficient of subgrade reaction, the undrained strength of the clay, and the pile diameter. This relationship is also used by Shibata et al. (1982)
• Broms and Fredriksson perform a parametric study using their analytical model to investigate the influences of the following on pile bending moments: Pile modulus, pile length, settlement magnitude, undrained shear strength of clay, restraint conditions of the pile, variation of shear strength with depth, and the presence of a desiccated crust.</td></tr>
</table>

Appendix A.1, Overview and initial impressions of existing methods to calculate downdrag-induced bending moment in batter piles

<table>
<tr><th>Method</th><th>Pros/Cons</th><th>Assumptions</th><th>Remarks/ Other findings of study</th></tr>
<tr><td></td><td colspan="3">Assessment
• There is not a usable form of the expression for bending moment readily available.
• Insufficient guidance is provided in the paper to reproduce the trigonometric series used by Broms and Fredriksson to solve the differential expression for bending.
• This approach appears to have no advantages over the method by Shibata et al. (1982), except that Broms and Fredriksson show their approach applied to both hinged and fixed conditions at the head of the pile.</td></tr>
<tr><td>Shibata et al. (1982)</td><td>• Simple closed-form solution
• Limited applicability to realistic field conditions</td><td>• Pile considered to be an elastic beam
• Clay is considered as Winkler soil, therefore ground reaction is linear
• Pile considered to be pinned at base of clay layer, therefore there is no settlement or moment at the pile tip
• Linear variation of settlement through clay layer
• Moments and deflections are zero at either end of pile
• Contribution of axial pile loads to deflections and moments are insignificant.</td><td>Experimental model findings
• A linear relationship exists between bending moment and applied consolidation pressure
• A linear relationship exists between downdrag load and consolidation pressure
• A 20% reduction in max. bending moment was observed when bitumen was used for batter piles.
• For small batter angle, the bending moment at a particular location along the axis of the pile is proportional to batter angle</td></tr>
<tr><td>(continued) Shibata et al. (1982)</td><td colspan="3">Assessment
• The simple closed-form solution proposed by Shibata et al. can be used to predict the maximum bending moment measured in laboratory and field-scale studies with good accuracy, provided that the right value is used for the horizontal subgrade reaction coefficient assumed over the pile length.
• The method is suited for batter piles with a pinned top connection which are embedded in uniform clay and bear on a stiff underlying stratum. The method loses accuracy for bending moment distribution of piles that pass through an embankment layer or extend above the ground surface.
• Reliable use of this method would require a way to confidently estimate the coefficient of horizontal subgrade reaction for local soils.
• It does not appear that the model by Shibata et al. can be extended to include other boundary conditions, variable ground conditions, or nonlinearity within the scope of this project. However, such extensions may be possible in the future by developing adjustment factors or adding an extra calculation step.</td></tr>
</table>

Appendix A.1, Overview and initial impressions of existing methods to calculate downdrag-induced bending moment in batter piles

Method	Pros/Cons	Assumptions	Remarks/ Other findings of study
Takahashi (1985)	• No closed form solution • Insufficient details are provided to implement this approach • More realistic treatment of settling clay • Considers case where pile penetrates the embankment • Boundary condition are not explicitly given	• Pile considered to be an elastic beam • Clay is considered as Winkler soil, therefore ground reaction is linear • Non-linear distribution of clay settlement according to double-drained assumed strain profile • Bending moment induced by embankment through component of overburden pressure normal to the pile axis • Pile considered to be pinned at base of clay layer, therefore there is no settlement or moment at the pile tip	• Takahashi's model incorporates four conditions: 1) bearing stratum, 2) consolidating clay, 3) embankment layer, 3) free portion • The pile is loaded normal to the pile axis both through the embankment and the consolidating clay. • Takahashi does not provide details on how to solve for unknown constants and implement his approach. • Possible typo in Equation 6 of the paper. • Takahashi compared the deflections and moments measured in experimental and field-scale studies and found that his method, along with Sato's method (1970) outperformed the predictive ability of his 3D finite element model. *Experimental model findings* • A proportional relationship exists between maximum bending moment and pile inclination angle • A linear relationship exists between ground settlement magnitude and maximum bending moment. • Takahashi observed a linear relationship between settlement of the pile top and the pile inclination angle *Numerical study findings* • Takahashi found that a 3D FEM was necessary since his 2D model was unable to capture the pile behavior observed in the experimental model.

Appendix A.1, Overview and initial impressions of existing methods to calculate downdrag-induced bending moment in batter piles

<table>
<tr><th>Method</th><th>Pros/Cons</th><th>Assumptions</th><th>Remarks/ Other findings of study</th></tr>
<tr><td rowspan="2">(continued)
Takahashi
(1985)</td><td></td><td></td><td>Field study findings
The use of bitumen coating can significantly reduce downdrag loads on a batter pile, but can actually result in a slight increase in the measured maximum bending moment</td></tr>
<tr><td colspan="3">Assessment
There is not a usable form of the expression for calculating bending moment readily available.
The additional features incorporated into Takahashi’s Method over the Shibata Method appear to provide little added benefit to addressing the evaluation of bending moments in batter piles supporting T-Walls.
It does not appear that Takahashi’s Method can be extended to include other boundary conditions or nonlinearity within the scope of this project.</td></tr>
<tr><td rowspan="2">Sato et al.
(1987)
(Japanese)</td><td>A description of the method in English is not available</td><td>Assumes linear subgrade reaction up to an ultimate capacity and perfectly plastic response thereafter</td><td>It appears that this method is very similar to the method by Sato et al. (1970) with the addition of the consideration of the plastic yield of the soil.
Based on his experimental study, Sawaguchi (1989) showed that this model does reasonably well at predicting maximum bending moment</td></tr>
<tr><td colspan="3">Assessment
Since there is no English version of this paper, pursuing this method further would be difficult.
From the figures in the reference paper, it appears that this method is similar to the method by Sato et al. 1970 with the inclusion of a yield stress to the linear soil response.
It is unclear whether sufficient details are provided in the paper to implement the approach.</td></tr>
</table>

Appendix A.1, Overview and initial impressions of existing methods to calculate downdrag-induced bending moment in batter piles

<table>
<tr><th>Method</th><th>Pros/Cons</th><th>Assumptions</th><th>Remarks/ Other findings of study</th></tr>
<tr><td rowspan="2">Sawaguchi (1989)</td><td>Sawaguchi provides non-dimensional design charts to calculate the maximum bending moment.
The charts provided in the paper cannot be used to determine the distribution of bending moment.
No closed-form solution exists.
Sawaguchi does not provide details for implementation of his method beyond the use of the design charts.</td><td>Pile considered to be an elastic beam
Pile is considered to be loaded as a positive projecting conduit according to Spangler’s formula in upper “Loading zone”
Below loading zone, clay is considered as Winkler soil, therefore ground reaction is linear.
Linear variation of settlement through clay layer
Moments and deflections are zero at either end of pile</td><td>The portion of the pile that is considered within the “Loading zone” is determined in the solution using the boundary conditions of the problem.
To estimate the coefficient of subgrade reaction, Sawaguchi used an empirical relationship with unconfined compressive strength proposed by Sawaguchi (1986).
Using the field study data also reported by Sato et al. (1987) and Takahashi (1985), Sawaguchi compared the measured maximum bending moments to the values predicted using his method and the methods by Takahashi (1985), Sato et al. (1987) and found that all had good predictive ability.</td></tr>
<tr><td colspan="3">Assessment
The method does not offer significant advancements over the Shibata Method except for the inclusion of a “loading zone” near the pile top.
It does not appear that Sawaguchi’s method can be extended to include other boundary conditions, variable ground conditions, or nonlinearity within the scope of this project.
Evaluating the Sawaguchi Method would require digitizing the chart solutions provided in the paper to predict the maximum bending moment.</td></tr>
</table>

Appendix A.1, Overview and initial impressions of existing methods to calculate downdrag-induced bending moment in batter piles

Method	Pros/Cons	Assumptions	Remarks/ Other findings of study
Rao et al. (1994)	• Simple model, easy to implement • Some assumptions are questionable • Development includes incorrect consideration of pore pressures. • Poor predictive quality relative to other methods	• The pile is treated as a free spanning beam with either pinned-pinned or fixed-fixed connections • The pile is assumed to carry the foundation soil within a wedge-shaped volume defined based on the pile length, width, and inclination. The load imposed on the pile due to the foundation soil is equal to the weight of the wedge of soil minus the shear resistance acting between the sides of the wedge and the surrounding soil. • Fully-mobilized shear forces act on the sides of the wedge of soil supported by the pile but not on the face of the wedge. • The component of the supported weight of soil which acts normal to the pile axis is treated as a uniformly distributed load over the length of the pile.	*Experimental study findings* • Rao et al. compared their analytical model assuming pinned and fixed end supports to the experimental results for bending moment and found that the fixed support condition yielded better agreement.
	Assessment • This does not appear to be a suitable method due to the errors and unreasonable assumptions made during the development of the model.		

Appendix A.1, Overview and initial impressions of existing methods to calculate downdrag-induced bending moment in batter piles

Method	Pros/Cons	Assumptions	Remarks/ Other findings of study
Hance and Stemlau (2009)	• Procedure to determine the position of the neutral plane is incorrect. • Some assumptions used in the method are questionable	• The pile length below the neutral plane is considered to have an insignificant impact on the predicted values of maximum bending moment and is disregarded. • The pile length above the neutral plane considered to be a free-spanning beam with pinned end supports, therefore no displacement or moment is allowed at the neutral plane. • Pile tip resistance is incorrectly assumed to increases in linear proportion to shaft resistance. • Above the neutral plane, the pile is assumed to not make contact with the underlying soil. • The downdrag load on the pile is assumed to be equal to the integrated shaft resistance above the neutral plane. • The downdrag load is assumed to have a triangular distribution over the pile length above the neutral plane.	• This procedure predicts the maximum bending moment by 1) estimating the position of the neutral plane for a particular set of ground conditions and axial service load, 2) determining the downdrag force as the maximum shaft resistance above the neutral plane, 3) treating the pile above the neutral plane as a free-spanning beam with pinned end supports, 4)applying the component of the downdrag load which is perpendicular to the axis of the pile to the beam as a load with a triangular distribution.
	Assessment • This approach has flaws in the way the position of the neutral plane is estimated, which is required for estimation of bending moment. • This approach also makes some unreasonable assumptions in its development.		

Appendix A.1, Overview and initial impressions of existing methods to calculate downdrag-induced bending moment in batter piles

Method	Pros/Cons	Assumptions	Remarks/ Other findings of study
Stremlau and Hance (2009)	• Procedure to determine the position of the neutral plane is incorrect. • Some assumptions used in the method are questionable	• The pile length below the neutral plane is considered to have an insignificant impact on the predicted values of maximum bending moment and is disregarded. • The pile length above the neutral plane considered to be a free-spanning beam with pinned end supports, therefore no displacement or moment is allowed at the neutral plane. • The pile length above the neutral plane considered to be a free-spanning beam with pinned end supports, therefore no displacement or moment is allowed at the neutral plane. • When determining the soil pressure acting on the piles using the p-y curves from LPILE, the pile is assumed to be rigid.	• We have not been provided a complete example of the procedure for this method. • The position of the neutral plane is required for use of this procedure. The information provided on this method does not show how the neutral plane was determined, however it appears that it was estimated using the same approach that was used for the method by Hance and Stremlau (2009). • In this approach the maximum bending moment is predicted by 1) estimating vertical settlement through the clay profile, 2) obtaining p-y curves for a vertical pile embedded in the clay, 3) treating the pile above the neutral plane as a free-spanning beam with pinned supports, 4) determining the soil pressure distribution acting on the pile using the p-y curves and the component of settlement which acts perpendicular to the pile axis as the deflection for various points along the pile, 5) determine to maximum bending moment due to the non-uniform pressure acting on the beam.
	Assessment • Like Hance and Stremlau (2009), this approach makes some unreasonable assumptions in its development.		
Templeton (2009)	• This method or a derivative appears to be promising	• This approach uses the component of the soil displacement due to consolidation which acts normal to the batter pile axis as the magnitude of free-field soil displacement in LPILE.	• Usage of this approach will require reviewing the usage of p-y curves developed for vertical piles on battered piles.
	Assessment • A derivative of this approach appears to be promising.		

Appendix A.1, Overview and impressions of existing methods to calculate downdrag-induced bending moment in batter piles

Evaluation of the method by Shibata et al. (1982) to predict bending moment

Key findings:

- With calibration, this method yields good agreement with the measured value of peak bending moment using a simple closed-form expression.
- The method loses predictive accuracy if the pile passes through an embankment layer or extends above the ground surface.
- The model is very sensitive to the assigned value of coefficient of subgrade reaction. Shibata et al. use the correlation by Broms and Fredriksson (1976) which relates subgrade reaction at long-term loading to undrained shear strength and pile diameter. There are limitations to using this correlation for the general case, these include 1) it was originally intended for concrete piles and 2) the constant in the equation is often taken to be 10, however, Broms and Fredriksson report that values ranging from 7 to 27. In order to achieve good agreement with the measured results, constants ranging from 0.7 to 90 were applied to the clay foundation soils. The New Orleans district has found that a coefficient of 64 works well for many native clay soils.
- When the pile length is less than about 20 times the pile width, both measured and predicted bending moment distributions do not have an inflection point. Despite some discrepancies between the observed and predicted bending moment distributions, the values of peak bending moment are quite similar.
- When the pile length is greater than about 20 times the pile width, both measured and predicted bending moment distributions include an inflection point. For piles which do not pass through an embankment layer or extend above the ground surface, the method by Shibata et al. does a good job at predicting the distribution of bending moment. The peak predicted and measured value of bending moment occurs within 8 pile diameters for piles which do not extend through an embankment layer or above the ground surface.

Plots of bending moment distributions:

General notes:

- The bending moment distributions predicted by Shibata et al. (1982) were developed using a value of coefficient of subgrade reaction estimated using the relationship proposed by Broms and Fredriksson (1976). This relationship is provided in Equation 1, where S_u is the average undrained strength over the clay layer, D is the pile width or diameter, and N is a proportionality constant. Broms and Fredriksson observed values of N ranging from 7 to 27 for concrete piles. The practical recommendation used by the New Orleans District is 64 for many native soils. The value of N used to develop each plot is given in the accompanying table of input parameters. A single value of N was assigned to each soil type.

$$k_h = N\frac{S_u}{D} \qquad (1)$$

Laboratory model by Shibata et al. (1982)

Surcharge pressure = 20kPa

p_o	*5.5*	cm
Batter angle	*0.262*	rad
l	*60*	cm
S_u avg	*6*	kPa
D	*6*	cm
E	*2.10E+08*	kpa
I	*9.6*	cm^4
EI	*20.16*	
N	*10*	
k	*1000.00*	- N Cu/D (kN/m^3)
Beta	0.009	- (kD/4EI)^1/4
Beta *l	0.56	

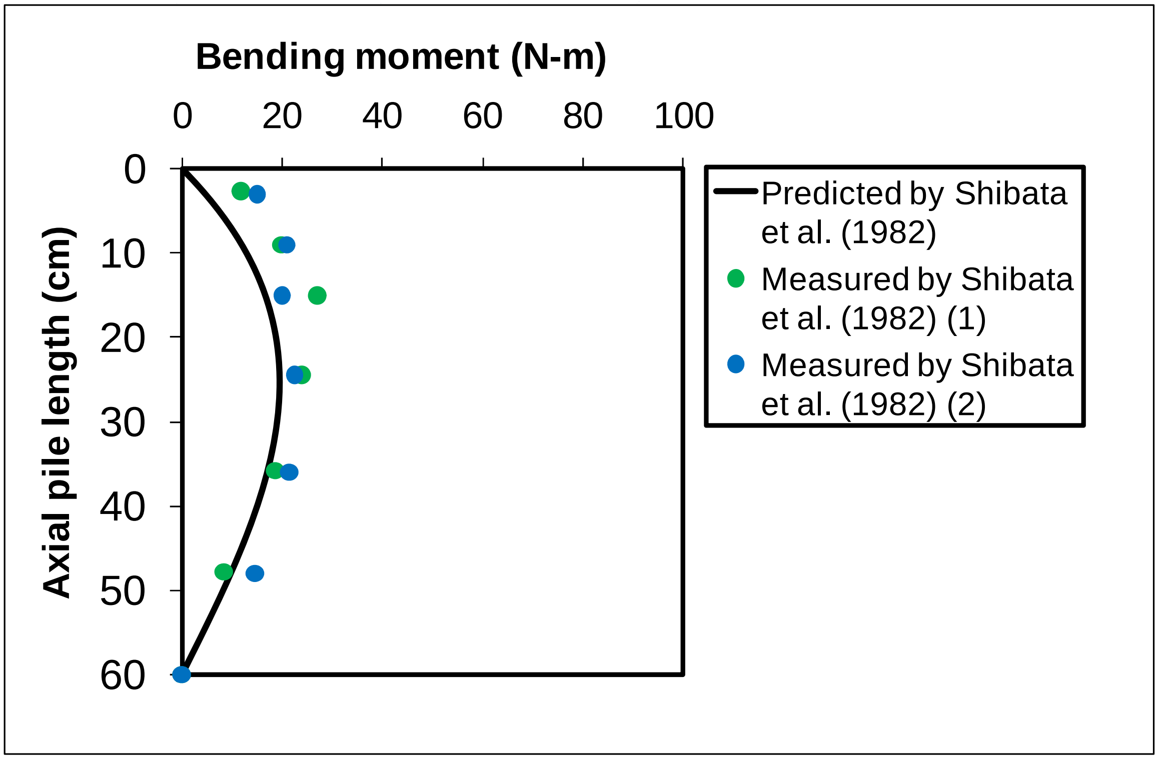

Surcharge pressure = 40kPa

p_o	6.65	cm	
Batter angle	0.262	rad	
l	60	cm	
S_u avg	12	kPa	
D	6	cm	
E	2.10E+08	kpa	
I	9.6	cm^4	
EI	20.16		
N	10		
k	2000.00		- 10 Cu/D (kN/m^3)
Beta	0.011		- (kD/4EI)^1/4
Beta *l	0.66		

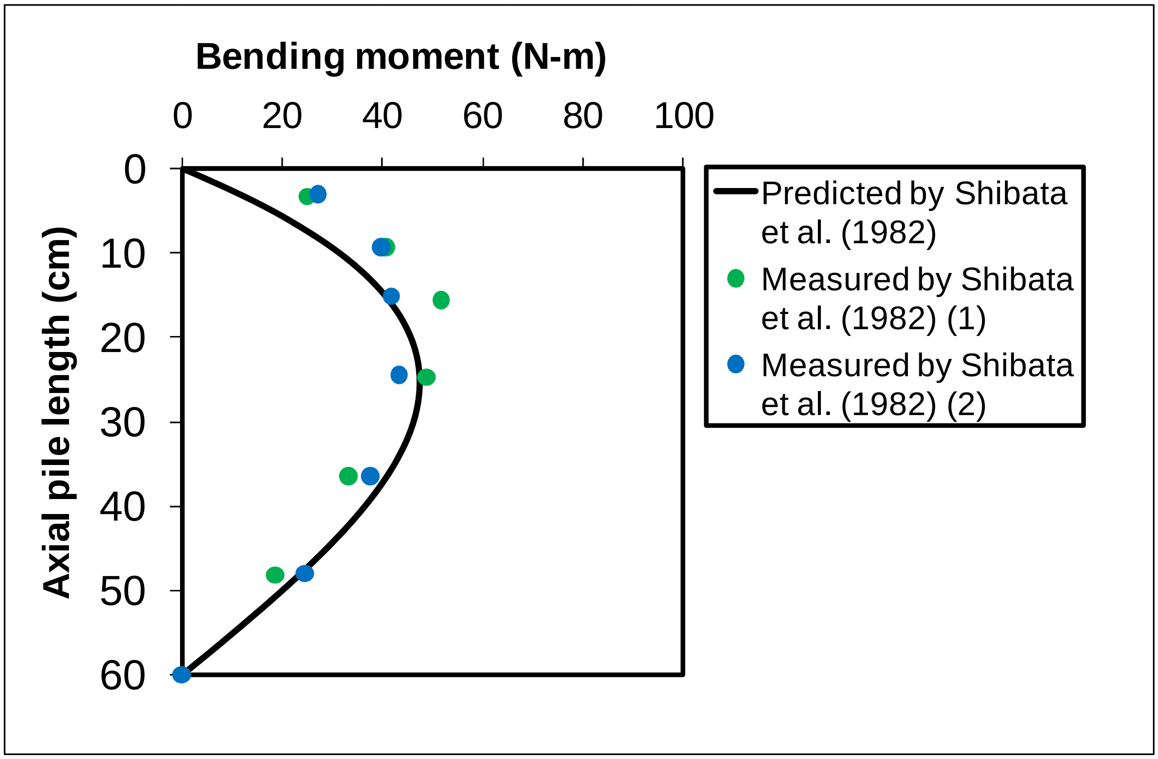

Surcharge pressure = 60kPa

p_o	*7.04*	cm
Batter angle	*0.262*	rad
l	*60*	cm
S_u avg	*18*	kPa
D	*6*	cm
E	*2.10E+08*	kpa
I	*9.6*	cm^4
EI	*20.16*	
N	*10*	
k	*3000.00*	- 10 Cu/D (kN/m^3)
Beta	0.012	- (kD/4EI)^1/4
Beta *l	0.73	

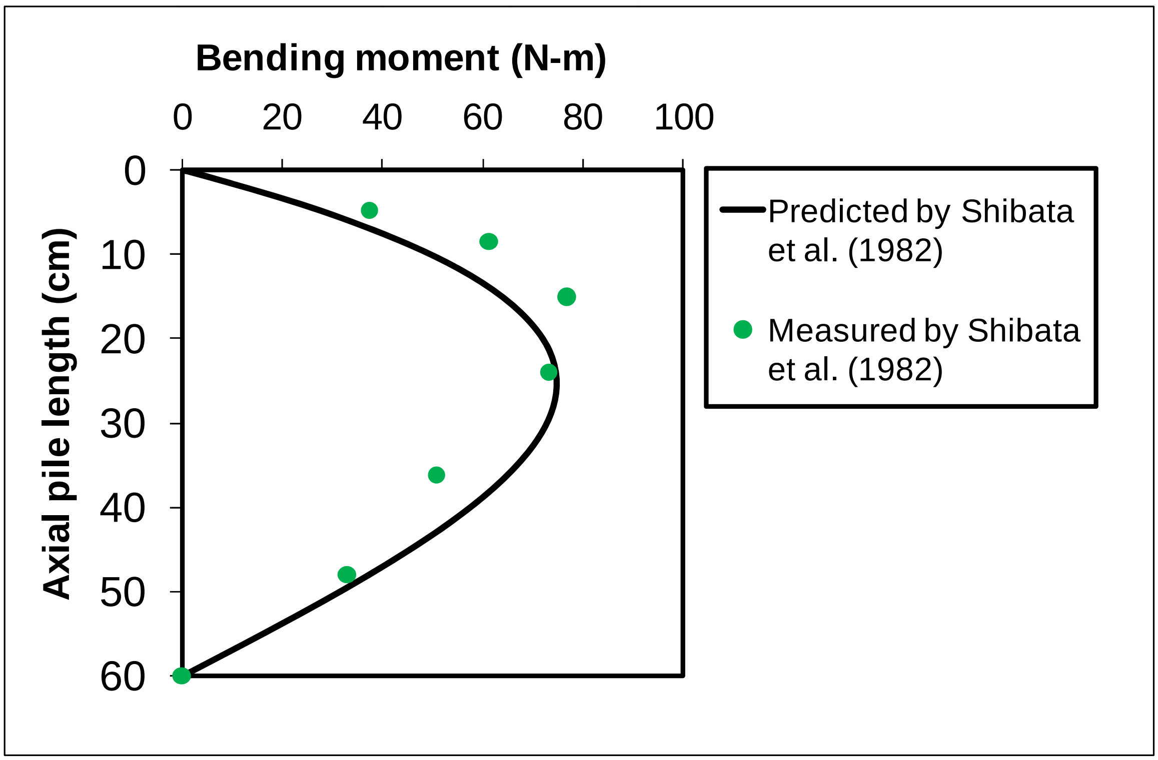

Laboratory model by Takahashi (1985)

In this model, the batter piles pass through an embankment layer and extend above the ground surface

Surface settlement after 1 week, batter angle of 20 deg

p_o	*0.046*	m
theta	*0.349*	rad
l	*1.78*	m
S_u avg	*5*	kPa
D	*0.075*	m
E	*2.00E+08*	kN/m2
I	*4.556E-09*	m^4
EI	*9.11E-01*	kN-m^2
N	*19*	
k	*1266.67*	- 10 Cu/D (kN/m^3)
Beta	2.260	- (kD/4EI)^1/4
Beta *l	4.02	

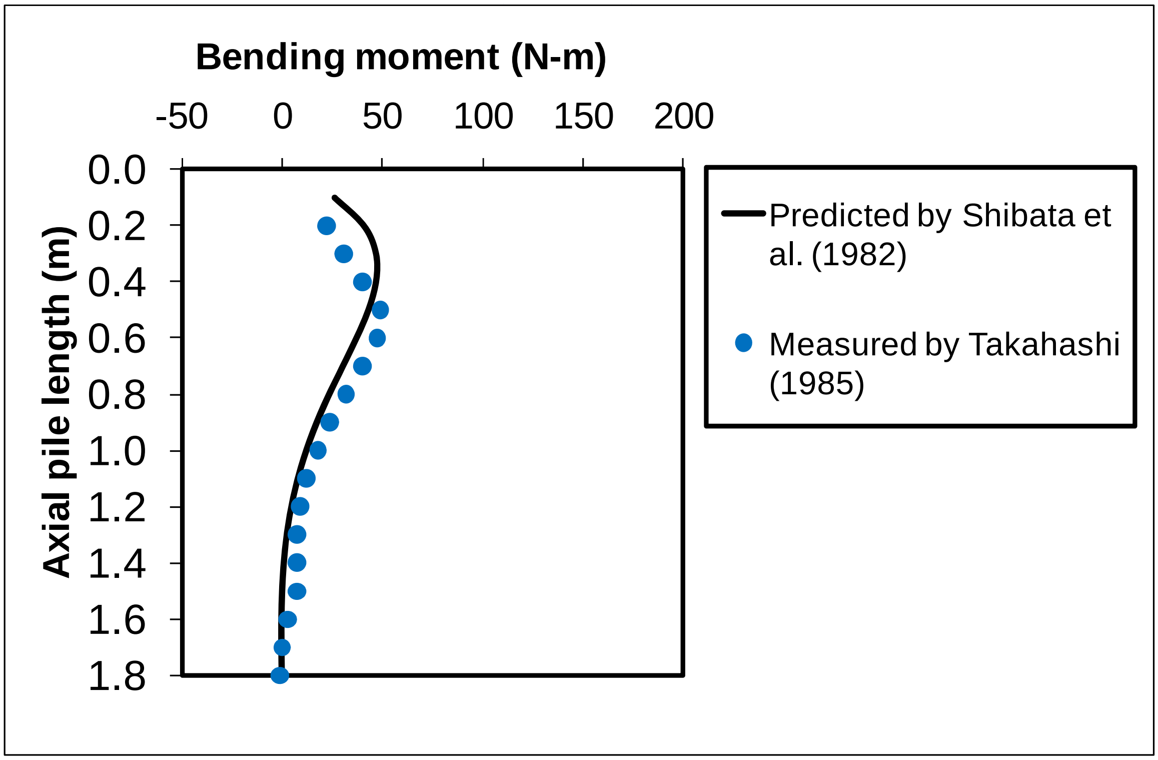

Surface settlement after 4 weeks, batter angle of 20 deg

p_o	0.101	m
theta	0.349	rad
l	1.78	m
S_u avg	5	kPa
D	0.075	m
E	2.00E+08	kN/m2
I	4.556E-09	m^4
EI	9.11E-01	kN-m^2
N	19	
k	1266.67	- 10 Cu/D (kN/m^3)
Beta	2.260	- (kD/4EI)^1/4
Beta *l	4.02	

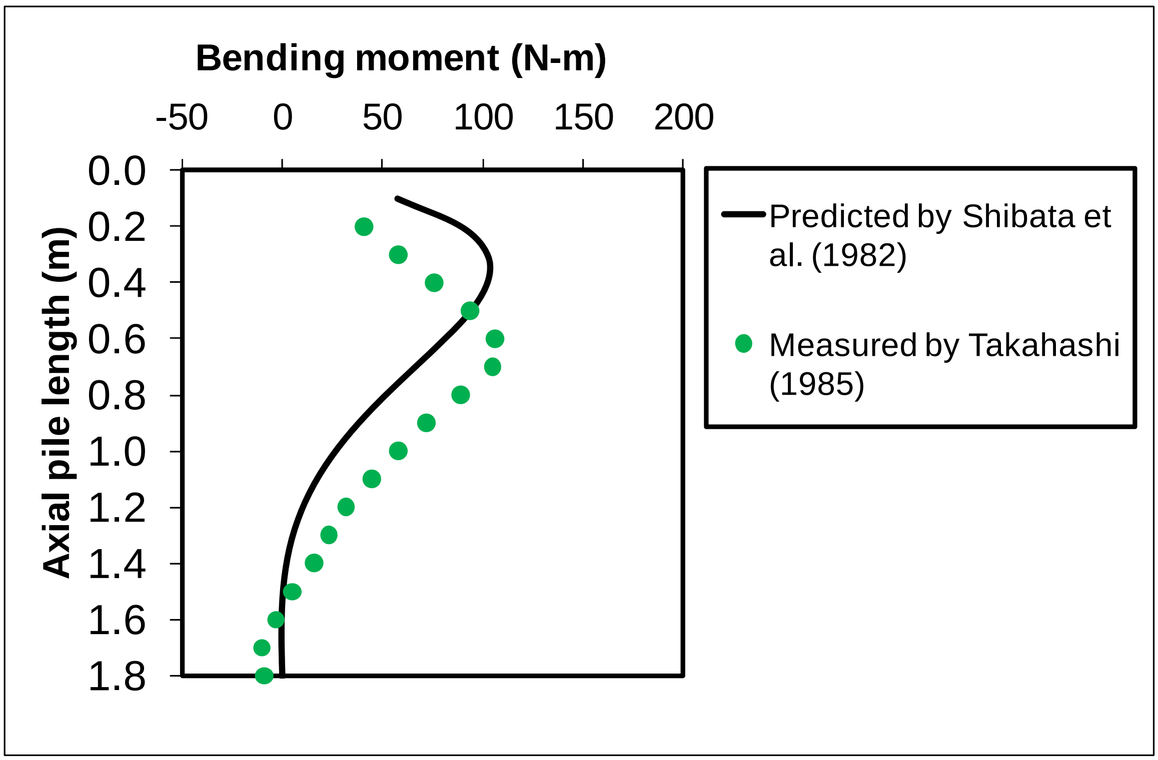

Surface settlement after 14 weeks, batter angle of 20 deg

p_o	*0.169*	m
theta	*0.349*	rad
l	*1.78*	m
S_u avg	*5*	kPa
D	*0.075*	m
E	*2.00E+08*	kN/m2
I	*4.556E-09*	m^4
EI	*9.11E-01*	kN-m^2
N	*19*	
k	*1266.67*	- 10 Cu/D (kN/m^3)
Beta	2.260	- (kD/4EI)^1/4
Beta *l	4.02	

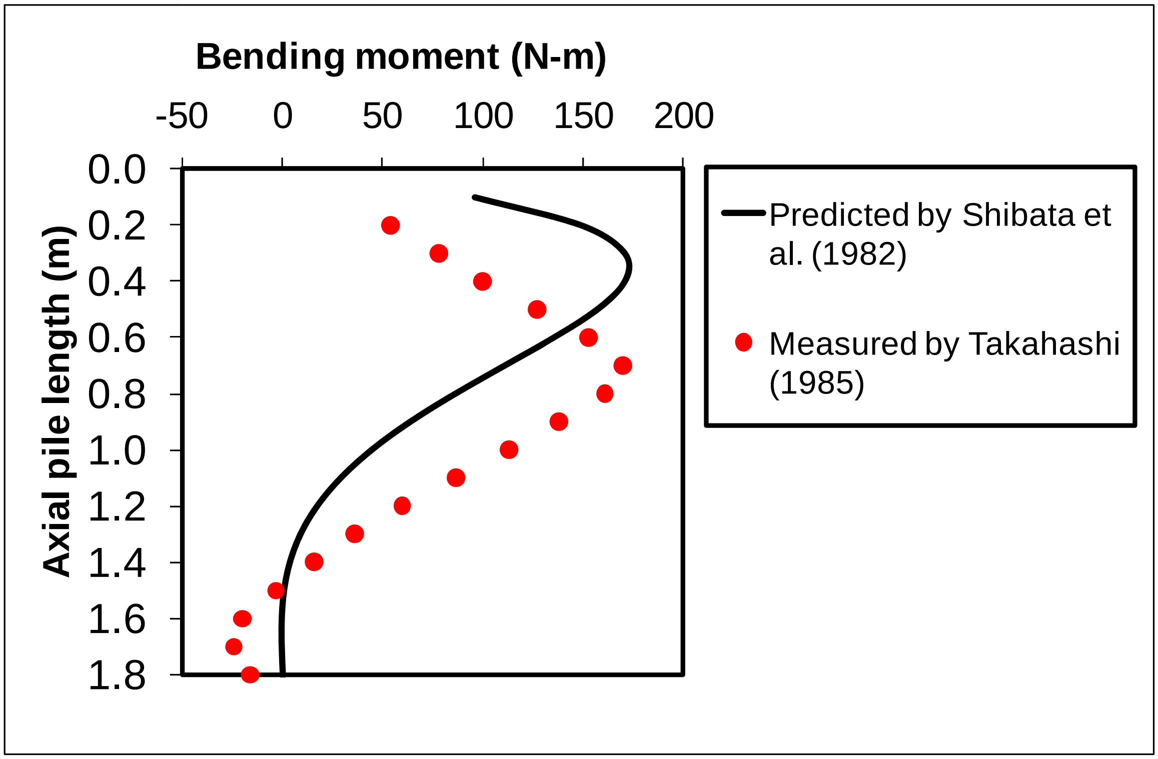

Surface settlement after 14 weeks, batter angle of 10 deg

p_o	*0.169*	m
theta	*0.175*	rad
l	*1.78*	m
S_u avg	*5*	kPa
D	*0.075*	m
E	*2.00E+08*	kN/m2
I	*4.556E-09*	m^4
EI	*9.11E-01*	kN-m^2
N	*19*	
k	*1266.67*	- 10 Cu/D (kN/m^3)
Beta	2.260	- (kD/4EI)^1/4
Beta *l	4.02	

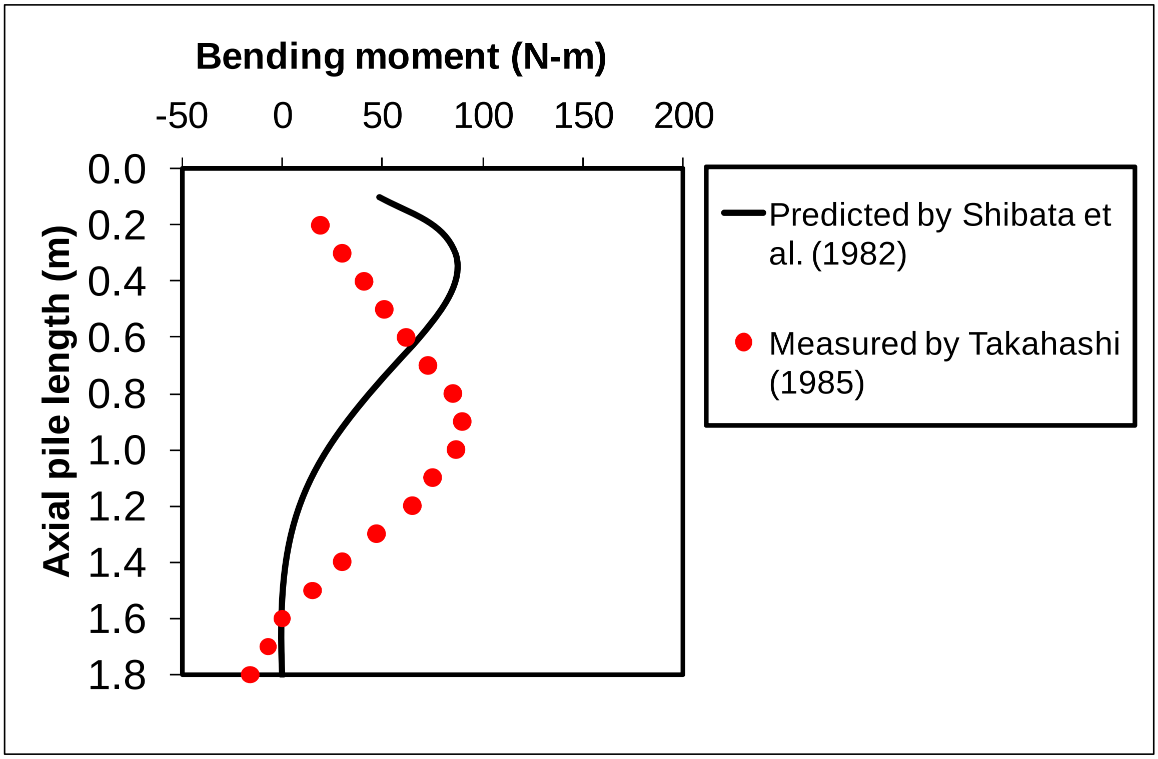

Field-scale study reported by Takahashi (1985)

In this model, the batter piles pass through an embankment layer.

Surface settlement after 55 days

p_o	*0.108*	m
theta	*0.262*	rad
l	*38.7*	m
S_u avg	*20*	kPa
D	*0.508*	m
E	*2.00E+08*	kN/m2
I	*0.00043927*	m^4
EI	*8.79E+04*	kN-m^2
N	*90*	
k	*3543.31*	- 10 Cu/D (kN/m^3)
Beta	0.268	- (kD/4EI)^1/4
Beta *l	10.35	

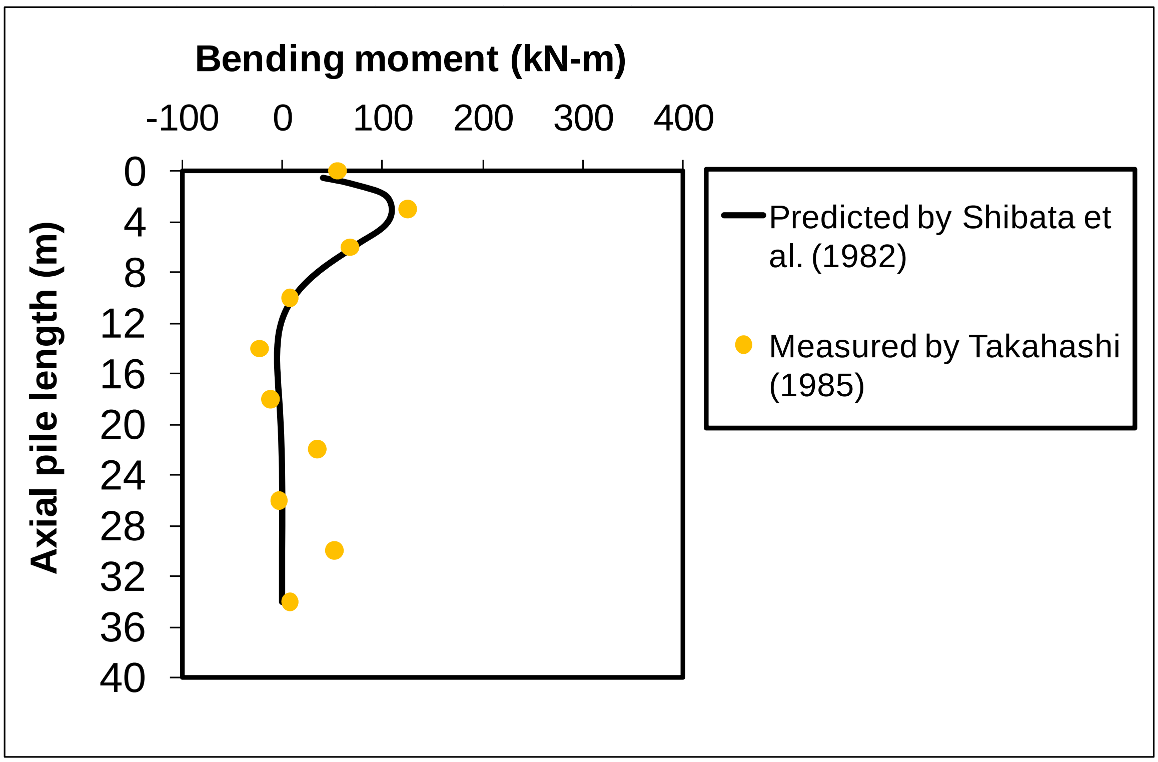

Surface settlement after 119 days

p_o	0.163	m
theta	0.262	rad
l	38.7	m
S_u avg	20	kPa
D	0.508	m
E	2.00E+08	kN/m2
I	0.00043927	m^4
EI	8.79E+04	kN-m^2
N	90	
k	3543.31	- 10 Cu/D (kN/m^3)
Beta	0.268	- (kD/4EI)^1/4
Beta *l	10.35	

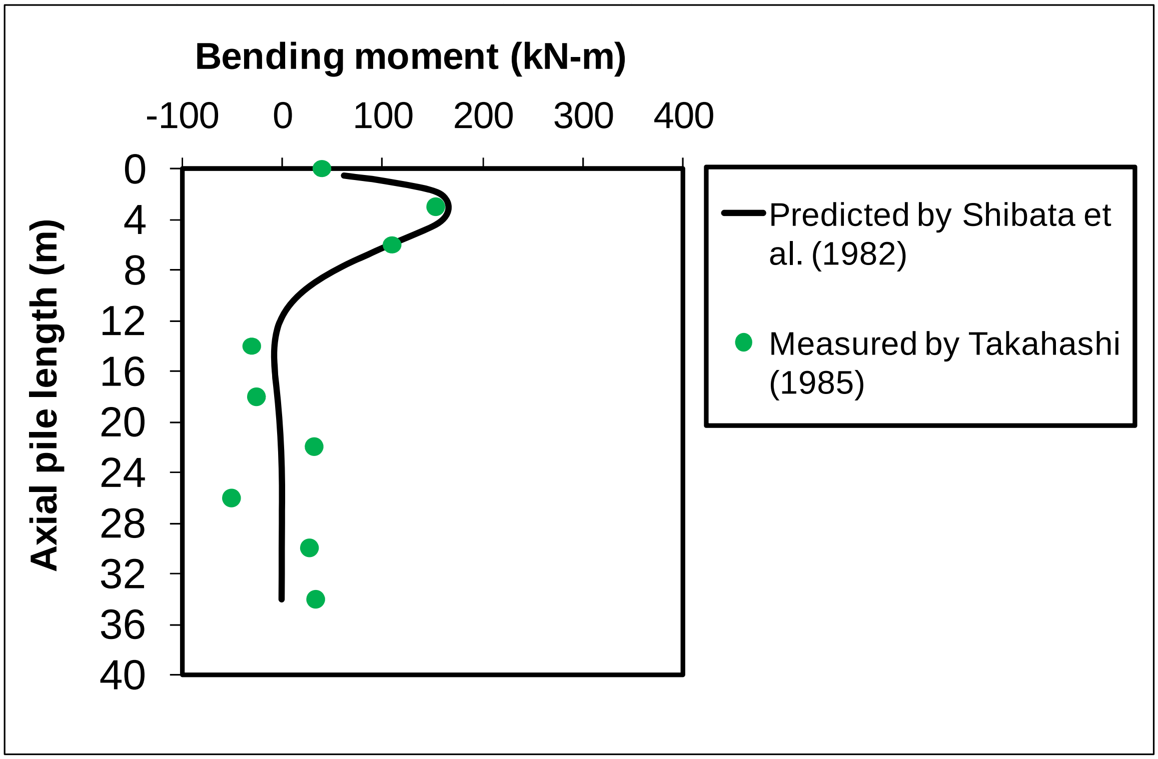

Surface settlement after 243 days

p_o	*0.23*	m
theta	*0.262*	rad
l	*38.7*	m
S_u avg	*22.5*	kPa
D	*0.508*	m
E	*2.00E+08*	kN/m2
I	*0.00043927*	m^4
EI	*8.79E+04*	kN-m^2
N	*90*	
k	*3986.22*	- 10 Cu/D (kN/m^3)
Beta	0.276	- (kD/4EI)^1/4
Beta *l	10.66	

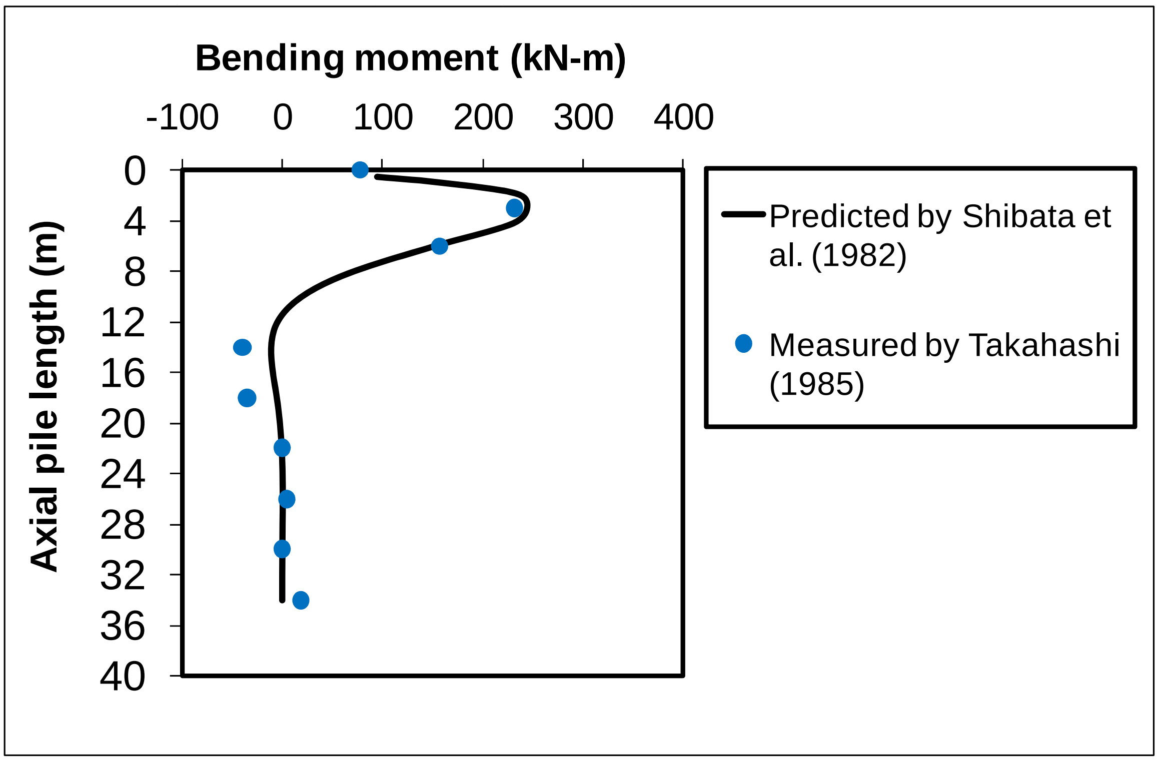

Surface settlement after 364 days

p_o	*0.263*	m
theta	*0.262*	rad
l	*38.7*	m
S_u avg	*25*	kPa
D	*0.508*	m
E	*2.00E+08*	kN/m2
I	*0.00043927*	m^4
EI	*8.79E+04*	kN-m^2
N	*90*	
k	*4429.13*	- 10 Cu/D (kN/m^3)
Beta	0.283	- (kD/4EI)^1/4
Beta *l	10.95	

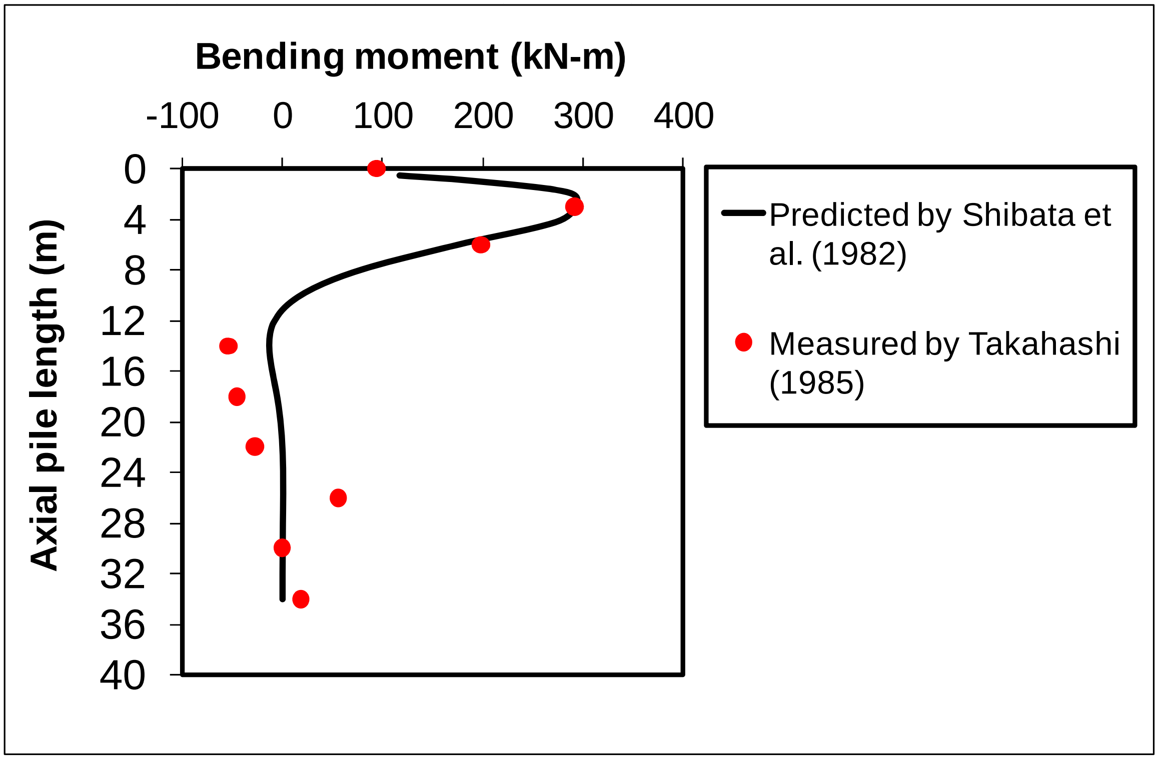

Field-scale study reported by Sawaguchi (1989)

p_o	0.263	m	
theta	0.262	rad	
l	33.65	m	
C_u avg	12	kPa	
D	0.508	m	
EI	179830	kN-m^2	
N	90		
k	5880.00	GIVEN	(kN/m^3)
k	2177.36	- 10 Cu/D	(kN/m^3)
Beta	0.254	- (kD/4EI)^1/4	
Beta *l	8.54		

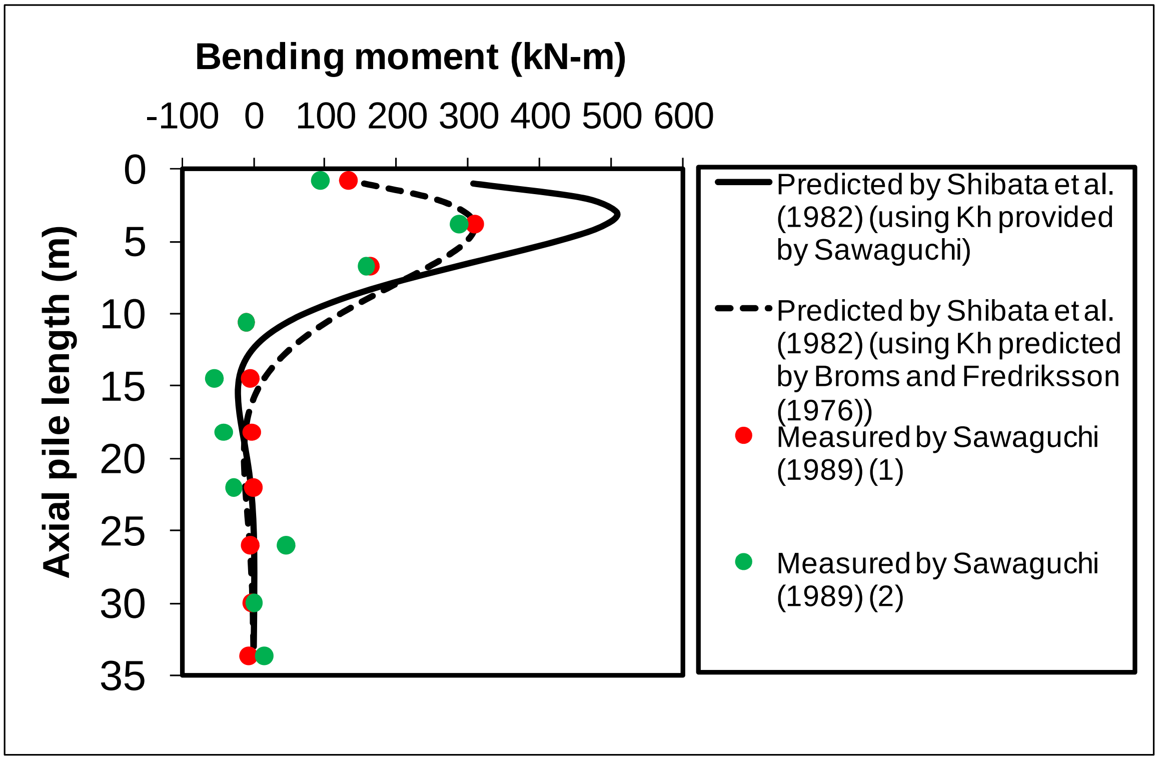

Laboratory model by Rao et al. (1994)

p_o	*0.0304*	m
theta	*0.175*	rad
l	*0.725*	m
S_u avg	*53*	kPa
D	*0.0381*	m
E	*7.00E+07*	kN/m2
I	*2.8928E-08*	m^4
EI	*2.02E+00*	kN-m^2
N	*0.7*	
k	*965.12*	- 10 Cu/D (kN/m^3)
Beta	1.460	- (kD/4EI)^1/4
Beta *l	1.06	

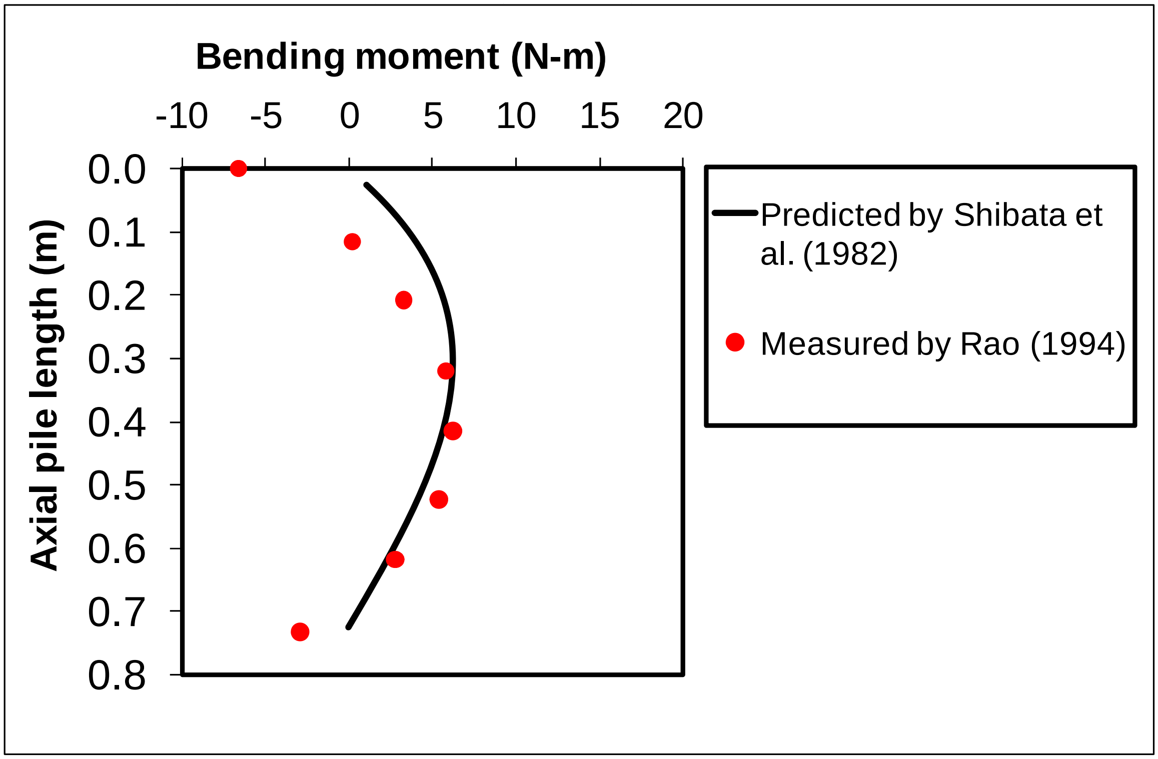

Appendix A.2, Overview of experimental and numerical studies and Available Data

Reference	Type of study	Description of Piles	Description of Foundation soil	Description of embankment / foundation loading	Results
Shibata et al. (1982)	Laboratory model	A 3x2 group of piles composed of steel pipe having an outer diameter of 6.0cm, wall thickness of 1.2mm, and a length of 60cm were installed in the apparatus at a batter angle of 15 degree from vertical. Vertical sections were welded on the tops of the battered portion of the piles. Three series of tests were performed, one of which used a bitumen coating on the piles. Test series were also performed on single vertical piles and vertical pile groups.	A slurry of kaolin was poured around the pile group. The kaolin had a LL = 52, a PL = 39, a clay fraction of 39%, and a specific gravity of 2.61. A 10cm thick sand drainage layer was provided at the base of the sample tank. The kaolin slurry was allowed to consolidate under its own weight prior to application of a surcharge pressure.	A vinyl plastic sheet placed over the top of the clay slurry and pile tops was used to create a seal that allowed a surcharge pressure to be applied using air pressure. Tests were performed at surcharge pressures of 20, 40, and 60 kPa.	Results for the battered pile groups include plots of downdrag pressure versus time for the various surcharge pressures used. Also plots of bending moment versus depth along the pile are provided in Figure 14 of the paper. Plots of bending moment at various positions along the pile versus consolidation pressure are provided in Figure 15 of the paper.
Takahashi (1985)	Laboratory model	Piles consisted of rectangular plates measuring 1780mm long, 75mm wide, and 9mm thick. Four pairs of pile were installed with	A remolded fully saturated clay sample was formed in the apparatus prior to pile installation. The clay had a LL=89.8, a PL=35.2, and a specific gravity of 2.72.	The clay was subjected to a consolidation pressure of 10kN/m^2 using 220mm of steel shot placed over an upper drainage layer of sand.	Results include six plots of max bending moment for all batter angles, the distribution of

Reference	Type of study	Description of Piles	Description of Foundation soil	Description of embankment / foundation loading	Results
		hinged tops at batter angles of 5, 10, 15, and 20 degrees from vertical. Piles are pinned at the base of the clay using hinges.	Figure 6 in the paper shows a profile of the saturated unit weight and unconfined compressive strength measured after the test. Coefficient of compressibility, m_v, is stated as $15m^2/MN$		bending moment for two pile inclinations, and a plot of maximum bending moment versus ground settlement magnitude.
Takahashi (1985)	Numerical model (3D) represents the laboratory tests	Piles treated as 3D elastic beam elements, likely with steel properties. Batter angles of 10 and 20 degrees were considered. Springs, presumably linear, are considered between the pile and the surrounding soil.	Clay is modeled as an elastic material with a Young's modulus of $44kN/m^2$ and a Poisson's ratio of 0.33.	Steel and upper sand layer applied as pressures in the model. No additional details are provided about loading.	Figure 15 of the paper shows the predicted distribution of bending moment for a batter angle of 20 degrees.
Takahashi (1985), Sato et. al (1987), and Sawaguchi (1989)	Field study	A 2x2 group of steel pile piles (ϕ508xt9xl38700mm) were installed through the test embankment at a batter angle of 15 degrees. The arrangement of the pile is not provided. Two of the piles were coated with	The foundation soil consisted of a 30m deposit of clayey soil containing shell fragments. Piles were terminated in a stiff clay containing gravel and having an N value of 20. A profile of moisture content, total unit weight, and unconfined compressive	A 2.5m high embankment with plan dimensions of 40m x 25m. Consolidation of the clay soil was monitored for one year	Figures 20 through 24 in Takahashi (1985) detail ground settlements and the distribution of axial force, bending moment, and elastic compression

Appendix A.2, Overview of experimental and numerical studies and Available Data

Reference	Type of study	Description of Piles	Description of Foundation soil	Description of embankment / foundation loading	Results
		bitumen. The tops of the piles were hinged and extended above the ground surface. Pile settlements are provided in Table 2 in the paper.	strength is provided in Figure 19 of the paper by Takahashi (1985).		observed in the piles.
Rao et al. (1994)	Laboratory model	The model consisted of a square grouping of piles set at a batter angle of 10 degrees and fixed at the top using steel plate. The piles were made from aluminum tubing having a diameter of 38.1mm, a thickness of 1.5mm, and measuring 725mm in length.	The piles were installed in an empty tank and 570mm of saturated clay was placed and tamped around the pile group. The clay had a LL=53, a PL=19, G_s=2.66, w=49%, unit weight of 17.2kN/m^3, and a vane shear strength of 60kN/m^2. Sand drainage layers 50 and 100mm thick were placed above and below the clay layer, respectively.	Loading of the clay was performed by placing weights on top of a steel plate at the top of the sand surface. It is not clear in the paper whether this is the same plate the piles are tied to. Two surcharge pressures were used in the study.	The results include plots of settlement versus time and distribution of bending moment for the two surcharge loads.
Veeresh (1996) as reported in Rajashree and Sitharam (2001)	Laboratory model	Isolated steel piles with a diameter of 19mm, a wall thickness of 2.1mm, and a length of 620mm were installed in soft clay. The top of the piles were left free. The following batter angles were considered: 0, +10, +30, -10, and -30	The soft clay used in the model was stated to have a liquid limit of 82% and a plastic limit of 2% which falls outside the limits of known soils. The clay was also has a water content of 50%, a unit weight of 17.2 kN/m^3, an undrained	Lateral loads were applied to the free ends of the piles at the ground surface elevation in 24N increments up to 120N. A cyclic load analysis was also included in this study.	The paper includes plots of lateral deflection against applied load and against depth at a load of 120N. Plots of the distribution of bending moment are also

Reference	Type of study	Description of Piles	Description of Foundation soil	Description of embankment / foundation loading	Results
		degrees.	strength of 7.5kPa, and a modulus of 415 kPa.		provided.
Navin (2009) *Baseline T-Wall model for St. Bernard Parish*	Numerical model	A 2D FLAC model considers three battered H-piles (two on protected side) and a sheet pile. Battered piles are HP14x89 and the sheet pile is PZ-22. The tip elevation for the H-piles is El -130 and EL -45 for the sheet pile. The spacing between H-piles perpendicular to the centerline of the wall is 6 ft. The batter angle of the H-piles is 3V:1H. The tops of the piles are pinned and are embedded 0.75ft into the T-Wall concrete to provide some moment capacity. 3D soil-pile interaction is represented using spring-slider elements between the piles and the soil in both normal and shear directions.	Soil properties for drained and undrained stages of the analysis are given in Tables 1 through 4 of the reference document.	The existing foundation soils are brought into equilibrium with gravity under drained conditions. The water table is established and the model is analyzed again. The piling is installed and the model is analyzed again. The embankment is placed (H=20 ft max, El +20) and the model is analyzed again. Soil properties are changed to reflect undrained conditions and the model is analyzed at increments of flooding ranging from 1.5 to 9 ft.	Profiles of shear load, axial load, moment, lateral displacement, and strain along the batter piles are provided.

Appendix A.2, Overview of experimental and numerical studies and Available Data

Reference	Type of study	Description of Piles	Description of Foundation soil	Description of embankment / foundation loading	Results
Navin (2009) *T-Wall model to assess settlement*	Numerical model	The model considers one batter pile on the protected side and one on the flood side with a sheet pile separating the two. Battered piles are HP14x89 and the sheet pile is PZ-22. The spacing between H-piles perpendicular to the centerline of the wall is not provided in the reference document. The batter angle of the H-piles was scaled from Figure 3 in the report to be 1H:3V.	The same soil properties used in the baseline analysis for St. Bernard Parish are presumably used in this analysis.	The loading conditions modeled in the baseline analysis for St. Bernard Parish was followed up to the point of flood load, where instead of incremental flood loads, a vertical line load of 13.3 kpf was applied to the wall under drained conditions	Horizontal profiles of vertical changes in stress are provided at various elevations over the length of the piles.

Digitized Bending Moment Distributions

Shibata et al. (1982)

Surcharge Pressure = 20kPa

Bitumen-coated piles (RED)		Uncoated piles (1) (GREEN)		Uncoated piles (2) (BLUE)	
Y	X	Y	X	Y	X
Axial Length	Bending Moment	Axial Length	Bending Moment	Axial Length	Bending Moment
m	N-m	m	N-m	m	N-m
3	10	2.6	11.8	3	15.1
8.6	12.6	9	19.8	9	21
15	18	15	27	15	20
24	17	24.4	24	24.4	22.5
36	13	35.8	18.7	36	21.5
47.6	10	47.8	8.4	48	14.5
60	0	60	0	60	0

Surcharge Pressure = 40kPa

Bitumen-coated piles (RED)		Uncoated piles (1) (GREEN)		Uncoated piles (2) (BLUE)	
Y	X	Y	X	Y	X
Axial Length	Bending Moment	Axial Length	Bending Moment	Axial Length	Bending Moment
m	N-m	m	N-m	m	N-m
3.3	17	3.3	25	3	27.2
9.3	25.4	9.3	40.7	9.3	39.7
15.6	38	15.6	51.7	15.1	41.8
24.6	35	24.7	48.8	24.4	43.4
36.6	24.5	36.5	33.2	36.4	37.5
48.2	17.5	48.2	18.6	48	24.5
60	0	60	0	60	0

Surcharge Pressure= 60kPa

Bitumen-coated piles (RED)		Uncoated piles (1) (GREEN)	
Y	X	Y	X
Axial Length	Bending Moment	Axial Length	Bending Moment
m	N-m	m	N-m
4.8	24.5	4.8	37.4
8.5	38.5	8.5	61.2
14.5	56	15	76.8
24	54	24	73.2
35.5	36.4	36.2	50.8
47	26	48	33
60	0	60	0

Plots of Moment Distribution

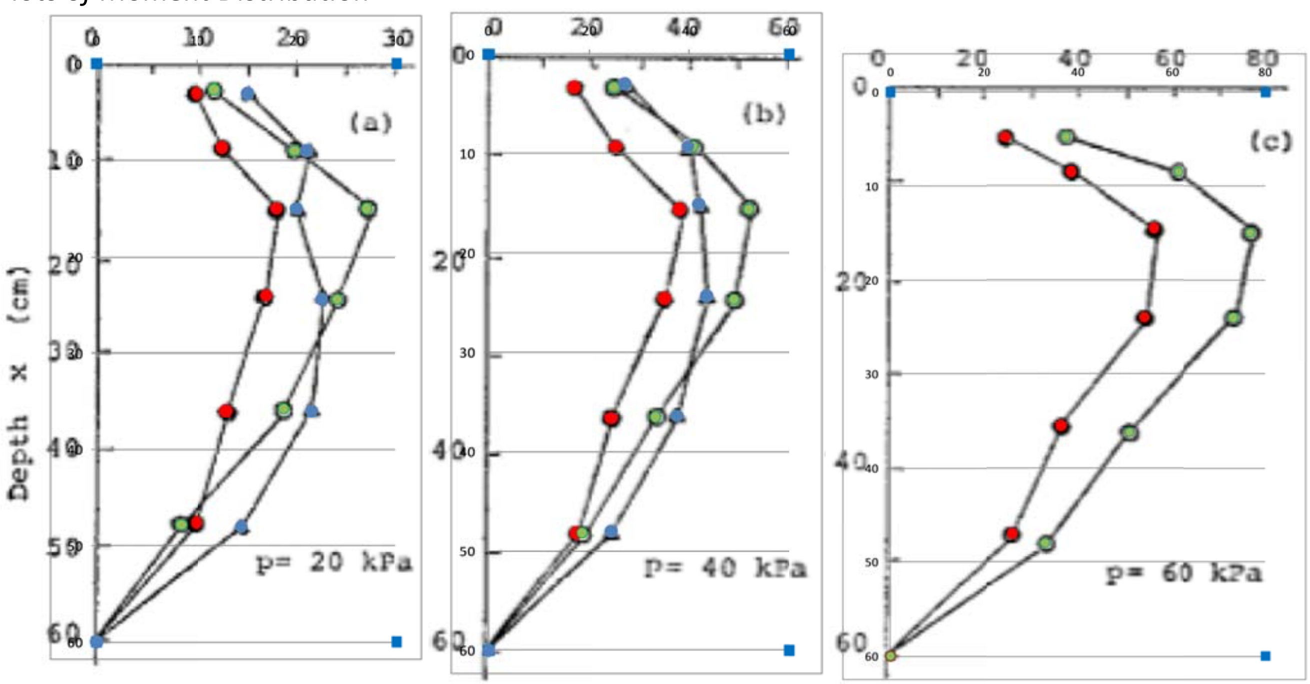

Takahashi (1985)

Experimental bending moment distributions after 1, 4, and 14 weeks of consolidation for batter angle of 20 degrees

1 Week		4 Weeks		14 Weeks	
Y	X	Y	X	Y	X
Axial Length	Bending Moment	Axial Length	Bending Moment	Axial Length	Bending Moment
cm	N-m	cm	N-m	cm	N-m
10	22	10	41	10	54
20	31	20	58	20	78
30	40	30	76	30	100
40	49	40	94	40	127
50	47.5	50	106	50	153
60	40	60	105	60	170
70	32	70	89	70	161
80	24	80	72	80	138
90	18	90	58	90	113
100	12	100	45	100	87
110	9	110	32	110	60
120	7.5	120	23.5	120	36
130	7.5	130	16	130	16
140	7.5	140	5	140	-3
150	3	150	-3	150	-20
160	0	160	-10	160	-24
170	-1	170	-9	170	-16

Plots of moment distribution

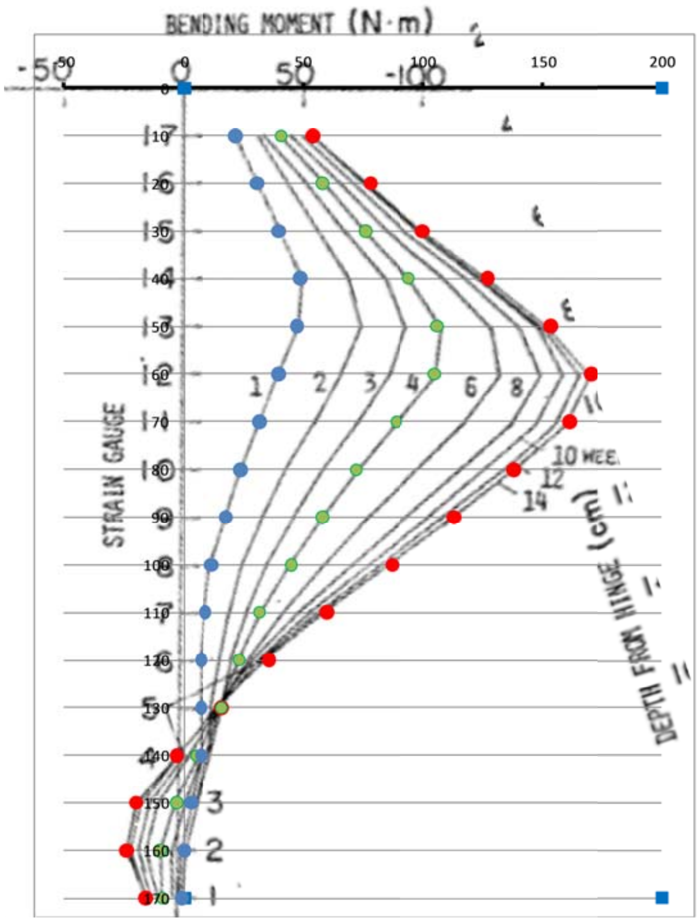

Experimental bending moment distributions after 14 weeks of consolidation for batter angle of 10 degrees

14 Weeks	
Y	X
Axial Length	Bending Moment
cm	N-m
20	19
30	30
40	41
50	51
60	62
70	73
80	85
90	90
100	87
110	75
120	65
130	47
140	30
150	15
160	0
170	-7

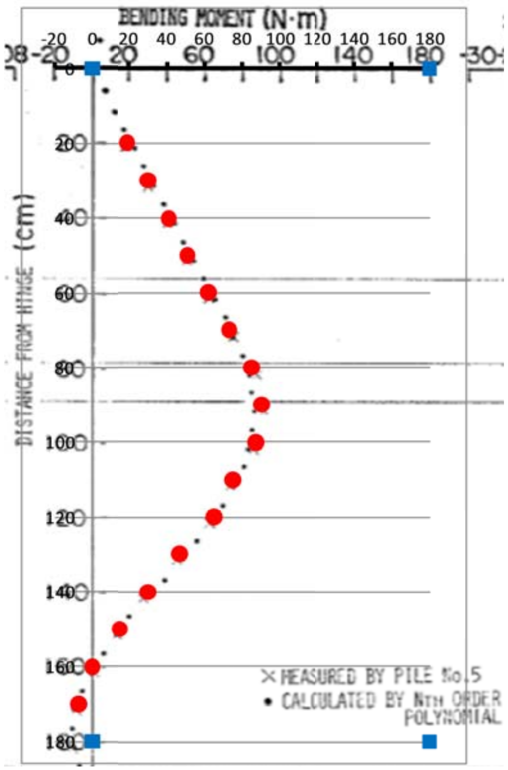

Field-scale study bending moment distributions after 55, 119,264, and 364 days of consolidation for batter angle of 15 degrees

55-days

Y	X
Axial Length	Bending Moment
m	kN-m
0	-55
3	-125
6	-68
10	-8
14	22
18	12
22	-35
26	3
30	-52
34	-8

119-days

Y	X
Axial Length	Bending Moment
m	kN-m
0	-40
3	-153
6	-110
14	30
18	25
22	-32
26	50
30	-27
34	-34

243-days

Y	X
Axial Length	Bending Moment
m	kN-m
0	-78
3	-232
6	-157
14	40
18	35
22	0
26	-5
30	0
34	-19

364-days

Y	X
Axial Length	Bending Moment
m	kN-m
0	-94
3	-292
6	-198
14	54
18	45
22	27
26	-56
30	0
34	-19

Plots of moment distribution

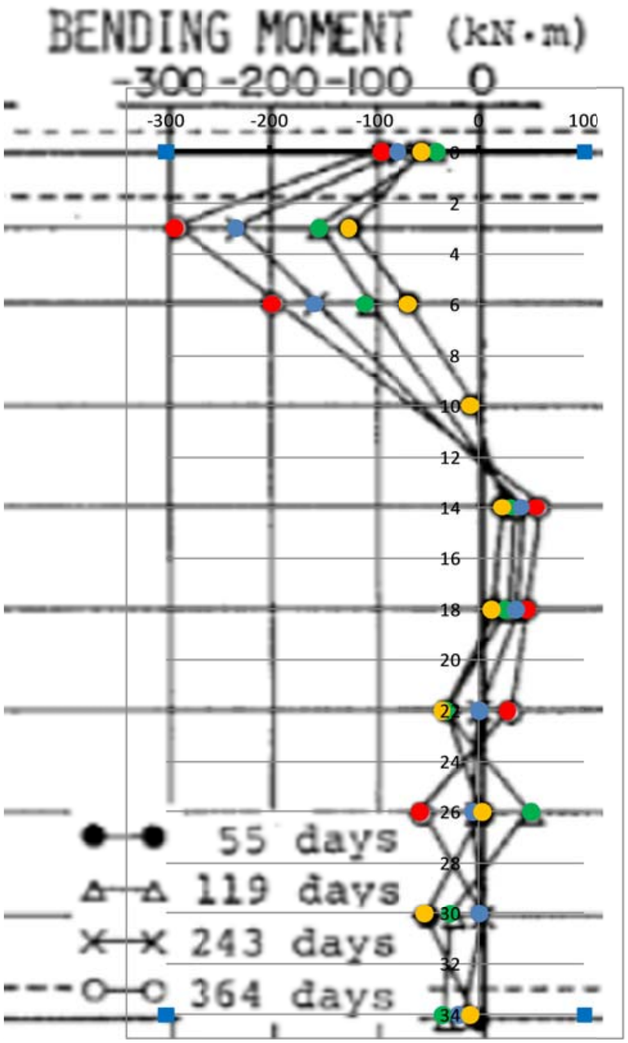

Sawaguchi (1989)

Field-scale bending moment distributions after one year of consolidation for batter angle of 15 degrees

Pile C		Pile D	
Y	X	Y	X
Axial Length	Bending Moment	Axial Length	Bending Moment
m	tf-m	m	tf-m
0.8	-13.5	0.8	-9.5
3.8	-31.5	3.8	-29.3
6.75	-16.65	6.75	-16.1
10.6	1	10.6	1
14.5	0.5	14.5	5.6
18.2	0.2	18.2	4.3
22	0	22	2.8
26	0.4	26	-4.6
30	0.3	30	-0.1
33.65	0.6	33.65	-1.5

Plots of moment distribution

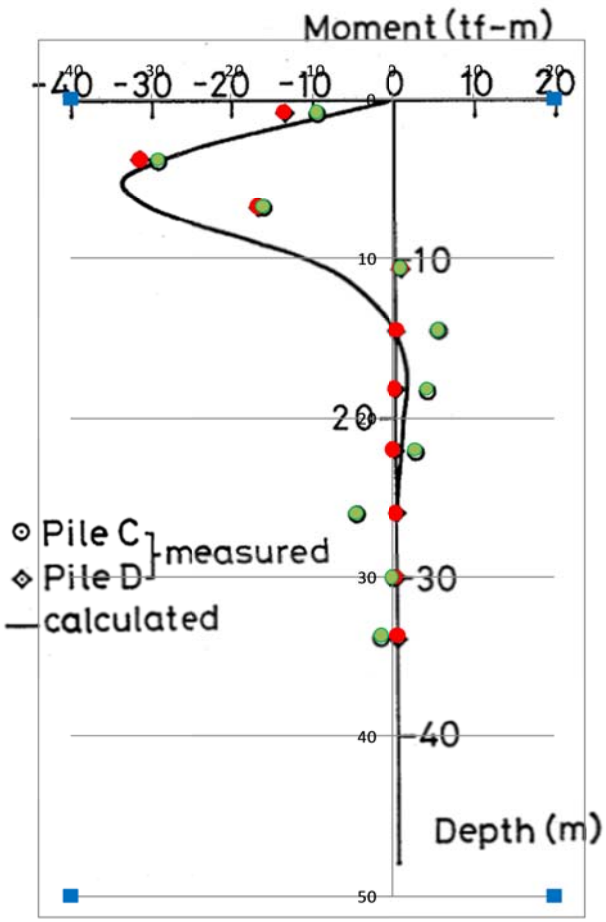

Rao et al. (1994)

Field-scale bending moment distributions after 400 hours of consolidation for batter angle of 10 degrees

Y	X
Axial Length	Bending Moment
m	N-m
0	-6.6
0.115	0.2
0.208	3.3
0.32	5.8
0.415	6.2
0.523	5.4
0.618	2.8
0.732	-2.9

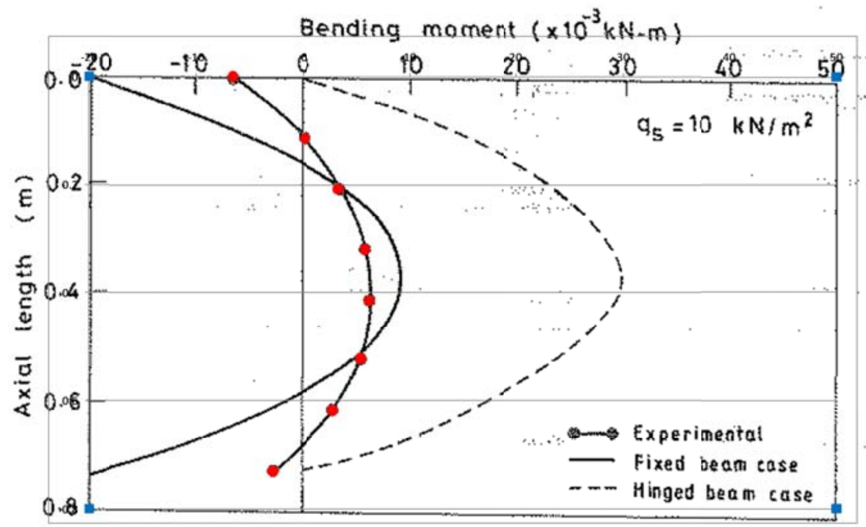

Navin (2009)

Moment distributions calculated using FLAC for T-Wall Foundation Elements in St. Bernard Parish

These plots are taken directly from the document "Overview of FLAC analysis for St. Bernard Parish." The plots representing the "Drained" condition apply to the analysis which considered drained conditions during stress initialization, pile installation, and fill placement and undrained conditions during the short-term flood loading. The plots representing the "Undrained" condition apply to the analysis which considered undrained soil properties for all phases.

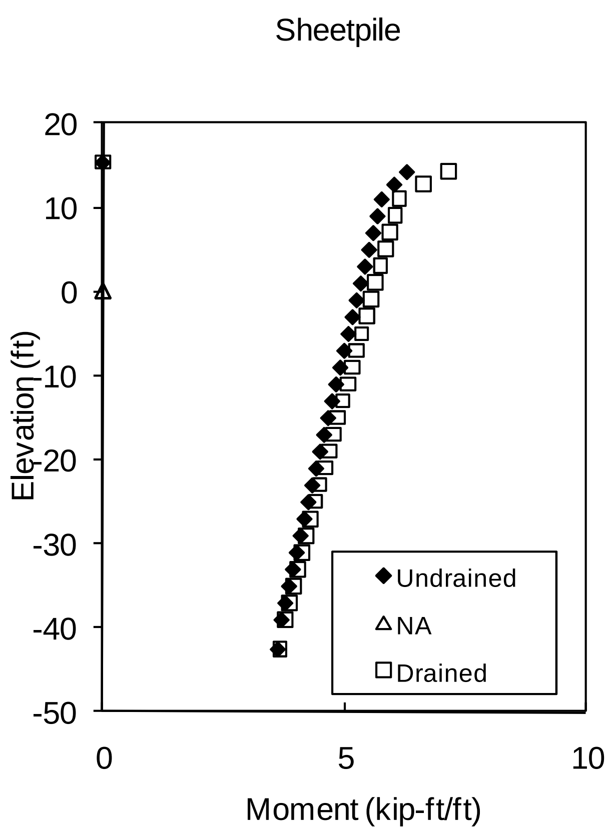

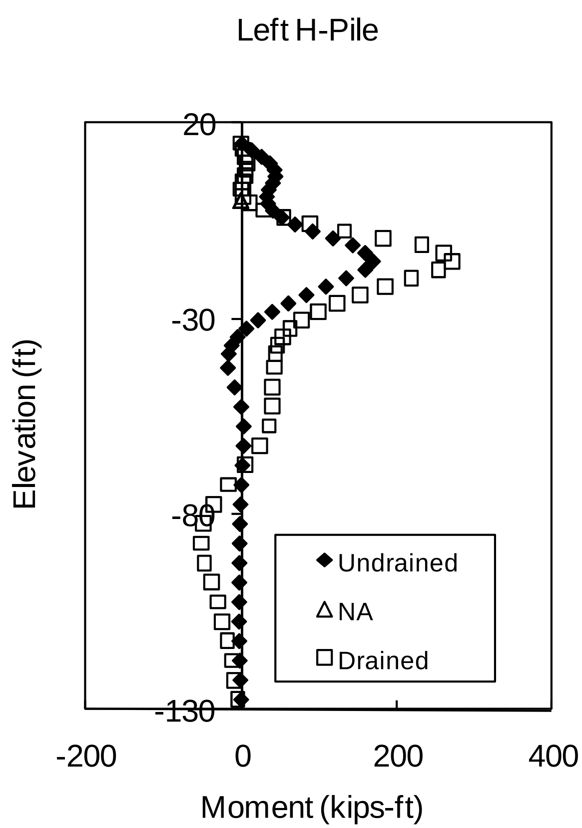

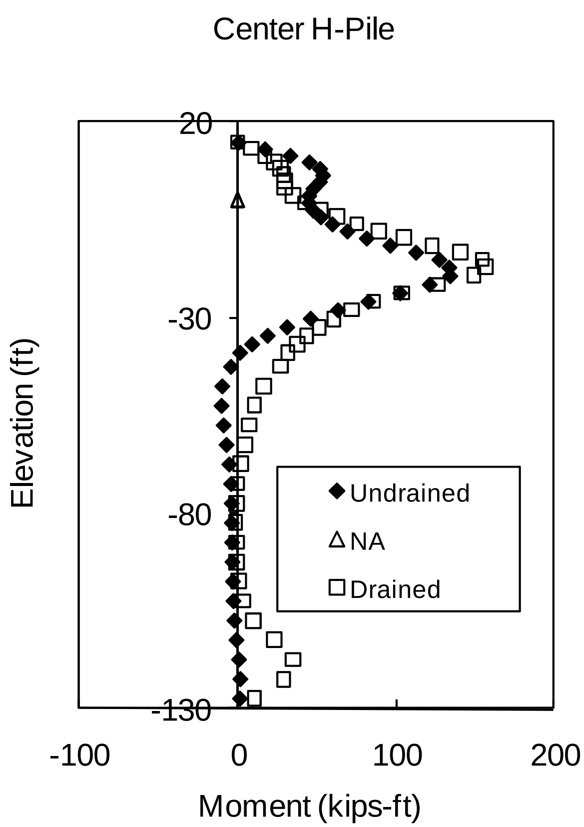
Center H-Pile
20
-30
-80
-130
-100
0
100
200
Elevation (ft)
Moment (kips-ft)
Undrained
NA
Drained

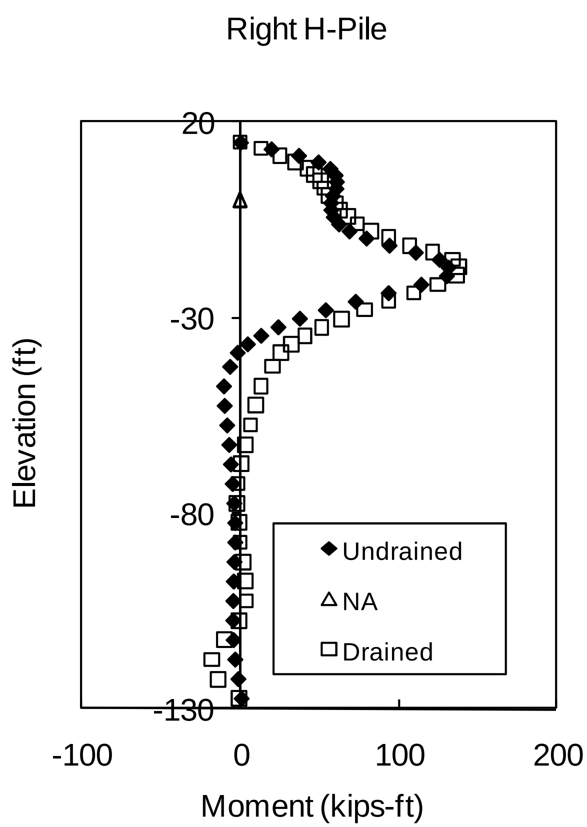
Right H-Pile
20
-30
-80
-130
-100
0
100
200
Elevation (ft)
Moment (kips-ft)
Undrained
NA
Drained

Reference:

Broms, B., and Fredericksson, A. (1976). "Failure of pile-supported structures caused by settlements." Proceedings of the 6th European Conference on Soil Mechanics and Foundation Engineering, 383-386.

Overview:

This study presents the development of an analytical model to estimate the deflection and bending moment induced in a batter pile due to downdrag. The model is then used to theoretically explore the influences of the following factors on bending moment and deflection: the modulus of the pile material, pile length, settlement magnitude, shear strength of the foundation soil, restraint conditions at the ends of the pile, the variation of shear strength with depth, and the presence of a dessicated upper crust. Also investigated was the magnitude of ground settlement that could be tolerated by a pile with a moment capacity of 41kNm installed at a certain inclination angle through a clay layer with a constant undrained strength.

Development of analytical model:

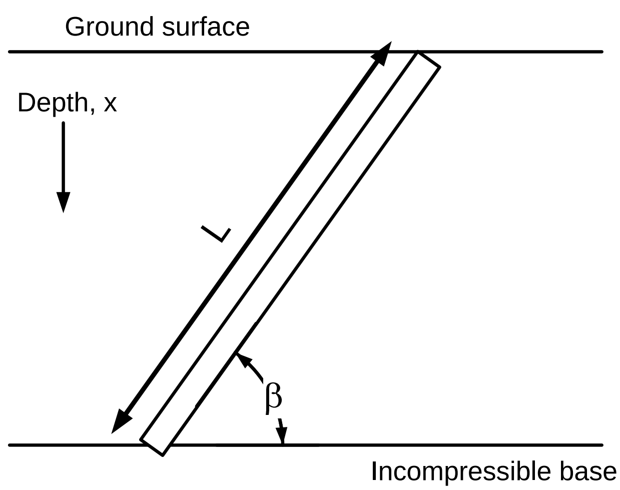

Figure 1: Analytical model proposed by Broms and Fredriksson

Broms and Fredriksson assume that bending moments are induced in batter piles due to the component of settlement of the surrounding soil that is perpendicular to the pile axis. They acknowledge that the component of downdrag force that acts axial to the pile, in addition to the imposed load at the pile head, has the effect of increasing the moment capacity of the pile, but this influence has been neglected in the model. Their model assumes a linear soil response to pile deflection by the use of a coefficient of subgrade reaction, k_h, which they assumed can be approximated from the undrained shear strength, S_u, of the clay, and the pile diameter, D, according to Equation 1.

$$k_h = 10\frac{S_u}{D} \qquad 1$$

Similar to the methods by Shibata (1982) and Takahashi (1985), the reaction of the soil is proportional to the relative displacement of the pile and the soil by Equation 2, which is equal to the difference between the component of settlement normal to the pile axis, $\delta_x \cos\beta$ and the lateral deflection of the pile, y_x. As indicated in Figure 1, β is the inclination of the pile from horizontal and δ_x is the vertical ground settlement.

$$q_x = k_h\left(\delta_x \cos\beta - y_x\right) \qquad 2$$

To relate the load-displacement relationship of the soil the to the lateral load-displacement relationship of the pile, Broms and Fredriksson use the principal of virtual work. They use trigonometric series out to eighty terms to apply the virtual work concept based on solutions by Hetenyl (1946) where the coefficient of subgrade reaction varies along the length of the pile. The internal work, V_1, from the moment of the pile is given by Equation 3 in the paper. The work by the surrounding soil, V_2, is given by Equation 4 and the work imposed by the soil on the pile, V_3, is given by Equation 5. Using the principal of virtual work, the work done by the soil on the pile, V_3, must equal the change in internal work, V_1. This equality is given in Equation 6 in the paper. Since the work by the external soil load depends on the magnitude of settlement acting normal to the pile axis, the distribution of the settlement with depth has important impacts on the model response. Broms and Fredriksson are not clear as to how they assume settlement varies along the length of the pile. The impression from the text and from Figure 3 in the paper is that the settlement is assumed to be uniform over the pile length. This means that the soil displacement normal to the pile is equal to the component of settlement at the ground surface which acts normal to the pile.

Results of parametric study using the analytical model:

Below are the results of the investigation for each of the parameters evaluated.

Modulus of elasticity of the pile

Broms and Fredriksson observed that the bending moment increases in the pile with an increase in modulus. They also observed that the location of the maximum bending moment moves away from the pile head as the pile becomes stiffer.

Pile length

The results of the theoretical investigation indicate that the maximum bending moment predicted in the pile is independent of pile length for lengths greater than 10m.

Settlement magnitude and shear strength of clay foundation soil

Broms and Fredriksson found that the predicted maximum bending moment increased linearly with the magnitude of surface settlement acting normal to the pile axis. Figure 3 in the paper shows that increasing the shear strength of the foundation soil increases the predicted maximum bending moment for a given magnitude of settlement. This conclusion is due to the increase in virtual work by the soil pressure acting on the pile since more work is required to displace the soil a given magnitude when the coefficient of subgrade reaction is higher.

End restraint

The model developed by Broms and Fredriksson predicts that the maximum bending moment is nearly three times higher when the pile head is fixed rather than pinned.

Variation of shear strength with depth

Broms and Fredriksson investigated the response of their model to an undrained shear strength profile that increases linearly with depth. Since the value of shear strength is used to estimate the coefficient of subgrade reaction, the variation affects the virtual work done by the soil on the pile. Based on Figures 4 and 5 in the paper, they concluded that there was not a significant difference in the magnitude or distribution of bending moments between the case where shear strength is constant and the case where shear strength increases with depth.

Presence of dessicated crust

Broms and Fredriksson studies the case where the upper 2 meters of foundation soil was assigned a shear strength that was 10 times higher than the underlying soil. This scenario was used to investigate the influence of a stronger, dessicated, layer of soil at the ground surface. Their model predicts that the maximum bending moment for a pile will be 4 times higher when a desiccated crust is present compared to a profile without such a crust.

Settlement at pile failure

Assuming a pile with a moment capacity of 41kN, Broms and Fredriksson varied the pile inclination angle from horizontal and determined the magnitude of settlement needed to produce failure. They found that piles with increasing batter failed at lower magnitudes of settlement. They also observed that piles become less tolerant of settlement (more prone to failure) when the undrained shear strength of the soil was high.

Reference:

Shibata, T., Sekiguchi, H., and Yukitomo, H. (1982). "Model test and analysis of negative friction acting on piles." *Soils and Foundations*, 22(2), 29-39.

Overview:

The study by Shibata et al. 1982 focuses on answering three question regarding the influence of negative friction of groups of piles: 1) What is the net effect of negative skin friction acting on a group of vertical piles?, 2) What bending moments and deflections are produced in batter piles due to negative skin friction?, and 3) What percent reduction in downdrag-induced loads and bending moments can be achieved through the use of bitumen as a friction reducer. The questions are addressed using a laboratory-scale model which can simulate the downdrag forces acting on piles due to an applied uniform pressure and by using a theoretical approach developed by Broms and Fredriksson (1976). Additional details of the investigation related to batter piles is given below.

Description of the experimental apparatus:

The apparatus developed by the authors consists of a cylindrical steel tank with an outside diameter of 1485mm and a height of 1000mm. The tank is used to contain the model piles and the clay which consolidates around the piles. The tank has a lid that, when secured, makes the tank air-tight. The bottom of the tank includes a base layer of sand and drainage ports to allow for water expelled from the clay during consolidation to exit the apparatus. The tips of the model piles react against load cells fixed to the bottom steel plate of the tank. In this arrangement, the neutral plane will be at the pile tips. The clay sample consists of kaolin and is formed around the model piles from slurry and allowed to consolidate under self-weight. During a test, a vinyl membrane is placed over the top of the model piles and clay sample. With the tank lid in place, air pressure is applied through a port in the lid which exerts a vertical pressure on the piles and clay. As the clay consolidates, the load acting on the pile is monitored using the load cells. Piezometers are also included in the tank to measures pore pressures in the clay and track the progress of primary consolidation.

Three series of tests were performed at different consolidation pressures using two rows of three piles set at a batter of 15 degrees from vertical. Each steel pile had an outer diameter of 60mm, a wall thickness of 1.2mm, and a length of 600mm. A series of strain gauges were installed on the inner surface of the battered model piles to measure bending moment. One of the three tests series used bitumen to determine its effectiveness at reducing downdrag loads and bending moments.

Experimental results for batter piles:

Downdrag load
The unit downdrag load acting on a single vertical pile is expressed by the authors according to Equation 3. In this expression, τ_z is the mobilized unit shaft friction at a depth *z* below the ground surface, $\delta_m^{'}$ is the mobilized effective interface friction angle between the pile and the surrounding clay, K is the lateral earth pressure coefficient, and $\sigma_v^{'}$ and $\sigma_h^{'}$ are the magnitudes of effective vertical and horizontal stress, respectively. The value of τ_z at a given depth increases with relative displacement of the soil relative to the pile to reach a limiting value.

$$\tau_z = \sigma_h^{'} \tan\delta_m^{'} = K\sigma_v^{'} \tan\delta_m^{'} \qquad 3$$

The contribution of group effects results in different magnitudes of downdrag force exerted on the piles depending of their position within the group. As shown in Figure 8 in the paper, piles with exposure to the perimeter of the pile group are subjected to higher downdrag loads than piles found in the interior of the group. This figure also shows that there exists an approximately linear relationship between the unit downdrag stress and the magnitude of applied consolidation pressure. This observation suggests that the lateral earth pressure coefficient and interface friction angle are not significantly affected by the magnitude of effective vertical stress for the modeling conditions used in the study. The ratio between the unit downdrag stress and the consolidation pressure for batter piles was determined by the authors to be only slightly smaller than the value of 0.18 observed using vertical piles. The authors contend that the relationship given in Equation 3 for vertical piles can be applied to batter piles and yield conservative results. In the test using bitumen as friction reducer, the authors observed a 50 percent reduction in measured downdrag load compared to the uncoated cases.

Flexural behavior

Shibata et al. use the layout given in Figure 1 to present their discussion of the flexural behavior of batter piles. Here, x represents the distance measured from along the length of the batter pile, with length, *L,* penetrating the clay stratum. The authors chose to average the bending moment measured in the piles at the different positions in the group. They observed that for a position along the x-axis, the measured bending moment increased more or less linearly with consolidation pressure. This linear relationship contrasts to the nonlinear relationship between applied consolidation pressure and settlement. They also found that the used of bitumen resulted in a 20% reduction in the maximum bending moment compared to the uncoated case.

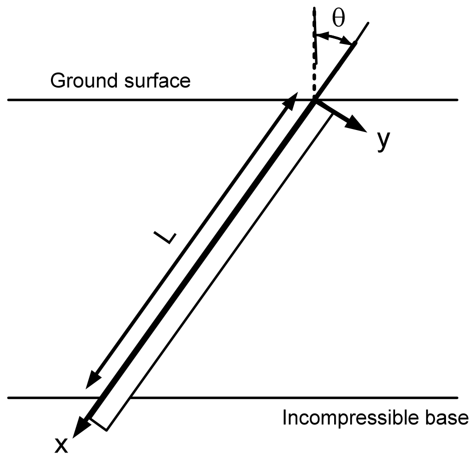

Figure 2: Local axes and orientation for batter pile

Theoretical consideration of the flexural behavior of batter piles

In an effort to theoretically model the flexural behavior of a batter pile subjected to downdrag forces, the authors decided to model the pile as a horizontal elastic beam supported by a Winkler spring foundation. Using these representations, the force relationship given in Equation 4 holds.

$$\frac{EI}{D}\frac{d^4y}{dx^4} + k\left(y - y_s\right) = 0 \qquad 4$$

In this expression *E* is the Youngs modulus of the pile, *I* is the moment of inertia, *D* is the pile diameter, *k* is the coefficient of subgrade reaction, *y* is the pile deflection, and y_s is the ground displacement normal to the x-axis. The authors assume that the ground displacement, y_s, can be related to the vertical surface settlement according to Equation 5 where ρ_o is the magnitude of surface settlement, and ▯ is the inclination of the pile from vertical. This approach assumes that settlement varies linearly along the length of the pile.

$$y_s\left(x\right) = \rho_o\left(1 - \frac{x}{L}\right)\sin\theta \qquad 5$$

Substituting Equation 5 into Equation 4 yields the differential equation given by Equation 6

$$\frac{d^4y}{dx^4} + 4\beta^4 y = 4\beta^2\rho_0\left(1 - \frac{x}{L}\right)\sin\theta \qquad 6$$

where β is defined by

$$\beta = \left(\frac{kD}{4EI}\right)^{1/4}$$

The authors chose to establish boundary conditions by assuming no pile deflection or moment, *M*, occurs at either end of the pile.

$$\left.\begin{array}{l} y = 0 \text{ at } x = 0 \text{ and } x = L \\ M = 0 \text{ at } x = 0 \text{ and } x = L \end{array}\right\} \qquad 7$$

Using the boundary conditions given in (7), the differential equations can be solved to yield solutions for deflection and moment along the pile according to Equations 8 and 9, respectively.

$$y = \rho_o \sin\theta \left[\frac{\cosh\beta x \cdot \cos(\beta x - 2\beta L) - \cosh(\beta x - 2\beta L)\cdot \cos\beta x}{\cosh 2\beta L - \cos 2\beta L} + \left(1 - \frac{x}{L}\right)\right] \qquad 8$$

$$M = \frac{2\rho_o \sin\theta \cdot EI\beta^2}{\cosh 2\beta L - 2\cos\beta L}\left[\sinh\beta x \cdot \sin(\beta x - 2\beta L) - \sinh(\beta x - 2\beta L)\sin\beta x\right] \qquad 9$$

To assign a value for the modulus of subgrade reaction, Shibata et al. chose to use the recommendation by Broms and Fredriksson (1976) and assume that $k = 10S_u/D$, where S_u, is the undrained strength of the clay. Using the relationships given in Equations 8 and 9, the authors obtained good agreement between the predicted and measured value sof bending moment. They also found that when the batter angle is small, that the bending moment at any value of *x* is proportional to the batter angle.

Reference:

Takahashi, K. (1985). "Bending of a batter pile due to ground settlement." *Soils and Foundations*, 25(4), 75-91.

Overview:

The study by Takahashi applies theoretical modeling, laboratory and field scale experimental modeling, and numerical modeling to the problem of predicting bending moments generated in batter piles due to downdrag forces.

Background on theoretical models:

The author presents a general overview of the existing theoretical methods which treat the pile as an elastic beam which rests on a Winkler spring foundation. The existing approaches include the method develop by Broms and Fredriksson (1976), the method by Sato et al. (1970) which is presented in Japanese, and the method by Shibata et al. (1982). These methods are all fairly similar in their assumptions and treatment of the pile and consolidating clay. The author asserts that the method by Shibata et al. was developed primarily for comparison to their experimental model which was for the case of an end bearing pile. The model by Shibata et al. also assumed that the settlement of the clay varied linearly along the axis of the batter pile. The method by Broms and Fredriksson solves the differential expressions for stress and deflection using trigonometric series, which Takahashi claims make the approach impractical for general use.

The method by Sato et al. (1970) treats the batter pile as an elastic beam which supports the weight on the consolidating clay over an “effective width” and “effective length” which are chosen using judgement. The weight of the soils is thought to act over the area defined by the effective width and length. Below the zone where the pile is considered to carry the weight of the soil, the pile is considered to supported elastically by the bearing stratum. This arrangement is shown in Figure 1, where L’ is the effective length of the pile.

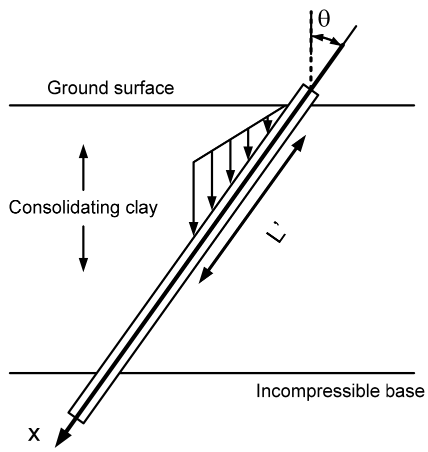

Figure 3: Treatment of pile and foundation soil interaction in method by Sato et al. (1970)

Development of theoretical model by Takahashi:

The theoretical model developed in the current study treats the pile-soil model according to Figure 2. Similar to the other models mentioned above, the current model considers the pile to be an elastic beam resting on a Winkler spring foundation. The enhancements of this model compared to the preceding models in the inclusion of four distinct foundation characteristics and consideration of the non-linear strain profile within the consolidating clay layer. The model also does not assume that displacement and moment is zero at the base of the clay layer, but rather uses the reaction of the pile in the bearing stratum (Layer 1).

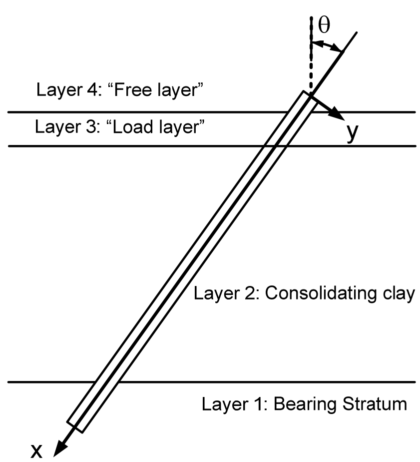

Figure 4: Takahashi's model for soil-pile interaction

Using Winkler springs, the pile is loaded proportionally to the product of the coefficient of subgrade reaction and the relative displacement between the pile and the component of ground settlement normal to the pile axis.

Takahashi provides the assumption of Winkler subsoil according to Equation 1, where *E* represents Youngs modulus of the pile, *I* is the moment of interia of the pile, *W* is the pile width, θ is the pile inclination form vertical, *k* is the coefficient of subgrade reaction, *x* is the distance along the pile axis, and *y* is the deflection normal to the pile axis. The function S(x) represents the vertical ground settlement as a function of the position, x, along the pile axis.

$$\frac{EI}{W}\frac{d^4y}{dx^4} = k\left(S(x)\sin\theta - y\right) \qquad 1$$

For Layer 1, which represents the bearing stratum, the ground settlement is assumed to be zero and Equation 1 reduces to an elastic subgrade reaction for pile deflection.

For Layer 2, which represents the consolidating clay, the function S(x) developed based on the strain profile for one-dimensional consolidation that is occurring with drainage layers at both the top and bottom of the clay layer. The author uses a third-order polynomial to model the settlement profile developed by integrating a second-order (parabolic) strain profile given by Mikasa (1963). This profile is shown in Figure 3 of the paper. Takahashi provides the expression for S(x) according to Equation 2.

$$S(x) = S_\infty\left\{\frac{x}{d/\cos\theta} - (1-U)\left(\frac{x}{d/\cos\theta}\right)^2 \cdot \left(3 - 2\frac{x}{d/\cos\theta}\right)\right\} \qquad 2$$

In this expression S_∞ is the settlement of the ground surface at the end of primary consolidation, *U* is the degree of consolidation, and *d* is the original thickness of the clay layer. Takahashi warns that the assumed strain profile given in Figure 3 of the paper is only valid when at least a third of the primary consolidation has completed. Solving Equation 1 for Layer 2 yields the expression for pile deflection normal to the pile axis given by Equation 3 where A_1 through A_4 are constants and z_1 through z_4 are defined below.

$$y = A_1z_1 + A_2z_2 + A_3z_3 + A_4z_4 + S(x)\sin\theta \qquad 3$$

$$z_1 = \cos\beta x \cdot \cosh\beta x$$

$$z_2 = \frac{1}{2}\left(\sin\beta x \cdot \cosh\beta x + \cos\beta x \cdot \sinh\beta x\right)$$

$$z_3 = \frac{1}{2}\sin\beta x \cdot \sinh\beta x \qquad 4$$

$$z_4 = \frac{1}{4}\left(\sin\beta x \cdot \cosh\beta x - \cos\beta x \cdot \sinh\beta x\right)$$

$$\beta = \sqrt[4]{\frac{Wk}{4EI}}$$

Layer 3 is defined as the "load layer" and is used to represent the embankment load. Takahashi does not provide a clear explanation of how this layer contributed to the deflection and bending moment produced in the pile, however the adapted form of Equation 1 for the Layer is given by Equation 5. In this expression, γ is the unit weight of the embankment material and x_o is the distance along the pile axis from the pile tip to the top of Layer 3.

$$\frac{EI}{W}\frac{d^4y}{dx^4} = \gamma\left(x_o - x\right)\sin^2\theta\cos\theta \qquad 5$$

Inspection of Equation 5 allows for an explanation of the contribution of Layer 4 to the deflection and bending moment to be developed. The vertical stress at a depth, z, measured from the top of Layer 4 is equal to $\gamma\left(x_o - x\right)\cos\theta$ and the component of the vertical stress which acts normal to the pile axis is equal to $\gamma\left(x_o - x\right)\cos\theta\sin\theta$. The sine in Equation 5 is squared and at this time is it not understood why this is. Using Takahashi's expression given by Equation 5, the deflection of the pile can be determined according to Equation 6, where, A_1 through A_4 are constants and A_5 and A_6 and given below.

$$y = A_1 + A_2x + A_3x^2 + A_4x^3 + A_5x^4 + A_6x^5 \qquad 6$$

$$A_5 = \frac{1}{24}\frac{W\gamma}{EI}x_o\sin^2\theta\cos\theta$$

$$A_6 = -\frac{1}{120}\frac{W\gamma}{EI}\sin^2\theta\cos\theta \qquad 7$$

Layer 4 is the "free layer" which corresponds to the portion of the pile that extends above the ground surface. Since the free layer has a coefficient of subgrade reaction equal to zero the solution to Equation 1 for Layer 4 is equal to Equation 8.

$$y = A_1 + A_2x + A_3x^2 + A_4x^3 \qquad 8$$

Takahashi applies linear algebra to set up the expressions relating the pile behavior to the soil deflections for each of the four layers. These expressions are given by Equations 9 through 14 in the paper. The process to solve the systems of equations is left unclear. Takahashi mentions limiting the number of rows in the matrices to four, which in the case of Layer 2 requires eliminating a row, to make solving the expressions possible. He also does not provide details on how the unknown constants should be determined other than that the “sixteen constants could be solved by the use of twelve continuity conditions at three boundaries between the layers and of four boundary conditions at pile top and pile tip.”

Experimental Model Tests:

The test apparatus used in this study consists of a cylindrical steel tank with an inside diameter of 2520mm and a height of 1700mm. A 1130mm sample of clay was prepared saturated in a remolded state and was sandwiched between upper and lower sand drainage layers (50-100mm thick each). The piles used consist of thin rectangular steel plates with a length of 1780mm, a width of 75mm, and a thickness of 9mm. A group of eight piles was installed into the remolded clay sample at a batter angles of 5, 10, 15, or 20 degrees. The piles in opposing pairs were installed at the same batter angle and all four angles of batter were present in the group simultaneously. Takahashi doesn’t describe installation process or how much smearing occurs, but mentions that a ‘special device’ was used. Each pile was instrumented with seventeen strain gauges spaced every 10 cm along its length to measure the bending moment.

Consolidation of the clay was induced by placing a 220mm layer of steel shot over the upper sand layer corresponding to a consolidation pressure of $10kN/m^2$. The ground settlement, pile deflection, and bending moments were monitored for 100 days after placement of the steel shot. The distribution of bending moment if the pair of piles inclined at 20 degrees is shown in Figure 7 of the paper. Takahashi observed a proportional relationship between the maximum bending moment and the pile inclination angle. This is similar to the result observed by Sabata et al. (1982). Takahashi also found that the relationship between the magnitude of surface settlement and maximum bending moment to be near linear. Shibata et al. (1982) observed a near linear relationship between the bending moment at a given position along the pile and the consolidation pressure.

Finite element analysis of model tests:

Takahashi does not provide much detail on the methods or software used to generate a finite element model of the experimental conditions. He used elastic constitutive relations for both the pile and soil and modeled the experimental tests in two dimensions. He was not able to obtain reasonable agreement between the numerical and experimental results and determined it was necessary to model the problem in 3D. Using the 3D model he was able to obtain reasonable agreement for the magnitude of maximum bending moment for inclination angles of 10 and 20 degrees.

Evaluation of experimental results using Sato's Method:

Takahashi was able to obtain good agreement between the measured and predicted values of deflection, deflection angle, bending moment, shear force, and soil pressure acting on the pile for an inclination angle of 20 degrees. It seems like a trial and error approach is necessary to adjust the effective width and length values to get the predicted values to agree with the experimental results. Sato et al. recommend an effective width that is three times the pile width. The data fit obtained using Sato's method, once calibrated, was better than the fit obtained using the 3D FE model.

Evaluation of experimental results using Takahashi's method:

Takahashi achieved good agreement between the measured and predicted values of deflection, deflection angle, bending moment, shear force, and soil pressure acting on the pile for an inclination angle of 20 degrees. He found the best fit was obtained when he assumed an elastic soil reaction for both the clay and sand layers and treated the steel shot as a load layer.

Field tests:

An instrumented field test consisting of a 2x2 group of steel pipe piles with a batter angle of 15 degrees was reported by Takahashi (1985), Sato et al. (1987) and Sawaguchi (1989). An 2.5m embankment with plan dimensions of approximately 40m x 25m was placed to initiate consolidation of the roughly 30m thick soft clay deposit. The piles were installed through the embankment and the clay to bear on a stratum of stiff clay stratum with gravel. The piles extended above the ground surface and were hinged in pairs. The spacing between the piles is not provided in the paper. Two of the piles were coated with bitumen to observe the effects on deflection and moment. Extensive instrumentation was used in this study to monitor settlement, pile deflection, and pile moment. A summary of the instrumentation is given in Table 1 of the paper. The instrumentation was monitored for a year while consolidation proceeded. The distributions of axial force and bending moment for the coated and uncoated piles is shown in Figures 22 and 23 of the paper. Takahashi found that while the bitumen coating significantly reduced down drag loads, the coating actually resulted in slightly higher bending moments in the upper portion of the pile. Takahashi 's laboratory finding that the maximum bending moment increased linearly with the ground settlement was again observed at the field scale.

Finite element analysis of model tests:

In an attempt to model the field results, Takahashi again found that 2D finite element modeling did not adequately capture the interaction between the pile and the soil. He did not pursue modeling the field tests in 3D.

Evaluation of experimental results using Sato's Method:

Takahashi again applied a trial and error approach to selecting appropriate values for the effective width and length. In the paper, he notes the strong influence of the choice of effective width on the results. He was able to obtain reasonable prediction of bending moment along the length of the pile, although the predicted location of maximum moment did not correspond to the measured location.

Evaluation of experimental results using Takahashi's method:

Takahashi provides some detail on how he decided to divide the soil profile at the field test site into the Layers used in his theoretical model. He ultimately decided break the pile into four sections. He included a free layer, a load layer to capture the influence of the embankment, and two clay layers to simulate the soft clayey soil. He found some sensitivity of the model to the location where he divided the clay layer in to upper (compressible) and lower (less compressible) regions. His model did not show much sensitivity to the choice of soil unit weight, which is equivalent to changing the width adjustment factor. Takahashi also found that the selection of the thickness for the embankment layer made little difference on the results. Again, he found that his model was able to capture the interaction between the pile and soil better than either Sato's method or finite element analysis.

Reference:

Sawaguchi, M. (1989). "Prediction of bending moment of a batter pile in subsiding ground." *Soils and Foundations*, 29(4), 120-126.

Overview:

The technical note by Sawaguchi briefly discussions existing methods by Sato et al. (1970), Shibata et al. (1982), Takahashi (1985), and Sabato et al. (1987) for estimating the bending moment induced in a batter pile due to settling ground. Sawaguchi draws from elements from each of the aforementioned methods and presents his analytical model of the problem. He provides chart solutions developed from computer solutions of his model.

Development of analytical model:

Sawaguchi's approach introduces a different way to consider the vertical loading of the batter pile near the ground surface. Rather than use a "loading layer" like Takahashi, Sawaguchi assumes that the upper portion of the pile is loaded in a way similar to a positive projecting conduit. For the remainder of the pile, Sawaguchi adopts the assumption of Winkler ground common to the other methods. The justification for the treatment of the upper pile as a positive projecting conduit is based on numerous field observations of ground deformation around the batter pile. This deformation can be generalized as having a zone directly over the surface projection of the pile where significantly less surface settlement occurs compared to other areas. Sawaguchi's analytical model is shown in Figure 1.

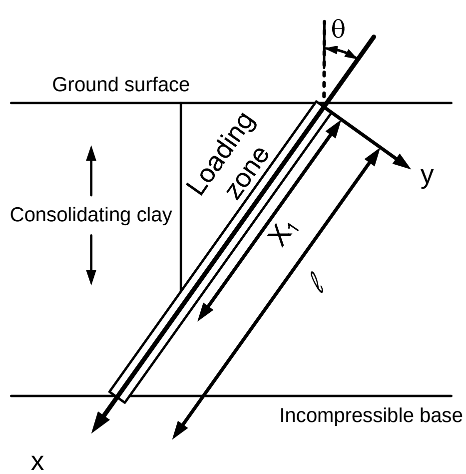

Figure 5: Analytical model developed by Sawaguchi (1989)

Using the assumption of a positive projecting conduit for loading within the upper portion of the pile, the earth pressure acting on the pile can be estimated using Spangler's formula. For a pile top flush with the ground surface, the relationship between pile deflection and soil pressure in the loading zone ($0 \le x \le X_1$) is given by Equation 1.

$$EI\frac{d^4 y_1}{dx^4} = \frac{B^2 \gamma \sin^2\theta}{2K\mu}\left(\exp\frac{2K\mu\cos\theta}{B}X - 1\right) \qquad 1$$

In the expression above, Young's Modulus of the pile is represented by E, the moment of inertia of the pile by I, B is the pile width, $y_1$is the deflection of the pile within the loading zone, γ is the unit weight of the surrounding soil, K is the coefficient of lateral earth pressure, μ is the coefficient of friction between the soil supported by the pile and the surrounding soil, θ is the inclination f the pile from vertical, and y_1 is the pile deflection within the loading zone. Below the loading zone ($X_1 \le x \le \ell$), Sawaguchi considers the pile to be supported by Winkler soil according to Equation 2.

$$EI\frac{d^4 y_2}{dx^4} = Bk_h\left(S(x)\sin\theta - y_2\right) \qquad 2$$

Here, y_2, is the deflection of the pile below the loading zone, k_h is the horizontal coefficient of subgrade reaction, and S(x) expresses the variation of vertical settlement along the pile axis. Sawaguchi applies the same assumption as Shibata et al. (1982) and assumes linear variation of the vertical settlement with depth according to Equation 3, where S_o is the settlement at the ground surface.

$$S(x) = S_o\left(1 - \frac{x}{\ell}\right) \qquad 3$$

After substituting Equation 3 into Equation 2, Sawaguchi solves Equations 1 and 2 assuming no moment exists at either end of the pile and that the deflection, deflection angle, moment, shear force, and pressure in the pile at the interface of the loading layer with the Winkler soil layer are equal.

Since no closed solution for the equations exists, Sawaguchi developed normalized design charts. The charts relate normalized moment, $\left(M\ell / EI\right)$, to non-dimensional parameters listed below.

$$\beta\ell = \sqrt[4]{\frac{k_h B}{4EI}}\ell$$

$$\nu\ell = \frac{2K\mu\ell\cos\theta}{B}$$

$$\varepsilon\ell^3 = \frac{B^2\gamma\ell^3\sin^2\theta}{2K\mu EI} \qquad 4$$

$$\xi = \frac{S_o}{\ell}\sin\theta$$

Field Scale Tests:

An instrumented field test consisting of a 2x2 group of steel pipe piles with a batter angle of 15 degrees was reported by Takahashi (1985), Sato et al. (1987) and Sawaguchi (1989). An 2.5m embankment with plan dimensions of approximately 40m x 25m was placed to initiate consolidation of the roughly 30m thick soft clay deposit. The piles were installed through the embankment and the clay to bear on a stratum of stiff clay stratum with gravel. The piles extended above the ground surface and were hinged in pairs. The spacing between the piles is not provided in the paper. Two of the piles were coated with bitumen to observe the effects on deflection and moment. Extensive instrumentation was used in this study to monitor settlement, pile deflection, and pile moment. A summary of the instrumentation is given in Table 1 of the paper. The instrumentation was monitored for a year while consolidation proceeded. The distributions of axial force and bending moment for the coated and uncoated piles is shown in Figures 22 and 23 of the paper. Takahashi found that while the bitumen coating significantly reduced down drag loads, the coating actually resulted in slightly higher bending moments in the upper portion of the pile. Takahashi 's laboratory finding that the maximum bending moment increased linearly with the ground settlement was again observed at the field scale. The measured bending moments induced by the settlement were compared to values predicted using Sawaguchi's analytical model. Sawaguchi applied an empirical correlation using the unconfined strength of the clay to estimate the coefficient of horizontal subgrade reaction. Using the input parameter values given in Table 1 of the paper, Sawaguchi was able to obtain good agreement between the measured and predicted values of bending moment. He concludes the discussion of the field-scale study by comparing the measured value of maximum bending moment to the values predicted using the methods by Sato et al. (1987) and Takahashi (1985). For the case at hand, the two existing methods and the Sawaguch's method all predicted values close to the measured maximum bending moment.

Reference:

Rao, S. N., Murthy, T. V. B. S. S., and Veeresh, C. (1994). "Induced bending moments in batter piles in settling soils." *Soils and Foundations*, 34(1), 127-1

Overview:

The study by Rao et al. (1994) includes the development of an analytical model for estimating the pressure acting on a single batter pile due to settlement of the surrounding soil. The model divides the consolidating soil surrounding the pile into three zones: 1) a wedge-shaped zone overlying the pile that is completely supported by the pile, 2) a transitional 3D zone of arching that sheds vertical stress to the pile, 3) the soil beyond the zone of arching that is unaffected by the presence of the pile. The principal deviation of the proposed method to the methods by Sata, Takahashi, and Shibata, is the consideration of separation developing between the pile and the underlying soil. The authors contend that soil settlement can leave the pile unsupported and it is more appropriate to model the pile as a clear spanning beam with either free or fixed end supports. The pressure acting on the free spanning beam representing the batter pile is determined using the combined pressures produced by the fully –supported and arching zones.

The study also includes a description of a laboratory scale study carried out to support the provide support for the proposed theoretical model.

This paper contains several errors in the presentation of the mathematical development of the model. These errors include typographical mistakes, unreasonable assumptions, and improper application of soil mechanics. These problems are pervasive enough to essentially discredit the authors' assertions.

Development of analytical model:

Estimation of pressure acting on the batter pile

The authors introduce the concept for their analytical model by describing the probably shape of the volume of soil that is either directly supported by the pile or supported by arching. The end result of this discussion is the treatment of the soil mass supported by the pile as a three-dimensional wedge that is defined by a vertical plane extending from the tip of the pile and a width equal to two pile diameters. This defined soil volume is provided in Figure 1 of the paper, however the figure and supporting text suggest that the width of the wedge is three pile diameters instead of two. It is not until the mathematical development is presented that is becomes apparent that the soil wedge has a thickness of two pile diameters. The concept behind the use of a wedge, is that the soil mass within the wedge is considered to be completely supported by the pile and that shear resistance between the sides of the wedge and the surrounding soil reduces the load carried by the pile. No shear force is considered to develop between the face of the wedge and the surrounding soil. This concept is illustrated in Figure 1.

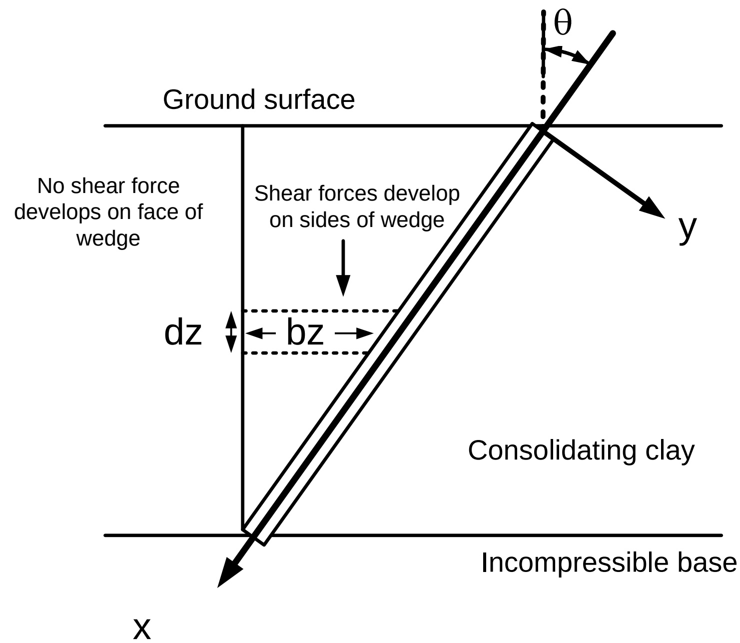

Figure 6: Wedge of soil supported by pile used in the analytical model developed by Rao et al.

Using the wedge defined in Figure 1 and assuming that shear strength is fully mobilized between the sides of the wedge and the surrounding consolidating soil, vertical equilibrium is satisfied by Equation 1.

$$\sigma_{vz}(2R)b_z + \gamma(2R)b_z dz - \left(\sigma_{vz} + \frac{d\sigma_{vz}}{dz}dz\right)(2R)(b_z) - 2\tau_z b_z dz = 0 \qquad 1$$

In this expression 2R, is the width of the soil wedge and R is assumed to be equal to the diameter of the pile, b_z and dz are the dimensions of a unit of soil within the wedge, τ_z is the peak shear strength along the side of the wedge, σ_{vz} is the total vertical stress, and γ is the total unit weight of the soil.

The authors then mistakenly define the peak shear strength at the sides of the wedge at a particular elevation according to Equation 2 where k is the at-rest earth pressure coefficient estimated using Jaky's formula, $k = (1 - \sin\theta)$.

$$\tau_z' = c' + (k\sigma_{vz} - u)\tan\phi' \qquad 2$$

The error of multiplying the total vertical stress by the earth pressure coefficient is incorporated into subsequent development of the analytical model. Later in the development, Rao et al. decide to set pore pressure to zero using an rationale that is incorrect on the basis of soil mechanics and the model development. This adjustment does however remedy the improper calculation of horizontal stress acting on the face of the wedge. Any potential user of this method should know to use effective unit weights and drained strength parameters as input. The end result of the expression used to estimate the pressure acting on the pile is given by Equation 3, where *x* is the distance along the pile axis from the head of the pile, *d* is the pile diameter and, q_s is the applied surcharge due to the embankment.

$$P_{vx} = q_s d + \gamma(d + 2R)x\cos\theta + 2R\left(q_s - \frac{Q}{P}\right)\cdot\left(1 - \exp(-P \cdot x\cos\theta)\right) \qquad P = \frac{k\tan\phi}{R} \qquad Q = \gamma - \frac{c}{R} \tag{3}$$

Rao et al. use Equation 4 to resolve the vertical pressure P_{vx} determined using Equation 3 into components acting normal and coincident to the pile axis. Here, f_{nx} is the component of vertical stress acting along the pile axis and q_{tx} is the component which acts normal to the pile.

$$f_{nx} = P_{vx}\cos\theta \qquad q_{tx} = P_{vx}\sin\theta \tag{4}$$

As shown in Equation 5, the next step in the procedure by Rao et al. is to integrate the pressure acting normal to pile over its length to get the total lateral force. They then divide this force by the pile length to yield a uniformly distributed pressure which induced bending moment. This approach completely disregards the impact of non-uniformly distributed lateral soil pressure on the induced bending moment. Rao et al. also make the assumption that the axial force in the pile has no influence on measured bending moment.

$$w = \frac{1}{L}\int_0^L q_{tx}\,dx \tag{5}$$

Using the uniform pressure, w, Rao et al. estimate bending moment in the pile by considering two typical support conditions for a free spanning beam. The first condition is for pinned-pinned end supports, for which the bending moment along the pile is given by Equation 6, and the second is for fixed-fixed end supports given by Equation 7.

$$M_x = \frac{wx}{2}\left(L - x\right) \tag{6}$$

$$M_x = \frac{w}{12}\left(6Lx - L^2 - 6x^2\right) \tag{7}$$

<u>Verification of proposed analytical model using experimental model:</u>

An experimental model consisting of a square steel tank with dimensions of 1200mm x 1200mm x 1200mm was constructed to house a square grouping of batter piles with a batter angle of 10 degrees. The model piles consisted of aluminum pipes with a length of 725mm, an outer diameter of 38.1mm, and a wall thickness of 1.5mm. The four piles were fixed to a square top plate and arranged so that a pile extend from each face of the plate. This arrangement is shown in Figure 4 of the paper.

To conduct a test, the piles were placed in the empty tank and a 50mm layer of sand was placed to provide drainage. Next, 570mm of clay was placed and tamped moist in 50mm lifts. Above the compacted clay layer, another 100mm of sand was provided for a upper drainage layer. A surcharge was applied to the steel plate fixed to the piles to induce settlement of the compacted clay. At this point, the text and figures are confusing as to whether the steep plate covered the entire sample surface or just the 200mm x 200mm plate shown in Figure 4.

The model piles were instrumented using strain gauges to measure bending moment. The results on tests performed using different surcharge loads are shown in Figures 6 and 7 of the paper. The authors use this information to assess their proposed model. First they calculated the pressure acting normal to the pile axis using Equation 3. After integrating the soil pressures over the length of the pile and determining an equivalent uniform distributed pressure, the authors estimated bending moments using the beam support conditions given in Equations 6 and 7. They concluded that the bending moment distribution estimated assuming the fixed-fixed end supports more closely matched the experimental results.

Reference

Hance, J., and Stremlau, T. (2009). "Lateral load on piles subjected to downdrag." Internal document, Eustis Engineering, Metairie, Louisiana.

Summary of Method:

This approach considers that the pile is loaded by downdrag above the neutral plane and that the distribution of the force acting normal to the pile axis can be approximated by a triangular distribution. The magnitude of downdrag force is determined by treating the batter pile as a vertical pile and estimating the static capacity of the pile shaft and tip. The neutral plane is estimated using an approach which will be described below. The portion of the ultimate shaft capacity that is above the neutral plane is taken to be the downdrag load. The method estimates bending moment induced in the batter pile by treating the length of pile above the neutral plane as a free spanning elastic beam supported at both ends by pinned connections. The portion of the pile below the neutral plane is neglected in the analysis.

Development and implementation of the Method:

This method is described below following the example provided in the reference. Calculation errors or questionable assumptions will be pointed out, however for the purposes of maintaining continuity with the reference document, the original values and assumptions will be carried through the procedural steps.

1. *Assign the structural loads, pile elevations, and amount of pile batter*.

   For the example:

Butt elevation	=	El 0
Tip elevation	=	El -110
Pile batter (θ)	=	2V:1H or 26.56^{o} from vertical

   For the elevations provided the required length of the batter pile, L, would be

   $$L = \left[0^{EL} - \left(-110^{EL}\right)\right] \big/ \cos\left(26.56\right) \approx 123ft$$

   The length used in the calculation is L = 110 ft, which does not account for the pile batter. The structural loads considered in the example problem range from 53 to 103 kips.

2. *Determine the static capacity and ratio of the structural load to the ultimate static capacity*

The authors consider this ratio to be the factor of safety, but it does not account for the downdrag load. The ultimate static capacity of the 14” H-pile was calculated by the authors using a software program. They do not indicate what software was used or the method of estimation. The breakdown of the ultimate pile capacity is given below:

Ultimate shaft capacity (L = 110ft)	=	279 kips
Ultimate tip capacity	=	14 kips
Combined ultimate capacity	=	293 kips

The ratio of the structural load to the ultimate load, R_L, for the range of structural loads is given below.

$$R_L = \frac{293kips}{53kips} = 5.5$$

$$R_L = \frac{293kips}{103kips} = 2.8$$

3. *Determine the neutral plane of the pile.*

For this step the authors develop their own technique for estimating the location of the neutral plane. The primary assumptions of this approach are given below.

i. The neutral plane can be determined relative to the pile axis and does not depend on batter angle
ii. The downdrag pressure increases linearly with depth.
iii. The pile cross section is assumed to be constant with depth
iv. The ultimate tip resistance is assumed to increase as a fraction of the shaft resistance

Figure 1 shows the forces acting on a vertical pile subjected to downdrag where P_i is the applied load, F_D is the total down drag load, F_R is the ultimate resisting skin friction, and Q_T is the ultimate tip resistance. The unit skin friction between the pile and soil, k, is defined, but the author’s do not explain how it is determined. One approach for estimate the unit skin friction given by Equation 1, γ' is the effective unit weight of the surrounding soil, USR is the Undrained Strength Ratio of the clay, and α is a coefficient relating undrained strength to shaft resistance. For an increment of length along the pile, dx, the shaft friction, f_s, is given by Equation 2, where *s* is the surface area of the pile over the length increment.

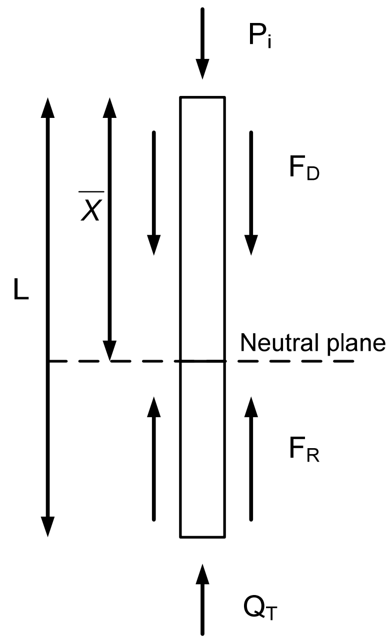

Figure 7: Forces acting on vertical pile subjected to downdrag

$$k = \alpha\gamma'(USR) \quad (1)$$

$$f_s(x) = kxsdx \quad (2)$$

For a pile with a constant cross-sectional area, the ultimate shaft friction over the entire length of the pile is given by Equation 3.

$$F_S = \frac{ksL^2}{2} \quad (3)$$

The authors assume that the ultimate tip resistance can be expressed as a fraction, n, of the ultimate shaft capacity calculated in Equation 3. Such a relationship is given in Equation 4.

$$Q_T = \frac{nksL^2}{2} \quad (4)$$

Typically, static capacity analyses determine ultimate tip resistance as $Q_T = q_t A_T$, where q_t in the unit tip resistance and A_T is the area enclosed by the outer edges of the pile tip. For piles in cohesive soils, the unit tip resistance depends on the ultimate bearing capacity of the clay and can be estimated by Equation 5, where S_u is the undrained strength of the clay.

$$Q_T = 9 S_u A_T \tag{5}$$

For clays with a constant USR, Equation 5 can be modified to Equation 6.

$$Q_T = 9(USR)L\gamma' A_T \tag{6}$$

The assumption that the ultimate tip resistance can be expressed as a fixed ratio of the shaft resistance is unreasonable. Combining Equations 1, 3, 4, and 6 into Equation 7 shows that the ratio between tip capacity and shaft capacity cannot be expressed independently of pile length.

$$\frac{Q_T}{F_s} = n = \frac{\alpha s L}{18 A_T} \tag{7}$$

Using the proposed method, the ultimate capacity of the pile, F_U, is equal to the sum of the shaft resistance and the tip resistance. The combination of Equations 3 and 4 yields the ultimate pile capacity given by Equation 8.

$$F_U = (1+n)\frac{ksL^2}{2} \tag{8}$$

The applied structural load, P_i, can be expressed using the ratio R_L according to Equation 9. The authors do not point out that the ratio, R_L, is determined for a specific pile length if the applied load is known.

$$P_i = \frac{(1+n)ksL^2}{2R_L} \tag{9}$$

The down drag force, F_d, and the ultimate shaft resistance below the neutral plane is given by Equations 10 and 11. In Equation 10, the authors chose to divide the negative shaft resistance by a constant,c. They do not provide guidance on the values to use for the constant and they use a value of unity in the example problem.

$$F_D = \frac{ks\overline{X}^2}{2c} \tag{10}$$

$$F_R = \frac{ks}{2}\left[L^2 - \overline{X}^2\right] \tag{11}$$

The determination of the neutral plane is accomplished by summing the forces acting along the axis of the vertical pile according to Equation 12.

$$P_i + F_D = F_R + Q_T \qquad 12$$

Using their assumptions, the authors express the ratio of the distance along the pile to the neutral plane to the pile length by Equation 13.

$$\frac{\overline{X}}{L} = \sqrt{(1+n)\left(\frac{R_L - 1}{R_L}\right)\left(\frac{c}{c+1}\right)} \qquad 13$$

The authors assert that Equation expresses the neutral plane as a non-dimensional fraction of pile length, however the ratio is only valid for the pile length at which *n* and R_L were evaluated.

4. Set up free-spanning elastic beam problem

Using the software evaluation performed in Step 2, the authors determine the ultimate shaft capacity at the elevation of the neutral plane estimated in Step 3. They consider this value of shaft resistance to be the downdrag load, F_D^*. Different notation is used since this value of downdrag force is evaluated differently than the down drag force used in Step 3 to estimate the neutral plane. The authors then take the value of downdrag force determined using the software and subtract it from the shaft capacity over the entire length of the pile to determine the shaft resistance, F_R^*. Next, they evaluate downdrag force again by taking the combined resistances of the shaft and tip and subtract the applied load. This process is expressed below.

$$F_R^* = F_S - F_D^* \qquad 14$$

$$F_D^{**} = F_R^* + Q_T - P_i \qquad 15$$

After the down drag force is determined according to Equation 15, the authors find the component that would act perpendicular to the axis of a batter pile. This force has a value of 102 kips in the example problem. There are mathematical errors in the use of trigonometry to find the perpendicular component of down drag load. First, they divide the value of down drag force by the pile batter expressed as a ratio of vertical run to horizontal run. In the example problem, this batter ratio is 1H:2V, so the downdrag force is divided by 2. This gives the downdrag force acting in the horizontal direction. Next the authors find how much of the horizontal downdrag force acts perpendicular to the pile, $F_{D,orth}$. To do this they multiply the value by the cosine of the batter angle. For the example problem, this translates to multiplying the vertical downdrag force by 0.5 and then again by 0.89 to yield a force of 55 kips, which is equivalent to multiplying the vertical force by the sine of the batter angle. The final step to this process is to convert the force into a triangular distributed pressure according to Equation 16.

$$w = \frac{2F_{D,orth}}{\overline{X}} \tag{16}$$

For the example problem triangular distributed load is found as shown below.

$$w = \frac{2\left(55kips\right)}{72.6ft} = 1.5\,kips/ft$$

5. Solve free-spanning elastic beam problem

The authors determine the maximum bending moment in the pile by treating the portion of the pile above the neutral plane as a free-spanning beam with pinned end connections. The soil pressure, W, acting perpendicular to the pile axis is considered to act as a triangular pressure distribution according to Equation 16. The maximum bending moment of a beam subjected to the loading and support scenario shown in Figure 2 can be determined according to Equation.

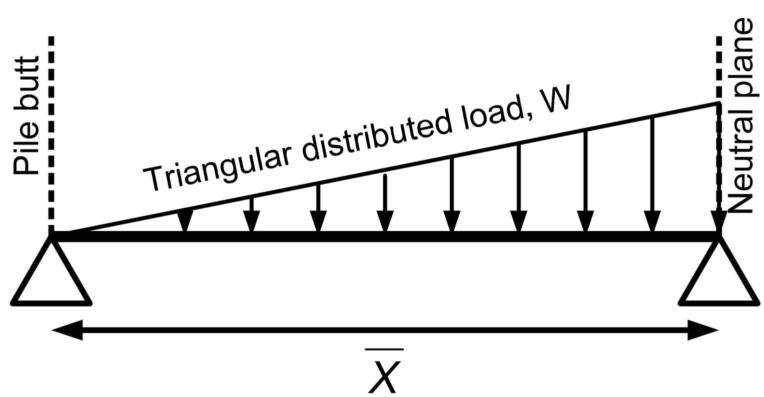

$$M_{\max} = \frac{wL^2}{9\sqrt{3}} \tag{17}$$

This equation was checked against published sources and found to be correct. For the example problem the maximum bending moment was determined to be 508 kip-ft/ft as shown below.

$$M_{\max} = \frac{1.5\,kips/ft\left(72.6ft\right)^2}{9\sqrt{3}} = 508\,\text{kip-ft}/ft$$

Determining the maximum bending moment in this way assumes the following:

i. There is no contact between the pile and the underlying soil above the neutral plane
ii. The bending moment at the top of the pile and at the neutral plane is zero.
iii. The distribution of downdrag force can be approximated by a triangular distribution

Reference:

Stremlau, T., and Hance, J. (2009). "Lateral loads on piles." Internal document, Eustis Engineering, Metairie, Louisiana.

Overview:

This approach uses the commercial software LPILE (Ensoft) to estimate the bending moments induced above the neutral plane in batter piles subject to downdrag force. The procedure requires determination of the vertical settlement resulting from fill placement. The authors used Settle^{3D} (RocScience) for their calculations which are for the Sellars Canal (WBV-74). The relative vertical settlement between the soil and the pile is determined by subtracting a magnitude of vertical pile displacement. In the example problem, the value of vertical pile displacement is 1.9 inches. It is not clear how this value was determined but the method assumes that the entire length of the pile displaces vertically by the same amount. The component of relative vertical settlement which acts perpendicular to the pile axis is determined by multiplying the relative settlement magnitude by the sine of the batter inclination from vertical. The component of relative settlement normal to the pile axis is used as the displacement magnitude, y, on p-y curves developed in LPILE for several positions along the length of the pile. The soil pressures corresponding to the displacements are determined for the portion of the pile above the neutral plane and plotted as shown in Figure 1. From the available information, it appears that the neutral plane is determined using the approach proposed by Hance and Stremlau (2009).

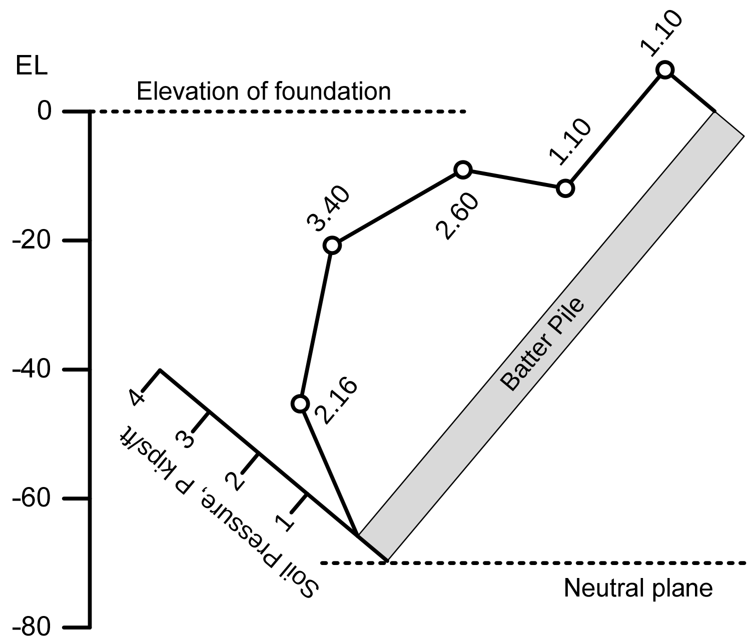

Figure 8: Distribution of soil pressure above the neutral plane

A plot like the one shown in Figure 1 is used to express the distribution of soil pressures acting normal to the axis of the batter pile. The reference explaining this approach does not carry the procedure through to the point of calculating bending moment. From the available information, it appears that the pile length above the neutral plane is treated as an elastic beam with pinned end supports. The bending moments are calculated by applying the pressure distribution determined using the p-y curves from LPILE to the elastic beam representing the pile.

Broms, B., and Fredericksson, A. (1976). "Failure of pile-supported structures caused by settlements." Proceedings of the 6th European Conference on Soil Mechanics and Foundation Engineering, 383-386.

Ensoft. (2008). *LPILE 5.0 Plus User's Manual*, Ensoft, Inc., Austin, TX.

Geomatrix Consultants, I. (2007). "Soil-structure interaction and load transfer mechanism of pile-supported T-Wall for New Orleans levees, Project 12048.001." Prepared for U.S. Army Engineer Research & Development Center, Waterways Experiment Station, Vicksburg, Mississippi, Okland, California.

Ghaly, A. M. (1995). "Discussion of "Induced bending moments in batter piles in settling soils" by S. Narasimha Rao et al." *Soils and Foundations*, 35(1), 174-175.

Hance, J., and Stremlau, T. (2009). "Lateral load on piles subjected to downdrag." Internal document, Eustis Engineering, Metairie, Louisiana.

ITASCA. (2002). "FLAC Fast Lagrangian Analysis of Continua." ITASCA Consulting Group, Minneapolis, Minnesota.

Kelesoglu, M. K., and Cinicioglu, S. F. (2010). "Free-field measurements to disclose lateral reaction mechanism of piles subjected to soil movements." *Journal of Geotechnical and Geoenvironmental Engineering*, 136(2), 331-343.

Matlock, H. (1970). "Correlations for design of laterally loaded piles in sift clay." 2nd Annual Offshore Technology Conference, OTC1204 Vol 1, Houston, Texas, pp. 577-594.

Navin, M. (2009). "FLAC analyses for T-Wall downdrag investigation." Internal document, USACE, St. Louis, Missouri, pp.24.

Navin, M. (2009). "Overview of FLAC analysis for St. bernard Parish." Internal document, USACE, St. Louis, Missouri, pp17.

Rajashree, S. S., and Sitharam, T. G. (2001). "Nonlinear finite-element modeling of bater piles under lateral load." *Journal of Geotechnical and Geoenvironmental Engineering*, 127(7), 604-612.

Rao, S. N., Murthy, T. V. B. S. S., and Veeresh, C. (1994). "Induced bending moments in batter piles in settling soils." *Soils and Foundations*, 34(1), 127-133.

Rao, S. N., Murthy, T. V. B. S. S., and Veeresh, C. (1995). "Closure to "Induced bending moments in batter piles in settling soils" " *Soils and Foundations*, 35(1), 175.

Reese, L. C., Cox, W. R., and Koop, F. D. (1974). "Analysis of laterally loaded piles in sand." 5th Annual Offshore Technology Conference, OTC 2080, Houston, Texas.

Reese, L. C., and Van Impe, W. F. (2001). *Single piles and pile groups under lateral loading*, Taylor and Francis, London, U.K.

Sato, S., Akai, K., Funahashi, T. (1970). "Study on methods to calculate negative skin friction and bending in a batter pile." Laboratory Report of Japan Road Corporation, pp. 31-49 (*in Japanese*).

Sato, S., Iwashita, F., and Ohmori, H. (1987). "The calculation method on the bending moment of a batter pile
induced by ground settlement." *Soils and Foundations*, 27(2), 75-84 *(in Japanese)*.

Sawaguchi, M. (1989). "Prediction of bending moment of a batter pile in subsiding ground." *Soils and Foundations*, 29(4), 120-126.

Shibata, T., Sekiguchi, H., and Yukitomo, H. (1982). "Model test and analysis of negative friction acting on piles." *Soils and Foundations*, 22(2), 29-39.

Stremlau, T., and Hance, J. (2009). "Lateral loads on piles." Internal document, Eustis Engineering, Metairie, Louisiana.

Takahashi, K. (1985). "Bending of a batter pile due to ground settlement." *Soils and Foundations*, 25(4), 75-91.

Templeton, A. E. (2009). "Settlement and settlement induced stress." Burns Cooley Dennis, Inc., Ridgeland, Mississippi, pp. 49.

Tominaga, M., and Hashiimoto, M. (1987). "Discussion of "Bending of a batter pile due to ground settlement" by Kunio Takahashi." *Soils and Foundations*, 27(1), 102-104.

Wang, S. T., and Reese, L. C. (1993). "COM624P-Laterally loaded pile analysis program for the microcomputer, Version 2.0." FHWA-SA-91-048, Federal Highway Administration, Washington, D.C., pp.504.

Wenz, K. P. "Large scale tests for determination of lateral loads on piles in soft cohesive soils." *Proceedings of the 8th International Conference of Soil Mechanics and Foundation Engineering*, 247-255.

B. Development of LPILE Method

B.1 Background

A method utilizing the program LPILE Plus 5.0, produced by Ensoft, Inc., has been developed to estimate the bending moments generated in batter piles subjected to downdrag. The approach uses the soil movement option in LPILE 5.0 Plus to apply the component of downdrag that acts normal to the pile axis when the pile is battered. As shown in Figure B.1, the soil movement is treated as displacement of the back side of the nonlinear p-y springs that act on the pile. For embankment surcharge loading that produces symmetrical compression on the flood side and protected side of the T-Wall, the primary direction of soil displacement due to consolidation under the embankment loading is assumed to be vertical. For embankment loading that produces asymmetric compression, there may be a significant component of lateral soil movement. The most straightforward approach to estimating the component of soil displacement that acts normal to the pile axis, $d_{N,z}$, is to multiply the vertical component of soil displacement, $d_{V,z}$, by the sine of the batter angle taken from vertical and add the result to the product of the horizontal component of soil displacement, $d_{H,z}$, and the cosine of the batter angle.

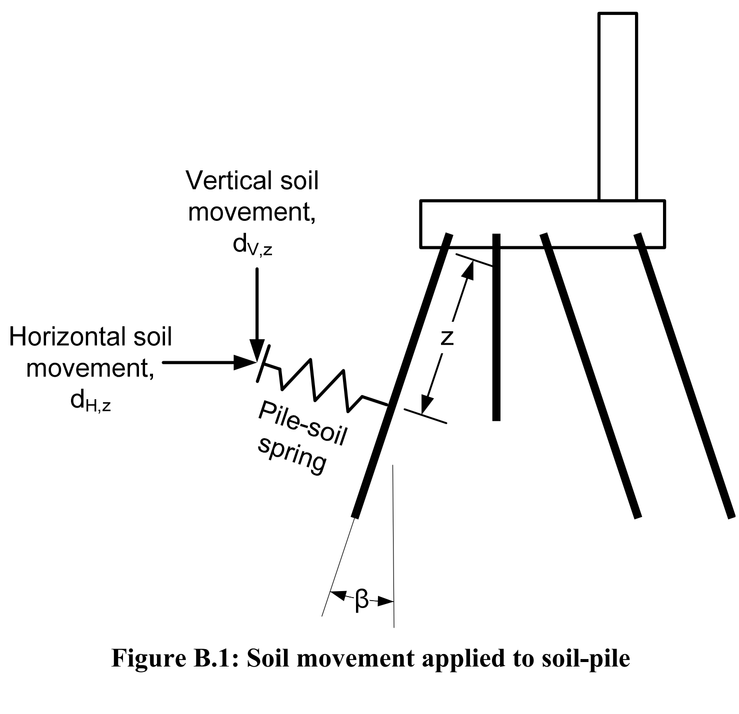

Figure B.1: Soil movement applied to soil-pile

Using the concept described above, the main issues to be addressed to apply this approach to T-Walls in the New Orleans area are:

1. What p-y soil response curves should be used in LPILE to represent the relationship between the soil pressure exerted on the pile and the soil movement due to consolidation?
2. How should pile batter be accounted for in LPILE?
3. What type of boundary conditions for moment and displacement should be applied to the top of the pile in LPILE?
4. What are the influences of the T-Wall, a sheet pile cut-off, stiff near-surface material beneath the T-Wall footing, and a second batter pile on the protected side on the downdrag-induced bending moments?
5. How can vertical compression calculated using straightforward hand calculations be adjusted to factor in the support provided by the piles and the T-Wall?
6. How can the impact of lateral soil displacement due to asymmetric fill be accounted for in the soil movements used as input to LPILE?

The following steps and observations led to answers to the above questions:

a) LPILE was applied to the experimental field scale study described by Takahashi (1985), Sato et al. (1987), and Sawaguchi (1989). LPILE was also applied to the laboratory studies conducted by Takahashi (1985) and Shibata et al. (1982).
b) Successful validation of the LPILE Method against the experimental results was achieved using a simple approach for determining soil movement due to vertical consolidation, the p-y relationships built into LPILE to model the soil layers, and an appropriate sign convention for entering the batter angle.
c) A parametric study was performed using the finite difference analysis program FLAC (Itasca 2002) for a pile-supported T-Wall on a simple foundation soil profile that was based on the profile used in the numerical model developed by GeoMatrix Consultants (2007) for analysis of T-Walls in the New Orleans area.
d) The results of the FLAC study were used as the basis for exploring the influence of the T-Wall, the sheet pile cut-off, existing fill or stiff near-surface soils beneath the T-Wall footing, and a second batter pile on the protected side on downdrag-induced bending moments. These analyses permitted determining which of these influences are significant for USACE T-Wall projects in the New Orleans area.

e) Compression of the foundation soil profile determined from the FLAC analyses in Step (c) was compared to the result of hand calculations performed using conventional geotechnical calculations without the stiffening effect of the T-Wall and piles. When the T-Wall and piles were removed from the FLAC model, the compressions calculated by hand agreed with the values determined using FLAC. When the T-Wall and piles were left in place in the FLAC model, the compressions in the vicinity of the piles were considerably smaller than those estimated by hand. The agreement between the experimental studies and the LPILE Method was based on using the reported settlements, which were influenced by the piles. Therefore, an approach had to be developed to adjust the hand-calculated soil compressions to account for the settlement reducing influence of the piles and the T-Wall.

f) The form of the LPILE Method that was validated against the experimental results in Step (b), together with the method for adjusting hand calculated settlements described in Step (e), were successfully used to calculate bending moments in agreement with those from the FLAC analyses in Step (c) for the case where the embankment fill is symmetrical with respect to the T-Wall. This result suggested that the LPILE Method was also applicable to pile-supported T-Walls that have a more complex soil-structure interaction than the A-frame pile configurations used in the experimental studies.

g) The FLAC model was then used to investigate the impact of asymmetric fill on the flood and protected sides of the T-Wall. A simple procedure was developed to relate soil compression determined by hand on the flood and protected sides of the T-Wall to the magnitude of horizontal soil movement which, when applied normal to the pile in LPILE, yielded bending moments that agreed with those determined by FLAC analyses.

B.2 Basics of the Method

B.2.1 Application of Soil Movements in LPILE

As described previously, the most straightforward way to determine the magnitude of soil movement normal to the pile axis at a position along the pile is to multiply the vertical component of soil displacement by the sine of the batter angle from vertical and add the result to the product of the horizontal component of soil displacement and the cosine of the batter angle. Rigorous application of this approach would require determining the soil movements at many locations along the length of the pile. Because the pile is battered, such an operation would require calculating movements along many different vertical profiles and using the settlement where the vertical profile intersects the pile. In the methods developed by Shibata et al. (1982) and Sawaguchi (1989) to estimate downdrag-induced bending moments, soil movements due to vertical compression are determined based on settlement evaluated at a single location. These methods make the simplifying assumption that soil movements are distributed linearly along the length of the pile from the value at the top of the pile to a value of zero at the pile tip. For piles that penetrate an embankment with significantly lower compressibility than the foundation soils, Takahashi (1985) assumed that the soil movements are constant over the length of the pile within the embankment.

A refinement of the approach described above for applying soil movement normal to the pile axis is to assume that soil movements along the pile are distributed according to the distribution of settlement evaluated along a single profile rather than a linear approximation. Using the measured or calculated settlement profile allows consideration of the compressibility of each soil layer and applies soil movements to the pile based on the cumulative compression at a particular elevation.

The LPILE Method adopts the assumption that soil movements will be distributed along the pile according to the distribution of vertical compression determined along a profile from the base of the T-Wall to the top of the bearing stratum or pile tip for profiles lacking a bearing stratum. The location of the profile where vertical compression is calculated for the complete LPILE Method is described in Section B.4.1. For validation of the basic LPILE Method described in Section B.3, some of the source material only reports measured ground surface settlement and lacks sufficient information to determine the distribution of soil compression. In these instances, a linear distribution of soil movement from the top of the pile to the tip of the pile was assumed.

Figure B.2 shows the relevant components and dimensions of the T-Wall and embankment configurations considered in this project for cases where the T-Wall is positioned within the compressible clay foundation soil or within an existing embankment. In this figure, L_e equals the length of pile within the existing embankment, L_c equals the length of pile in the clay, and z equals the distance along the pile starting from an origin at the base of the T-wall.

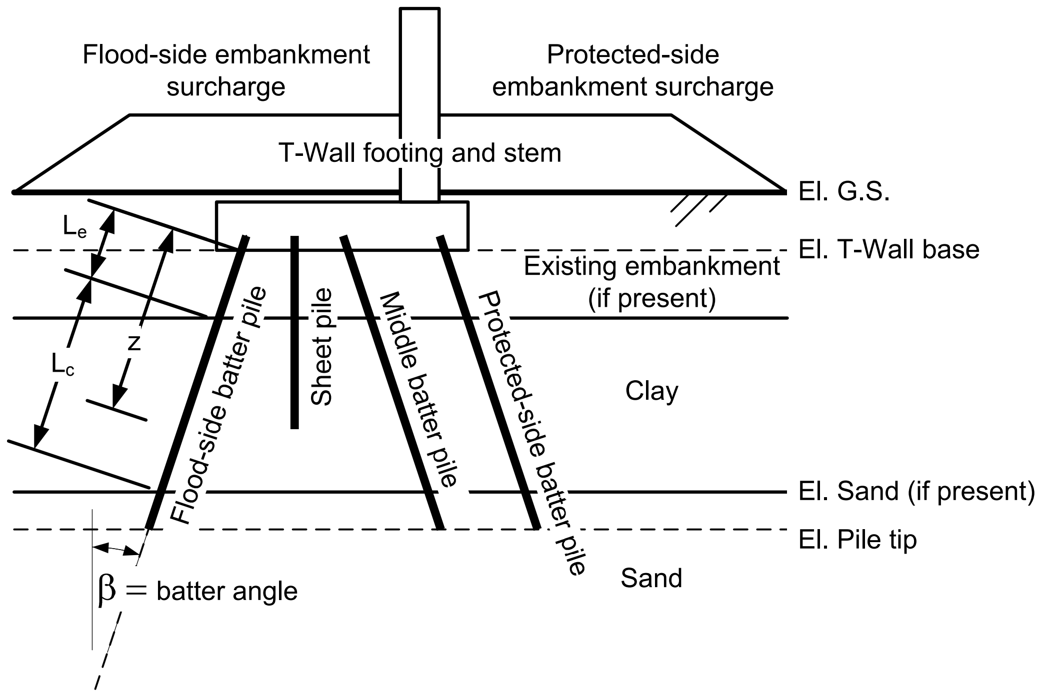

Figure B.2: Schematic diagram of pile-supported T-Wall, embankment, and sub-surface profile.

Soil movement applied as the spring support displacements along the pile, $d_{N,z}$, in LPILE is based on the distribution of settlement determined along a vertical profile. The spring support displacement at the top of the pile, $d_{N,0}$, is composed of the normal components of the vertical and lateral soil movements at the pile top, $d_{V,0}$ and $d_{H,0}$, according to Equation B.1, where β is the pile batter angle measured from vertical. Downward vertical soil movements have positive sign for piles on both the flood and protected sides. For the flood-side batter pile, horizontal soil movement from the flood side to the protected side has a positive sign. For piles on the protected side, horizontal soil movement from the protected side to the flood side has a positive sign. The spring support displacements along the pile length within the clay equal the spring support displacement at the pile top multiplied by the ratio of the profile settlement at the depth corresponding to the location along the pile, z, to the profile settlement at the elevation of the T-Wall base, $s_{z*\cos\beta}/s$. For T-Walls positioned with an existing embankment, the compression of the existing embankment due to the application of the new embankment surcharge is assumed to be insignificant relative to the compression of the clay foundation. Therefore, the spring support displacements over the length of pile within the existing embankment equal the displacement at the top of the pile. The calculations for $d_{N,z}$ are expressed in Equations B.2 and B.3.

$$d_{N,0} = d_{V,0}*\sin\beta + d_{H,0}*\cos\beta \quad \text{for } z = 0 \tag{B.1}$$

$$d_{N,z} = d_{N,0} \qquad \text{for } (0 < z \leq L_e) \qquad (B.2)$$

$$d_{N,z} = d_{N,0}(s_{z*\cos\beta}/s) \qquad \text{for } (L_e < z \leq L_e + L_c) \qquad (B.3)$$

B.2.2 Soil Response

The soil response for the clay is applied in LPILE using the built-in p-y relationship for soft clay developed by Matlock (1970) for clay with undrained strength less than or equal to 1250 psf and the p-y relationships for stiff clay developed by Reese et al. (1975) and Reese and Welch (1975) for clay with undrained strength greater than 1250 psf. Even though downdrag is a long-term consolidation phenomenon, the standard p-y curves for clays that are incorporated in LPILE provided a good fit to the results of the experimental studies, as shown in Section B.3 of this appendix. The undrained strengths used in LPILE should be based on experience or available laboratory and field data. A sand bearing layer located beneath the clay can be applied in LPILE using the p-y relationship proposed by Reese et al. (1974). The yield strength and stiffness parameters for the p-y response curves are assigned using guidance in the LPILE 5.0 Plus User's Manual (Ensoft, 2008). In the absence of specific information regarding selection of the values of strain at 50% of maximum stress, ε_{50}, for the soft clay and the soil modulus parameter, k, for sand, the default values in LPILE are recommended. The default values are assigned by entering zero in the ε_{50} and k input fields in LPILE.

LPILE considers a wedge type failure mode in determining the ultimate resistance of near-surface soils surrounding a pile that is subject to an applied load at the top and whose lateral movement is resisted by the soil. In the current application, the ultimate load able to be applied to the pile by movement of near-surface soil against the pile due to downdrag is limited by the weight and shear strength of the soils comprising the wedge. The soil above the elevation of the T-Wall base ($z < 0$) is considered in LPILE using guidance in the LPILE 5.0 Plus User's Manual (Ensoft, 2008) and the guidance provided in Section B.2.3 for transforming the soil profile to account for pile batter.

B.2.3 Batter Angle

The following three steps are taken to account for pile batter in the LPILE Method described here:

- The pile length is measured along the pile, and the soil layer thicknesses are transformed to match, as shown in Figure B.3.
- The unit weights of the soils are adjusted to produce the same vertical effective stress in the transformed soil profile as in the real soil profile at corresponding positions along the pile length. This is done by multiplying the soil unit weight, γ, by the cosine of the pile batter angle to produce an adjusted unit weight, $\gamma_z = \gamma * \cos(\beta)$. Total unit weights should be multiplied by the cosine of the pile batter angle for soils above the water table, and buoyant unit weights should be multiplied by the cosine of the pile batter angle for soils below the water table.
- LPILE provides for the possibility of a wedge type of failure mode near the ground surface for laterally loaded piles, and this failure mode depends on the batter angle of the pile. The sign convention for a pile that is subject to an applied load at the top and whose lateral movement is *resisted by the soil* is shown in Figure 3.9 in the LPILE User's Manual. When the *soil is moving against a pile* that is restrained at the top, the sign convention in Figure 3.9 of the LPILE User's Manual should be reversed, and the sign convention shown in Figure B.4 should be applied. For soil movement, this means that a positive batter angle should be input to LPILE for calculating bending moments due to downdrag.

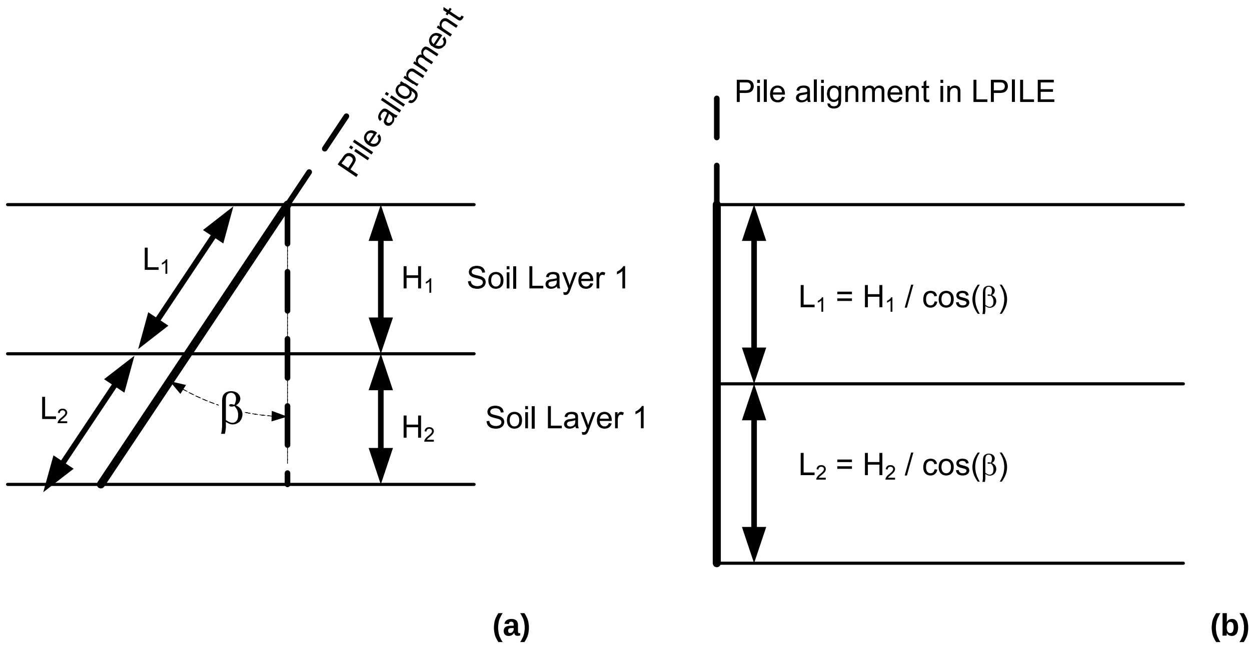

Figure B.3: (a) Actual soil stratigraphy, (b) Soil stratigraphy modified for pile batter angle

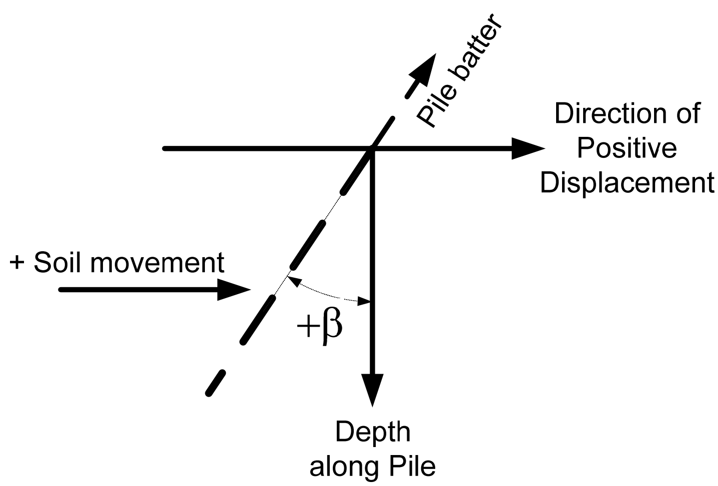

Figure B.4: Sign convention in LPILE for soil movement and pile batter

B.3 Validation of Basic LPILE Method

The LPILE Method described in the preceding sections was applied to the experimental results from the field tests reported by Takahashi (1985), Sato et al. (1987), and Sawaguchi (1989), as well as laboratory studies by Takahashi (1985) and Shibata et al. (1982). The details of these studies can be found in Appendices E and F of this report. For the field test, an embankment of unspecified material was constructed over a soft clay stratum to induce consolidation. Two battered piles were then installed through the embankment and soft clay stratum to a bearing layer of stiff clay and sand. A portion of the battered piles extended above the ground surface and were pinned together with a hinge at the top. Bending moments were measured in the piles over the year-long duration of the experiment. The input used in LPILE for the field experiment is shown below in Table B.1, Table B.2, and, Table B.3. The value for the moment of inertia shown in Table B.1 was determined according to $\pi/4*(r_o^4 - r_i^4)$, where r_o and r_i are the inner and outer radii of the pipe pile section determined from information given in the referenced papers. This value of moment of inertia is different from the value reported by Sato et al. (1987). Default LPILE values for ε_{50} were used for all soil layers. The results of the field-scale study include a vertical settlement profile obtained from six reference points embedded in the ground. None of the papers describing the field study explicitly indicate the location of the settlement profile relative to the piles; however, based on the width of the surcharge embankment provided by Sawaguchi (1989) and the horizontal projection of the piles from the center of the embankment, it can be assumed that the measured settlements must have been influenced by the presence of the piles. Measured compression of the embankment was insignificant relative to compression of the clay foundation.

Table B.1: Pile properties for field experiment

Pile Length (m)	Dist above ground (m)	Batter angle (deg)	Diameter (m)	Moment of Inertia (m^4)	Area (m)	Young's Modulus (kN/m^2)
38.7	0.9	15	0.508	0.0004623	0.0148	2e8

Table B.2: Soil layer input in LPILE for field experiment

Layer	Depth along pile (m)	Unit weight, γ_z (kN/m^3)	Undrained strength, S_u (kN/m^2)
Stiff Clay	0.9 to 3.5	7.0	25†
Soft Clay	3.5 to 9.9	7.0	20 to 16.6
Soft Clay	9.9 to 28.0	7.0	16.5 to 50
Stiff Clay	28.0 to 34.6	7.7	50 to 62
Stiff Clay	34.6 to 38.7	7.7	62

Table B.3: Soil movements applied normal to the pile in LPILE

Depth along pile (m)	364-day Soil Movement (m)	243-day Soil Movement (m)	119-day Soil Movement (m)	55-day Soil Movement (m)
0	0	0	0	0
0.9	0	0	0	0
0.9	0.0681	0.0590	0.0422	0.0280
3.5	0.0681	0.0590	0.0422	0.0280
5.4	0.0600	0.0520	0.0372	0.0247
11.8	0.0104	0.0090	0.0064	0.0043
24.2	0.0024	0.0021	0.0015	0.0010
36.4	0	0	0	0

The results of the LPILE analyses are shown in Figure B.5, where it can be seen that the LPILE results are in good agreement with the field data.

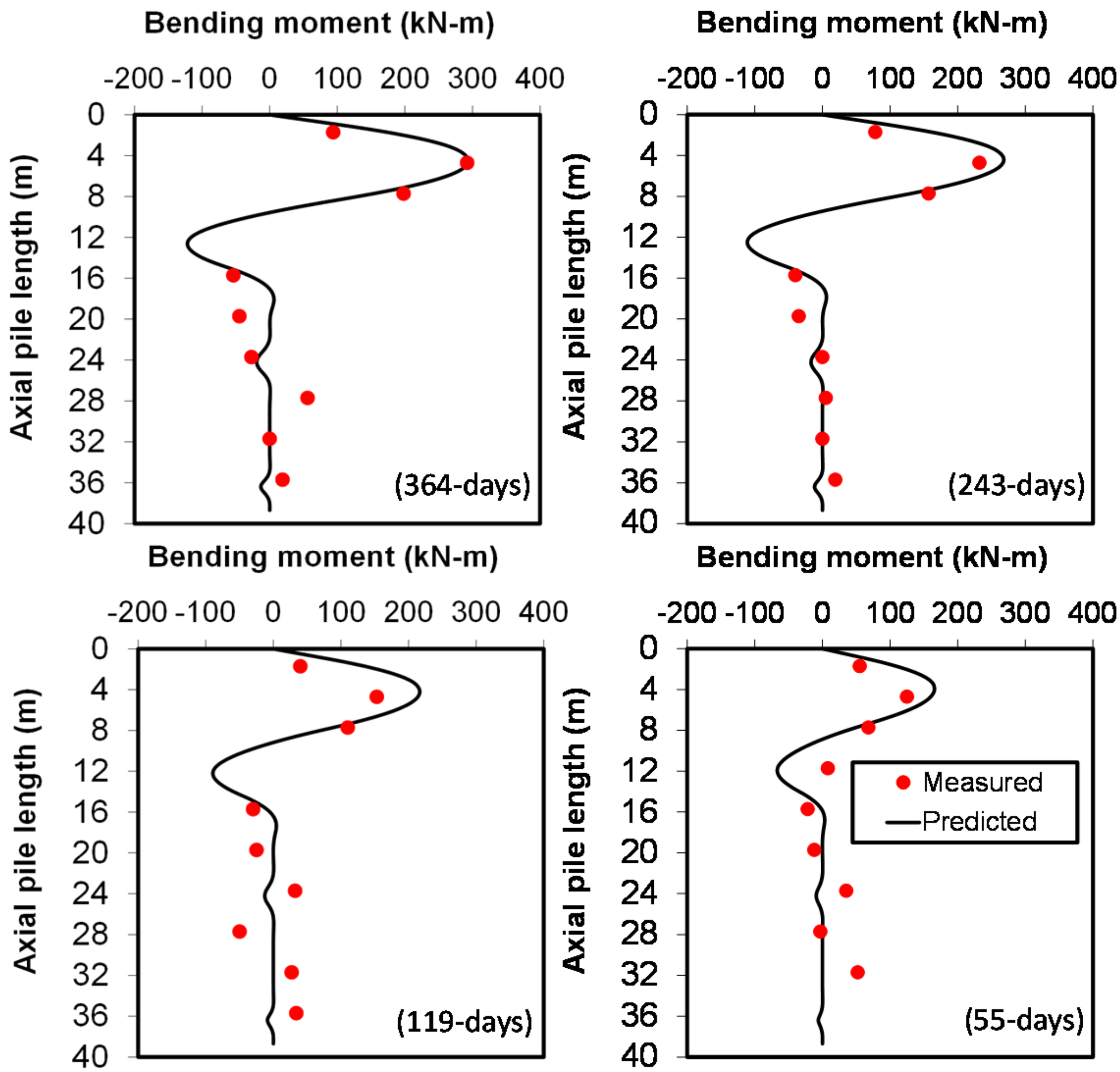

Figure B.5: Comparison of LPILE-predicted moments versus moments measured during field experiment

In addition to the field study, the basic LPILE Method was compared to laboratory-scale experiments performed by Takahashi (1985) and Shibata et al. (1982). The laboratory study performed by Takahashi (1985) included four pairs of piles at different batter angles. A layer of sand and steel shot was used to load the clay around the piles. A portion of the piles extended above the surface of the sand and shot; and each pair was connected with a hinge at the top. Bending moments in the piles and settlement of the sample surface were measured at various times during the year-long experiment for piles with two different batter angles. The input values used in the LPILE analysis of the laboratory experiments conducted by Takahashi (1985) are shown in Table B.4, Table B.5, and Table B.6. Due to the very low effective stresses present at the model scale, it is unclear whether the guidance for the stiffness parameter k given in the LPILE User's Manual is directly applicable. Accordingly, a range of values for k were used to represent the sand and steel shot layer used in the experiment to apply the surcharge pressure. In this instance, the LPILE analysis was not sensitive to values of k above 10,000 kN/m^3. The results of the LPILE analysis for k equal to 1,000 and 10,000 kN/m^3 are shown in Figure B.6, where it can be seen that a value of 1,000 kN/m^3 produced reasonably good agreement between the calculated and measured values of maximum bending moment. Default values of the stiffness parameter ε_{50} were used for the clay layers.

Table B.4: Pile properties for lab experiment by Takahashi (1985)

Pile Length (m)	Batter angles (deg)	Dist. above ground 20^o (m)	Dist. above ground 10^o (m)	Diameter (m)	Moment of Inertia (m^4)	Area (m)	Young's Modulus (kN/m^2)
1.78	20,10	0.237	0.308	0.075	4.556e-9	0.000675	2e8

Table B.5: Soil layer input in LPILE for lab experiment by Takahashi (1985)

Layer	Depth along pile (m)		Unit weight, γ_z (kN/m^3)		Undrained strength, S_u (kN/m^2)	Effective friction angle, φ'	Soil modulus parameter, k (kN/m^3)
	20^o batter	10^o batter	20^o batter	10^o batter			
Sand and steel shot	0.237 to 0.578	0.308 to 0.633	29.4	30.8	--	35	1,000 or 10,000
Soft Clay	0.578 to 1.000	0.633 to 1.000	4.8 to 4.7	5.1 to 4.9	5	--	--
Soft Clay	1.000 to 1.780	1.000 to 1.780	4.7 to 5.1	4.9 to 5.3	5 to 10	--	--

Table B.6: Soil movements applied normal to the pile in LPILE for lab experiment by Takahashi (1985)

Depth along pile (m)	14-week Soil Movement (m) 20° batter angle	4-week Soil Movement (m) 20° batter angle	1-week Soil Movement (m) 20° batter angle	14-week Soil Movement (m) 10° batter angle
0	0.0561	0.0338	0.0157	0.0285
1.78	0	0	0	0

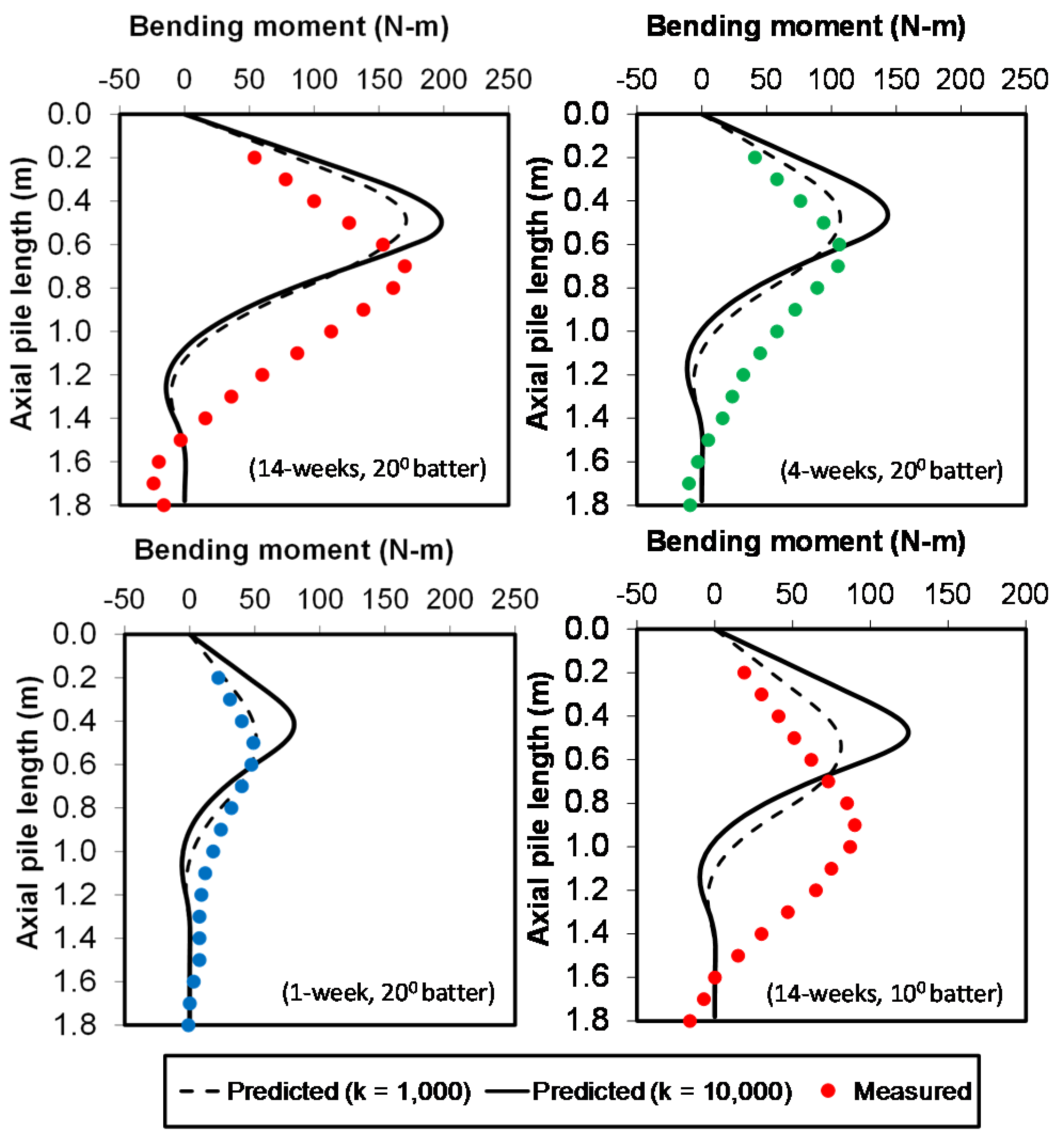

Figure B.6: Moments predicted in LPILE analysis of laboratory study by Takahashi (1985)

The inputs used in the LPILE analysis of the laboratory study performed by Shibata et al. (1982) are shown in Table B.7, Table B.8, and Table B.9. Shibata's study involved measuring settlement of the sample surface and bending moments in model piles subjected to downdrag produced by applying three magnitudes of surcharge pressure: 20 kPa, 40 kPa, and 60 kPa. Since the piles in this model were pinned at both the top and bottom, a pinned boundary connection was needed at the bottom of the pile in LPILE. This was accomplished by adding a length of pile with a very low flexural rigidity beyond the actual pile tip. The flexible portion of the pile was embedded in a very strong rock layer. These modifications resulted in a pinned condition of essentially no moment or displacement at the tip of the pile. Figure B.7 shows the results of the LPILE analysis performed for the laboratory study by Shibata et al. (1982), and it can be seen that the agreement is reasonably good.

Table B.7: Pile Properties for laboratory study by Shibata et al. (1982)

Pile Length (m)	Batter angles (deg)	Diameter (m)	Moment of Inertia (m^4)	Area (m)	Young's Modulus (kN/m^2)
0 to 0.6	15	0.06	9.6e-8	0.000222	2.1e8
0.6 to 1	15	0.06	1e-8	0.000222	100000

Table B.8: Soil layer input in LPILE for laboratory study by Shibata et al. (1982)

Layer	Depth along pile (m)	Unit weight, γ_z (kN/m^3)	Undrained strength, S_u† (kN/m^2)	Strain at 50% maximum stress, ε_{50}	Unconfined compressive strength (kN/m^2)
Soft Clay	0 to 0.6	6.5	3 (*6*), 6 (*12*), 9 (*18*)	0.02	
Rock	0.6 to 1.0	22			100,000

Table B.9: Soil movements applied normal to the pile in LPILE for laboratory study by Shibata et al. (1982)

Depth along pile (m)	20 kPa Soil Movement (m)	40 kPa Soil Movement (m)	60 kPa Soil Movement (m)
0	0.0142	0.0172	0.0182
0.6	0	0	0
1.0	0	0	0

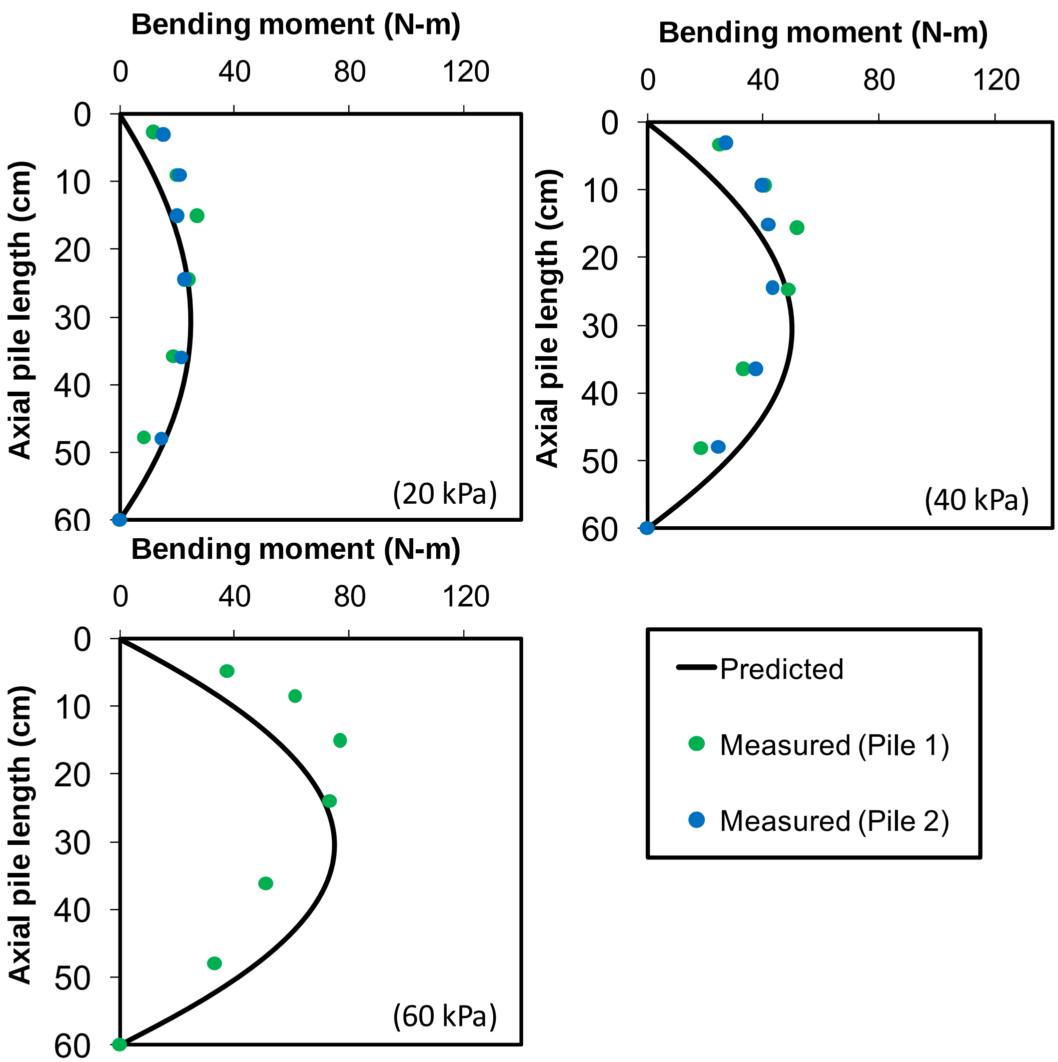

Figure B.7: LPILE analysis of laboratory study by Shibata et al. (1982)

The soil movements used in LPILE for the laboratory studies by Takahashi (1985) and Shibata et al. (1982) are based on reported values of surface settlement of the samples; however, the locations in the tank relative to the piles where the settlements were measured were not reported. Since the apparatuses used in both laboratory studies were too small for the measured settlements to reflect a free field condition, it can be reasonably assumed that the reported settlements are influenced by the presence of the piles.

Reported values of undrained shear strength were used in LPILE for the field study and laboratory study by Takahashi (1985). For the laboratory study performed by Shibata et al. (1982) the clay was placed around the piles as a slurry and allowed to consolidate under self-weight, therefore the undrained strength of the clay at the start of the test when the surcharge pressure was applied was likely very low, with an average value of about 0.5 kPa. The undrained strengths used in analyses by Shibata et al. (1982) are based on an assumed undrained strength ratio of 0.3 multiplied by the value of the surcharge pressure. It is likely that this approach significantly overpredicts the undrained strength of the clay for the majority of the consolidation-induced soil movement. This is supported by the fact that LPILE significantly overpredicts bending moments when the assumed strength values listed in the paper are used. If strengths equal to half the reported values are used, to approximately represent the average strength during the consolidation process, the agreement with the measured moments for the three surcharge pressures is quite good, as shown in Figure B.7.

B.4 Refinement of the Basic LPILE Method

The validation of the LPILE Method described in Section B.3 of this appendix left the following issues still to be addressed to develop a practical method that can be applied to the T-walls typically used by the USACE in New Orleans and vicinity:

A. The stiffening effect of the piles on soil settlements, as compared to conventional settlement calculations without piles.
B. The shielding effect of the T-wall, which may reduce stress changes in the compressible soil from the fill load.
C. The effect of an existing embankment.
D. The effects of multiple batter piles on the protected side.
E. The effects of a sheet pile cutoff wall.
F. The effects of asymmetry of embankment fill, which could cause an additional bending moment on the pile closest to the greater fill load.
G. The effects of an all clay profile without a sand bearing layer.

These factors were investigated for the geometries shown in Figures B.8 and B.9 for the cases listed in Table B.10 using an adaptation of the FLAC model developed by Geomatrix Consultants, Inc. (Geomatrix, 2007). Table B.10 also includes the maximum bending moment, M_{max}, in the batter piles calculated from the FLAC analyses. The existing embankment layer included in Geometry (e) was of broad lateral extent. The property values used in FLAC for the piles are listed in Table B.11. The existing embankment material, clay, and sand used in the FLAC model were assigned property values listed in Table B.12. For the purpose of settlement calculations for Geometries (a) through (d), the preconsolidation pressure of the clay was assumed to be equal to the initial effective vertical stress below El. -20 ft and to be equal to the initial effective vertical stress at El. -20 ft for elevations above -20 ft. For Geometry (e), the clay was assumed to be normally consolidated under the load from the existing embankment. Figure B.10 shows the undrained shear strength profiles used in LPILE to establish the p-y curves for the clay. The ground water level was assumed to be at the ground surface, El. -2. The bottom of the model is at El. – 140 ft, and no displacements are allowed below this level.

The new embankment geometry extended laterally such that the mid-point of the side slopes was 75 ft from the protected-side face of the T-Wall stem in either direction for cases where the fill is symmetric and only on the flood side for cases with asymmetric fill. The embankment load was applied as a pressure on the ground surface in the FLAC model, rather than adding elements of soil to the mesh. This approach simplified the process of evaluating many different magnitudes of surcharge pressure. To evaluate the impact of this simplification, FLAC analyses were performed to compare the moments in the piles when the embankment was modeled using elements of soil versus applied pressure. When the embankment was symmetric on the flood and protected sides, the difference between the moments was small, with the case using applied pressure producing slightly higher moments than the case using soil elements. This outcome means that using applied pressures instead of soil is conservative when the fill loading is symmetric. When the embankment was asymmetric, the difference between the moments was more significant and depended on the pile being compared. This outcome, and the implications on the calibration of the LPILE Method, is discussed in detail in Section B.4.4.

Issues (A) through (G) listed above are addressed in the sections that follow. Issue (A) is discussed in Section B.4.1, Issue (B) is discussed in Section B.4.2, Issue (C) is discussed in Sections B.4.1, B.4.4, and B.4.6, Issue (D) is discussed in Sections B.4.3 and B.4.4, Issue (E) is discussed in Sections B.4.3 and B.4.4, Issue (F) is discussed in Section B.4.4, and Issue (G) is discussed in Section B.4.5.

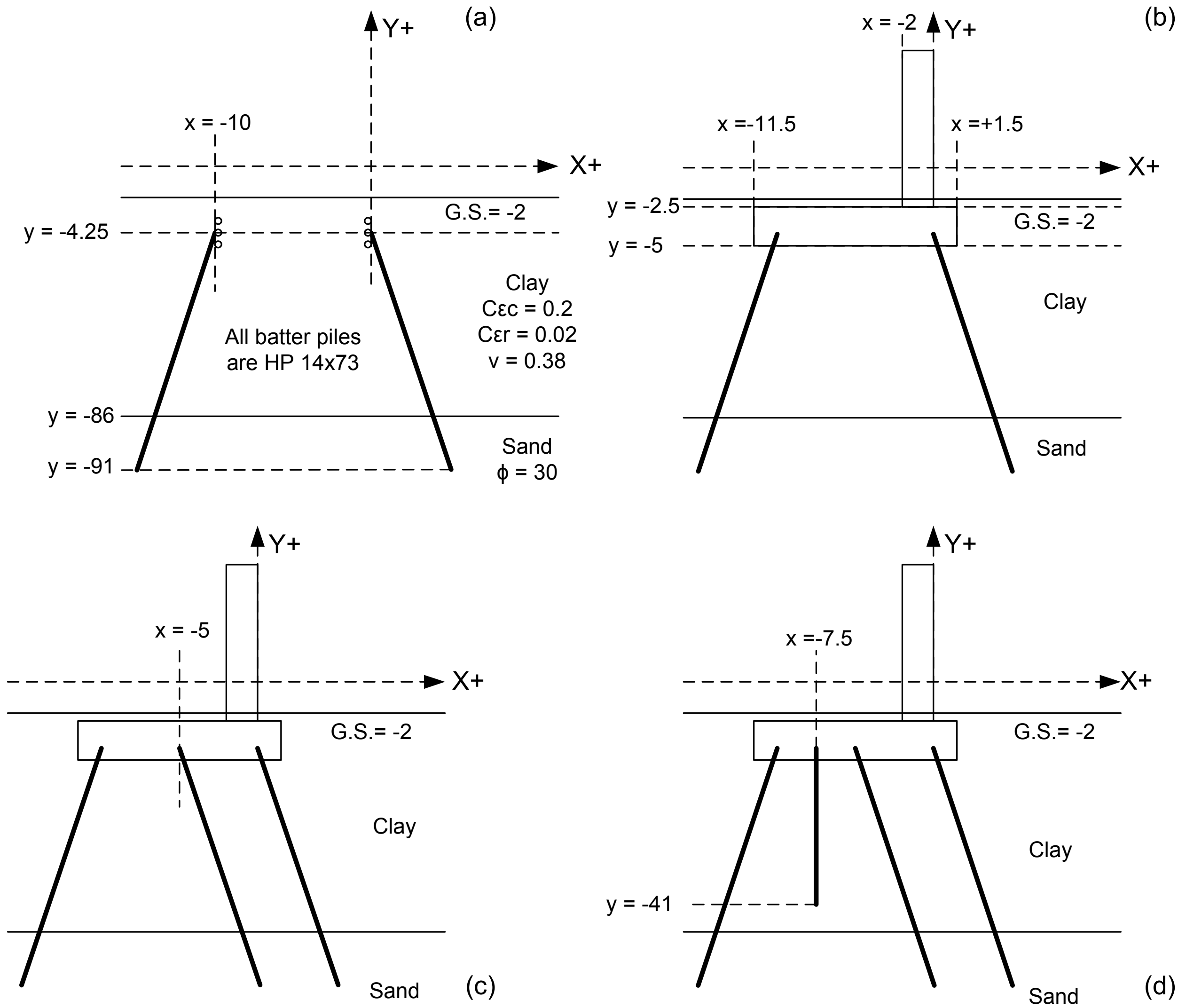

Figure B.8: Geometries evaluated in FLAC for the purpose of developing the LPILE Method with T-Wall positioned in soft clay: (a) Pair of batter piles with roller supports, (b) Pair of batter piles pinned at base of T-Wall footing, (c) Three batter piles pinned at base of T-Wall footing, (d) Three batter piles plus sheet pile pinned at base of T-Wall footing. In all cases shown, the flood side is to the left of the T-Wall stem. The coordinate values shown for each portion of the figure also apply to all subsequent portions of the figure. All piles at 3V:1H batter. All distances and elevations in feet.

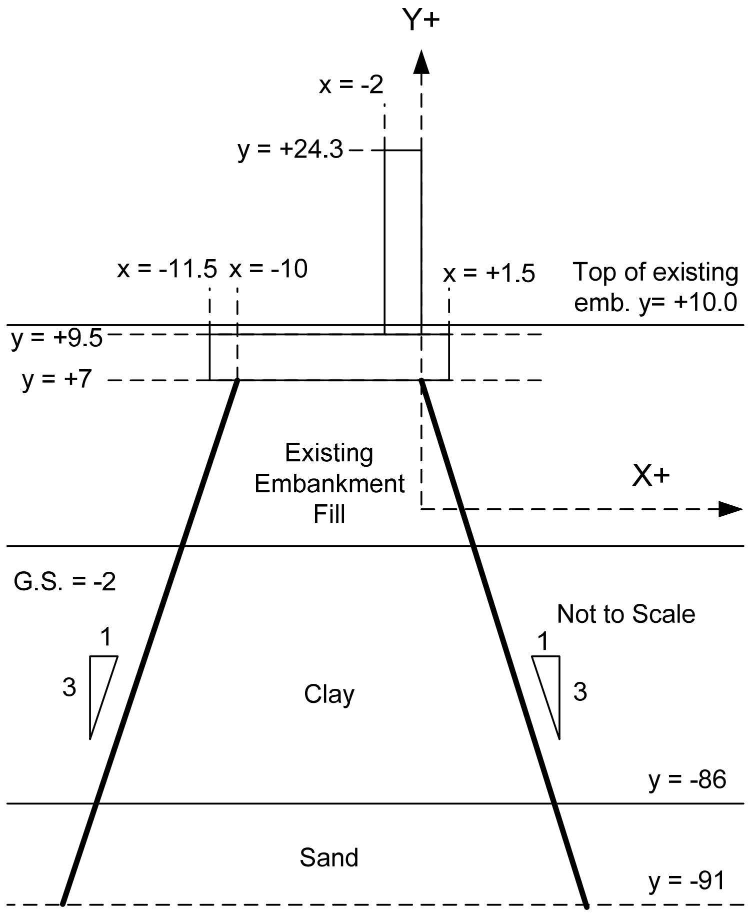

Figure B.9: Geometry (e) evaluated in FLAC for the purpose of developing the LPILE Method with the T-Wall positioned within existing embankment. The flood side is to the left of the T-Wall stem. All distances and elevations in feet.

Table B.10: FLAC analyses in parametric study

CASE	Geometry	Flood-side, FS, Surcharge (psf)	Protected-side, PS, Surcharge (psf)	FS pile M_{max} (k-ft)	Middle pile M_{max} (k-ft)	PS pile M_{max} (k-ft)
1	a	660	660	112	--	-111
2	a	330	330	57	--	-57
3	a	990	990	164	--	-164
4	b	330	330	63	--	-52
5	b	660	660	117	--	-100
6	b	990	990	168	--	-148
7	b	330	0	88	--	27
8	b	660	0	120	--	16
9	b	990	0	120	--	-33
10	c	660	660	116	44	-84
11	c	660	0	159	57	47
12	d	660	660	86	44	-96
13	d	660	0	136	51	42
14[a]	a	660	660	118	--	-117
15[a]	d	660	660	100	-59	-109
16	c	330	0	88	32	27
17	c	990	0	216	76	64
18	b	1320	0	118	--	-78
19	c	1320	0	270	94	79
20	b	165	0	45	--	18
21	c	165	0	42	16	15
22	b	495	0	111	--	27
23	c	495	0	126	45	37
24	b	825	0	120	--	-16
25	c	825	0	188	67	56
26	b	1155	0	118	--	-54
27	c	1155	0	246	86	72
28	b	1320	1320	229	--	-190
29	c	330	330	61	27	-47
30	c	990	990	162	61	-114
31	c	1320	1320	205	77	-149
32	b	165	165	30	--	-21

a. No sand bearing layer included in profile (i.e. all clay).

Table B.11 continued: FLAC analyses in parametric study

CASE	Geometry	Flood-side, FS, Surcharge (psf)	Protected-side, PS, Surcharge (psf)	FS pile M_{max} (k-ft)	Middle pile M_{max} (k-ft)	PS pile M_{max} (k-ft)
33	c	165	165	27	17	-21
34	b	495	495	94	--	-78
35	c	495	495	92	37	-68
36	b	825	825	147	--	-119
37	c	825	825	141	54	-98
38	b	1155	1155	204	--	-167
39	c	1155	1155	184	69	-130
40	e	660	660	83	--	-83
41	e	990	990	144	--	-141
42[b]	e	1320	1320	227	--	-220
43	e	1320	1320	216	--	-212
44[b]	e	1320	1320	225	--	-222
45	e	660	0	139	--	59
46	e	990	0	208	--	82
47	e	1320	0	273	--	94
48	b	1650	1650	282	--	-232
49	e	330	330	38	--	-41
50	e	1650	1650	280	--	-276
51	e	330	0	71	--	32
52	e	1650	0	322	--	100

b. Undrained strength of existing embankment equal to 400 psf for Case 42 and 1,600 psf for Case 44.

Table B.11: H-Pile (HP 14x73) properties used in FLAC analyses to calibrate LPILE Method

Moment of Inertia (in.^{4})	726
Depth and Width of Section (in.)	13.6 x 14.6
X-Sectional Area (in.^{2})	21.4
Young's Modulus (psi)	29 x 10^6

Table B.12: Soil properties used in FLAC analyses to calibrate LPILE Method

	Existing Embankment	Soft Clay	Sand
Effective unit weight[1], γ (pcf)	110	50	60.5
Compression ratio, $C_{\varepsilon c}$ Recompression ratio, $C_{\varepsilon r}$		0.2 0.02	
Preconsolidation pressure, p_p (psf)		$\text{Max}\begin{cases}900\\ \sigma_v'\end{cases}$	
Undrained strength, s_u (psf)	800	$\text{Max}\begin{cases}200\\ \frac{2}{9}(\sigma_v')\end{cases}$	
Effective friction angle, φ' (deg)		23	30
Effective cohesion (psf)		0	0
Effective Poissons Ratio		0.38	0.35
Effective Youngs Modulus (psf)	500(s_u)	varies	423,000

1. Ground water was located at the elevation of the original ground surface, El. -2

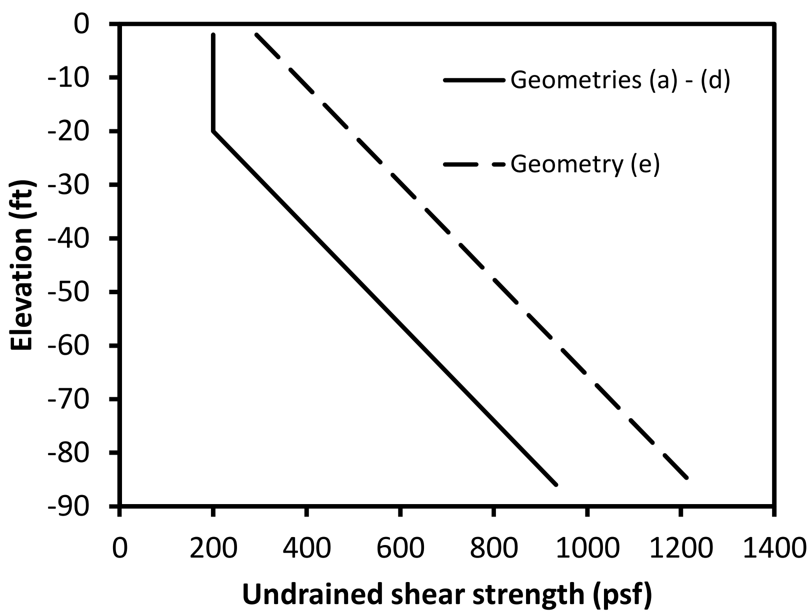

Figure B.10: Undrained shear strength of clay layer in the FLAC model

B.4.1 Effect of Piles on Soil Settlements

As described in Section B.2.1, vertical soil movement acting on the pile in LPILE is determined by the magnitude of settlement calculated along a vertical profile over the elevation interval from the base of the T-Wall to the top of the pile bearing layer, or pile tip, for profiles lacking a distinct bearing layer. Settlements determined without the presence of the piles, s, will over-predict the soil movement and therefore the maximum bending moment calculated using LPILE. This section describes selection of a consistent location to evaluate soil compression and a method to account for the stiffening effect of the piles.

A vertical profile that intersects the pile at 25 percent of the vertical distance from the base of the T-Wall footing to the top of the bearing layer, or pile tip if no bearing layer is present, was selected for the location to evaluate compression because it is near the point along the pile that experiences the maximum bending moment. This location is a horizontal distance measured from the location where the pile intersects the T-Wall base equal to $0.25(L_e + L_c)\sin(\beta)$. Settlement along this profile location can be computed using ordinary geotechnical procedures for hand or spreadsheet calculation of 1-D compression beneath a finite located area. A sample calculation is provided in Appendix H. The fill overlying the base of the T-Wall is excluded from the calculation since this material is primarily supported by the T-Wall and piles, and it does not impose a significant load on the foundation soil. The locations of the profiles for calculating settlement are shown Figures B.11 and B.12. When the calculation is performed for the profile on the flood side, the resulting compression is referred to herein as s_F. On the protected side, the settlements s_M and s_P are determined along profiles that intersect the middle and protected-side piles, respectively.

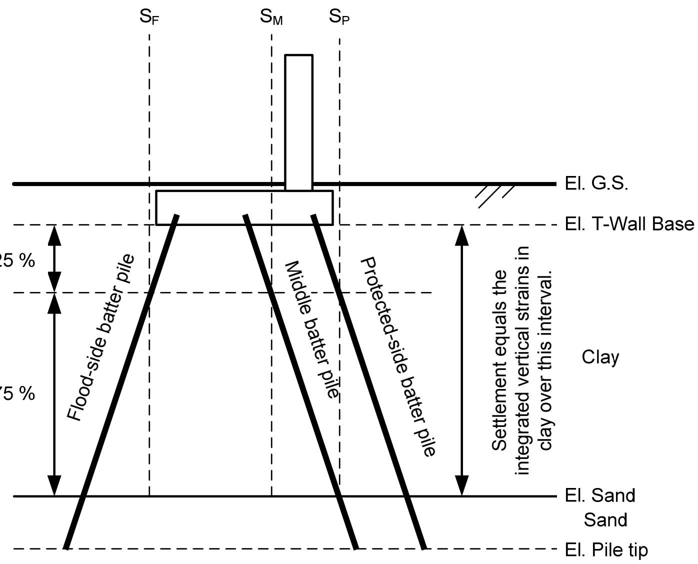

Figure B.11: Location of settlement profiles, when the T-Wall is positioned within the clay foundation, for determining soil movements used in LPILE

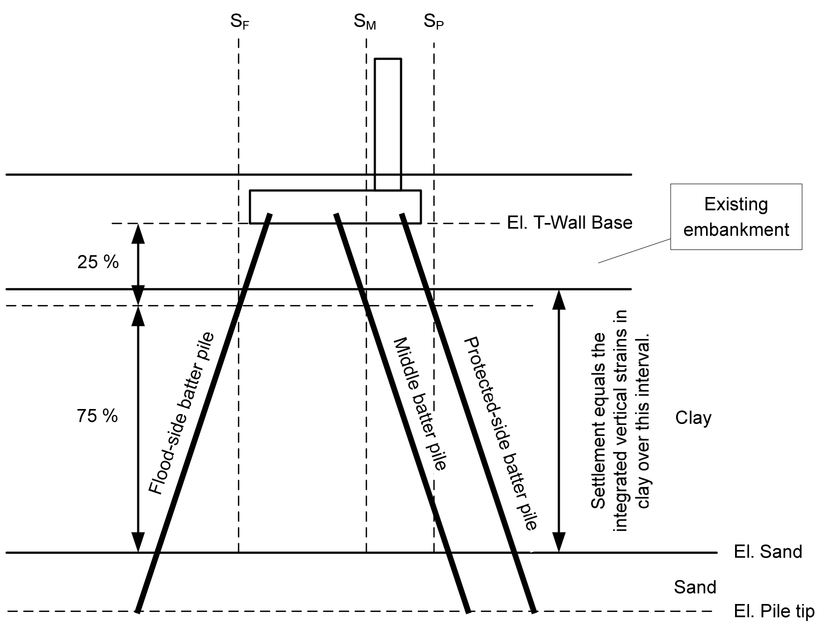

Figure B.12: Location of settlement profiles, when the T-Wall is positioned within an existing embankment, for determining soil movements used in LPILE

The stiffening effect of the piles was investigated in two ways: 1) by comparing s_F to FLAC calculations of soil compression with piles present using Geometries (b) and (e) in Figures B.8 and B.9, and 2) by comparing the value of s to the magnitude of vertical soil compression, $d_{V,0}^{FLAC}$, whose normal component, when applied to the p-y spring supports in LPILE, produces the same value of the maximum moment as calculated in FLAC.

Using the first approach, the value of s_F was compared to s_F^{FLAC}, which is the FLAC-calculated compression at the same location with piles, for Geometries (b) and (e) with symmetric embankment loading. An example of the comparison between s_F and s_F^{FLAC} is provided in Appendix H. For symmetric loading, an equivalent calculation of compression on the protected-side would be essentially the same. The comparisons of s_F to s_F^{FLAC} given by the open symbols in Figure B.13 for Geometries (b) and (e) show that, at least for the range of hand-calculated compressions evaluated, the stiffening effect of the piles significantly reduces the magnitude of compression relative to the case where no piles are present. This comparison is important because the basic LPILE Method was validated against the experimental results using reported values of settlement that were influenced by the stiffening effect of the piles. If compressions determined by hand were used instead of the reported values of settlement, it is likely that the LPILE Method would have predicted moments that were significantly higher than the measured values.

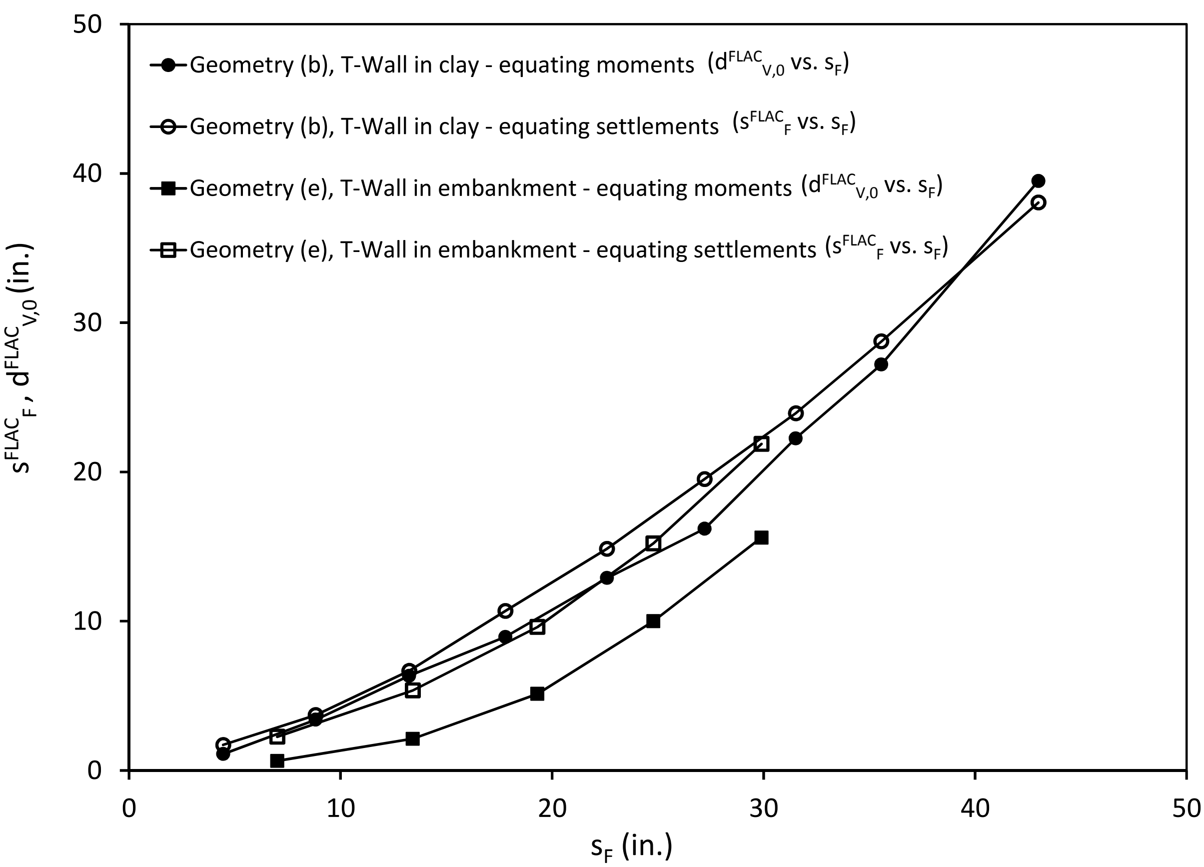

Figure B.13: Relationship between 1-D hand-calculated settlement on flood side, s_F, and settlement calculated by FLAC and relationship between s_F and $d_{V,0}$ applied in LPILE that produces maximum moment calculated by FLAC.

Another way to consider the stiffening effect of the piles on soil compression is to compare the magnitude of vertical soil compression, $d_{V,0}^{FLAC}$, whose normal component, when applied to the p-y spring supports in LPILE, produces the same maximum moment as calculated in FLAC for the flood-side batter pile. An example of the comparison between s_F and $d_{V,0}^{FLAC}$ is provided in Appendix H. The moment in the flood-side pile is used for this comparison because, as described in Section B.4.2, it experiences higher bending moments than the protected-side pile for symmetric loading. The approach of basing the stiffening effect of the piles on $d_{V,0}^{FLAC}$ is different from the approach using s_F^{FLAC} described above in that $d_{V,0}^{FLAC}$ is a fixed value for a particular set of conditions whereas s_F and s_F^{FLAC} depend on the location of the vertical profile over which compression is evaluated. This feature makes $d_{V,0}^{FLAC}$ a benchmark that, unlike s_F^{FLAC}, is not sensitive to the choice of profile location. The filled symbols in Figure B.13 show the relationships between s_F and $d_{V,0}^{FLAC}$ for Geometries (b) and (e) using the results from the FLAC parametric study.

From Figure B.13, it can be seen that the relationships comparing s_F with d_F^{FLAC} and $d_{V,0}^{FLAC}$ are quite similar for Geometry (b) and reasonably similar for Geometry (e). This suggests that selection of the plan-view location for calculating compressions is fairly representative of the vertical soil movements applied in LPILE to generate moments that are in agreement with the FLAC results (i.e. $s_F^{FLAC} \approx d_{V,0}^{FLAC}$). Due to the similarity between the relationships and because the USACE has developed confidence in using FLAC to calculate soil-structure interactions for pile-supported T-walls, the stiffening effect of the piles is accounted for in the LPILE Method using the comparison between s_F and $d_{V,0}^{FLAC}$. As described below in Section B.4.4, the settlement corresponding to the pile being analyzed by the LPILE Method is used as the input value in Figure B.14 to obtain the vertical soil movement, $d_{V,0}$, to be used at the top of the pile in the LPILE Method. The relationships provided in Figure B.14 were developed for values of s ranging from 4.5 to 43 inches for cases where the T-Wall is positioned within the clay foundation and from 6.5 to 30 inches for cases where the T-Wall is positioned within an existing embankment. Extrapolation of the relationships should be done at the discretion of the designer, but $d_{V,0}$ never needs to be greater than s.

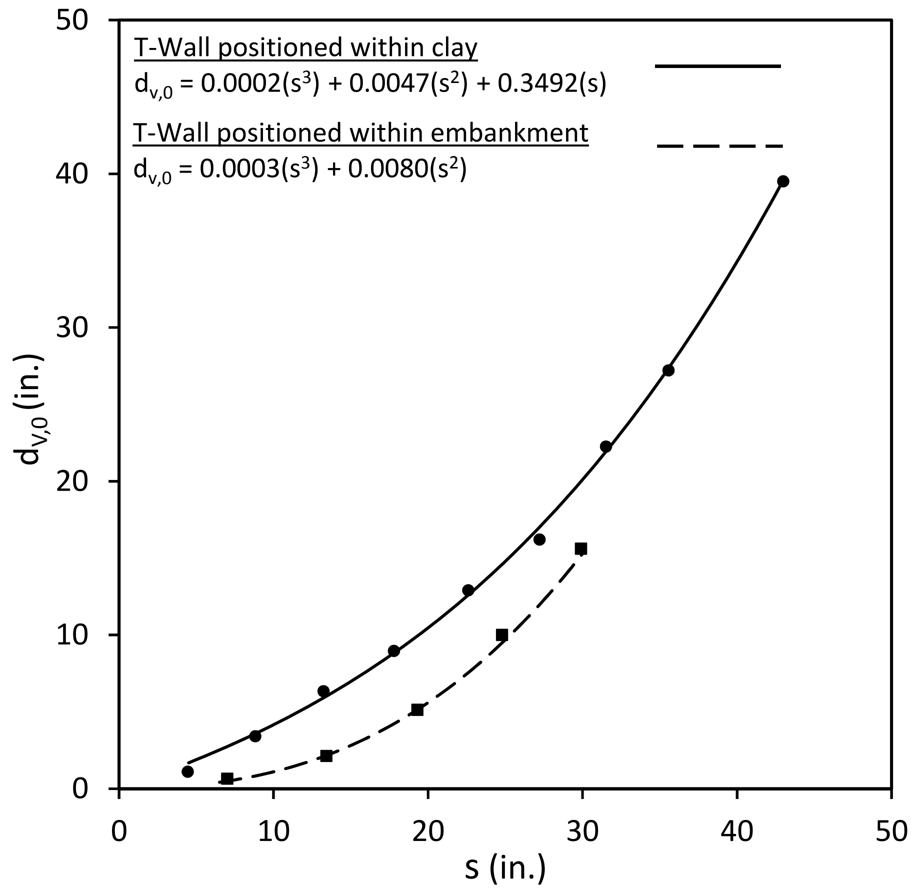

Figure B.14 Relationship between s and $d_{V,0}$ to account for stiffening effect of piles on compression

B.4.2 Effect of T-Wall

The presence of the T-Wall can influence downdrag-induced bending moments by: 1) shielding foundation soils in the vicinity of the piles from the full surcharge pressure produced by the embankment and 2) moving the tops of the batter piles by the effect of frame action between the piles and the T-Wall footing.

The shielding effect of the T-wall can be evaluated by comparing the results listed in Table B.10 for Cases 2, 1, and 3 for fill pressures of 330, 660, and 990 psf, respectively, with the average absolute value of maximum moment for the flood-side and protected-side piles for Cases 4, 5, and 6. This comparison shows that the shielding effect of the T-wall does not produce much change in the maximum bending moments. The lack of a shielding effect may be due, in part, to the fact that the maximum bending moment in the batter piles occurs at about Elevation -20 ft, which is beyond the T-wall limits for the batter piles. Also, while the fill load between the piles for Cases 1, 2, and 3 generates additional vertical settlement, which increases bending moments, the lack of shielding for these cases reduces the inward lateral component of soil movement produced by the fill beyond the T-Wall, thus reducing bending moments. The LPILE Method for symmetric fill was calibrated using only vertical soil movements, $d_{V,0}$, and the fill overlying the T-Wall base is not included in the compression calculations. This approach yields good agreement between the FLAC and LPILE moments, and it is slightly conservative overall because the fill loads in the FLAC analyses were imposed by surcharge pressures instead of fill soil, which tends to reduce the shielding effect.

The effect of frame action between the batter piles and the T-Wall base can be evaluated by comparing the maximum bending moments in the flood-side and protected-side batter piles when the embankment fill is symmetrical. The frame action develops due to the effect of the eccentric location of the wall stem. Figure B.15 shows the absolute value of the maximum bending moments in the flood-side and protected-side batter piles determined using FLAC for Geometry (b) versus the applied embankment pressure. The figure shows that the maximum bending moments are higher, on average by about 23 percent, for the flood-side batter pile than for the protected-side pile when no middle pile is present. As discussed in Section B.4.3, the presence of a middle batter pile reduces the maximum moment in the outer protected-side pile. This effect results in the maximum bending moment in the flood-side pile being larger by about 45 percent, on average, than the maximum bending moment in the protected-side pile. Therefore, for the conditions evaluated using symmetric loading, the critical pile for down-drag induced bending moments is the flood-side batter pile.

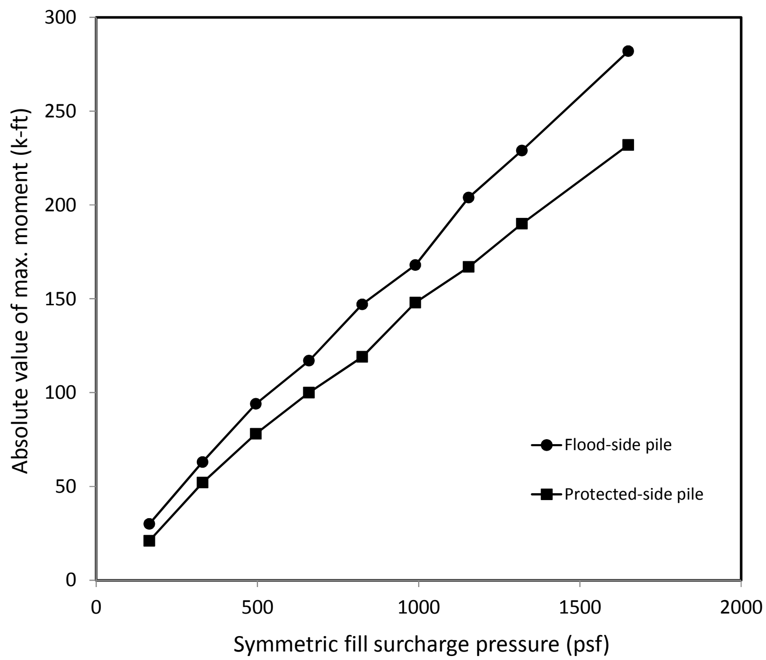

Figure B.15: Absolute value of the maximum bending moment in the flood-side and protected-side batter piles determined using FLAC for Geometry (b) versus symmetric surcharge pressure

B.4.3 Effect of Additional Piles

The FLAC analyses performed using Geometries (c) and (d) permitted evaluating the effect of a middle batter pile and a sheet pile cut-off on downdrag-induced bending moments. Figure B.16 shows that, for symmetric loading, the presence of the middle batter pile has very little influence on the bending moment in the flood-side batter pile. It can be concluded that the middle batter pile does not need to be considered when the LPILE Method is applied to the flood side pile and the fill is symmetric.

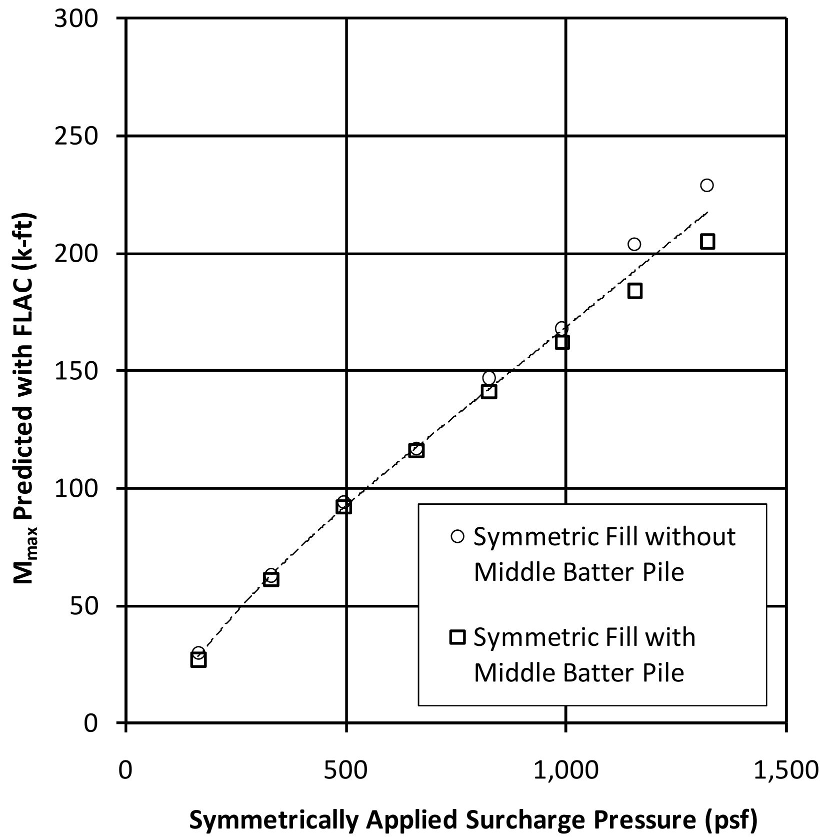

Figure B.16: Influence of middle batter pile on maximum moment in the flood-side batter pile

Figure B.17 shows the influence of the middle batter pile on moments produced in the protected-side pile when the fill is symmetric. The figure shows that the middle batter pile significantly reduces moments in the protected-side pile, particularly for high embankment pressures. This effect is likely due to the additional support provided by the middle pile to the protected-side pile and nearby soil.

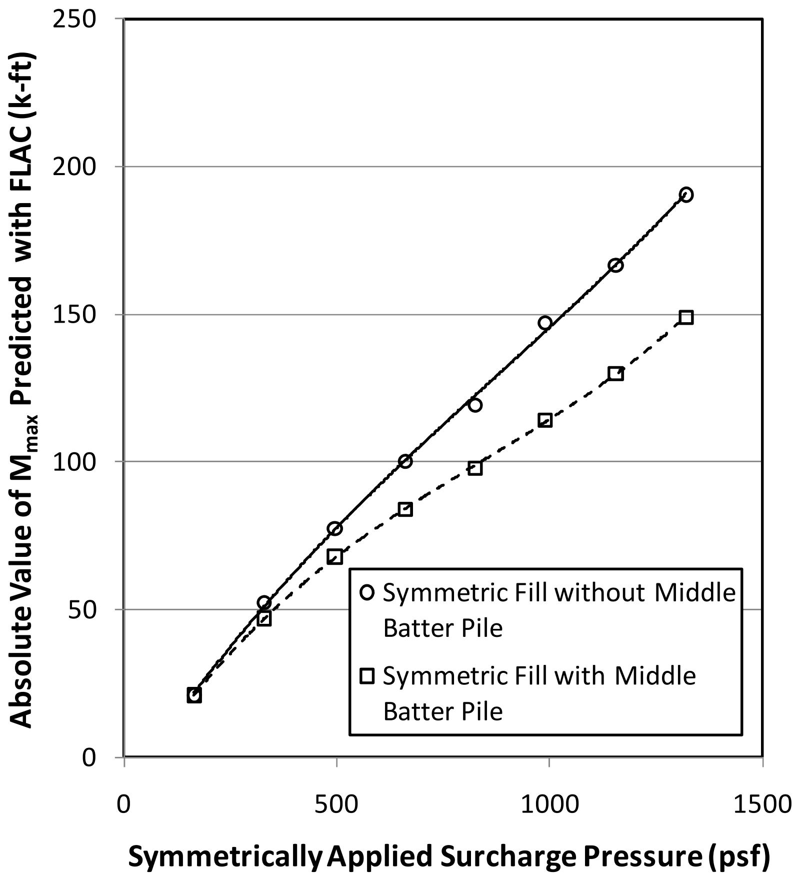

Figure B.17: Influence of middle batter pile on maximum moment in the protected-side batter pile

The influence of the sheet pile cut-off for cases with symmetric fill can be evaluated by comparing Case 10 with the results of Case 12 in Table B.10. From these cases it is seen that the sheet pile cutoff wall reduces maximum bending moments. The magnitude of this reduction is expected to be sensitive to the depth and the lateral position of the sheet pile with respect to the battered piles, and its influence can be conservatively neglected from the LPILE Method.

B.4.4 Effect of Fill Asymmetry

The FLAC analyses permit consideration of cases where the magnitude and/or lateral extent of the embankment fill on the flood and protected sides of the T-Wall is asymmetric and results in $s_F \neq s_P$. When compression of the clay foundation resulting from embankment loading is asymmetric, there can be horizontal soil displacement that acts on the piles and the T-Wall. Excluding the possibilities of lateral spreading and heave, Figure B.18 shows the directions of vertical and horizontal soil movement for symmetric and asymmetric loading cases. When the components of vertical and horizontal soil movement that act normal to the pile have the same sign, the effect of fill asymmetry acts to increase the magnitude of the bending moment produced in the pile. When normal components of vertical and horizontal soil movement have opposite signs, the bending moment due to horizontal soil movement may counteract the moment due to vertical soil movement. For the middle loading case shown in Figure B.18, the flood-side pile experiences the highest downdrag-induced bending moment, while the protected-side pile experiences the highest downdrag-induced bending moment for the loading case shown in right-hand figure in Figure B.18. The middle load case shown in Figure B.18 is critical for the effects of fill asymmetry since the flood-side pile lacks the additional support provided to the protected-side pile by the middle pile in the right-hand loading case shown in Figure B.18. Therefore it is conservative to use the middle load case in Figure B.18 to evaluate the effects of fill asymmetry on downdrag-induced bending moment. As shown in Table B.10, FLAC analyses were performed using Geometries (b), (c), and (e) where the embankment surcharge was only applied to the flood side. This load case corresponds to the middle figure in Figure B.18, except that there is no surcharge applied to the protected-side. The FLAC analyses incorporating asymmetric fill on the flood side were used to calibrate the LPILE Method by evaluating the moment calculated for the flood-side pile, since this pile experiences the highest downdrag-induced bending moment for the asymmetrical loading condition evaluated. For middle and protected-side piles, the net effect of the vertical and horizontal soil movements produced by the particular asymmetric fill geometry used in the FLAC analyses caused the middle and protected-side piles to bend away from the centerline of the T-Wall. This direction of bending is opposite of the direction the flood-side pile bends in response to the asymmetric fill. Since the maximum bending moments produced in the flood-side pile were used to calibrate LPILE Method to the FLAC results, the LPILE Method is not currently equipped to calculate bending moments in the middle and protected-side piles when asymmetric fill produces more compression on the flood side of the T-Wall. Further discussion of the application of the LPILE Method to the flood-side, middle, and protected-side piles for difference fill conditions is discussed in Section B.6.

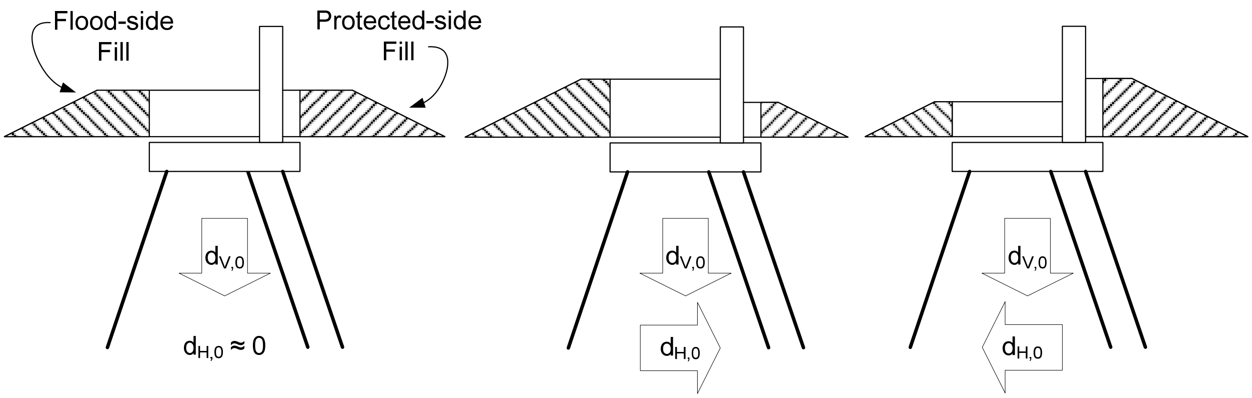

Figure B.18 Possible load cases

As previously discussed in Section B.4, the embankment surcharge was applied in the FLAC model as a pressure placed on the ground surface rather than constructing the embankment in the mesh and assigning soil properties to the embankment elements. This approach simplified the process of evaluating many different magnitudes of surcharge pressure. However, when an asymmetric fill was applied to Geometry (b), which lacks a middle pile, the T-Wall exhibited an unrealistic lack of lateral restraint allowing it to slide in the direction of lateral soil movement. When the T-Wall is permitted to slide, the top of the flood-side pile moves laterally causing the pile to relax some of the downdrag-induced bending moment. The tendency for the T-Wall to slide was not observed for Geometry (c) since the inclusion of the middle pile significantly stiffens the frame action of the piles and the T-Wall. The FLAC analyses using Geometry (e) also did not show significant sliding of the T-Wall since the existing embankment soils are stronger and stiffer than the soft clay and resist sliding of the T-Wall. Because the T-Wall would have to slide against the resistance provided by a soil embankment surcharge regardless of whether a middle pile or existing embankment layer were present, the LPILE Method was calibrated to account for the effects of horizontal soil movement based on the FLAC analyses performed using Geometries (c) and (e) only.

To account for the additional bending moment due to horizontal soil movement, the following procedure was performed for each different asymmetric fill surcharge pressure analyzed in FLAC for Geometries (c) and (e):

1. Calculate s_F and s_P using hand-calculations.
2. Determine Δs as the absolute value of $s_F - s_P$.
3. Determine $d_{v,o}$ using s_F and the appropriate trend provided in Figure B.14.

4. Perform LPILE analyses and determine the value of $d_{N,0}$ that, when applied along the pile according to the distribution of settlement over the profile producing s_F, yields the same maximum moment as calculated by FLAC.
5. Using the value of $d_{V,0}$ determined in Step 3 and the value of $d_{N,0}$ determined in Step 4, determine the value of $d_{H,0}$ according to: $d_{H,0} = d_{N,0}*1/\cos(\beta) - d_{V,0}*\tan(\beta)$, which is simply Equation B.1 solved for $d_{H,0}$.
6. Plot $d_{H,0}$ versus Δs.

Using the procedure given above, the resulting relationships between $d_{H,0}$ and Δs are provided in Figure B.19 for cases where the T-Wall is positioned within the clay foundation or within an existing embankment. Based on the results shown in Figure B.19, the relationships between $d_{H,0}$ and Δs are similar for both T-Wall positions. Accordingly, a single trend line can be used to adequately account for the influence of fill asymmetry on downdrag-induced bending moments in the LPILE Method.

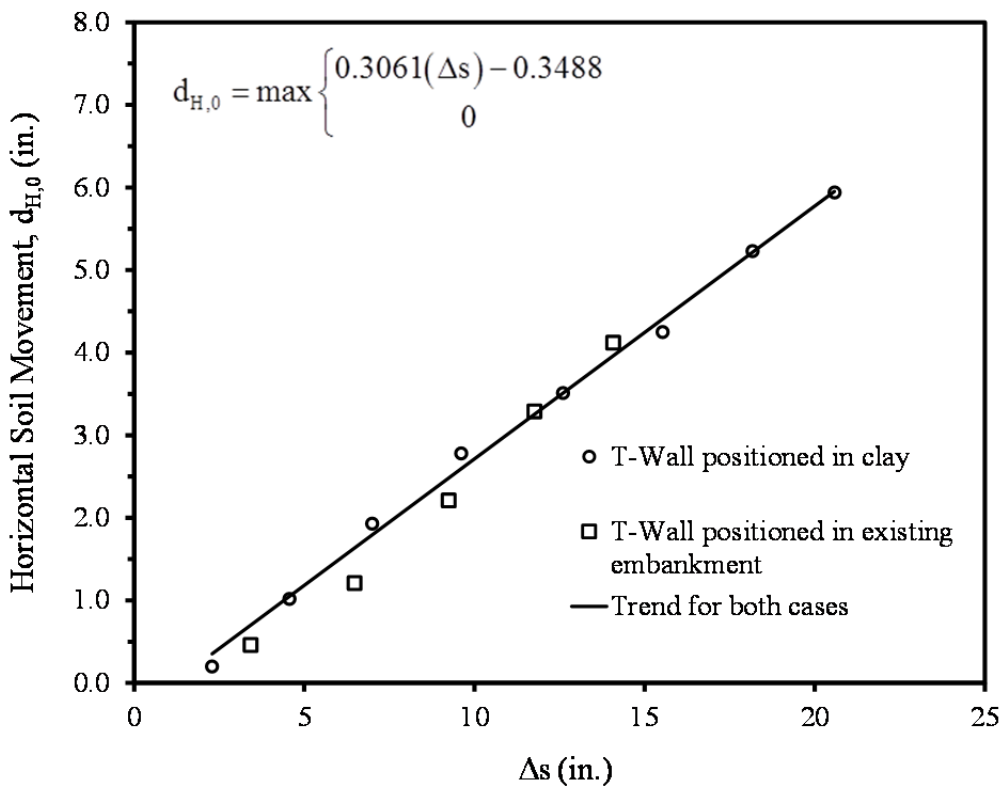

Figure B.19: Horizontal soil movement, $d_{H,0}$, applied at top of pile in addition to vertical soil movement versus difference between flood-side an protected-side settlements.

The influence of the sheet pile cut-off for cases with asymmetric fill can be evaluated by comparing Case 11 with the results of Case 13 in Table B.12. From these cases it is seen that the sheet pile cutoff wall reduces maximum bending moments. The magnitude of this reduction is expected to be sensitive to the depth and the lateral position of the sheet pile with respect to the battered piles, and its influence can be conservatively neglected from the LPILE Method.

B.4.5 Effect of an All Clay Profile

When piles are installed in a soil profile that lacks a distinct bearing layer, significant compression of the foundation soil due to the embankment surcharge may occur beyond the pile tip. For this case, s_{FS} and s_{PS} are calculated over the interval from the base of the T-Wall to the elevation of the pile tip. Soil movement is applied in LPILE using Equations B.2 and B.3 in the same way as for a profile with a bearing layer except that in this case L_c extends to the pile tip. The effect of an all clay profile without a sand bearing layer can be seen by comparing the FLAC results from Cases 1 and 14 and Cases 12 and 15 in Table B.12. Both comparisons show that the maximum moment is larger for an all clay profile. The average increase in maximum moment for these two comparisons is about 11 percent.

B.4.6 Effect of existing embankment layer

As shown in Figure B.14, for the same magnitude of s, the corresponding magnitude of $d_{V,0}$ used in LPILE is smaller for the case where the T-Wall is positioned in an embankment than when the T-Wall is positioned in the clay foundation. The reasons for this difference can be explored by comparing Case 34 (T-Wall in clay) and Case 40 (T-Wall in embankment) which have very similar values of s. In both cases, the fill surcharge is symmetrical on the flood and protected sides. In Table B.13, the values of s between the two cases are shown to be very similar and the maximum bending moments for Case 40 is 88% of the value for Case 34; however, the value of $d_{V,0}$ for Case 40 is only 38% of the value for Case 34. Recall that the values of $d_{V,0}$ were determined by back-calculating vertical soil movements that produce the same maximum moment by the LPILE Method as calculated using FLAC. One possible explanation for this outcome is that the pile-soil springs in the existing embankment are significantly stiffer than in the upper portion of the soft clay, thus they exert considerably greater force to the pile for the same magnitude of soil movement. In addition, the pile length is longer for Case 40 than Case 34, which means that, compared to Case 34, the pile in Case 40 is subjected to greater total soil force applied over a longer distance for the same magnitude of $d_{V,0}$.

Table B.13: Comparison of cases with and without an existing embankment having similar values of s_{max}.

Case	Surcharge (psf)	s (in.)	$d_{V,0}$ (in.)	FLAC M_{max} (k-ft)
34	495	13.25	6.76	94
40	660	13.42	2.55	83

The influence of the undrained strength of the existing embankment was investigated using Cases 42, 43, and 44. The results are summarized in Table B.14.

Table B.14: Influence of undrained strength of existing embankment on maximum bending moment

<table>
<tr><th>Undrained strength of embankment, S_u (psf)</th><th>Max. Moment in FS pile calculated by FLAC (k-ft)</th><th>s (in.)</th><th>$d_{V,0}$ (in.)</th><th>Max. Moment in FS pile calculated by LPILE Method (k-ft)</th></tr>
<tr><td>400</td><td>227</td><td rowspan="3">24.79</td><td rowspan="3">11.34</td><td>180</td></tr>
<tr><td>800</td><td>216</td><td>210</td></tr>
<tr><td>1600</td><td>225</td><td>304</td></tr>
</table>

Table B.14 shows that the maximum bending moment calculated by FLAC does not change significantly, or in a consistent way, when the undrained strength of the existing embankment ranges from 400 to 1,600 psf. Over the same range of undrained strength, the LPILE Method calculates significantly higher maximum bending moment as undrained strength increases. This result is due to the fact that the pile-soil springs used in LPILE become stiffer as undrained strength increases, thus applying greater soil force for the same magnitude of soil movement. Since the LPILE Method is calibrated to the FLAC results, which showed low sensitivity to the value of undrained strength for the existing embankment layer, it is recommended that an undrained strength equal to 800 psf be used in the LPILE Method for existing embankment soils with undrained strengths between 400 and 1,600 psf.

B.5 Comparison of LPILE Method with FLAC Results

The complete LPILE Method was compared to the FLAC analyses described in Section B.4 for the cases listed in Table B.15. Figures B.20 through B.23 show that the agreement between the maximum moment values determined from the LPILE Method and FLAC is quite good, although the elevation of the maximum bending moment differs for several cases.

Table B.15: Cases where LPILE Method was compared to FLAC analyses

Case	Geometry	FS Surcharge	PS Surcharge
32	b	165	165
6	b	990	990
54	b	1650	1650
21	c	165	0
17	c	990	0
19	c	1320	0
55	e	330	330
41	e	990	990
56	e	1650	1650
57	e	330	0
46	e	990	0
58	e	1650	0

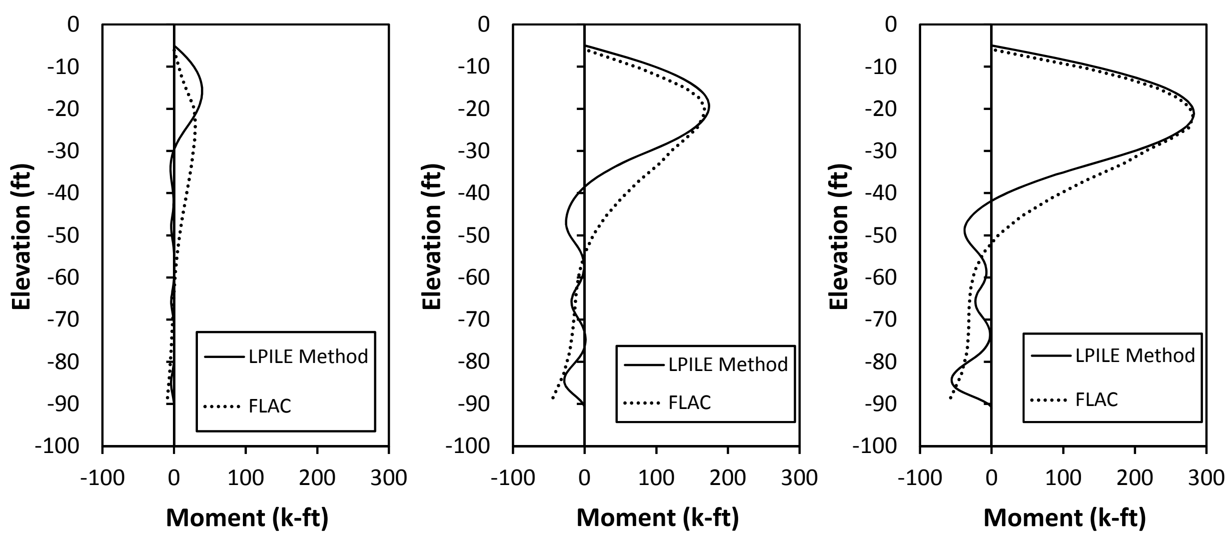

Figure B.20: (left to right) Comparison of bending moment diagrams for Cases 32, 6, and 54 from the LPILE Method and FLAC analyses

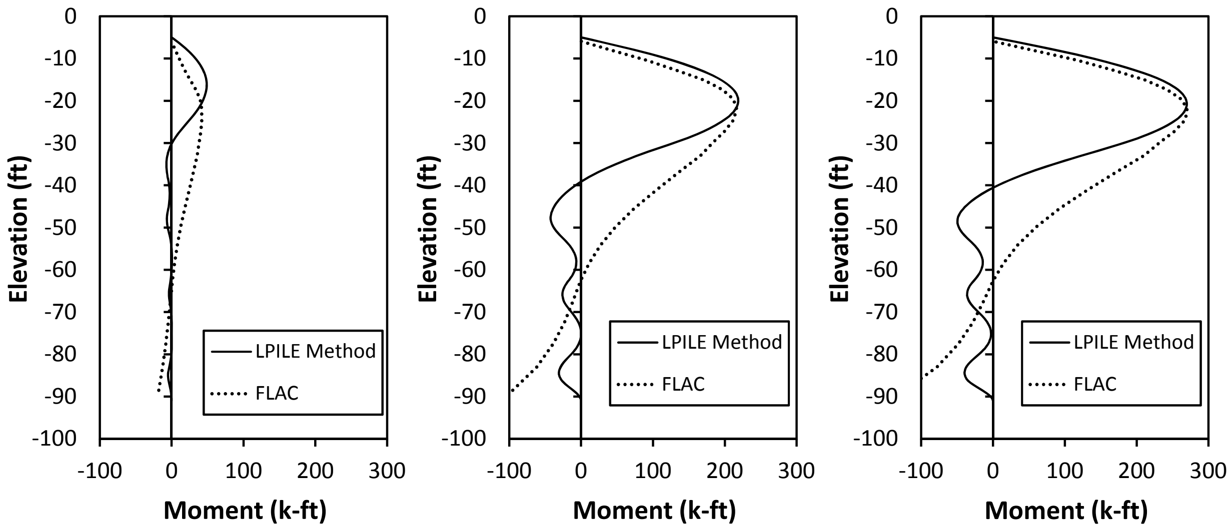

Figure B.21: (left to right) Comparison of bending moment diagrams for Cases 21, 17, and 19 from the LPILE Method and FLAC analyses

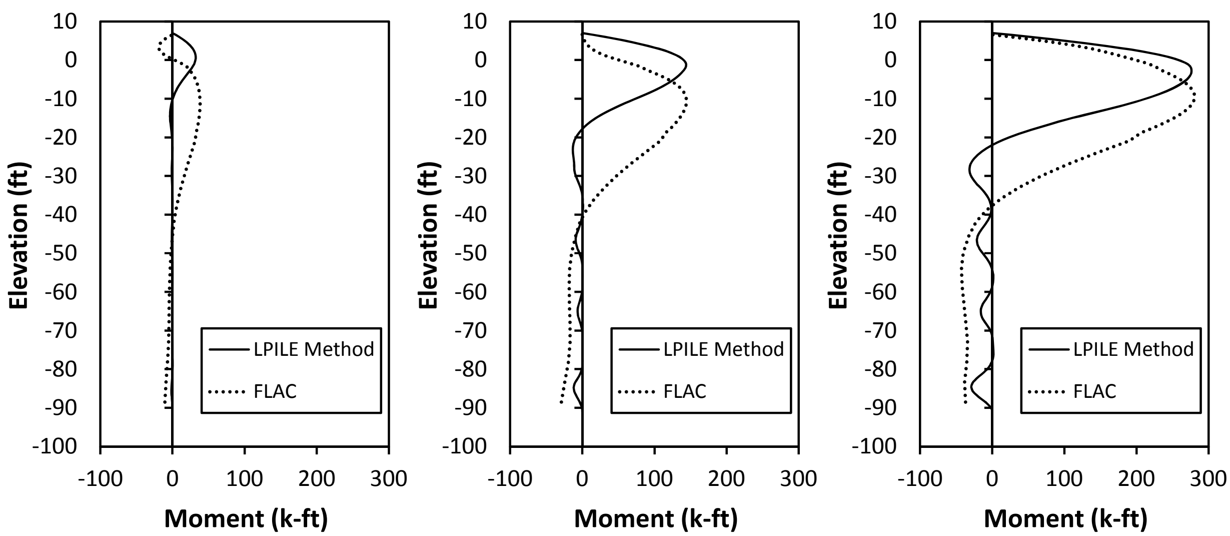

Figure B.22: (left to right) Comparison of bending moment diagrams for Cases 55, 41, and 56 from the LPILE Method and FLAC analyses

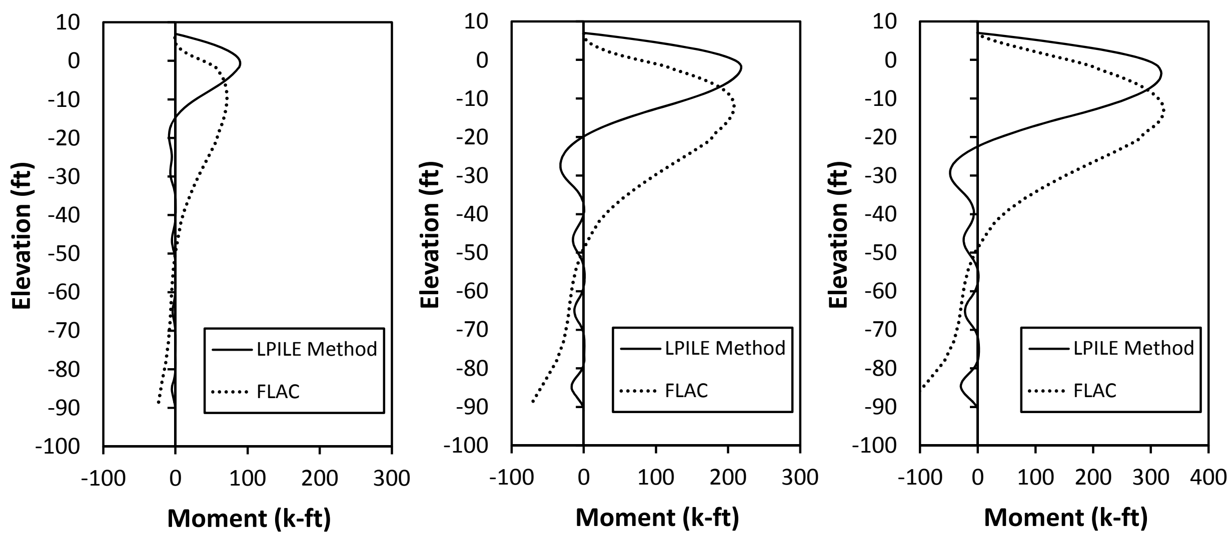

Figure B.23: (left to right) Comparison of bending moment diagrams for Cases 57, 46, and 58 from the LPILE Method and FLAC analyses

B.6 Applicability of LPILE Method

Table B.16 outlines the applicability of the LPILE Method to the flood side, middle, and protected side batter piles for combinations of fill loading and T-Wall position. The fill loading conditions considered were fills that produce symmetrical compression on the flood- and protected-sides of the T-Wall, fill that produces more compression on the flood side, and fill that produces more compression on the protected side. The T-Wall positions considered were the case where the T-Wall is positioned in the clay foundation and the case where the T-Wall is positioned within an existing embankment resting on a clay foundation that has already completed consolidation due to the load imposed by the existing embankment. For each combination of pile, fill condition, and T-Wall position, Table B.16 indicates how the maximum moment calculated by LPILE Method, in its current calibration, compares to the moments calculated by FLAC. In cases where the LPILE results compare closely to the FLAC results, the use of the LPILE Method is considered "okay". In cases where the maximum moment calculated by LPILE is greater than the maximum moment calculated by FLAC, the use of the LPILE Method is considered conservative. The degree of conservatism is indicated by the descriptors "somewhat" for results within 25% of the FLAC values, "fairly" for results within 50% of the FLAC values, and "very" for results exceeding 50% larger than the FLAC values. In cases where the maximum moment calculated by LPILE is less than the maximum moment calculated by FLAC, the signs of the calculated moment are not the same (i.e., LPILE calculates the pile bending one way and FLAC calculates it bending the opposite way), or the current investigation does not provide enough information to make a judgment, the LPILE Method is considered to not be applicable in its current form. The last column in the table provides key supporting information for the conclusions about the use of the LPILE Method.

Table B.16: Application of the LPILE Method to flood-side, middle, and protected-side batter piles for different combinations of fill and T-Wall position.

Pile of interest	Fill condition	T-Wall position	Use of LPILE Method
Flood-side pile	Symmetrical compression on flood and protected sides	In clay foundation	▪ Okay Details: The maximum moment calculated by LPILE was calibrated to the FLAC results for soil movements based on S_F
Middle pile	Symmetrical compression on flood and protected sides	In clay foundation	▪ Very conservative Details: Values of S_M were not calculated as part of the development of the LPILE Method, but they are logically expected to be somewhat less than S_P due to greater shielding from the T-Wall. If S_M is assumed to equal S_P, the calculated maximum moment is 144% greater, on average, than the maximum moment calculated by FLAC.
Protected-side pile	Symmetrical compression on flood and protected sides	In clay foundation	▪ Somewhat conservative when middle pile is not present. ▪ Fairly conservative when middle pile is present. Details: When soil movements based on S_P are used in LPILE, the calculated maximum moment is 23% greater, on average, than the maximum moment calculated by FLAC when no middle pile is present. When a middle pile is present, the maximum moment calculated by LPILE is 45% greater, on average, than the maximum moment calculated by FLAC.
Flood-side pile	Symmetrical compression on flood and protected sides	In existing embankment	▪ Okay Details: The maximum moment calculated by LPILE was calibrated to the FLAC results for soil movements based on S_F.

Table B.16 (cont): Application of the LPILE Method to flood-side, middle, and protected-side batter piles for different combinations of fill and T-Wall position.

Pile of interest	Fill condition	T-Wall position	Use of LPILE Method
Middle pile	Symmetrical compression on flood and protected sides	In existing embankment	▪ Expected to be fairly to very conservative. Details: This case was not evaluated in the parametric study, but the results are expected to be fairly to very conservative
Protected-side pile	Symmetrical compression on flood and protected sides	In existing embankment	▪ Okay when middle pile is not present. ▪ Expected to be somewhat conservative when middle pile is present. Details: Using soil movements based on S_P, the maximum moment calculated by LPILE is within 2%, on average, of the maximum moment calculated by FLAC when no middle pile is present. The case where a middle pile is present was not evaluated in the parametric study, but results are expected to be somewhat conservative.
Flood-side pile	Asymmetrical with more compression on flood side	In clay foundation	▪ Okay Details: The maximum moment calculated by LPILE was calibrated to the FLAC parametric study for the case where a middle pile is present. Due to the way the fill soil was represented in the FLAC analyses as a pressure, there was potential for unconservative results if a separate calibration was developed for the flood side pile when a middle pile is not present (refer to Section B.4.4). Consequently, the calibration developed for the flood-side pile when the middle pile is present is also applied when a middle pile is not present.

Table B.16 (cont): Application of the LPILE Method to flood-side, middle, and protected-side batter piles for different combinations of fill and T-Wall position.

Pile of interest	Fill condition	T-Wall position	Use of LPILE Method
Middle pile	Asymmetrical with more compression on flood side	In clay foundation	▪ Does not apply, but a conservative design can be obtained by using the magnitude of the maximum moment from the LPILE Method for the flood-side pile. <u>Details:</u> Values of S_M were not calculated as part of the development of the LPILE method. If vertical soil movements are based on S_P in place of S_M and counteraction produced by lateral soil movement is ignored ($d_{H,0} = 0$), LPILE calculates a maximum bending moment that has an opposite sign of what was calculated by FLAC. This means that, for this case, the LPILE Method is not correctly considering the mechanics that determine the maximum bending moment in the middle pile. Even if the difference in sign of the moment is ignored, the maximum moment calculated by LPILE is less than the value calculated by FLAC (which is unconservative). However, in every case analyzed, the magnitude of the maximum moment in the flood-side pile exceeded the magnitude of the maximum moment in the middle pile. Consequently, if the magnitude of the maximum moment for the flood-side pile is applied to the middle pile, a safe design will result. If this approach is judged by the designer to be too conservative, then numerical analyses can be performed.

Table B.16 (cont): Application of the LPILE Method to flood-side, middle, and protected-side batter piles for different combinations of fill and T-Wall position.

Pile of interest	Fill condition	T-Wall position	Use of LPILE Method
Protected-side pile	Asymmetrical with more compression on flood side	In clay foundation	▪ Does not apply, but a conservative design can be obtained by using the magnitude of the maximum moment from the LPILE Method for the flood-side pile. Details: If vertical soil movements based on S_P are used in LPILE and counteraction produced by lateral soil movement is ignored ($d_{H,0} = 0$), LPILE calculates a maximum bending moment that has an opposite sign of what was calculated by FLAC. This means that, for this particular case, the LPILE Method is not correctly considering the mechanics that determine the maximum bending moment in the protected-side pile. Even if the difference in sign of the moment is ignored, the maximum moment calculated by LPILE is less than the value calculated by FLAC (which is unconservative). However, in every case analyzed, the magnitude of the maximum moment in the flood-side pile exceeded the magnitude of the maximum moment in the protected-side pile. Consequently, if the magnitude of the maximum moment for the flood-side pile is applied to the protected-side pile, a safe design will result. If this approach is judged by the designer to be too conservative, then numerical analyses can be performed.

Table B.16 (cont): Application of the LPILE Method to flood-side, middle, and protected-side batter piles for different combinations of fill and T-Wall position.

Pile of interest	Fill condition	T-Wall position	Use of LPILE Method
Flood-side pile	Asymmetrical with more compression on flood side	In existing embankment	▪ Okay when middle pile is not present ▪ Expected to be okay if maximum moment is increased by 7%. <u>Details:</u> The maximum moment calculated by LPILE was calibrated to the FLAC parametric study for the case where a middle pile is not present. The case where a middle pile is present for a T-Wall positioned within an existing embankment was not evaluated in the parametric study. Since the middle pile provides additional restraint against T-Wall movement, which increases bending moment in the flood-side pile, it is recommended to increase the maximum moment calculated by LPILE by 7% (refer to Appendix D for details).
Middle pile	Asymmetrical with more compression on flood side	In existing embankment	▪ Does not apply, but it is expected that a conservative design can be obtained by using the magnitude of the maximum moment from the LPILE Method for the flood-side pile. <u>Details:</u> The case where a middle pile is present was not evaluated in the parametric study; however it logical to expect the magnitude of the maximum moment in the flood-side pile to be greater than the maximum moment in the middle pile. Consequently, if the magnitude of the maximum moment for the flood-side pile is applied to the middle pile, a safe design will result. If this approach is judged by the designer to be too conservative, then numerical analyses can be performed.

Table B.16 (cont): Application of the LPILE Method to flood-side, middle, and protected-side batter piles for different combinations of fill and T-Wall position.

Pile of interest	Fill condition	T-Wall position	Use of LPILE Method
Protected-side pile	Asymmetrical with more compression on flood side	In existing embankment	▪ Does not apply, but a conservative design can be obtained by using the magnitude of the maximum moment from the LPILE Method for the flood-side pile. <u>Details:</u> If vertical soil movements based on S_P are used in LPILE and counteraction produced by lateral soil movement is ignored ($d_{H,0} = 0$), LPILE calculates a maximum bending moment that has an opposite sign of what was calculated by FLAC. This means that, for this particular case, the LPILE Method is not correctly considering the mechanics that determine the maximum bending moment in the protected-side pile. Even if the difference in sign of the moment is ignored, the maximum moment calculated by LPILE is less than the value calculated by FLAC (which is unconservative). However, in every case analyzed, the magnitude of the maximum moment in the flood-side pile exceeded the magnitude of the maximum moment in the protected-side pile. Consequently, if the magnitude of the maximum moment for the flood-side pile is applied to the protected-side pile, a safe design will result. If this approach is judged by the designer to be too conservative, then numerical analyses can be performed.

Table B.16 (cont): Application of the LPILE Method to flood-side, middle, and protected-side batter piles for different combinations of fill and T-Wall position.

Pile of interest	Fill condition	T-Wall position	Use of LPILE Method
Flood-side pile	Asymmetrical with more compression on protected side	In clay foundation or in existing embankment	▪ Does not apply, but it is expected that a conservative design can be obtained by using the magnitude of the maximum moment from the LPILE Method for the protected-side pile. <u>Details:</u> Asymmetrical fill with more compression on the protected side was not considered in the parametric study; however it logical to expect the magnitude of the maximum moment in the protected-side pile to be greater than the maximum moment in the flood-side pile. Consequently, if the magnitude of the maximum moment for the protected-side pile is applied to the flood-side pile, a safe design will result. If this approach is judged by the designer to be too conservative, then numerical analyses can be performed.
Middle pile	Asymmetrical with more compression on protected side	In clay foundation	▪ Expected to be fairly to very conservative <u>Details:</u> Asymmetrical fill with more compression on the protected side was not considered in the parametric study; however, it is expected that using the LPILE Method calibrated for the flood side pile when compression is greater on the flood side for the middle pile will produce results significantly higher than FLAC would calculate due to the shielding provided by the T-Wall and protected-side pile.

Table B.16 (cont): Application of the LPILE Method to flood-side, middle, and protected-side batter piles for different combinations of fill and T-Wall position.

Pile of interest	Fill condition	T-Wall position	Use of LPILE Method
Protected-side pile	Asymmetrical with more compression on protected side	In clay foundation	▪ Expected to be okay when middle pile is not present ▪ Expected to be somewhat conservative when middle pile is present <u>Details:</u> Asymmetrical fill with more compression on the protected side was not considered in the parametric study; however, it is expected that using the LPILE Method calibrated for the flood side pile when compression is greater on the flood side for the protected side pile will produce results that are reasonably close to what would be calculated by FLAC, with results being somewhat conservative if a middle pile is present.
Middle pile	Asymmetrical with more compression on protected side	In existing embankment	▪ Expected to be fairly conservative <u>Details:</u> The case where a middle pile is present for a T-Wall positioned within an existing embankment was not evaluated in the parametric study; however it is expected that using the LPILE Method calibrated for the flood side pile when compression is greater on the flood side and no middle pile is present for the middle pile will produce results that are fairly conservative.

Table B.16 (cont): Application of the LPILE Method to flood-side, middle, and protected-side batter piles for different combinations of fill and T-Wall position.

Pile of interest	Fill condition	T-Wall position	Use of LPILE Method
Protected-side pile	Asymmetrical with more compression on protected side	In existing embankment	▪ Expected to be okay Details: Asymmetrical fill with more compression on the protected side was not considered in the parametric study; however, it is expected that using the LPILE Method calibrated for the flood side pile, when a middle pile is not present and compression is greater on the flood side, for the protected-side pile will produce results that are reasonably close to what would be calculated by FLAC. When a middle pile is present, the results of the analysis presented in Appendix D show that the increase in the maximum bending moment in the flood-side pile due to the additional restraint provided by a middle pile is expected to be less than 7% for the conditions considered. The supporting effect of the middle pile, which acts to reduce bending of the protected-side pile, is expected to exceed the restraining effect of the middle pile, which acts to increase the bending of the protected-side pile. Therefore, it is recommended that no adjustment be made to the maximum bending moment calculated by the LPILE Method for the protected-side pile when a middle pile is present.

C Example of Settlement Calculation and Calibration Process

C.1 Introduction:

This appendix is a companion to the background provided in Section B.4.1 of Appendix B which describes the stiffening effect of piles on soil settlements. Provided here are sample calculations of s_F, s_F^{FLAC}, and $d_{V,0}^{FLAC}$ for Case 36 defined in Table B.11 in Appendix B, which uses Geometry (b) and a symmetric embankment surcharge pressure of 825 psf. The calculated values are part of the data set used to produce Figure B.13 in Appendix B, which is ultimately used to develop the relationship between s_{FS} and $d_{V,0}$ given in Figure B.14.

C.2 Calculation of s_F, s_F^{FLAC} and $d_{V,0}^{FLAC}$:

Figure 1 shows a simplified cross section of the soil profile, T-Wall, and pile configuration for Geometry (b). Figure 1 also shows the height and lateral extent of the embankment which produces compression of the foundation soils.

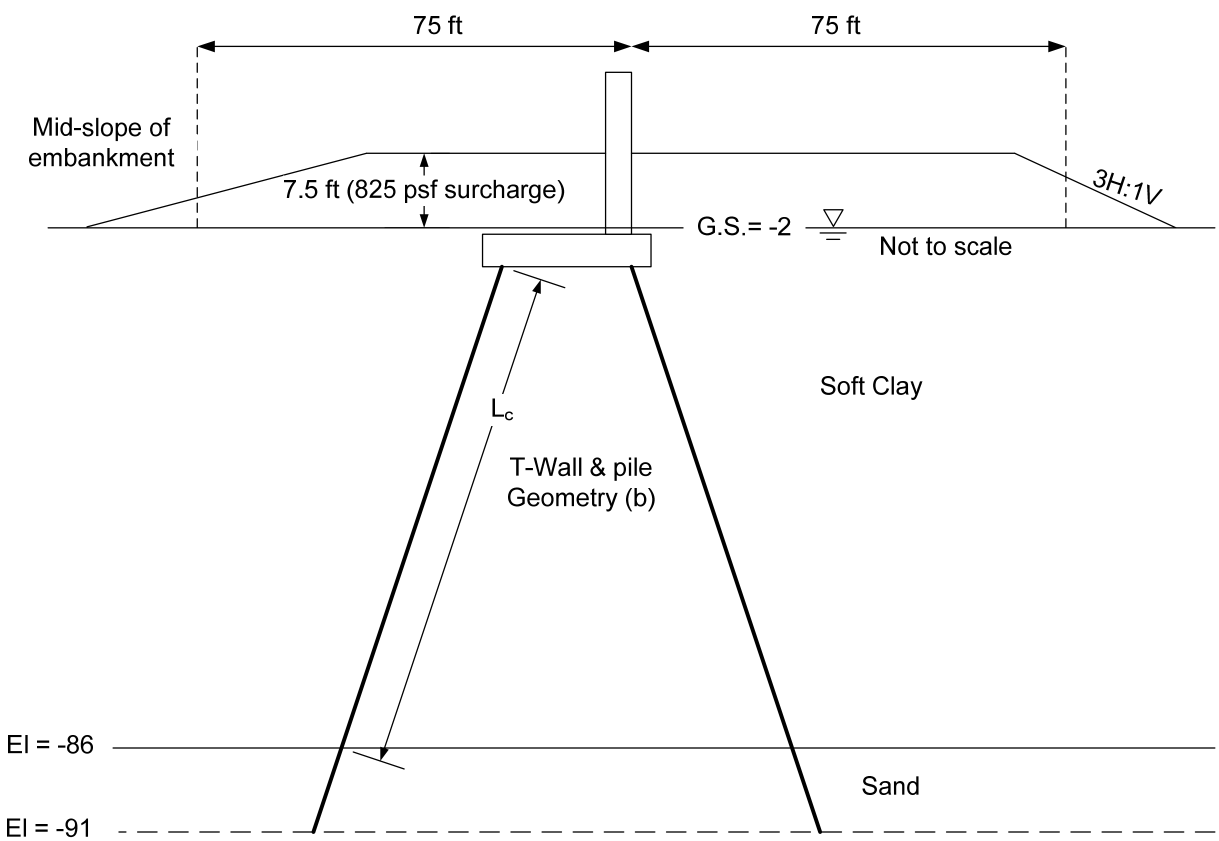

Figure C.1: Simplified cross section of Geometry (b) with 7.5 ft embankment surcharge

Figure 2 shows a plan view of the uniform finite loaded areas used to represent the embankment surcharge. The x-coordinates are based on an origin at the protected-side face of the wall stem. As described in the report, the weight of the T-Wall and overlying fill are excluded for the settlement calculations.

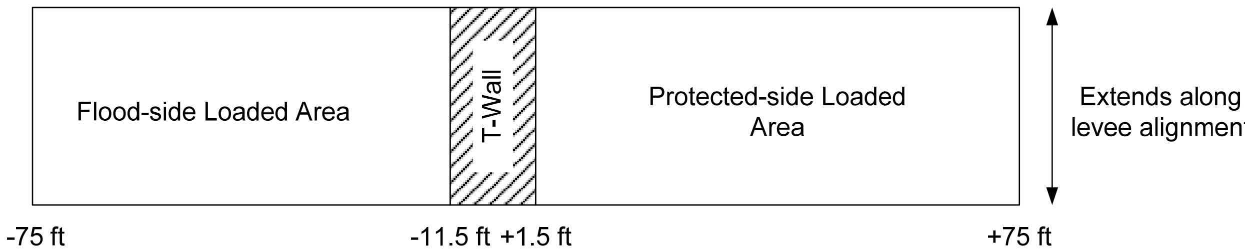

Figure C.2: Finite loaded areas used to represent the embankment surcharge

The compression of the foundation soils was evaluated from the base of the T-Wall at El. -5 to the top of the sand bearing layer at El. -86. For this case, compression was calculated along a vertical profile a distance $x = 0.25 \cdot L_c(\sin\beta)$ from where the flood-side pile intersects the T-Wall base. Calculation of x is provided below:

$$L_c = \frac{(\text{bottom of T-Wall - top of bearing layer})}{\cos(\beta)}$$

$$L_c = \frac{(El.\text{-}5 - EL.\text{-}86)}{\cos(18.43)} = 85.38\,ft$$

$$x = 0.25(85.38)\sin(18.43)$$

$$x = 6.75\,ft$$

Since the embankment surcharge is symmetrical, compression only needs to be calculated on the flood side. The flood-side pile intersects the T-Wall base 10 ft from the origin, so the vertical profile for calculating compression is 16.75 ft from the origin, at an x-coordinate of -16.75. The closest grid line in the FLAC model to this position is at an x-coordinate of -17.14, so this location was used as the flood-side profile for the hand calculation of compression.

The foundation soil profile was divided into layers corresponding to the horizontal grid lines of the FLAC model. The change in stress due to the embankment surcharge was determined at the mid-height of each layer using Boussinesq elastic solutions. The elevation of the top of each soil layer and the computed stress change at mid height are provided below in Table 1.

Compression of each soil layer was determined for clay layers using Equations 1 and 2 depending on whether the layer is overconsolidated or normally consolidated and Equation 3 for sand layers. In these equations, t is the thickness of the soil layer, $C_{\varepsilon r}$, is the recompression ratio, $C_{\varepsilon c}$, the virgin compression ratio, P_o, is the initial overburden stress, P_p, the preconsolidation stress, ΔP, the change in stress, P_f, the final stress equal to $P_o + \Delta P$, and M is the one-dimensional compression modulus of the sand. In this case, M has a value of 423,240 psf. The compression of each soil layer as well as the cumulative settlement at the top of each layer is listed in Table 1.

Table C.1: Settlement calculation along profile

Elevation of top of layer (ft)	Stresses at mid-height of layer: Initial stress, P_o (psf)	Preconsolidation stress, P_p (psf)	Stress change, ΔP (psf)	Final stress, P_f (psf)	Layer compression (ft)	Settlement at top of layer (in.)
-2.0	13	900	825	838	0.018	24.3
-2.5	38	900	825	863	0.014	24.0
-3.0	63	900	823	886	0.012	23.9
-3.5	88	900	820	908	0.010	23.7
-4.0	113	900	816	928	0.010	23.6
-4.5	138	900	809	947	0.011	23.5
-4.9	165	900	802	967	0.015	23.4
-5.7	210	900	784	994	0.022	23.2
-6.8	270	900	759	1029	0.027	22.9
-8.0	330	900	734	1064	0.028	22.6
-9.2	390	900	712	1102	0.030	22.3
-10.4	450	900	693	1143	0.032	21.9
-11.6	510	900	676	1186	0.035	21.5
-12.7	570	900	663	1233	0.042	21.1
-14.1	645	900	651	1296	0.057	20.6
-15.8	735	900	641	1376	0.070	19.9
-17.6	825	900	635	1460	0.077	19.1
-19.4	915	915	630	1545	0.082	18.1
-21.1	1005	1005	630	1635	0.089	17.2
-23.2	1125	1125	630	1755	0.099	16.1
-25.9	1263	1263	631	1893	0.092	14.9
-28.3	1388	1388	633	2020	0.094	13.8
-31.2	1550	1550	635	2185	0.108	12.7
-35.0	1750	1750	636	2386	0.110	11.4
-39.0	1958	1958	636	2593	0.104	10.1
-43.3	2175	2175	633	2808	0.097	8.8
-47.7	2393	2393	629	3022	0.088	7.6
-52.0	2608	2608	623	3231	0.081	6.6
-56.3	2825	2825	616	3441	0.075	5.6
-60.6	3043	3043	608	3650	0.071	4.7
-65.1	3275	3275	598	3873	0.070	3.9
-70.0	3525	3525	585	4110	0.067	3.0
-74.9	3775	3775	574	4349	0.065	2.2
-80.4	4050	4050	560	4610	0.059	1.5
-85.6	4300	n/a	548	4848	0.006	0.8
-89.9	4533	n/a	535	5068	0.007	0.7
-95.6	4858	n/a	518	5376	0.009	0.6
-102.5	5250	n/a	499	5749	0.011	0.5
-110.9	5750	n/a	475	6225	0.014	0.4
-123.6*	6475	n/a	443	6918	0.016	0.2

*bottom of layer at El. -139.4

$$s_i = t\left[C_{\varepsilon r}\log\left(\frac{P_p}{P_o}\right) + C_{\varepsilon c}\log\left(\frac{P_f}{P_p}\right)\right] \text{ for } \mathrm{P}_o < P_P \le P_f \tag{1}$$

$$s_i = t\left[C_{\varepsilon c}\log\left(\frac{P_f}{P_o}\right)\right] \text{ for } P_P \le \mathrm{P}_o \le P_f \tag{2}$$

$$s_i = t\left[\frac{\Delta P}{M}\right] \tag{3}$$

Figure 3 provides a plot of the cumulative settlement at the top of each soil layer versus elevation. The value of s_{FS} for these conditions is determined to be 22.6 inches by taking the settlement at the elevation of the T-Wall base, El. -5, and subtracting the settlement at the top of the bearing layer, El. -86.

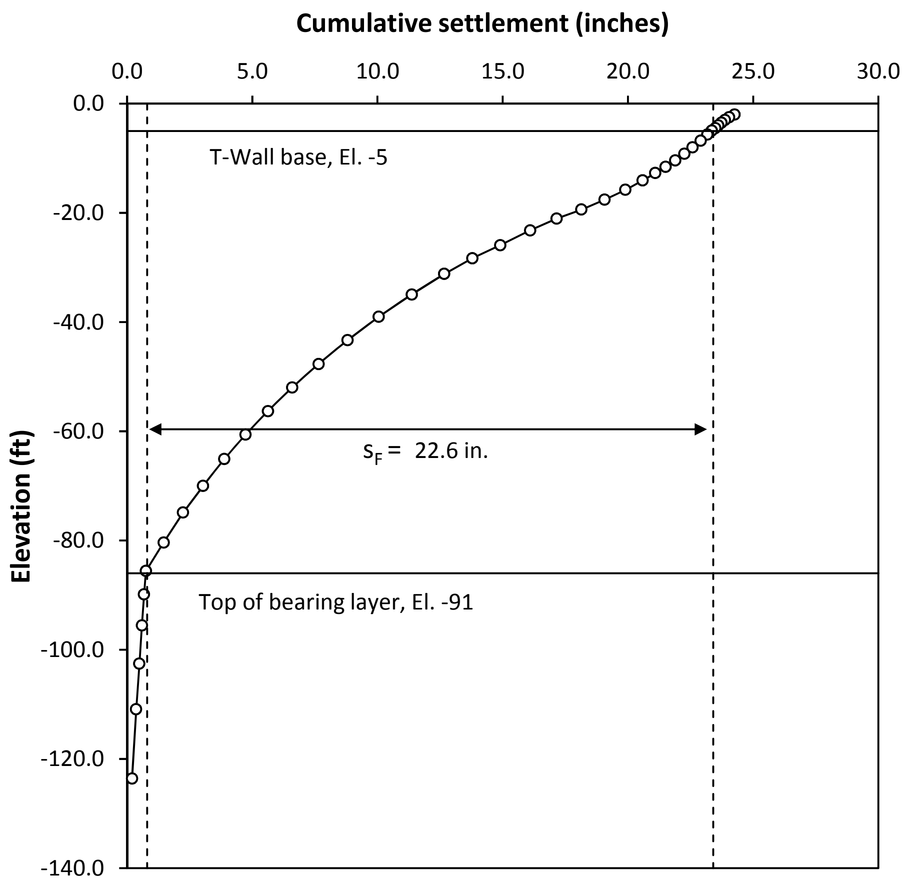

Figure C.3: Settlement versus elevation showing calculation of s_F

The magnitude of s_F is compared to s_F^{FLAC}, which is the corresponding compression calculated with the presence of piles in FLAC. The value of s_F^{FLAC} is determined by subtracting the vertical soil displacement along the flood-side profile at El. -86 from the displacement at El. -5. In this case, for Geometry (b) subjected to a symmetrical surcharge of 825 psf, s_F^{FLAC} is equal to 14.8 inches.

An excerpt from Figure B.11 for the case where the T-Wall is positioned within the clay foundation is reproduced here as Figure 4 which highlights the comparison of s_F with s_{FS}^{FLAC} for the current conditions.

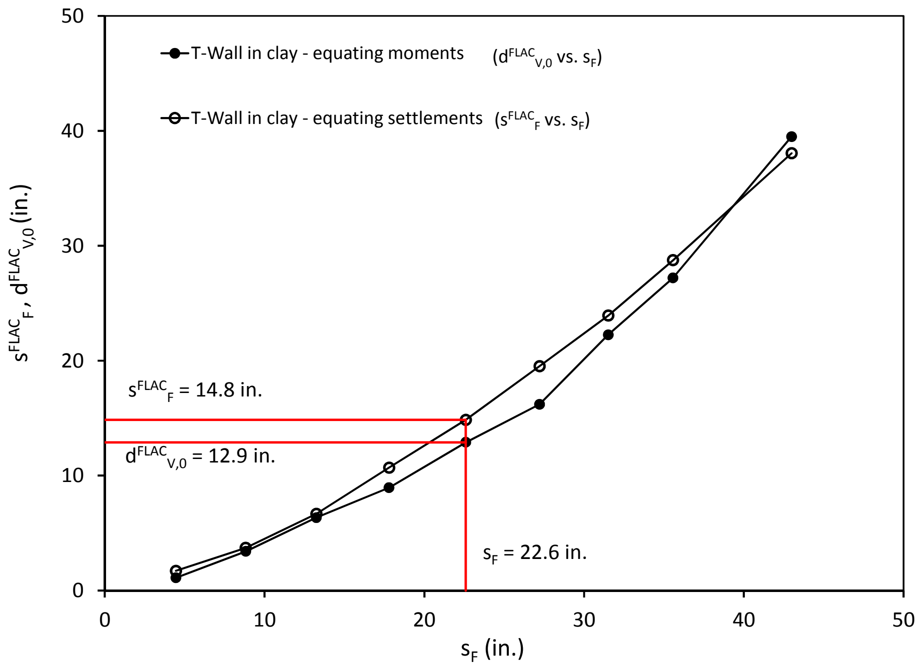

Figure C.4: Reproduction of Figure B.11 in Appendix highlighting results for 825 psf symmetrical surcharge pressure

As described in Section B.4.1 of the report, the value of $d_{V,0}^{FLAC}$ is the value of vertical soil movement, whose normal component, when applied in LPILE produces the same maximum moment as FLAC. For this example, Figure 5 shows the moment distribution calculated for the flood-side pile using FLAC, with a maximum moment of 147 kip-ft. The magnitude of soil movement normal to the pile, $d_{N,0}$ required for the maximum moment in LPILE to equal 147 kip-ft is 4.36 inches. Using Equation 1 of the report, the magnitude of vertical soil movement which produces 4.08 inches of normal movement is the value of $d_{V,0}^{FLAC}$ and is equal to 12.9 inches. The comparison of this value to s_F is shown in Figure 4.

The remainder of the values shown in Figure 4 correspond to values of $s_{F,}$ s_F^{FLAC}, and $d_{V,0}^{FLAC}$ determined using the same procedure described above for different magnitudes of embankment surcharge.

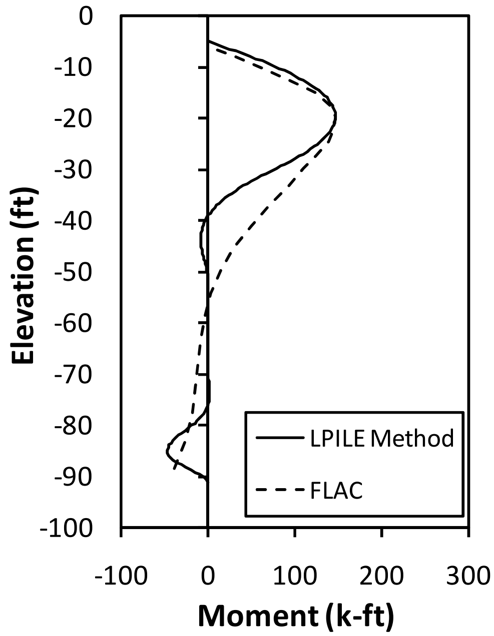

Figure C.5: Moment distributions calculated in LPILE and FLAC both having the same maximum moment

D Application of LPILE Method to T-Wall Positioned within Existing Embankment with Three Batter Piles

This appendix presents a summary of the analysis performed to determine how the LPILE Method should be applied when the new embankment fill produces asymmetric compression of the clay foundation soils (i.e. $\Delta s \neq 0$) and the T-Wall is supported by three rows of batter piles and positioned within an existing embankment. The LPILE Method was calibrated using FLAC analyses as described briefly in Section 2.1 of the main body of the report and in greater detail in Section B.4 of Appendix B. In total, five geometries, designated Geometry (a) through Geometry (e), were analyzed using FLAC. The geometries, which are shown in Figures 2.5 and 2.6 of the report, consider the case where the T-Wall is positioned in the clay foundation (Geometries (b), (c), and (d)) and the case where the T-Wall is positioned within a 12-ft high existing embankment of broad lateral extent (Geometry (e)). FLAC analyses were performed for both T-Wall positions to evaluate the effect on downdrag-induced bending moments of an asymmetric new embankment load producing more compression on the flood side of the T-Wall. When the T-Wall was positioned within the clay foundation in the FLAC model, analyses were performed in which the T-Wall was supported by a flood-side row and a protected-side row of batter piles, referred to herein as the 2-Pile Case, as well as the case where the T-Wall was supported by an additional row of batter piles on the protected side (a.k.a. middle piles), referred to herein as the 3-Pile Case. When the T-Wall was positioned within the existing embankment in the FLAC model, analyses were performed for the 2-Pile Case only. In order to provide the Corps with guidance on how to use the LPILE Method for the 3-Pile Case when the T-Wall is positioned within an existing embankment and $\Delta s \neq 0$, the analysis described in this appendix was performed to estimate the impact of the middle pile on the maximum downdrag-induced bending moment.

The notation used in the analysis is defined below:

$M_{max,F,2\text{-}Pile}$ = Maximum moment calculated for the flood-side pile by FLAC for the 2-Pile Case (i.e. no middle pile is present).

$d_{N,z,2\text{-}Pile}$ = The set of soil movements applied normal to the pile in LPILE so that the LPILE Method calculates $M_{max,F,2\text{-}Pile}$.

$M_{max,F,3\text{-}Pile}$ = Maximum moment calculated for the flood-side pile by FLAC for the 3-Pile Case (i.e. middle pile is present).

$d_{N,z,3\text{-}Pile}$ = The set of soil movements applied normal to the pile in LPILE so that the LPILE Method calculates $M_{max,F,3\text{-}Pile}$.

Δv = vertical movement of pile top, taken to be at El. -5, in FLAC. Downward movement has positive sign.

Δh = horizontal movement of pile top, taken to be at El. -5, in FLAC. Movement has positive sign to the protected side for the flood-side pile.

$y_{top,\ FLAC}$ = movement of the pile top in FLAC normal to the pile axis.

= $\Delta v*\sin(\beta) + \Delta h*\cos(\beta)$

$\Delta y_{top,FLAC}$ = change in movement of the pile top in FLAC with addition of the middle batter pile (i.e. change in $y_{top,FLAC}$ with change from 2-Pile Case to 3-Pile Case).

$\Delta y_{top,LPILE}$ = movement of the pile top applied in LPILE along with $d_{N,z,2\text{-}Pile}$ to obtain $M_{max,F,3\text{-}Pile}$

Table D.1 provides the maximum bending moment and pile top displacement in the flood-side pile calculated by FLAC for the 2-Pile and 3-Pile Cases. The upper portion of the table provides the results from analyses performed when the T-Wall is positioned within the clay foundation soils and the lower half of the table provides the results from analyses performed when the T-Wall is positioned within an existing embankment.

Normally, a zero displacement, zero moment, boundary condition is specified at the top of the pile in the LPILE Method. Therefore, the impact of pile top displacement on bending moments is lumped into the calibration of the LPILE Method since the pile top displacements calculated by FLAC are non-zero. As discussed in Section B.4.4 in Appendix B, when asymmetric fill was applied to the flood side when the T-Wall was positioned in the clay foundation, the T-Wall slid laterally to the protected side to a much greater extent for the 2-Pile Case than for the 3-Pile Case. The T-Wall movements for the 2-Pile and 3-Pile Cases can be compared in Table D.1 by looking at the movement of the top of the flood-side pile. Lateral sliding of the T-Wall to the protected side reduces the bending moment in the flood-side pile. Therefore, as shown in Table D.1, the maximum bending moments for the 3-Pile Case become significantly greater than the 2-Pile Case as the fill load increases and results in greater movement of the T-Wall.

Table D.1: Maximum downdrag-induced bending moments and movements of the top of the flood-side pile for 2-Pile Case and 3-Pile Case subjected to asymmetric fill loads on the flood side. The values in *red italics* are values estimated by the current analysis.

T-Wall in clay foundation (asymmetric fill load on flood side)

	New Fill Load on Flood side (psf)								
	165	330	495	660	825	990	1155	1320	1650
$M_{max,F,2\text{-}Pile}$ (k-ft) (Geometry b)	45	88	111	120	120	120	118	118	
$M_{max,F,3\text{-}Pile}$ (k-ft) (Geometry c)	42	88	126	159	188	216	246	270	
$y_{top,\ FLAC}$ for 2-Pile Case (Geometry b) (in.)	0.56	2.09	4.23	6.93	9.79	12.57	15.26	17.73	
$y_{top,\ FLAC}$ for 3-Pile Case (Geometry c) (in.)	0.05	0.50	1.00	1.54	2.06	2.56	3.04	3.52	
$\Delta y_{top,\ FLAC}$ (in.)	-0.51	-1.59	-3.23	-5.39	-7.73	-10.01	-12.22	-14.21	
$\Delta y_{top,\ LPILE}$ (in.)	0.07	0.00	-0.52	-1.42	-2.54	-3.78	-5.25	-6.45	

T-Wall in 12 ft existing exbankment (asymmetric fill load on flood side)

	New Fill Load on Flood side (psf)								
	165	330	495	660	825	990	1155	1320	1650
$M_{max,F,2\text{-}Pile}$ (k-ft) (Geometry e)		71		139		208		273	322
$M_{max,F,3\text{-}Pile}$ (k-ft) (estimated)		*71*		*141*		*219*		*291*	*344*
$y_{top,\ FLAC}$ for 2-Pile Case (Geometry e) (in.)		0.77		1.81		2.84		3.91	5.05
$y_{top,\ FLAC}$ for 3-Pile Case (estimated) (in.)		*0.15*		*0.36*		*0.57*		*0.78*	*1.01*
$\Delta y_{top,\ FLAC}$ (in.)		-0.62		-1.45		-2.27		-3.13	-4.04
$\Delta y_{top,\ LPILE}$ (in.)		*0.00*		*-0.05*		*-0.29*		*-0.57*	*-0.90*

As discussed in Section B.4.4, it was decided during calibration of the LPILE Method that the degree of T-Wall sliding calculated by FLAC for the 2-Pile Case when the T-Wall is positioned with the clay foundation may not be realistic. Therefore, a conservative approach was adopted whereby only the 3-Pile Case analyses were used to calibrate the LPILE Method for the effects of fill asymmetry when the T-Wall is positioned within the clay foundation. When the T-Wall was positioned in an existing embankment, the T-wall movements for the 2-Pile Case were much less than the T-Wall movements for the 2-Pile Case when the T-Wall was positioned in the clay foundation. In fact, as Table D.1 shows, movement of the flood-side pile top for the 2-Pile Case when the T-Wall in positioned within an existing embankment is similar to the corresponding 3-Pile Case when the T-Wall is positioned in the clay foundation. As such, there was not the same concern with using the 2-Pile Case to calibrate the LPILE Method for the effects of fill asymmetry when the T-Wall is positioned with an existing embankment as there was when the T-Wall was positioned in the clay foundation.

The process used to calibrate the LPILE Method is discussed in detail in Section B.4 of Appendix B. The calibration process consisted of determining the soil movement that, when applied along the length of the pile in LPILE according to Equations 2 and 3 in the main body report, produces the same maximum moment as calculated by FLAC. For the 3-Pile Case, the soil movements applied in LPILE to produce the maximum moment calculated for the flood-side pile by FLAC, $M_{max,F,3\text{-}Pile}$, are referred to in this appendix as $d_{N,z,3\text{-}Pile}$. If this calibration process is repeated for analyses of the 2-Pile Case when the T-Wall is in the clay foundation, the set of soil movements produced is $d_{N,z,2\text{-}Pile}$, since they result in calculation of $M_{max,F,2\text{-}Pile}$ when applied in LPILE. The bottom row in the upper half of Table D.1 provides the pile top displacement applied in LPILE, $\Delta y_{top,LPILE}$, that is needed to calculate the maximum moment for the 3-Pile Case, $M_{max,F,3\text{-}Pile}$, when soil movements are used from the corresponding 2-Pile Case, $d_{N,z,2\text{-}Pile}$. The values of $\Delta y_{top,LPILE}$ developed from the case where the T-Wall is in the clay foundation gives the basis for recommendations provided herein for use of the LPILE Method when the T-Wall is positioned within an existing embankment and a middle batter pile is present.

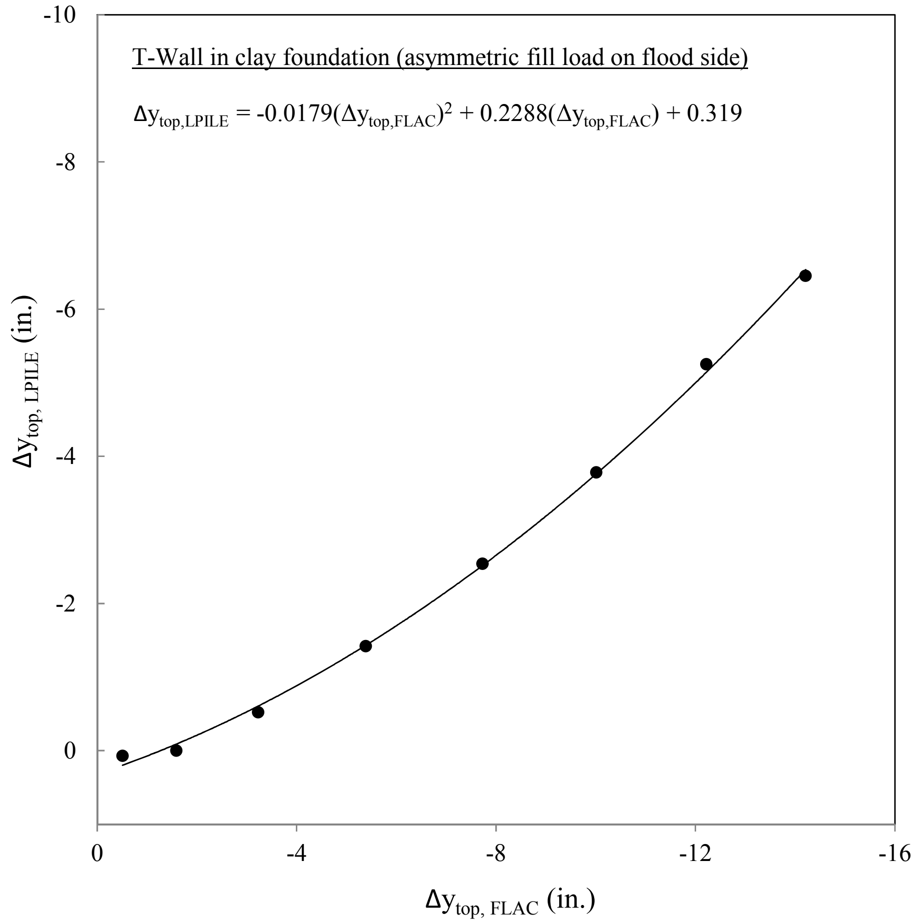

Figure D.1: Relationship between $\Delta y_{top,FLAC}$ and $\Delta y_{top,LPILE}$ when the T-Wall is positioned in the clay foundation an is subjected to asymmetric fill on the flood side.

The difference between the displacement of the top of the flood-side pile calculated by FLAC for the 3-Pile Case and the 2-Pile Case equals $\Delta y_{top,FLAC}$. Figure D.1 shows the relationship between $\Delta y_{top,FLAC}$ and $\Delta y_{top,LPILE}$ when the T-Wall is positioned in the clay foundation and subjected to asymmetric fill on the flood side. The relationship shows that to increase the maximum moment calculated in LPILE from $M_{max,F,2\text{-}Pile}$ to $M_{max,F,3\text{-}Pile}$ using soil movements based on the 2-Pile Case, the displacement magnitude applied at the pile top in LPILE is significantly less than the change in pile top displacement calculated by FLAC for the conditions evaluated. When the T-Wall is positioned within the existing embankment considered in the FLAC parametric study, the pile-soil springs for the upper portion of the pile in the existing embankment are stiffer than the pile-soil springs for the same length of pile in the clay foundation when the T-Wall is positioned in the clay foundation. The stiffer springs in the existing embankment impose more load to the pile for the same magnitude of imposed pile top displacement. Therefore, it is conservative to base the relationship between $\Delta y_{top,LPILE}$ and $\Delta y_{top,FLAC}$ on the relationship provided in Figure D.1 when the T-Wall is positioned within the existing embankment. Equation D.1 provides the relationship used herein between $\Delta y_{top,LPILE}$ and $\Delta y_{top,FLAC}$ when the T-Wall is positioned within an existing embankment subjected to asymmetric fill on the flood side.

$$\Delta y_{top,LPILE} = \mathrm{Min}\begin{cases} -0.0179\left(\Delta y_{top,LPILE}\right)^2 + 0.2288\left(\Delta y_{top,LPILE}\right) + 0.319 \\ 0 \end{cases} \tag{D.1}$$

When the T-Wall is positioned in the clay foundation, $\Delta y_{top,FLAC}$ is approximately equal to -0.8($y_{top,FLAC}$) for the 2-Pile Case. As shown in Table D.1 by comparing pile top displacements, the T-Wall is more restrained against lateral movement for the 2-Pile case when it is positioned within existing embankment soils, than when it is positioned in softer clay foundation soils. Therefore, it is logical to expect that the additional lateral restraint (as observed by the reduction in the magnitude of pile top displacement, $\Delta y_{top,FLAC}$) provided to the T-Wall by adding a middle pile when the T-Wall is positioned within an existing embankment would not exceed the increment of restraint provided by the middle pile when the T-Wall is positioned in the clay foundation. Since it is likely that $0 \geq \Delta y_{top,FLAC} \geq -0.8(y_{top,FLAC})$ when the T-Wall is positioned within an existing embankment, the relationship between $\Delta y_{top,FLAC}$ and $y_{top,FLAC}$ for the 2-Pile Case when the T-Wall is positioned in the clay foundation can be conservatively applied to $y_{top,FLAC}$ for the 2-Pile Case when the T-Wall is positioned within an existing embankment. Equation D.2 provides the relationship used between $\Delta y_{top,FLAC}$ and $y_{top,FLAC}$ for the 2-Pile Case when the T-Wall is positioned in an existing embankment subjected to asymmetric fill on the flood side.

$$\Delta y_{top,FLAC} = -0.8\left(y_{top,FLAC}\right) \text{ for the 2-Pile Case} \tag{D.2}$$

The estimated values of $\Delta y_{top,LPILE}$ provided in red italics in the lower half of Table D.1 were developed using values of $y_{top,FLAC}$ for the 2-Pile Case and applying Equations D.1 and D.2. The estimated values of $M_{max,F,3\text{-}Pile}$ were obtained by performing analyses using the LPILE Method with the estimates of $\Delta y_{top,LPILE}$ and soil movements associated with the 2-Pile Case, $d_{N,z,2\text{-}Pile}$, as input. The results indicate that the addition of a middle pile increases $M_{max,F,2\text{-}Pile}$ by less than 7 percent in all cases considered. Therefore, it is recommended that designers increase the maximum downdrag-induced moment obtained from the LPILE Method by 7 percent when it is applied to the 3-Pile Case for a T-Wall positioned within an existing embankment and subjected to asymmetric fill that produces differential settlement on the flood and protected sides less than or equal to 14 inches ($\Delta s \leq 14$ in.). As addressed in Section B.4.3 of Appendix B, no adjustment is recommended when the fill is symmetric ($\Delta s = 0$). This approach should produce conservative results when applied to conditions similar to those considered in the development of the LPILE Method. If the designer judges the conditions to be too dissimilar, then numerical analyses are recommended.